International Atomic Energy Agency

INDC(NDS)-103/M

INDC INTERNATIONAL NUCLEAR DATA COMMITTEE

PROCEEDINGS OF THE ADVISORY GROUP MEETING ON NUCLEAR DATA FOR REACTOR DOSIMETRY, VIENNA, 13-17 NOVEMBER 1978

May 1979

IAEA NUCLEAR DATA SECTION, KÄRNTNER RING 11, A-1010 VIENNA

Reproduced by the IAEA in Austria

May 1979

79-3204

INDC(NDS)-103/M

PROCEEDINGS OF THE ADVISORY GROUP MEETING ON NUCLEAR DATA FOR REACTOR DOSIMETRY

VIENNA, 13-17 NOVEMBER 1978

May 1979

FOREWORD

The Advisory Group Meeting on Nuclear Data for Reactor Dosimetry was convened by the IAEA Nuclear Data Section at IAEA Headquarters in Vienna, Austria, from 13-17 November 1978. The meeting was attended by 20 representatives from 10 Member States and 2 international organizations.

The primary objective of this meeting was to finalize the details for the creation of a new international file of evaluated neutron cross section data for reactor dosimetry applications, and to establish a procedure for the testing and adjustment of these data.

The conclusions and recommendations of this meeting are contained in three separate reports produced at the meeting:

- The General Guidelines for the Creation of the International Reactor Dosimetry File, consisting of a general set of recommendations on the creation, maintenance and up-keep of the basic reactor dosimetry data file, which contains the evaluated energy dependent cross section data and their uncertainties,

- The Report of the Working Group on Benchmark Fields and Integral Data, recommending the creation of a complementary benchmark data file containing data on reference benchmark fields and recommended evaluated integral cross sections measured in these fields, and

- The Report of the Working Group on Data Testing, Spectrum Unfolding and Data Adjustment, which recommends the methodology to be used in testing the data contained in the reactor dosimetry (differential) data file, in unfolding neutron flux density spectra, and in performing data adjustments on the basis of information from integral experiments.

The Summary Report of this meeting including the full text of the conclusions and recommendations has been issued as INDC report INDC(NDS)-100/M in January 1979.

These proceedings contain the papers presented at the meeting. Papers which had been or were to be published elsewhere have not been included in these proceedings.

TABLE OF CONTENT

AG/160-1 Status of the Dosimetry File for ENDF/B-V. B.A. Magurno 1

AG/160-2 Evaluations of the Cross Sections for the Reactions $^{24}Mg(n,p)^{24}Na$, $^{64}Zn(n,p)^{64}Cu$, $^{63}Cu(n,2n)^{62}Cu$ and $^{90}Zr(n,2n^{89}Zr$, S. Tagesen, H. Vonach, B. Strohmaier. (Not included in this report; this paper is to be published in Physics Data Nr. 13-1-1979, by the Fachinformationszentrum Energie, Physik, Mathematik GMBH Karlsruhe)

AG/160-3 Measurement of the Activation Cross Section of the Reaction $^{93}Nb(n,n')^{93m}Nb$ for 0-25 MeV Neutrons. M.F. Hegedüs, M.W. Guinan, J.R. Meadows, N.F. Peek and L.R. Greenwood 23

AG/160-4 The Analysis of the $^{59}Co(n,p)$ and $^{54}Fe(n,\alpha)$ Cross Sections for their Use in Reactor Dosimetry. G. Vasiliu, S. Mateescu 26

AG/160-5 The Measurements and Evaluation of Fast Neutron Cross Section Data for Reactor Dosimetry. A. Marcinkowski 40

AG/160-6 Status of the $^{45}Sc(n,2n)^{44}Sc$ Reaction. K. Okamoto. (Not included in this report; this paper is to be incorporated in a forthcoming BNL report.)

AG/160-7 Summary Remarks and Recommended Reactions for an International Data File for Dosimetry Applications for LWR, FBR, and MFR Reactor Research, Development and Testing Programmes. W.N. McElroy, E.P. Lippincott, J.A. Grundl, A. Fabry, R. Dierckx and U. Farinelli 50

AG/160-8 The Data Covariance Files for ENDF/B-V. F.C. Perey. (Not included in this report; published as ORNL/TM-5938 (July 1977)

AG/160-9 Neutron Fields Available at the National Physical Laboratory and the Need for Low Energy Neutron Standards. E.J. Axton, A.G. Bardell 59

AG/160-10 Fast Neutron Standard Fields at the Accelerators of the PTB. M. Cosack, H. Lesiecki, H. Klein and R. Jahr 77

AG/160-11 Accelerator-based Dosimetry Benchmarks. R. Dierckx 89

AG/160-12A Iteration Acceleration in the ITER-2 Unfolding Code. M. Panko and M. Najzer 98

AG/160-12B Multispectrometer Unfolding by the ITER Code. B. Glumac and M. Najzer 117

AG/160-13A Progress Report on the IAEA Programme on the Standardization of Reactor Dosimetry Measurements. C. Ertek, B. Cross and V. Chernyshev 131

AG/160-13B Influence of Cross-Section Structure on Unfolded Neutron Spectra. C. Ertek, M.F. Vlasov, B. Cross, P.M. Smith 149

AG/160-13C Errors Involved in the Folding and the Unfolding of Neutron Spectrum by SAND-II. C. Ertek. (Not included in this report, paper published separately as IAEA report IAEA/RL/51, August 1978).

AG/160-13D Seibersdorf-Helsinki Intercomparison of Neutron Flux Density Spectra by using the SAND-II and the LOUHI Unfolding Programmes. C. Ertek. (Not included in this report; paper published separately as IAEA report IAEA/RL/52, September 1978).

AG/160-14 Integral Cross Section Measurements in the Reference Field NISUS. G.D. Burholt, G.P. Dixon, S. Ghanbarzadeh, M. Rahbar and J.G. Williams 157

AG/160-15 Average Cross Sections in the Neutron Benchmark Field of Cf-252. A Status Report. W. Mannhart. (Not included in this report; this paper is published as report PTB-FMRB-72 (April 1978) by the Physikalisch-Technische Bundesanstalt, Braunschweig).

AG/160-16 Integral Cross Section Measurements in the Cf-252 Neutron Spectrum. Z. Dezsoe, J. Csikai 176

AG/160-17 On the Consistency between Integral Differential Cross Section Data. W.L. Zijp 187

AG/160-18 Attempts at the Adjustment of Detector Cross Sections. A.K. McCracken and A. Packwood 220

AG/160-19 Review of Advanced Methods for Data Adjustments. A. Gandini 234

STATUS OF THE DOSIMETRY FILE FOR ENDF/B-V*

Benjamin A. Magurno

National Nuclear Data Center
Brookhaven National Laboratory
Upton, New York 11973
U.S.A.

INTRODUCTION

Since the new Dosimetry File will not be ready for distribution until February-March, 1979, this presentation is submitted as a progress report and/or an extension of a paper[1] read at a previous conference[2] where the schedule for release and dissemination of the library was reported. The dates of release and distribution were predicated on the use of pre-determined standards (March, 1976)[3] for use with the new Dosimetry File. Subsequently, one of the most important standards, i.e. ^{235}U (n,f) has been re-evaluated, causing the delay that is responsible for the above mentioned release date.

STATUS OF THE DOSIMETRY FILE

Table I lists the isotopes submitted for the ENDF/B-V Dosimetry File, the laboratory responsible, the current status of the isotopes and whether or not a Covariance File is presently available. The only unfinished evaluations on the list are ^{6}Li (n, total He), ^{10}B (n, total He) and ^{45}Sc (n,γ). These evaluations are in progress and are expected by mid-December of this year.

The ^{27}Al (n,p) and the ^{27}Al (n,α) cross sections are from the General Purpose File and are the same as the Version-IV cross sections with the addition of the Covariance Files.

^{32}S (n,p) is also from the General Purpose File. The evaluation as a whole was adopted from the "Evaluated Nuclear Data Library" (ENDL) of R. Howerton, Lawrence Livermore Laboratory (LLL).

---

* Work carried out under the auspices of the U.S. Department of Energy.

^{23}Na (n,γ), Mn (n,2n) (curve and explanations included in the previous conference[1] for this isotope), ^{59}Co (n,2n), ^{59}Co (n,γ), ^{59}Co (n,α), and ^{237}Np (n,f) are taken directly from the General Purpose File.

^{232}Th (n,γ) and ^{238}U (n,γ) have minor adjustments necessary but in essence are ready. The ^{232}Th (n,f) and ^{238}U (n,f) both have ^{235}U (n,f) dependence and the cross sections are being verified or re-evaluated at this time.

^{239}Pu (n,f) is being re-evaluated using a new set of fission ratios.

The ^{197}Au (n,γ) cross section was amply described by Mughabghab in Appendix I of the previous description of the file.[1] There are minor changes being made in this isotope due to the change in ^{235}U but these changes are of little significance to the Dosimetry File.

The ^{235}U (n,f) cross section as a standard was set in March, 1976. In June of that year, however, at the Argonne Specialists' Meeting,[4] a 5% scatter was noted in the cross section between 0.25 MeV and 0.4 MeV. The need for new measurements was suggested. At a Standards Meeting[5] in March, 1977, Poenitz called for a re-evaluation of ^{235}U (n,f) because he felt that the existing evaluation was not a good representation of the current experimental data base.

Following that meeting, the measurements of ^{235}U (n,f) up to the summer of 1978 were reviewed at a special workshop[7] held at the National Bureau of Standards and led by C.D. Bowman with the participation of several U.S. laboratories.

The Specialists Meeting and the Standards Meeting led to the conclusion that the ^{235}U (n,f) cross section that had previously been proposed for ENDF/B-V should be re-evaluated and all evaluations dependent on ^{235}U (n,f) as a standard would also be required to change.

A final discussion group met at Brookhaven on September 11-12, 1978. This group recommended that W. Poenitz, using methods discussed[5] and all data available since the other evaluation, re-evaluate ^{235}U (n,f). Figure 1 shows the data in the 100 keV-700 keV range. The new Poenitz data[8] and a single point by Zhuravlev[9] are superimposed on the older data that was used as input for the original evaluation. The Poenitz data is in excellent agreement with Szabo data[10] and the University of Michigan data.[11] The other data shown in the Figure are the older Poenitz numbers,[12] Wasson,[13] Czirr,[14] and White.[15] At higher energies (not shown) the new Szabo data[10] in the 2-5.5 MeV energy region is lower than

Czirr[16] and Barton[17] by $\sim$ 6% but again agrees well with the Poenitz measurements. Neither of these sets was available at the time of the original ENDF/B-V ^{235}U (n,f) evaluation.

The Poenitz re-evaluation was submitted to the Normalization and Standards Subcommittee of the Cross Section Evaluation Working Group (CSEWG) on October 24, 1978. The evaluation is being documented.[18] and will be published in the near future as an Argonne report. The evaluation is an extension of Poenitz's previous work and "uses all the available data, not just those most recently measured". The normalization of the fission data was readjusted in part by the subcommittee but was within 1.5% of that proposed by Poenitz. The subcommittee's final choice of the options presented will appear in Poenitz's document. A comparison between the new evaluation and that used in Version IV is shown in Figures 2-5. Figures 2 and 3 show the curves between 100 to 700 keV and 1 to 3 MeV and the similarities between the two evaluations. Figures 4 and 5 from 1 MeV to 6 MeV and 6 MeV to 20 MeV detail the comparisons of the rest of the "standard" fission cross section. At energies greater than 7 MeV the Version V evaluation is generally lower than that of Version IV.

Table II lists the ^{235}U (n,f) "standard" cross section in an ENDF-like format. Columns 1, 3 and 5 are energies in eV and columns 2, 4 and 6 are the fission cross sections in Barns.

ENDF/B-V will present a different approach to the fission spectrum, i.e. an energy dependent Watt Spectrum as opposed to previous versions which were Maxwellian at a defined nuclear temperature. The procedure for Version V is to calculate $\bar{E}$ of ^{239}Pu using the parameters a and b given in the ^{239}Pu file. The relation observed by Adams, i.e. $\bar{E}_{239}/\bar{E}_{235} = 1.04$ is then utilized to deduce $\bar{E}_{235}$. Then b at low energies is considered constant (10^{-5} eV - 1.5×10^{6} eV) and calculated from $\bar{E}_{235}$ and the Adams assumed value, a = 0.998. A small energy dependence is then built into a and b to produce the correct $\bar{E}_{235}$.

The Dosimetry File contains reaction cross sections whose isotopes were evaluated as part of the job of evaluating elemental cross sections for the General Purpose File. These include the isotopes of Nickel, isotopes of Titanium, isotopes of Iron and the isotopes of Copper. Nickel has been covered in Appendix II of the previous paper.[1] Titanium was also covered, but in a sketchy

manner and is worth a note here. ^{46}Ti (n,p) and ^{47}Ti (n,p) have minor changes in evaluation for Version V and the discrepancies between integral and differential data will not change significantly. ^{48}Ti has had a large change in cross sections below 12 MeV. Figure 6 shows the Version V evaluation compared to that of Version IV. The Version V evaluation is documented as ANL/NDM-27.[19]

^{54}Fe (n,p) shown in Figure 7 is the same as Version IV, except that the cross section below 2 MeV is a Hauser-Feshbach calculation, normalized to low energy data (i.e. Data < 3 MeV). The change as it appears in the Figure between 6 and 12 MeV is the data of Smith and Meadows.[20] Although it doesn't show in the threshold area on Figure 8, there is a 10% reduction in the ^{56}Fe (n,p) cross section between threshold and 6 MeV. There is a 2 to 3% reduction between 6 and 10 MeV. Smith and Meadows[21] data (4 to 10 MeV) were relative to ^{238}U (n,f) and were renormalized for Version V. These changes were reflected in a $\sim$ 3% effect in the fission spectrum average. The final value, of course, is dependent on the final ^{238}U evaluation. ^{58}Fe (n,γ) has no change in the fast region from Version IV to Version V.

Figure 9 shows the high energy end of ^{63}Cu (n,γ) cross section. The smooth cross section, i.e. the end of the resonance region, starts at 50 keV. For the cross sections above 50 keV, Fu has adopted the evaluation of Drake and Fricke.[23] Figure 10, ^{63}Cu (n,α) is higher for Version V and is keyed to the 15 MeV value of Vonach[24], i.e. $\sigma_{n\alpha}$ (15 MeV) = 39.0 $\pm$ 0.8 mb. The threshold region, i.e. below 5.5 MeV, is an extrapolation of the evaluation guided by a Hauser Feshbach calculation.[21] This is in essence renormalizing the cross section curve by 1.17. Two high points of Paulsen[26] which were rejected by Alter[27] are restored having the effect of an additional 8% increase in the cross section from 10-11 MeV.

Figure 11 shows the 65Cu (n,2n) which, for the most part, is the Version IV evaluation. The difference lies in the addition of the Mannhart data[28] which is 10% lower than the Version IV curve. The weight given the Mannhart data by Fu is somewhat "arbitrary" but results in lowering the Version V evaluation $\sim$ 5% between 12-18 MeV.

A comparison of the fast cross section of ^{115m}In (n,γ) for Versions IV and V are shown in Figures 12a and 12b. Schmittroth renormalized the Grench values to Version V Au standard cross section and re-evaluated the cross sections in

the 14 MeV energy region. All experimental values were then used as input in a nuclear model code. The method used is documented[29] and will be available shortly. ^{115}In (n,n') to the 4.486 H isomer for Version IV and V are compared on Figure 13. This evaluation is based entirely on experimental differential data. The significant differences between Versions IV and V are that the new evaluation takes cognizance of structural detail in the excitation function and predicts larger cross sections in the regions from 2 to 3 and 4 to 6 MeV. This evaluation is documented[30] and available from Argonne National Laboratory (ANL).

^{127}I (n,2n) evaluated for Version IV will be carried over to Version V. The only data not included in the original evaluation is that of Santry.[31] The Santry data is measured from threshold to 19.6 MeV. The evaluation and the Santry data are compatible up to 11 MeV. Since this is the only data in that energy region, the evaluation remains unchanged. From 12-15 MeV the Santry data averaged into the other measurements leaves the evaluation unchanged. From 15-20 MeV the evaluation is lower than the experimental data would now indicate, but the evaluator feels scattering might tend to render the measured cross sections too high and, therefore, leaves the evaluated cross sections unchanged.

SUMMARY

The ENDF/B-V Dosimetry File is nearing completion with a target release date of March, 1979. The renormalization problems caused by the change in ^{235}U (n,f) standard cross section to the Dosimetry File have been overcome. The addition of Covariance Files to the Dosimetry reactions fulfills one of the major recommendations of the last meeting.[2]

ACKNOWLDEGEMENTS

I would like to thank all the evaluators who have contributed to the Dosimetry File, the members of the ILRR program, the members of the SAFE subcommittee and the Normalizatiwn and Standards Subcommittee both of CSEWG for their discussions, criticism and general support of the Dosimetry File. I would also like to thank the IAEA and M. Vlasov in particular for the support of this presentation.

REFERENCES

1. B.A. Magurno, ENDF/B Dosimetry File for Version V, Reference 2, p. 375.
2. Neutron Cross Sections for Reactor Dosimetry, IAEA-208, Volumes I and II, Vienna, November 15-19, (1976).
3. Task Force Meeting of CSEWG, March (1976).
4. Proc. at the NEANDC/NEACRP Specialists Meeting on Fast Neutron Fission Cross Sections of U-233, U-235, U-238 and Pu-239, ANL-76-90, Poenitz and Smith (editors).
5. Neutron Standards and Applications, Proc. of a Symposium, NBS Special Publication 493, (1977).
6. W.P. Poenitz, IBID, p. 261 (1977).
7. ^{235}U Coordination Workshop, National Bureau of Standards, July 11-12, 1978.
8. W.P. Poenitz, Nuc. Sci. and Eng. 64, 894 (1977).
9. Zhuravlev, et al., Proc. Int. Conf. on the Interactions of Neutrons with Nuclei, Lowell 2, 1417 (1976).
10. I. Szabo and G.P. Marquette ANL-76-90, p. 208 (1976).
11. Davis et al., IBID, p. 225 (1976).
12. W. Poenitz, Nuc. Sci. and Eng. 53, 370, (1974).
13. O.A. Wasson, ANL-76-90, p. 183 (1976).
14. J.B. Czirr, Nuc. Sci. and Eng., 60, 383, (1976).
15. P.H. White, Jour. Nuc. Energy, 19A/B, 325, (1965).
16. J.B. Czirr and G.S. Sidhu, Nuc. Sci. and Eng., 57, 18 (1975).
17. Barton, et al., Nuc. Sci. and Eng., 60, 369 (1976).
18. W.P. Poenitz, ANL/NDM 45, (1978) to be published.
19. J.M. Adams, Inelastic Scattering and Fission Neutron Spectra, AERE-R 8636 (1977).
20. Philis, et al., ANL/NDM 27 (1977).

21. D.L. Smith and J.W. Meadows, ANL/NDM 10 (1975).

22. D.L. Smith and J.W. Meadows, Nuc. Sci. and Eng. 58, 314 (1975).

23. M.K. Drake and M.P. Fricke, SAI-74-535-LJ (1974).

24. H. Vonach, Private Communication to M.F. Vlasov (1976).

25. C.Y. Fu and F.G. Perey, Jour. Nuc. Material 61, 153 (1976).

26. A. Paulsen and H. Liskien, Nukleonik 10, 91 (1976).

27. H. Alter Cu-63 Reactions for ENDF/B-IV, BNL-NCS-50446 (1975).

28. W. Mannhart and H. Vonach, Z. Phys. A272, 279 (1975).

29. F. Schmittroth, Varied Applications of a New Maximum Likelihood Code RSIC Seminar-Workshop, Theory and Applications of Sensitivity and Uncertainty Analysis, August (1978), to be published.

30. D.L. Smith, ANL/NDM-26, December, (1976).

31. D.C. Santry, PR-CMA-24, 13 (1973).

ISOTOPES SUBMITTED TO DOSIMETRY FILE FOR VERSION V

ISOTOPE/REACTION	LAB	STATUS	COVARIANCE FILE
^{6}Li (n, total He)	LASL	IP	
^{10}B (n, total He)	LASL	IP	
^{23}Na (n,γ)	ORNL	R (G.P.)	✓
^{27}Al (n,p)	LASL	R (G.P.)	✓
^{27}Al (n,α)	LASL	R (G.P.)	✓
^{32}S (n,p)	LLL	R (G.P.)	
^{45}Sc (n,γ)	BNL	IP	✓
^{46}Ti (n,p)	ANL	R	✓
^{47}Ti (n,p)(n,np)	ANL	R	✓
^{48}Ti (n,p)(n,np)	ANL	R	✓
^{55}Mn (n,2n)	BNL	R (G.P.)	✓
^{54}Fe (n,p)	HEDL	R	✓
^{56}Fe (n,p)	ORNL	R	✓
^{58}Fe (n,γ)	HEDL	R	✓
^{59}Co (n,2n)(n,γ)(n,α)	BNL	R (G.P.)	✓
^{58}Ni (n,2n)(μ,p)	BNL	R	✓
^{60}Ni (n,2n)	BNL	R	✓
^{63}Cu (n,γ)(n,α)	ORNL	R	✓
^{65}Cu (n, 2n)	ORNL	R	✓
^{115}In (n,n')	ANL	R	✓
^{115}In (n,γ)	HEDL	R	✓
^{127}I (n,2n)	STANFORD	R	✓
^{197}Au (n,γ)	BNL	R (G.P.)	✓
^{232}Th (n,f)(n,γ)	BNL	R*(G.P.)	✓
^{235}U (n,f)	BNL	R (G.P.)	✓
^{238}U (n,f)(n,γ)	ANL	R*(G.P.)	✓
^{237}Np (n,f)	LASL	R (G.P.)	✓
^{239}Pu (n,f)	GE	R*(G.P.)	✓

R = Received

G.P.= General Purpose File

✓ = Has or will have covariance file

IP = In progress

R* = Received, but may need final adjustment.

TABLE I

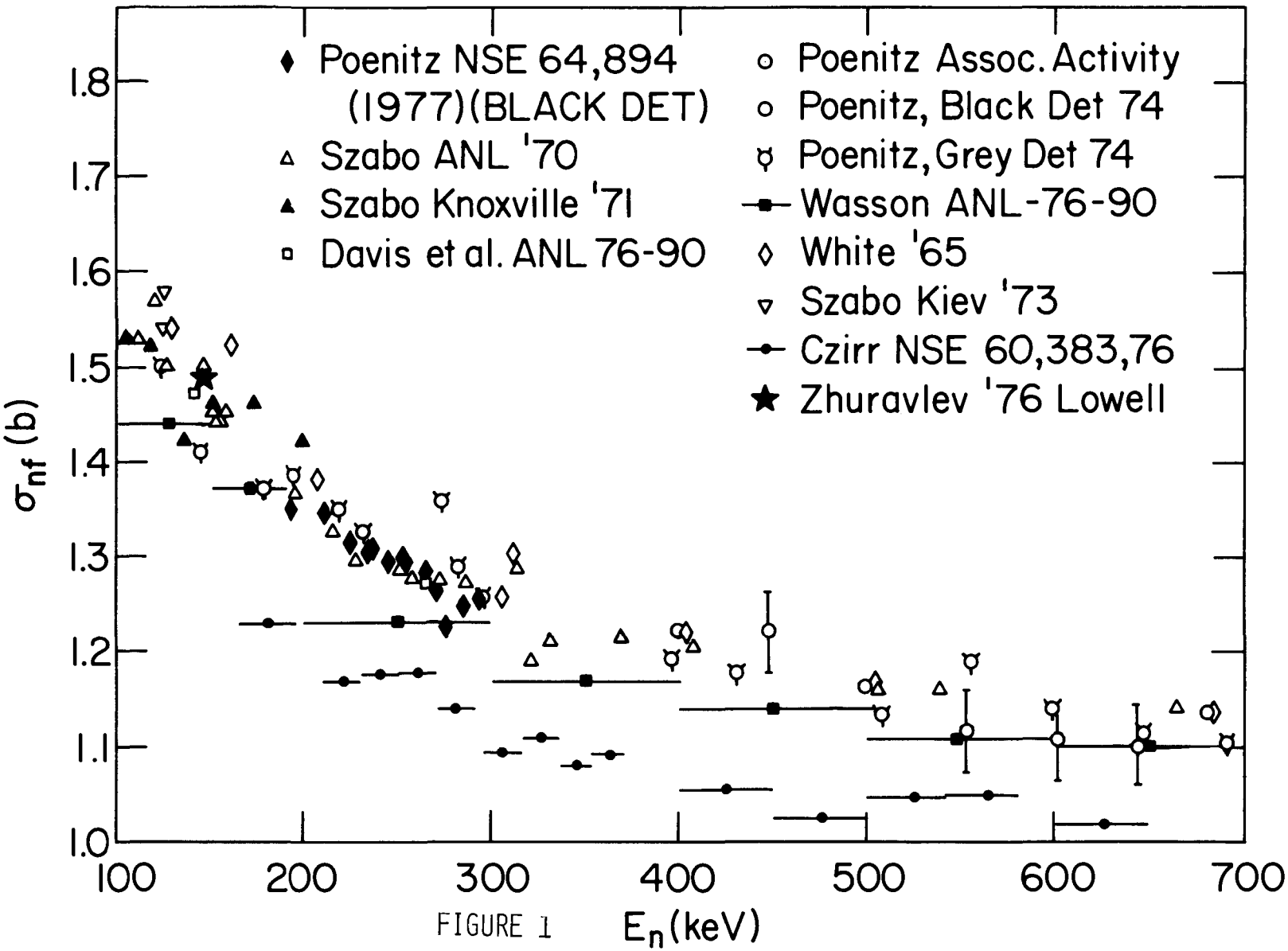
Poenitz NSE 64,894 (1977)(BLACK DET)
Szabo ANL '70
Szabo Knoxville '71
Davis et al. ANL 76-90
Poenitz Assoc. Activity
Poenitz, Black Det 74
Poenitz, Grey Det 74
Wasson ANL-76-90
White '65
Szabo Kiev '73
Czirr NSE 60,383,76
Zhuravlev '76 Lowell
σ_{nf} (b)
1.8
1.7
1.6
1.5
1.4
1.3
1.2
1.1
1.0
100
200
300
400
500
600
700
E_n(keV)

FIGURE 1

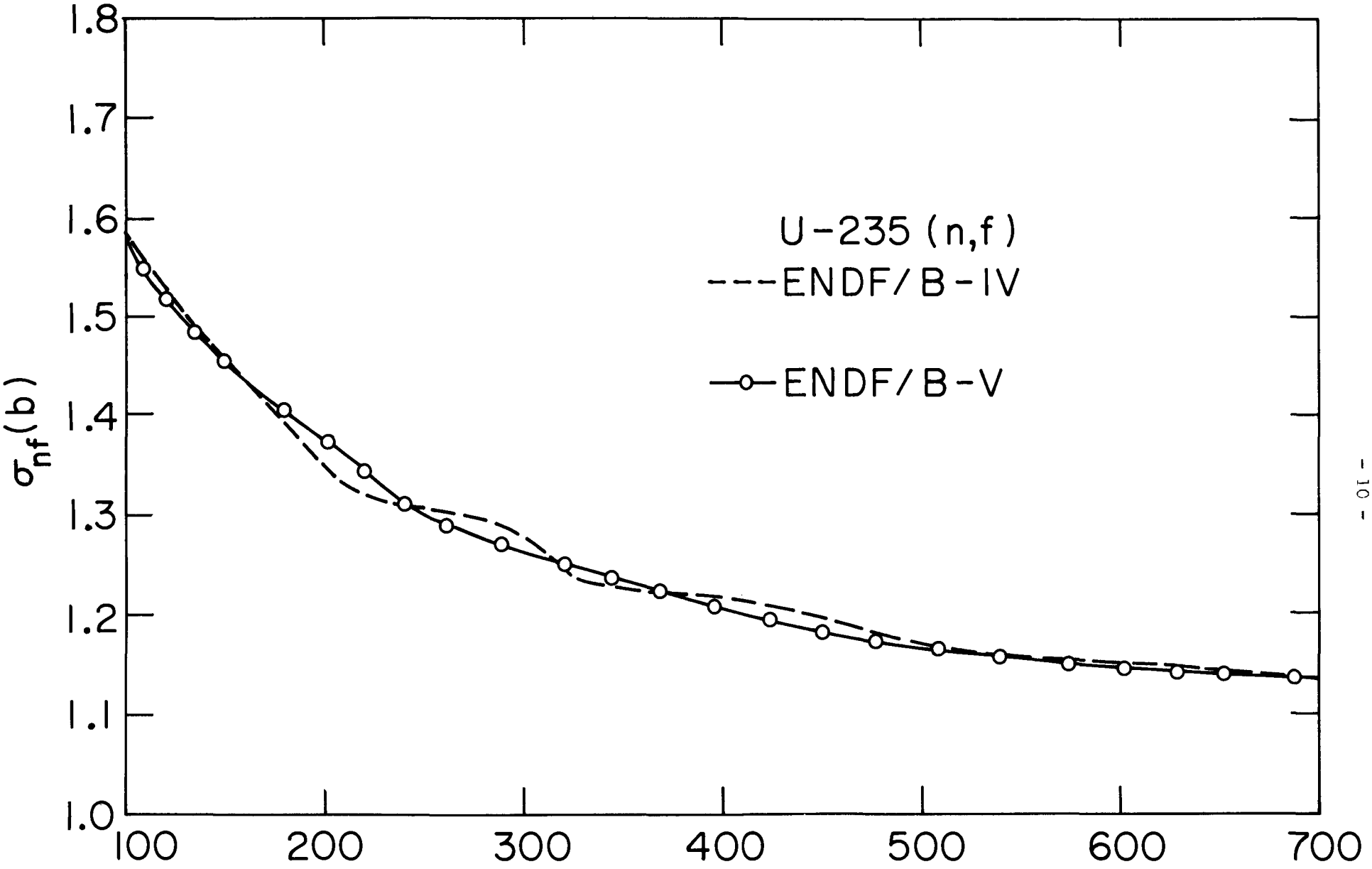
U-235 (n,f)
---ENDF/B-IV
—o—ENDF/B-V
σ_{nf}(b)
1.8
1.7
1.6
1.5
1.4
1.3
1.2
1.1
1.0
100
200
300
400
500
600
700
E_n (keV)

FIGURE 2

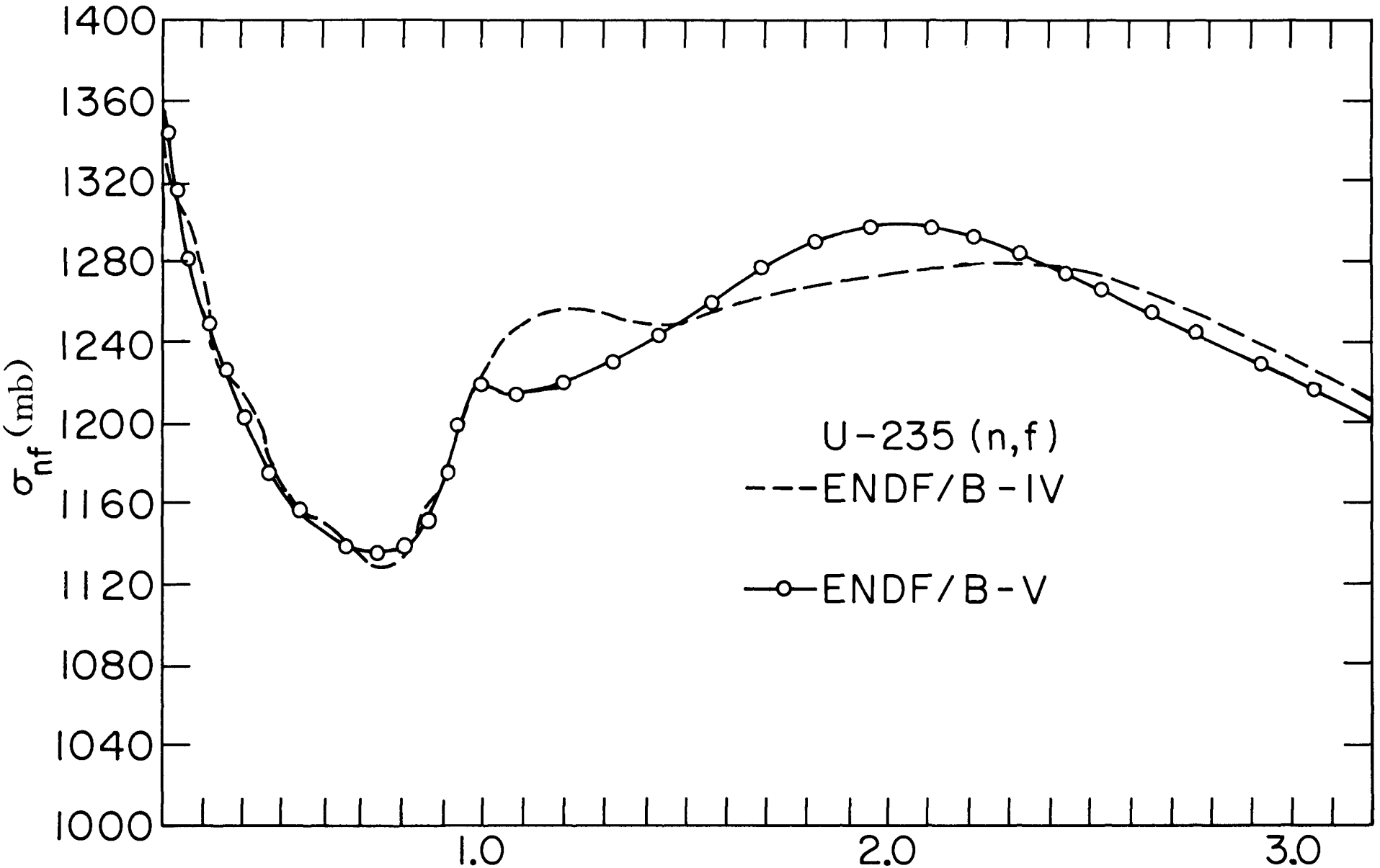
1400
1360
1320
1280
1240
1200
1160
1120
1080
1040
1000
σ_{nf} (mb)
1.0
2.0
3.0
E_n (MeV)
U-235 (n,f)
---ENDF/B-IV
—o—ENDF/B-V

FIGURE 3

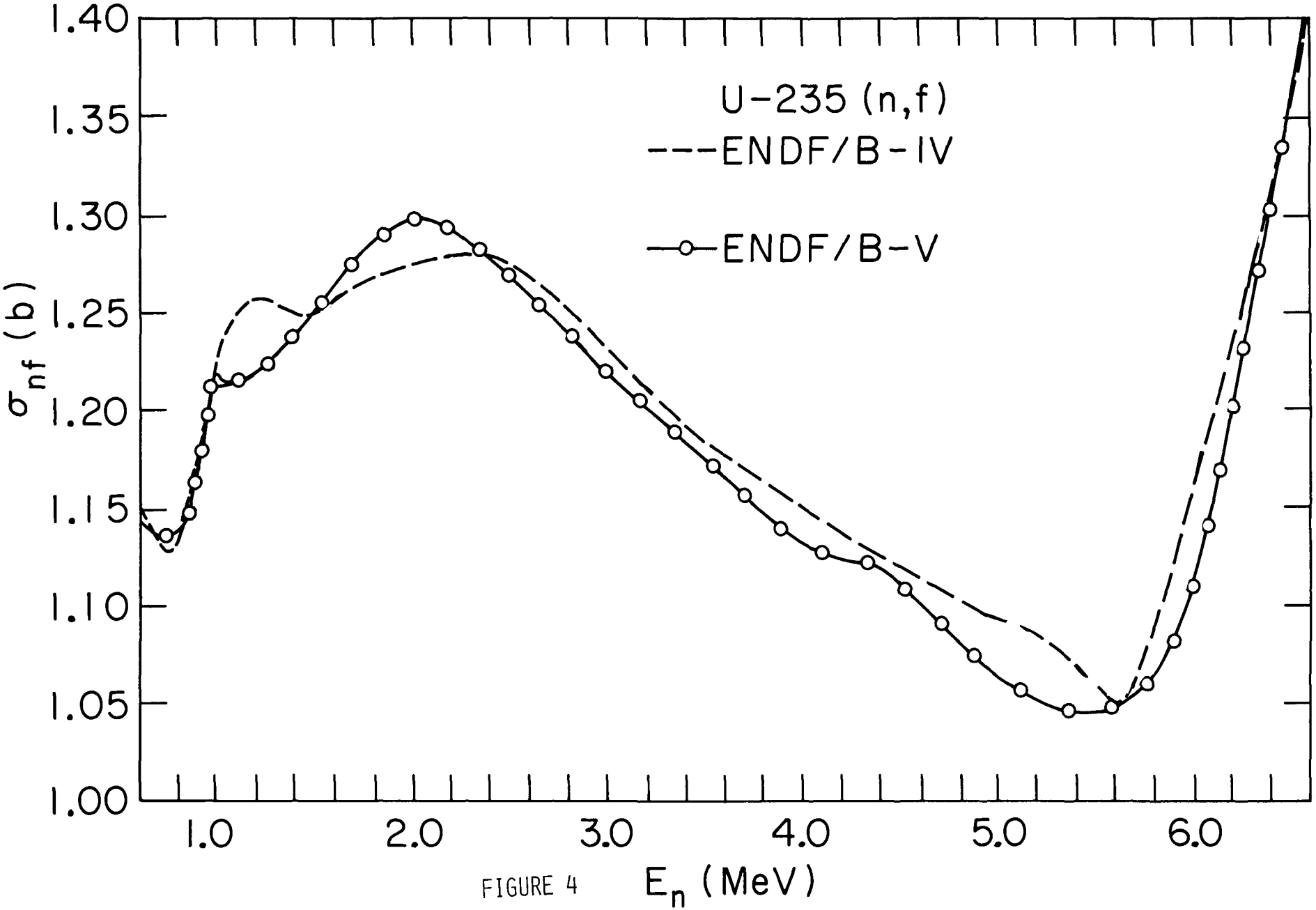
U-235 (n,f)
---ENDF/B-IV
—o—ENDF/B-V
σ_{nf} (b)
1.40
1.35
1.30
1.25
1.20
1.15
1.10
1.05
1.00
1.0
2.0
3.0
4.0
5.0
6.0
E_n (MeV)

FIGURE 4

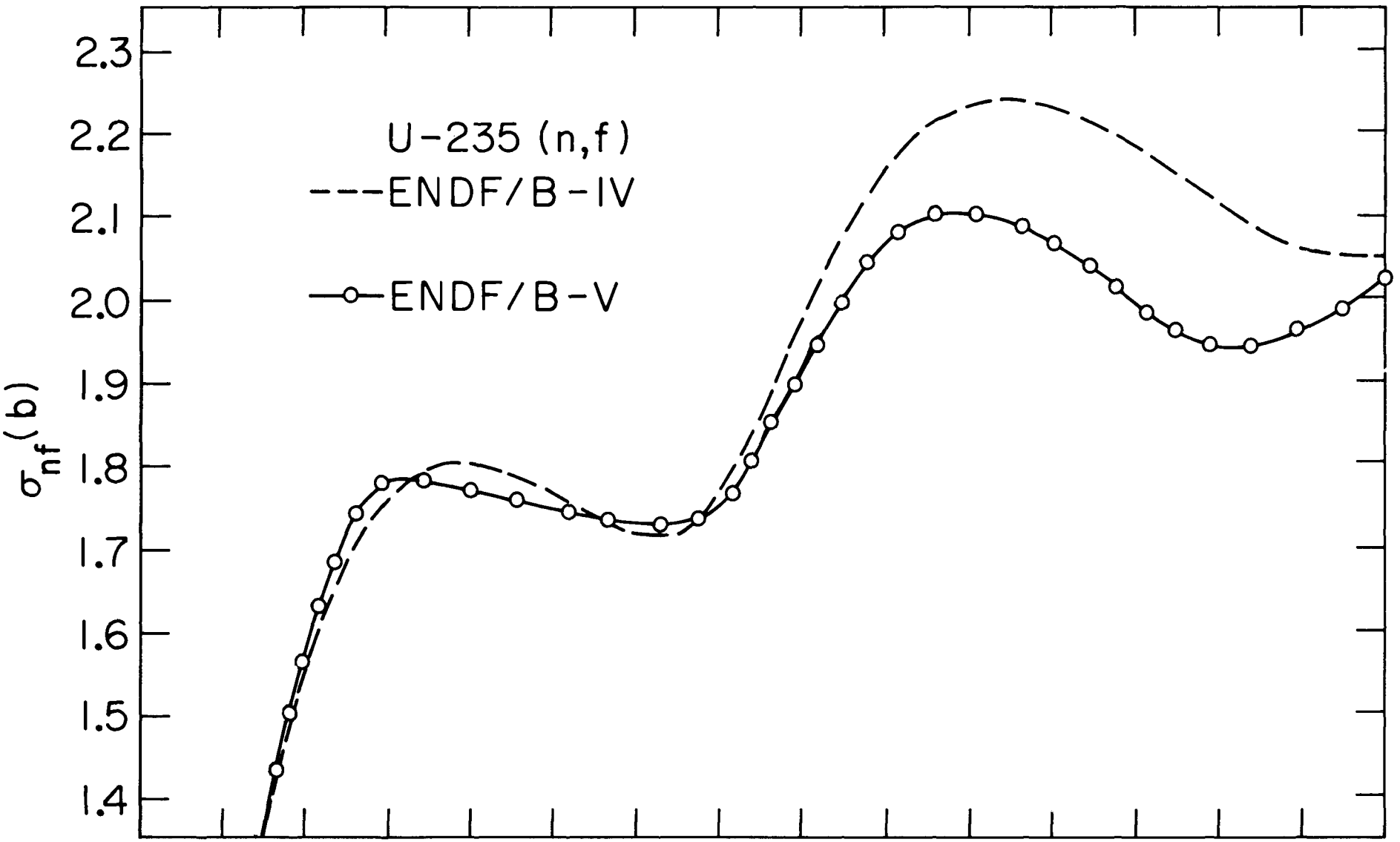
U-235 (n,f)
---ENDF/B-IV
—o—ENDF/B-V
σ_{nf} (b)
2.3
2.2
2.1
2.0
1.9
1.8
1.7
1.6
1.5
1.4
6
7
8
9
10
11
12
13
14
15
16
17
18
19
20
E_n (MeV)

FIGURE 5

9.2235	+ 4	2.33025	+ 2		0		99		0			05036	3	18
0.0	+ 0	1.9402	+ 8		0		0		1			1125036	3	18
	112		2									5036	3	18
9.99	+ 4	1.59924	+ 0	1.0	+ 5	1.581	+ 0	1.03	+ 5	1.572	+	05036	3	18
1.2	+ 5	1.520	+ 0	1.4	+ 5	1.476	+ 0	1.5	+ 5	1.457	+	05036	3	18
1.6	+ 5	1.440	+ 0	1.8	+ 5	1.408	+ 0	2.0	+ 5	1.377	+	05036	3	18
2.2	+ 5	1.343	+ 0	2.4	+ 5	1.314	+ 0	2.5	+ 5	1.302	+	05036	3	18
2.6	+ 5	1.291	+ 0	2.8	+ 5	1.272	+ 0	3.0	+ 5	1.262	+	05036	3	18
3.25	+ 5	1.249	+ 0	3.5	+ 5	1.235	+ 0	3.75	+ 5	1.221	+	05036	3	18
4.0	+ 5	1.209	+ 0	4.25	+ 5	1.196	+ 0	4.5	+ 5	1.184	+	05036	3	18
4.75	+ 5	1.174	+ 0	5.0	+ 5	1.167	+ 0	5.4	+ 5	1.157	+	05036	3	18
5.7	+ 5	1.151	+ 0	6.0	+ 5	1.145	+ 0	6.5	+ 5	1.140	+	05036	3	18
7.0	+ 5	1.137	+ 0	7.5	+ 5	1.137	+ 0	7.8	+ 5	1.137	+	05036	3	18
8.0	+ 5	1.139	+ 0	8.3	+ 5	1.142	+ 0	8.5	+ 5	1.147	+	05036	3	18
9.0	+ 5	1.168	+ 0	9.4	+ 5	1.195	+ 0	9.6	+ 5	1.207	+	05036	3	18
9.8	+ 5	1.217	+ 0	1.0	+ 6	1.220	+ 0	1.05	+ 6	1.215	+	05036	3	18
1.1	+ 6	1.215	+ 0	1.15	+ 6	1.216	+ 0	1.2	+ 6	1.220	+	05036	3	18
1.25	+ 6	1.223	+ 0	1.4	+ 6	1.239	+ 0	1.6	+ 6	1.264	+	05036	3	18
1.7	+ 6	1.278	+ 0	1.8	+ 6	1.288	+ 0	1.9	+ 6	1.294	+	05036	3	18
2.0	+ 6	1.298	+ 0	2.1	+ 6	1.297	+ 0	2.3	+ 6	1.286	+	05036	3	18
2.4	+ 6	1.278	+ 0	2.6	+ 6	1.259	+ 0	2.8	+ 6	1.240	+	05036	3	18
3.0	+ 6	1.219	+ 0	3.2	+ 6	1.201	+ 0	3.4	+ 6	1.184	+	05036	3	18
3.6	+ 6	1.165	+ 0	3.8	+ 6	1.148	+ 0	4.0	+ 6	1.132	+	05036	3	18
4.2	+ 6	1.125	+ 0	4.4	+ 6	1.120	+ 0	4.5	+ 6	1.111	+	05036	3	18
4.7	+ 6	1.092	+ 0	5.0	+ 6	1.064	+ 0	5.2	+ 6	1.052	+	05036	3	18
5.3	+ 6	1.048	+ 0	5.4	+ 6	1.047	+ 0	5.5	+ 6	1.047	+	05036	3	18
5.6	+ 6	1.049	+ 0	5.64	+ 6	1.051	+ 0	5.7	+ 6	1.055	+	05036	3	18
5.8	+ 6	1.066	+ 0	5.9	+ 6	1.083	+ 0	6.0	+ 6	1.112	+	05036	3	18
6.2	+ 6	1.207	+ 0	6.4	+ 6	1.306	+ 0	6.5	+ 6	1.364	+	05036	3	18
6.7	+ 6	1.456	+ 0	7.0	+ 6	1.553	+ 0	7.25	+ 6	1.650	+	05036	3	18
7.5	+ 6	1.719	+ 0	7.75	+ 6	1.763	+ 0	8.0	+ 6	1.782	+	05036	3	18
8.15	+ 6	1.784	+ 0	8.25	+ 6	1.784	+ 0	8.5	+ 6	1.782	+	05036	3	18
9.0	+ 6	1.772	+ 0	9.5	+ 6	1.762	+ 0	1.0	+ 7	1.749	+	05036	3	18
1.05	+ 7	1.738	+ 0	1.1	+ 7	1.732	+ 0	1.15	+ 7	1.732	+	05036	3	18
1.2	+ 7	1.748	+ 0	1.21991	+ 7	1.771	+ 0	1.22	+ 7	1.771	+	05036	3	18
1.25	+ 7	1.826	+ 0	1.3	+ 7	1.915	+ 0	1.35	+ 7	1.998	+	05036	3	18
1.4	+ 7	2.068	+ 0	1.45	+ 7	2.099	+ 0	1.5	+ 7	2.103	+	05036	3	18
1.55	+ 7	2.093	+ 0	1.6	+ 7	2.068	+ 0	1.65	+ 7	2.036	+	05036	3	18
1.7	+ 7	1.986	+ 0	1.75	+ 7	1.960	+ 0	1.8	+ 7	1.939	+	05036	3	18
1.85	+ 7	1.945	+ 0	1.9	+ 7	1.966	+ 0	1.95	+ 7	1.990	+	05036	3	18
2.0	+ 7	2.024	+ 0									5036	3	18
												5036	3	0
												5036	0	0
												0	0	0
												-1	0	0

TABLE II

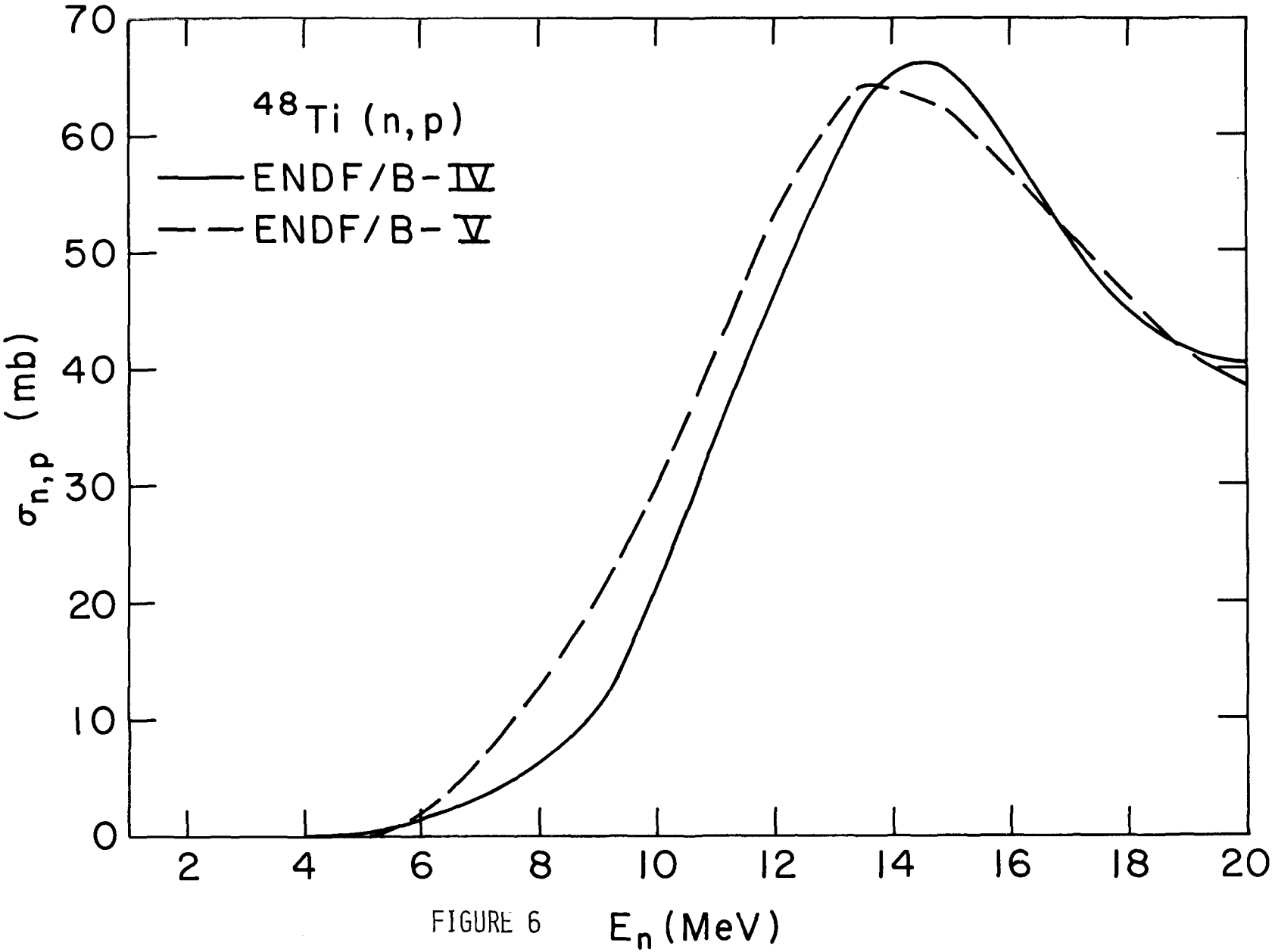
70
60
50
40
30
20
10
0
$\sigma_{n,p}$ (mb)
^{48}Ti (n,p)
ENDF/B-IV
ENDF/B-V
2
4
6
8
10
12
14
16
18
20
E_n (MeV)

FIGURE 6

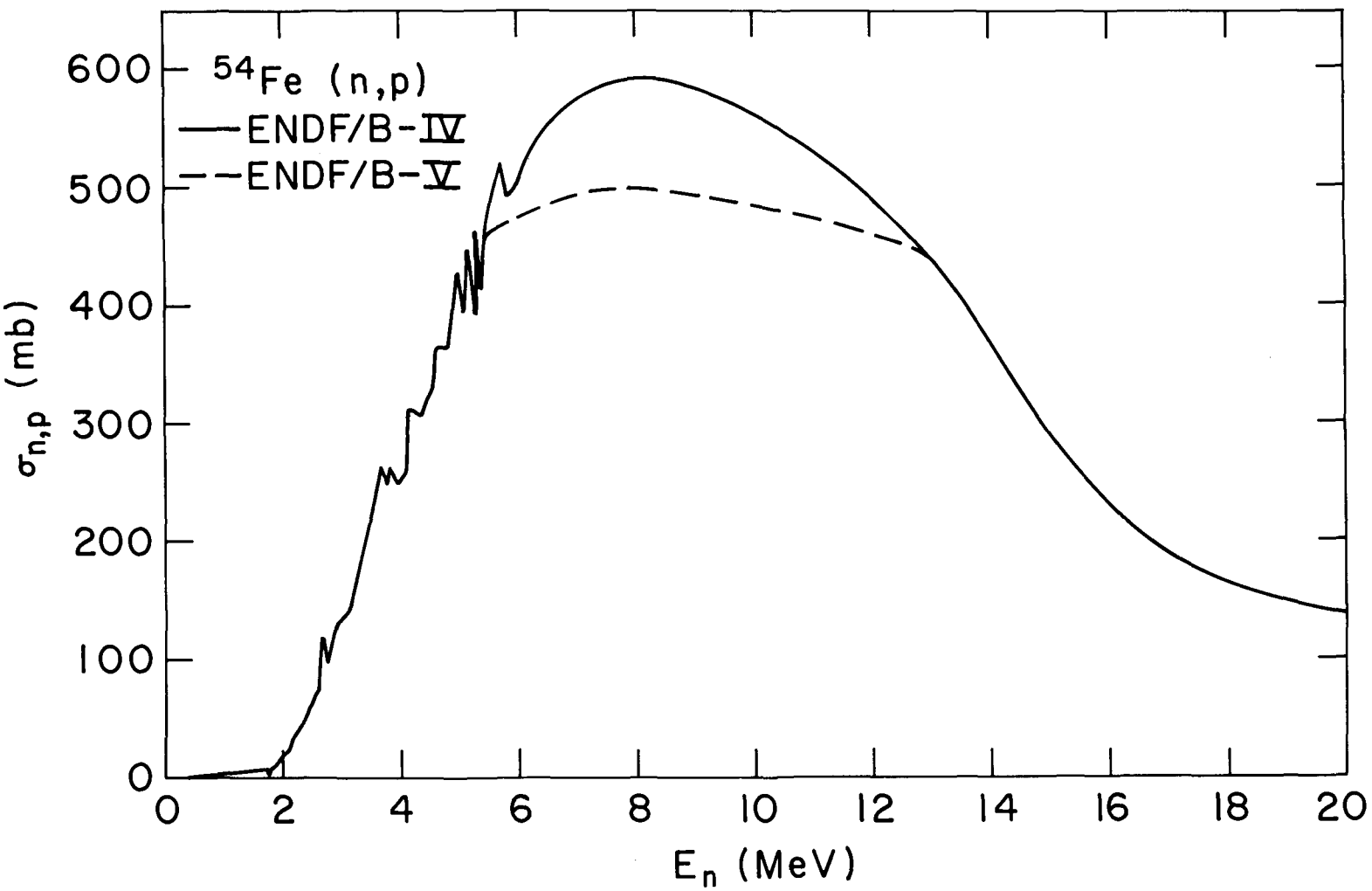

REVISED FIGURE 7
"STATUS OF DOSIMETRY FILE FOR ENDF/B-V" - B. Magurno, November, 1978 BNL-NCS-25200

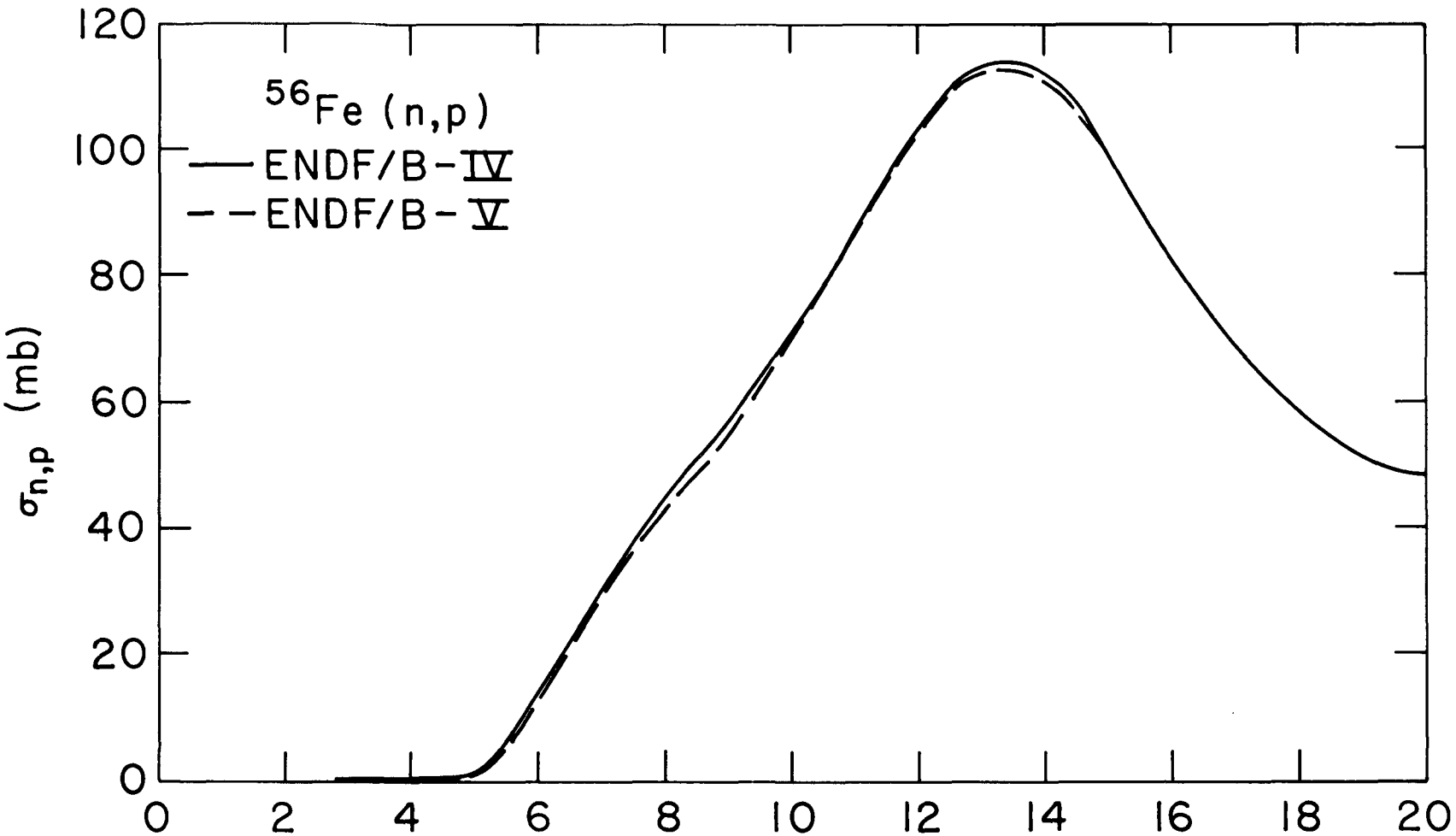
^{56}Fe (n,p)
ENDF/B-IV
ENDF/B-V
$\sigma_{n,p}$ (mb)
E_n (MeV)
0
20
40
60
80
100
120
0
2
4
6
8
10
12
14
16
18
20

FIGURE 8

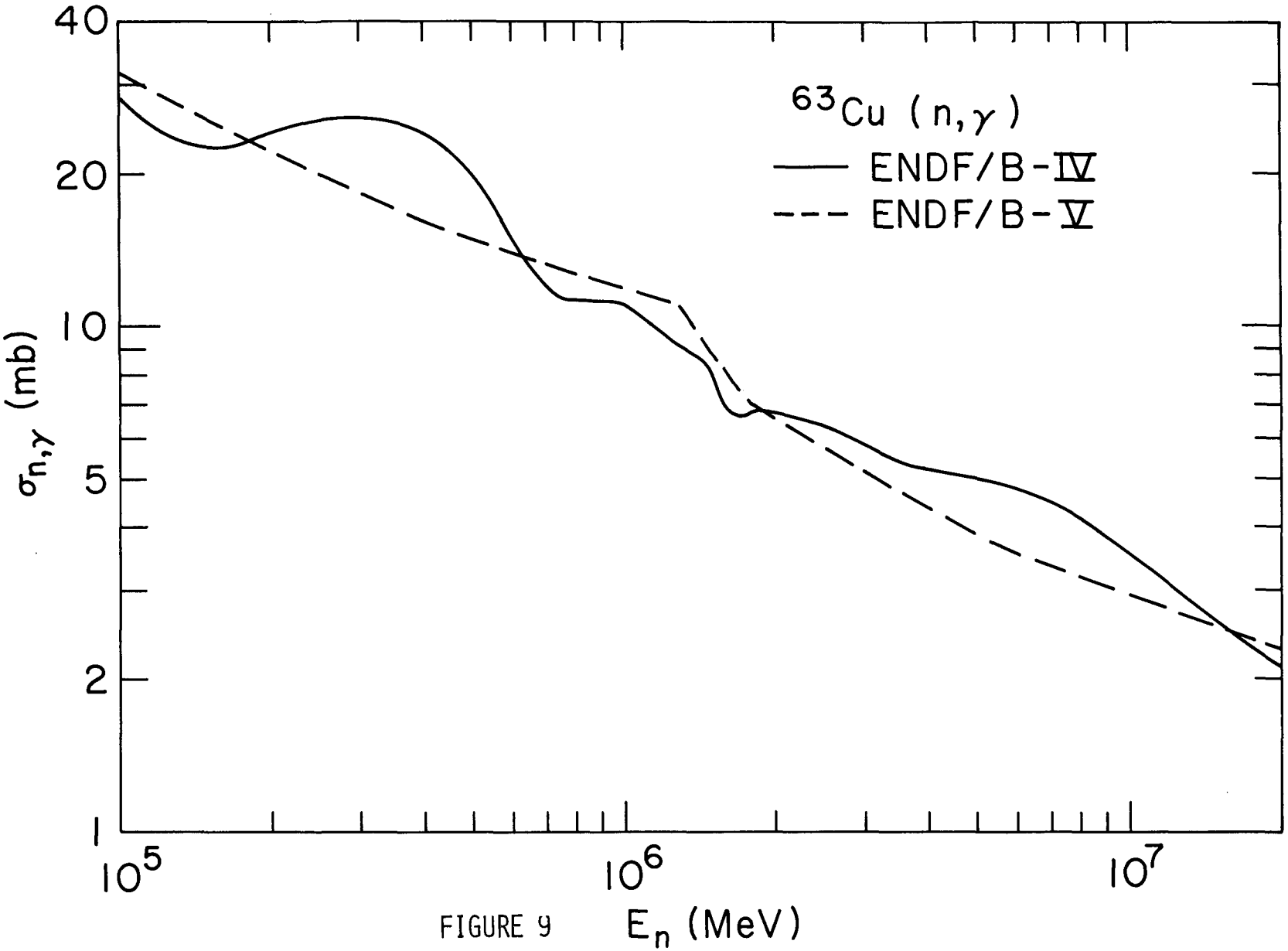
40
20
10
5
2
1
$\sigma_{n,\gamma}$ (mb)
^{63}Cu (n,γ)
ENDF/B-IV
ENDF/B-V
10^5
10^6
10^7
E_n (MeV)

FIGURE 9

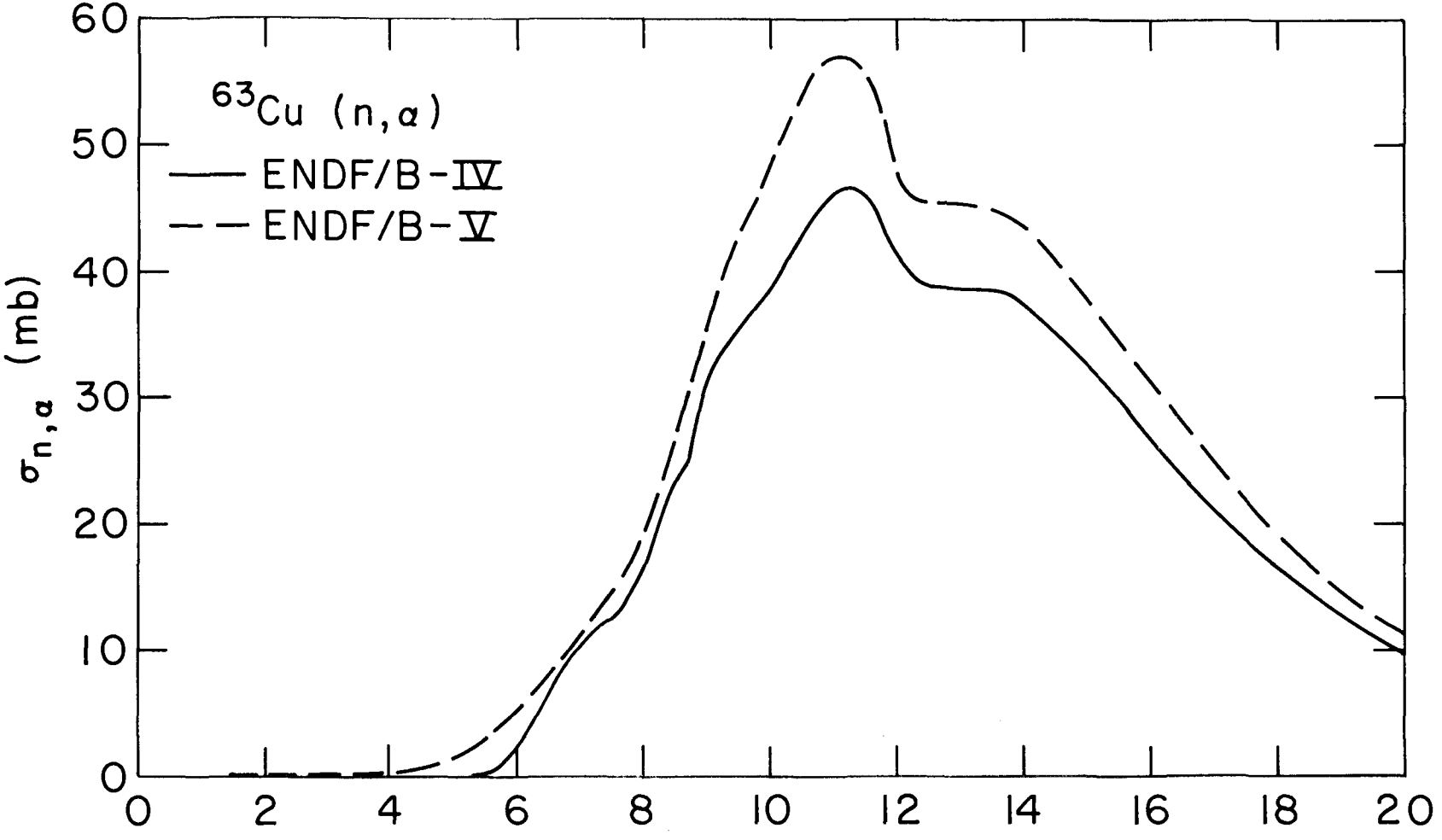
^{63}Cu (n,α)
ENDF/B-IV
ENDF/B-V
$\sigma_{n,\alpha}$ (mb)
E_n (MeV)
0
10
20
30
40
50
60
0
2
4
6
8
10
12
14
16
18
20

FIGURE 10

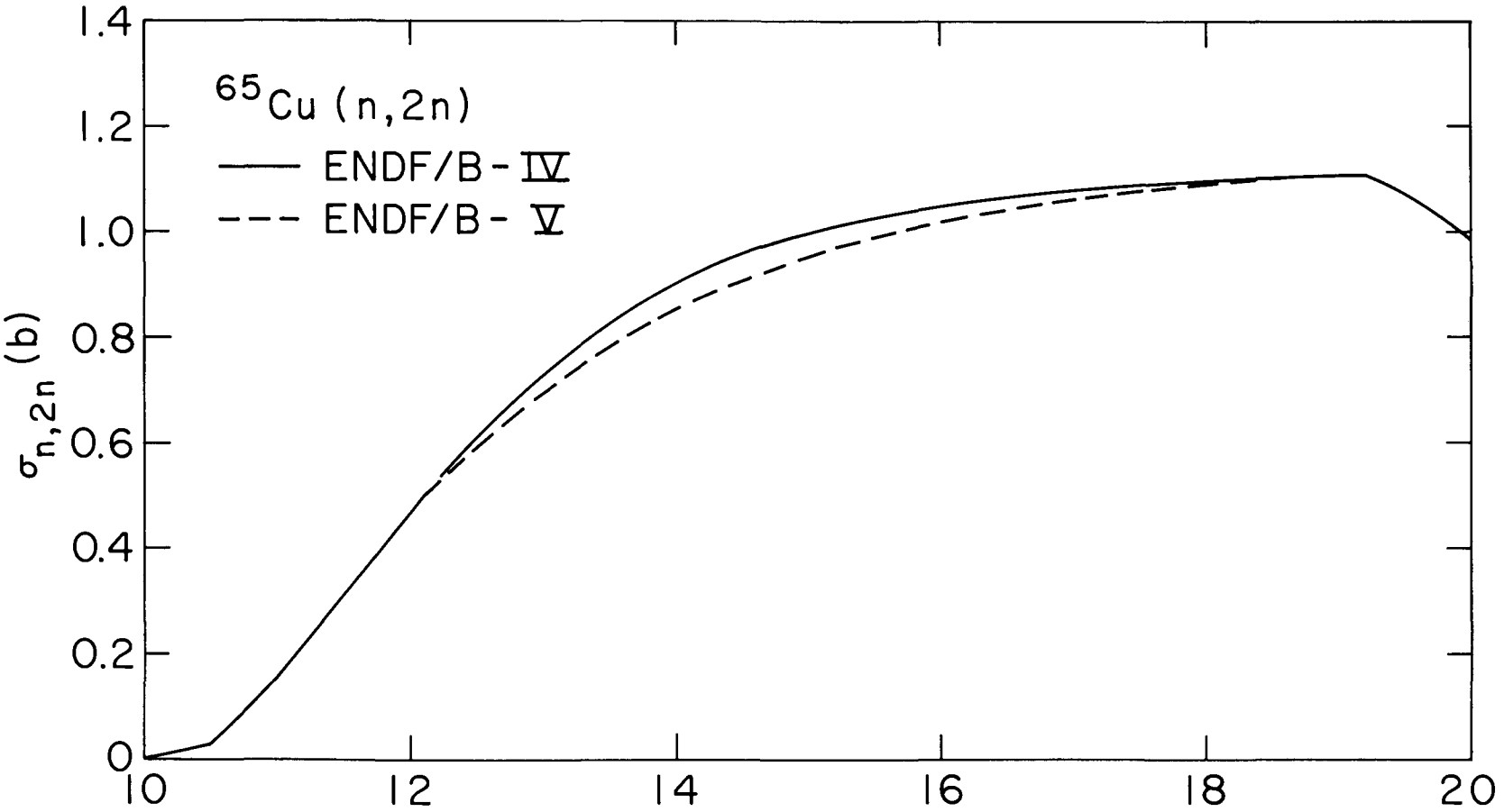
^{65}Cu (n,2n)
ENDF/B-IV
ENDF/B-V
$\sigma_{n,2n}$ (b)
1.4
1.2
1.0
0.8
0.6
0.4
0.2
0
10
12
14
16
18
20
E_n (MeV)

FIGURE 11

In 115 (n,g)In 116m

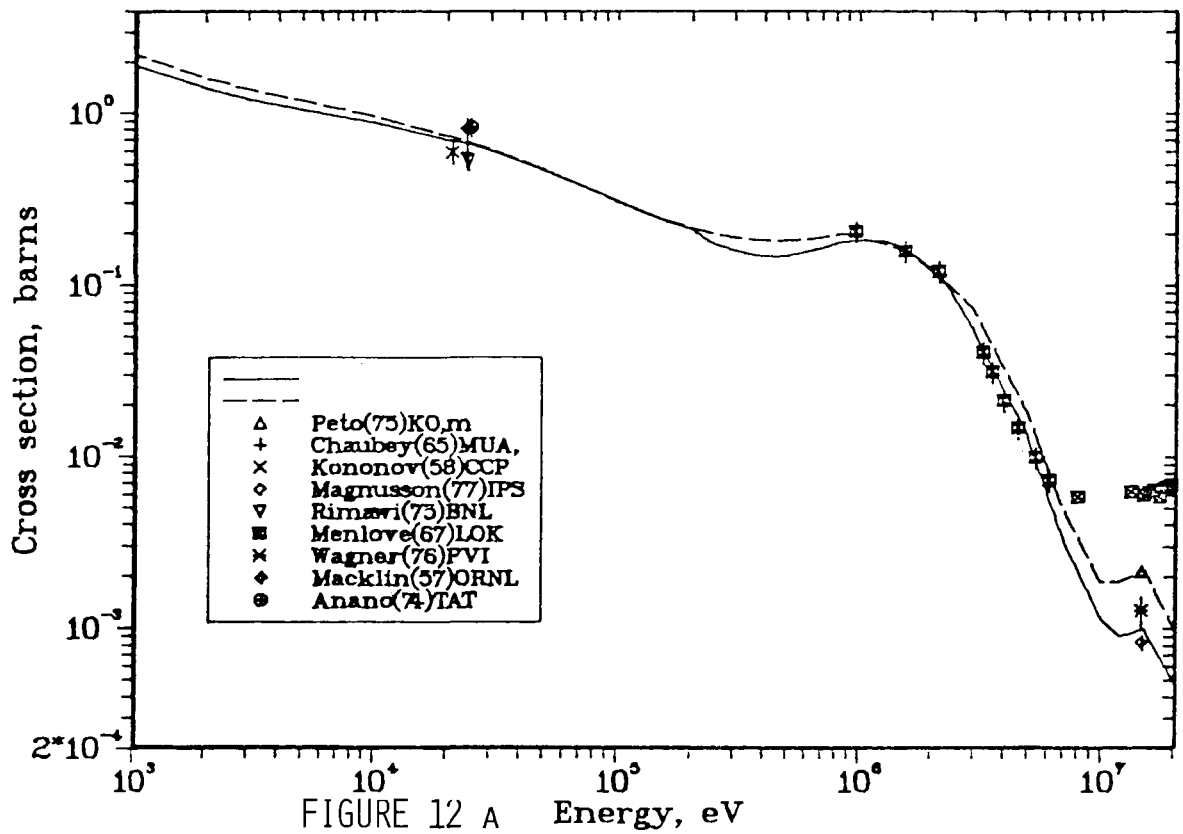

FIGURE 12 A

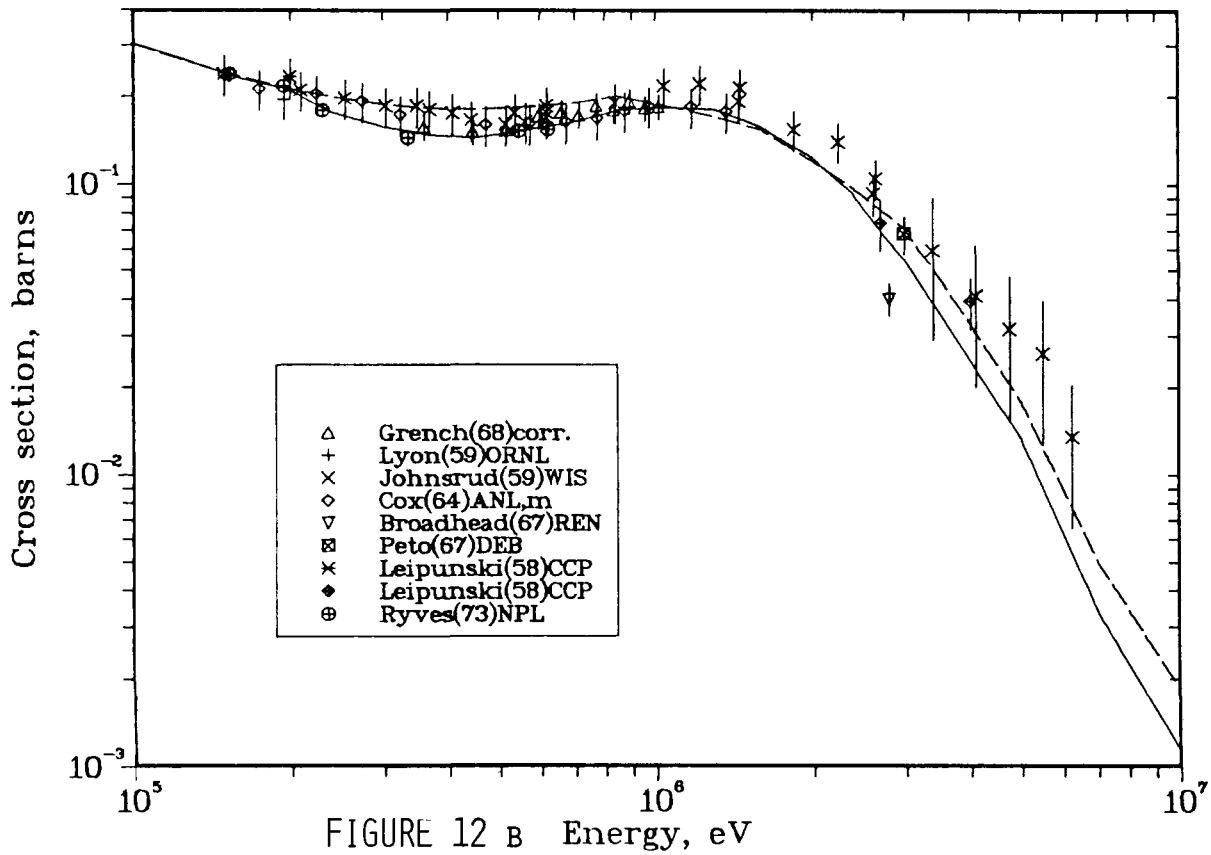

FIGURE 12 B

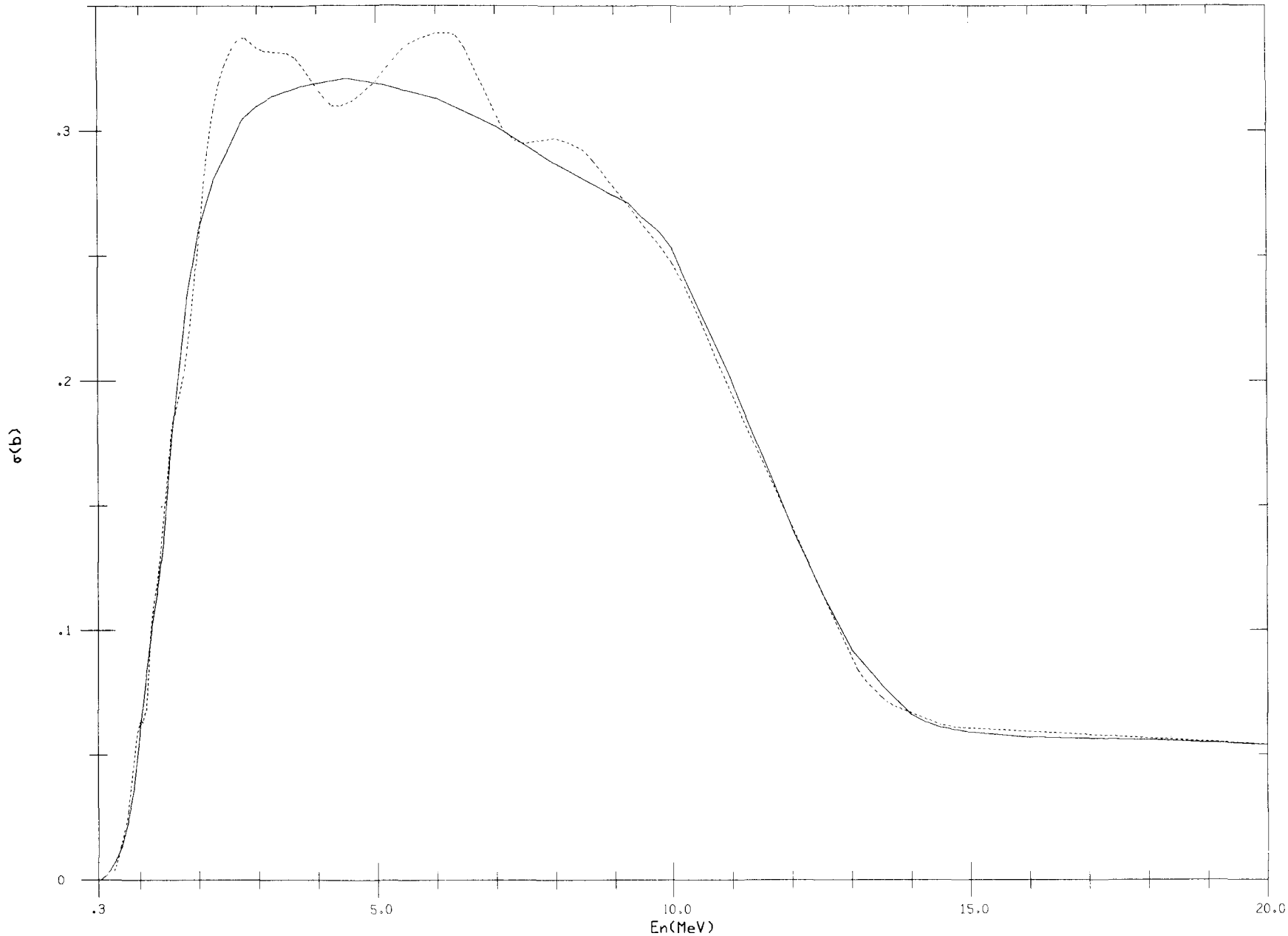

FIGURE 13

Measurement of the Activation Cross Section of the Reaction $^{93}Nb(n,n')^{93m}Nb$ for 0-25 MeV Neutrons

F. Hegedüs
Swiss Federal Institute for Reactor Research, CH-5303 Würenlingen

M.W. Guinan and J.R. Meadows
Lawrence Livermore Laboratory

N.F. Peek
University of California, Davis

L.R. Greenwood
Argonne National Laboratory

Introduction

The niobium is an excellent detector to monitor fast neutron fluence in power reactors (1,2,3,4). However its use is quite limited because the cross section is not well known. At the Second ASTM - Euratom Symposium on Reactor Dosimetry (Palo Alto, October 1977) delegates from several countries have shown interest in a more accurate measurement of the cross section in the neutron energy range of 0-25 MeV. By that means it would be possible to extend generally the use of niobium detectors which could improve the accuracy of the present material damage dosimetry in power reactors. Furthermore the niobium could be used for material damage dosimetry in accelerator facilities and fusion devices, too.

The main problem with the cross section measurement is that the activation by means of discrete energy neutron sources is weak, because of the half life of the product is very long (11.4 y). On the other hand the thickness of the samples is limited (<10 mg/cm^2) because the energy of the counted X_k - rays is low (16.6 keV). Therefore only strong sources with continuous neutron spectra could be used to measure $\sigma(E)$.

The principle is that the niobium samples are activated along with a set of threshold detectors. This allows the determination of the neutron spectra (5) furthermore by that means the unknown $\sigma(E)$ of niobium could be estimated by unfolding a number of integral experiments. Up to date only two measurements were published (1,4), both used space dependent fast neutron spectra in fission reactors. The obtained accuracy was poor because the shape of their neutron spectra was not appropriate for this purpose : the differential neutron flux was too strongly decreasing with increasing neutron energy.

The neutron spectra of d-Be accelerator neutron sources have more suitable shapes for this purpose (6). Specially the intense d-Be neutron source at the Crocker Nuclear Laboratory of the University of California at Davis (5) could be very appropriate to carry out the measurement of $\sigma(E)$ of niobium in the neutron energy range of 0-25 MeV.

Proposed Cross Section Evaluation

In 1977-78 a series of spectral determination experiments at d-Be sources were carried out at UC DAVIS, ANL & ORNL. In all these determinations the multiple foil technique was used in which the $Nb^{93}(n,2n)Nb^{92m}$ reaction was included. The Nb foils are presently available and will be counted for Nb^{93m}. Five spectra at 30 MeV covering the angular range from 0-60°, two at 40 MeV (0° & 15°) and two at 15 MeV (0° & 15°) have been determined. In addition foils irradiated with D-T neutrons ($\hat{E} \sim 14.8$ MeV) at the RTNS facility at Lawrence Livermore Lab are available. Since the spectra differ substantially over the range from 1-25 MeV the Nb^{93m} cross section can be extracted from the integral measurements with reasonable precision.

1. F. Hegedues: Utilization of the Reaction $^{92}Nb(n,n^1)^{93m}Nb$ for Fast Neutron Fluence Measurement.
Proceedings of the First ASTM-EURATOM Symposium on Reactor Dosimetry (Petten, 1975) EUR 5667 e/f.

2. R. Lloret: Application de la réaction $^{93}Nb(n,n^1)^{93m}Nb$ à la dosimètrie des irradiation de materiaux.
Proceedings (see ref. 1.).

3. F. Hegedues: Fast Neutron Dosimetry by the Reaction $^{93}Nb(n,n^1)$. Counting Technique for ^{93m}Nb Activity.
Proceedings of the Second ASTM-EURATOM Symposium on Reactor Dosimetry (Palo Alto, 1977).

4. W.H. Taylor: Some Studies of the $^{93}Nb(n,n^1)$ Reaction.
Proceedings (see ref. 3).

5. D.R. Nethaway, R.A. Van Konyenburg, M.W. Guinan and L.R. Greenwood : Neutron Spectra from 30 MeV Deuterons on a Thick Be-Target.
Proceedings of the Symposium on Neutron Cross Sections, Brookhaven 1977 BNL - NCS 50681.

6. P.J. Persiani, W. Becker and J. Donahue : Neutron Spectra and Basic Data Requirements for (d,Li) and d,Be) target Systems.
Proceedings (see ref. 5.)

7. F. Hegedues : EIR Report No. 195 (1971).

THE ANALYSIS OF THE $Co^{59}(n,p)Fe^{59}$ AND $Fe^{54}(n,\alpha)Cr^{51}$ CROSS SECTIONS FOR THEIR USE IN REACTOR DOSIMETRY

G.Vasiliu, S.Mateescu

Institute of Nuclear Power Reactors
Pitesti Romania

ABSTRACT

Based on experimental differential and integral data, as well as on integral computed data, after the renormalization and evaluation of experimental points, the $Co^{59}(n,p)Fe^{59}$ and $Fe^{54}(n,\alpha)Cr^{51}$ cross sections, have been carefully analyzed.

The consistency of newest differential experimental data for $Co^{59}(n,p)$ with the recommended average cross section value, and the discrepance between the same data type for $Fe^{54}(n,\alpha)$ cross section, are pointed out. New experimental differential and integral data, especially for the second reaction, are necesary for better estimation of these two excitation functions.

INTRODUCTION

The $Co^{59}(n,p)Fe^{59}$ and $Fe^{54}(n,\alpha)Cr^{51}$ threshold reactions have been recently proposed to be included into an international evaluated data file for reactor dosimetry purposes.

Contrary to the status of the experimental data for excitation functions of the most reactions already established for reactor dosimetry, in these two cases, the experimental measurements are very few, the data are discrepant, many of them are old data and the energy range of interest (from threshold up to 20 MeV) is only partially covered.

On the other hand, the integral data (experimental and recommended) available are affected by relatively high errors (10% for $Co^{59}(n,p)Fe^{59}$ and 30% for $Fe^{54}(n,\alpha)Cr^{51}$).

In these circumstances, an reevaluation process is a difficult task.

THE $Co^{59}(n,p)Fe^{59}$ CROSS SECTION ANALYSIS

The experimental data available until 1976 (1-12) are reported from 2.569 MeV (the threshold at 0.8 MeV (13)), up to 14-15 MeV, with two gaps: 10-14 MeV and 15-20 MeV (Fig.1).

Some of these data (the relative ones, with given standard(s)) have been renormalized according to the newest standards (ENDF/B-IV (26)), and the results are presented in the Table I.

After renormalization, the one-point measurements at 14.5 MeV are around 47 mb and 85 mb (where

the newest datum is reported by Dresler (6), in 1973).

Fig.1 shows also the ENDL, $Co^{59}(n,p)$ cross section, which is very closed of ENDF/B-IV data. The experimental data set available (Smith (1) from 1975 and Smith (2) from 1976) up to 10 MeV indicates a clear and significant disagreement in comparison with ENDL data, which are based on fewer experimental data and nuclear systematics (27) (the Smith's data are not included).

The Table II contains the status of averaged cross sections on U^{235} thermal fission spectrum comparatively, both, computed and measured (and recommended) values. The computed values are based on three data sets (I, III, based on Smith's data, and II on ENDL data set),

To obtain the sets I and III, the experimental data of Smith up to 10 MeV have been qualitatively forced to agree with the "evaluated" points in the 14-15 MeV energy range. The recommended integral data based on experimental values of Calamand (14) are given also,

The computed values are obtained using both, the Maxwell's (at 1.29 MeV and 1.32 MeV) and the Watt's spectra;

The typical formula (15) have been used:

$$N(E) = \sqrt{\frac{4E}{\pi\theta^3}}\, e^{-E/\theta} \qquad \text{(Maxwell)}$$

with θ - nuclear temperature in MeV, and

$$N(E) = c \cdot e^{-AE} \sinh \sqrt{BE} \qquad \text{(Watt)}$$

with $A = (1.012 \pm 0.0011)\ MeV^{-1}$

$B = (2.189 \pm 0.155)\ MeV^{-1}$,

the Adams' spectrum parameters recommended by Knitter (15) and $c = 2.214\ MeV^{-1}$ is the constant for spectrum normalization.

The computed values have been obtained via INTERX(BNL) computer code.

For the same data sets the average computed values for the 10-20 MeV energy range are also given.

It is obvious that the average cross section computed from Smith's data is in a good agreement in the limits of the experimental errors to the experimental recommended value (14), while the average cross section based on ENDL data set is much different from the lattest value,

It is obvious also, that the contribution to $\bar{\sigma}$ above 10 MeV is very small (4.2%-5.98%), because of the small percentage from fission spectrum at these energies (10-20 MeV), 0.143%-0.169%.

This situation makes impossible to take a decision about the validity of one or the other value of the cross section at 14-15 MeV.

For a better estimation of the excitation function for $Co^{59}(n,p)Fe^{59}$ reaction, new experimental measurements are desirable, and/or theoretical evaluations, to cover the gaps.

In this respect we already performed some theoretical calculations, based on statistical model including preequilibrium contributions, taking into account the competitive n, p, d, and α channels, and neglecting the t and He^3 channels which, even if are physicaly possible in this energy range, have small reaction probabilities (16). The choice of the optical model

parameters used to compute T_ℓ coefficients, and the parameters for level density, are to be assigned by fitting the evaluated total, elastic, inelastic, and (n,p) (up to 10 MeV and around 14 MeV) cross sections, as well as (n,α) and (n,2n) cross sections, which are quite well covered by experimental values.

The work is in progress and the results will be reported latter.

THE $Fe^{54}(n,\alpha)Cr^{51}$ CROSS SECTION ANALYSIS

The available experimental data (17-25) reported until 1976 cover the energy range from 2.23 MeV up to 6.2 MeV, between 13 MeV and 15 MeV, and includes only one point at 16.75 MeV, with gaps between 6.2-13 MeV, 15-16 MeV, and 17-20 MeV (Fig.2).

After the renormalization (Table III) we can see the same situation as for $Co^{59}(n,p)$, namely, between 13.5-15 MeV the experimental points tend to be around 95 mb and 130 mb. The Fig.2 shows the KEDAK (1970) evaluated data also.

In the Table IV the average cross sections are presented in the same manner as for the $Co^{59}(n,p)$ reaction.

It is to be noted the significant discrepances between the computed $\bar{\sigma}$ and the recommended one (14).

The same considerations as for $Co^{59}(n,p)$ reaction, makes impossible to select the correct value of the cross section around 14 MeV, and new measurements and/or theoretical calculations would be useful in this case too.

CONCLUSIONS

It seems that, based on the experimental values available at the moment, for both analyzed reactions, it is too early to be used in the dosimetry file. It is desirable to be stimulated new measurements for the excitation functions of both reactions, and, in particular, the $Fe^{54}(n,\alpha)$ differential and integral cross sections to be carefully analyzed, to obtain values with usual errors accepted for dosimetry purposes (less than 5%).

Of course, theoretical calculations can add useful information regarding these two reactions.

ACKNOWLEDGEMENTS

The authors wish to thank to IAEA-Nuclear Data Section which stimulated this analysis and kindly supplied us with the experimental data from EXFOR library, as well as to Dr.S.Rapeanu from the Institute of Nuclear Power Reactors for useful discussions.

TABLE I. Renormalization of data for $Co^{59}(n,p)$ reaction

Author (Reference)	Year	Energy (MeV)	Standard reaction	Standard value (mb)		Cross section (mb)	
				Old	New	Old	New
Preiss [4]	1960	14.8	$Ni^{58}(n,2n)$	52	35.1	82	55.35
Vonach [5]	1965	14.8	$Co^{59}(n,2n)$	750	696	53	49.18
Dresler [6]	1973	14.6	$Fe^{56}(n,p)$	105	104	84.1	83.3
Weingold [7]	1960	14.5	$Cu^{65}(n,2n)$	1030	959.5	80	77.524
Levkowsky [8]	1968	14.8	$Cu^{65}(n,2n)$	1000	984	37	36.423

TABLE II. Intercomparison of integral cross sections, of $Co^{59}(n,p)$ reaction averaged in the U^{235} thermal fission neutron spectrum

Data set	ΔE (MeV)	% of spect.	Maxwellian			$\bar{\sigma}_{recom.}$ (mb) from exp.-eval. (14)	WATT	
			Temp. (MeV)	$\bar{\sigma}$(computed)			$\bar{\sigma}$(computed)	
				% from total	(mb)		(mb)	% from total
I	$10^{-10} \div 20.$	100	1.29 1.32	100	1.3119 1.4054	1.42±0.14(±9.86%)	1.384	100
	10.÷20.	0.143 0.169	1.29 1.32	5.488 5.98	$7.2 \cdot 10^{-2}$ $7.85 \cdot 10^{-2}$	- -	$6.1 \cdot 10^{-2}$	4.4
II	$10^{-10} \div 20.$	100	1.29 1.32	100	2.8381 2.991	1.42 ± 0.14	2.95	100
	10.÷20.	0.143 0.169	1.29 1.32	4.2 4.68	$1.19 \cdot 10^{-1}$ $1.4 \cdot 10^{-1}$	- -	$1.03 \cdot 10^{-1}$	3.5
III	$10^{-10} \div 20.$	100	1.29 1.32	100	1.297 1.3875	1.42 ± 0.14 1.42 ± 0.14	1.372	100
	10.÷20.	0.143 0.169	1.29 1.32	4.4 4.83	$5.7 \cdot 10^{-2}$ $6.7 \cdot 10^{-2}$	-	$4.9 \cdot 10^{-2}$	3.57

TABLE III. Renormalization of data for $Fe^{54}(n,\alpha)$ reaction

Author (Reference)	Year	Energy (MeV)	Standard reaction	Standard value (mb)		Cross section (mb)	
				Old	New	Old	New
Singh [17]	1972	14.5	$Al^{27}(n,\alpha)$	114	119.36	139.5	146
Qaim [18]	1976	14.7	$Al^{27}(n,\alpha)$	121	116.776	88	84.9
Maslov [19]	1972	14.6	$Cu^{65}(n,2n)$	960	968.9	106	106.98
Cross [22]	1963	14.5	$Al^{27}(n,\alpha)$	115	119.36	94	97.5
Chittenden [23]	1961	14.8	$Al^{27}(n,\alpha)$	114	115.484	270	273
Venugopala [24]	1967	14.4	$Fe^{56}(n,p)$	100	108	90	97.2
		14.4	$Al^{27}(n,\alpha)$	114	120.428	90	95.07
Qaim [25]	1971	14.7	$Al^{27}(n,p)$	68	72.4	134	142.6
		14.7	$Al^{27}(n,\alpha)$	121	116.776	134	129.32

TABLE IV. Intercomparison of integral cross sections, of $Fe^{54}(n,\alpha)$ reaction, averaged in the U^{235} thermal fission neutron spectrum

Data set	ΔE (MeV)	% of spect.	Maxwellian			$\bar{\sigma}_{recom.}$ (mb) from exp.-eval. (14)	WATT	
			Temp. (MeV)	$\bar{\sigma}$(computed)			$\bar{\sigma}$(computed)	
				% from total	(mb)		(mb)	% from total
I	$10^{-10} \div 20.$	100	1.29	100	1.8462	0.6±0.2(±33%)	1.912	100
			1.32	100	1.9576			
	10.÷20.	0.143	1.29	5.96	$1.1 \cdot 10^{-1}$	-	$9.36 \cdot 10^{-2}$	4.9
		0.169	1.32	6.64	$1.3 \cdot 10^{-1}$	-		
II	$10^{-10} \div 20.$	100	1.29		1.7976	0.6 ± 0.2	1.86675	100
			1.32	100	1.9017			
	10.÷20.	0.143	1.29	4.99	$8.97 \cdot 10^{-2}$	-	$7.63 \cdot 10^{-2}$	4.1
		0.169	1.32	5.57	$1.06 \cdot 10^{-1}$			

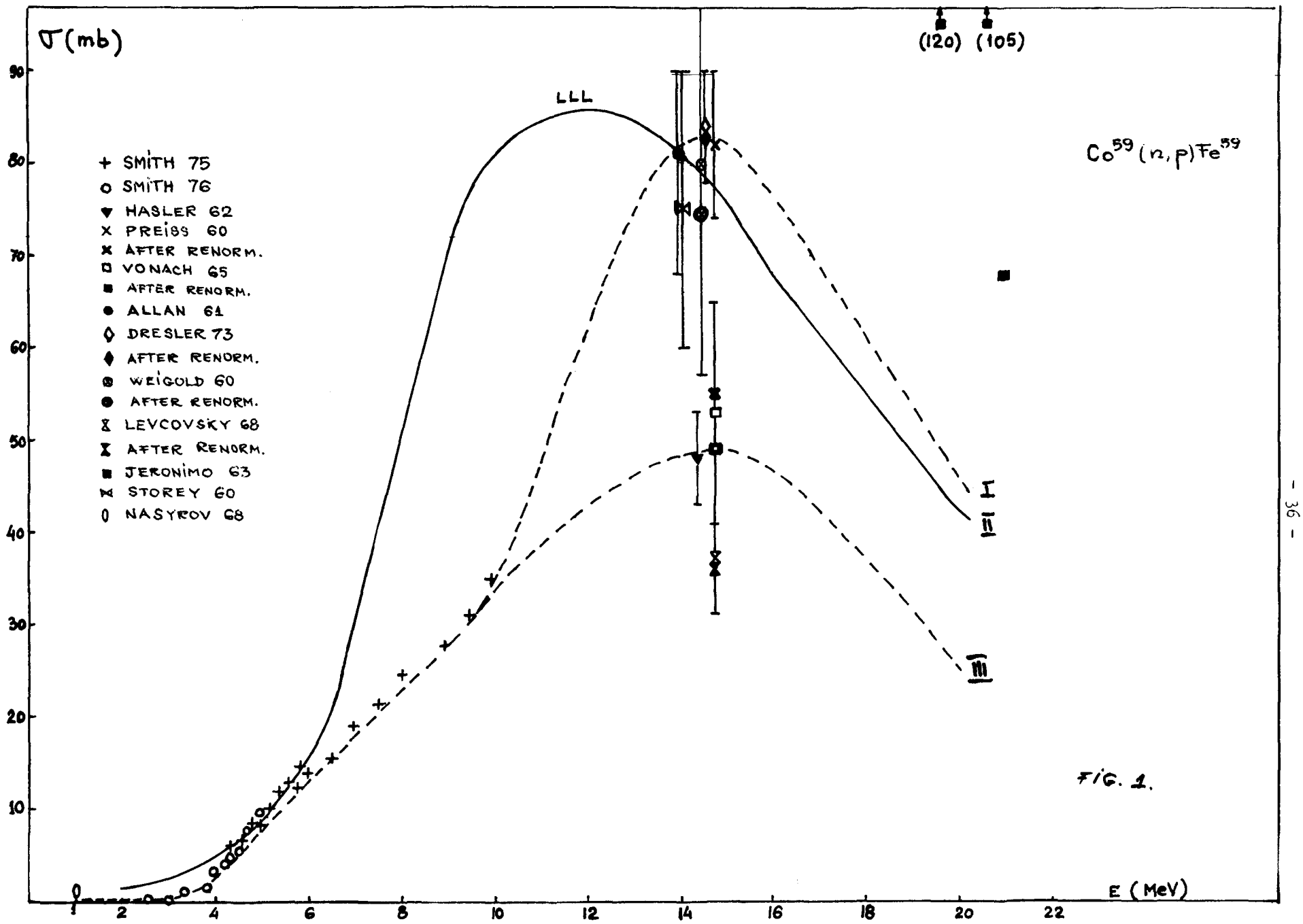
σ(mb)
(120) (105)
LLL
Co59 (n, p) Fe59
+ SMITH 75
o SMITH 76
▼ HASLER 62
× PREISS 60
✕ AFTER RENORM.
□ VONACH 65
■ AFTER RENORM.
● ALLAN 61
◇ DRESLER 73
◆ AFTER RENORM.
⊗ WEIGOLD 60
● AFTER RENORM.
⧖ LEVCOVSKY 68
⧗ AFTER RENORM.
■ JERONIMO 63
⋈ STOREY 60
0 NASYROV 68
I
II
III
E (MeV)
10
20
30
40
50
60
70
80
90
2
4
6
8
10
12
14
16
18
20
22

FIG. 1.

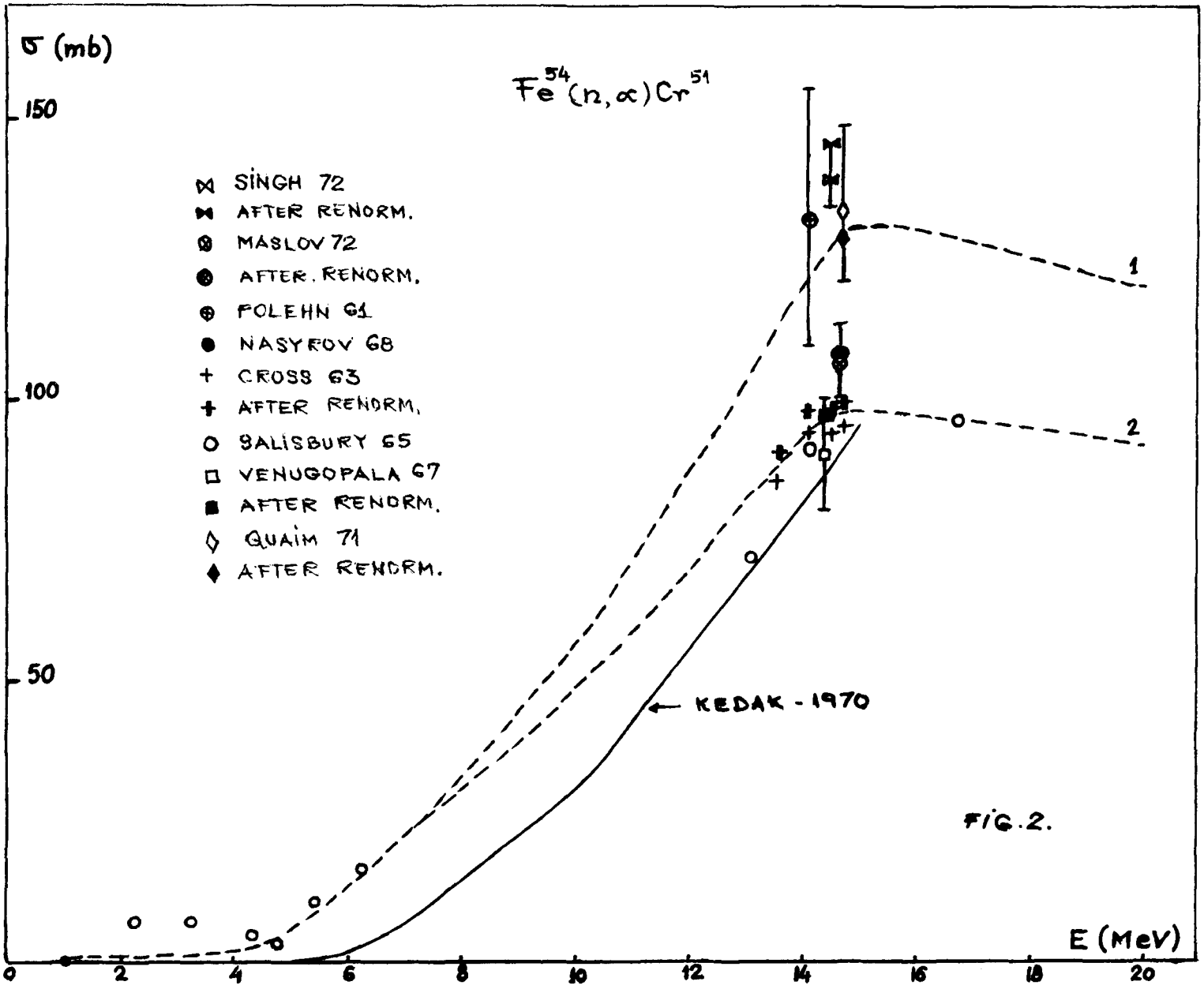
σ (mb)
$Fe^{54}(n,\alpha)Cr^{51}$
150
100
50
SINGH 72
AFTER RENORM.
MASLOV 72
AFTER. RENORM.
FOLEHN 61
NASYROV 68
CROSS 63
AFTER RENORM.
SALISBURY 65
VENUGOPALA 67
AFTER RENORM.
QUAIM 71
AFTER RENORM.
1
2
KEDAK - 1970
0
2
4
6
8
10
12
14
16
18
20
E (MeV)

FIG. 2.

References

1 D.L.Smith, Nucl.Sci.Eng.58,314,1975.

2 D.L.Smith, Priv.comm.to NDS Vienna,1976.

3 F.L.Hassler, Phys.Rev.125,1011,1962.

4 J.L.Preiss, Nucl.Phys.15,326,1960.

5 H.K.Vonach, Nucl.Phys.68,445,1965.

6 J.Dresler, Int.Phys.Jadovrej.INR-1464,12,1973.

7 E.Weigold, Austr.J.13,186,1960.

8 V.N.Levkovsky, Yad.Fiz.8(1),7,1968.

9 J.M.F.Jeronymo, Nucl.Phys.47,157,1963.

10 D.L.Allan, Nucl.Phys.24,274,1961.

11 R.S.Storey, Proc.Phys.Soc.75,526,1960.

12 F.Nasyrov, At.Energ.25,437,1968.

13 R.J.Howerton, UCRL-50400 vol.9,1970.

14 A.Calamand, INDC(NDS)-55/L,1973.

15 H.H.Knitter, Proc.of a Consultants' Meeting on Integral Cross Section Measurements in Standard Neutron Fields for Reactor Dosimetry, Vienna 1976, IAEA-208,183,1978.

16 D.I.Garber, R.R.Kinsey, "Neutron Cross Sections", vol.II, BNL-325,1976.

17 J.J.Singh, ANS,15,147,1972.

18 S.M.Qaim, Conf.Garmis,589,1976.

19 G.N.Maslov, Yad.Fiz.9,50,1972.

20 H.Pollehn, Z.Naturfors.16A,227,1961.

21 F.Nasyrov, At.Energ.25,431,1968.

22 W.G.Cross, EANDC(CAN)-16,1,1963.

23 D.M.Chittenden, Phys.Rev.122,860,1961.

24 P.Venugopala Rao, Phys.Rev.154,1023,1967.

25 S.M.Qaim, Conf.Canterbury, 121,1971.

26 B.A.Magurno, BNL-NCS-50446,1975, ENDF/B-IV Dosimetry File.

27 R.J.Howerton, M.H.MacGregor, UCRL-50400, vol.15, part D, Rev.1,1978.

The Measurements and Evaluation of Fast Neutron Cross Section Data for Reactor Dosimetry

A. Marcinkowski
Institute for Nuclear Research, Warsaw

The aim of arriving at an generally accepted, consistent and extended data file, containing sets of evaluated energy-dependent neutron cross sections for some reactions commonly used for reactor dosimetry purposes, remains the objectives of the programme initiated by the IAEA Consultants Meeting held in 1973 /1/ and 1976 /2/. Considerable evaluation efforts have been made in the last years resulting in the ENDF/B - file, consisting of a notable amount of evaluated differential neutron cross sections in a uniform, easily accesible format /3/. However, the recent reviews of differential data for reactor dosimetry by Paulsen and Magurno /4/ and by Vlasov, Fabry and McElroy /5/ revealed an unsatisfactory situation and little progress, particularly in determination of the accuracy of the evaluated data. The need for an international cooperative effort in establishing an accurate and reliable file was pointed out. Consequently the Nuclear Data Group in the Institute for Nuclear Research in Warsaw has been encouraged to participate in the Nuclear Data Sections cooperative programme on the evaluation of some reactions important for neutron spectra unfolding by the foil-activation technique, the final goal of which is the establishing of an internationally recommended neutron cross section data file for dosimetry applications.

Evaluation of the Cross Sections for /n,2n/ reactions

Cross sections of the two important, high negative Q value neutron dosimetry reactions ^{58}Ni/n,2n/^{57}Ni and

^{23}Na/n,2n/^{22}Na are evaluated in the neutron energy range from the threshold to 28 MeV and 20 MeV, respectively. The evaluation is based on the experimentally measured cross sections. The statistical model estimates do not facilitate the evaluation, the theoretical cross sections being higher by a factor of 4 than the experimental ones in case of the ^{58}Ni/n,2n/^{57}Ni reaction and not reliable for a nucleus so light like Na.

The experimental data were critically reviewed and some of the data sets were disregarded if obsolete, not well documented or deviating much from the average trend. The accepted data sets were normalized in order to adjust the standard cross-sections and decay schemes.

Concerning the ^{58}Ni/n,2n/^{57}Ni reaction cross sections three energy regions have been distinguished, in which different criteria of evaluation have been assumed. The first region extends from the threshold energy 12.4154 MeV /6/ up to about 16 MeV neutron energy. In this region the accepted data are consistent within the experimental errors and concentrated along a smoothly increasing, with energy, line. In the second region between 16 MeV and 20 MeV there exist four excitation curves measured by Prestwood et al /7/, Paulsen and Liskien /8/, Bormann et al /9/ and Bayhurst et al /10/. These four data sets diverge evidently with increasing neutron energy. The excitation curve of Bayhurst et al extends into the third region up to 28 MeV and therefore it was considered independently. In treating the remaining three excitation curves the polynomial $P/E/=\sum_{i\leq 6} a_i E^i$ has been fitted separately to each of the data sets in the energy interval from 15 MeV to 20 MeV supplying P_I, P_{II}, P_{III}. Separate polynomial fit P_{IV} has been performed to all the single energy data including the cross sections belonging to the above mentioned three data sets, which lie below the 15 MeV limit. The latter fit extended from 13 MeV to 18 MeV. The polynomial P_V has been then fitted to P_I, P_{II}, P_{III} and P_{IV} assuming

a constant energy step. Such a procedure ascribes an equal weight to the three excitation curves, with no regard on the number of experimental points in each curve.

As a next step the polynomial fit to the Csikai /11/ data, in the energy range 13.6 - 15.4 MeV, as well as an independent polynomial fit to the whole curve measured by Bayhurst et al /10/, both lying well above the average trend displayed by the remaining data, have been performed. The resulting polynomials were normalized to the P_V. The normalization constants being 0.79 and 0.76, respectively. After normalization the two latter polynomials and the P_I, P_{II}, P_{III} and P_{IV} were at last fitted to the $P/E/=\sum_{i=0}^{5} a_i E^i$ providing the recommended excitation curve.

The mean square deviation of the data points or sets of data from the recommended curve ϵ_{ext} together with the average experimental error ϵ_{int}, assumed to be 7.5% below 14 MeV and 8.0% above 14 MeV, were used to determine the errors of the recommended cross sections below 16 MeV $\epsilon^2 = \epsilon^2_{ext} + \epsilon^2_{int}$. The upper error limit above 22 MeV joins the lower limit of the error bars given by Bayhurst et al /10/.

The recommended cross sections are tabulated in 100 keV energy steps from 12.9 MeV to 28.0 MeV /12/. The errors exceed slightly the 10% error limit requested in WRENDA 76/77 by Michaudon, reaching 11.4% from the threshold up to 14 MeV. In the energy interval 14 - 16 MeV the accuracy has been estimated to be 8.7%. At still higher energies the accuracy is worse again because of the inconsistency of the results of Bayhurst et al /10/. The recommended cross sections are described by the 5^{th} order polynomial with the coefficients a_0=-3230.7, a_1=755.26, a_2=-70.268, a_3=3.2762, a_4=-0.075663 and a_5=0.0006865.

For the purpose of the ^{58}Ni/n,2n/^{57}Ni evaluation we have performed an additional experiment measuring the cross sections at four neutron energies 14.02, 16.42, 17.42 and 17.85 MeV. Reference being made to the cross sections of the ^{56}Fe/n,p/^{55}Mn reaction as well as to the ^{27}Al/n,α/^{24}Na

reaction. These two standards provided cross sections for the $^{58}Ni/n,2n/^{57}Ni$ reaction, which differed by about 8%. Average values have been adopted.

Table 1

$^{58}Ni/n,2n/^{57}Ni$

Cross Sections in mb

E_n/MeV/	
14.2	19.9 ± 2.3
16.42	53.4 ± 4.5
17.42	63.0 ± 6.6
17.85	66.6 ± 6.8

These values were corrected for summing of cascade γ-rays /13/ in the Ge/Li/ detector and thus are higher by about 13% than those reported in INR 1709/I/PL/A and INDC/POL/-8/L. This correction brought the results of our measurements into agreement with the older data obtained by β^- counting, by Prestwood et al /14/. The latter data are lower than the cross sections values obtained recently by Bayhurst et al, also by counting β^-, but are higher than all the data sets obtained with γ-ray detection. We did not account for the angular correlations of the cascading γ-rays in the calculations of the correction. The evaluated excitation curve is shown in fig. 1.

The evaluation of the cross sections for the ^{23}Na /n,2n/^{22}Na reaction encounters the difficulties very similar to those of the previous case. Again the result of the evaluation depends critically on the accepted data, which have to be chosen from a limited number of data sets. Despite of all these sets have been obtained in carefull experiments, they differ by more than three standard deviations. The sets in question consist of the excitation curves measured by Paulsen and Liskien /15/, Menlove et al /16/ and Picard and Williamson /17/. In this situation we have decided to remeasure the cross sections for the $^{22}Na/n,2n/$

reaction. The following preliminary results have been obtained at three neutron energies

Table 2

$^{23}Na/n,2n/^{22}Na$

Cross Sections in mb

E_n/MeV/	
15.5 ± 0.5	51.7 ± 4.2
16.3 ± 0.3	57.7 ± 4.5
16.6 ± 0.2	67.5 ± 4.4

These cross sections may be slightly changed to account for attenuation of γ-rays in the sample and adjustments of the cross sections of the reference reaction $^{27}Al/n,\alpha/$. They support the earlier data of Menlove et al /16/ and Picard and Williamson /17/, and are more than twice lower than those reported by Paulsen and Liskien /15/. Thus there is no need to disregard the lowest excitation curve measured by Picard and Williamson only because it was obtained in an experiment being a continuation of the project initiated at Saclay by Jeronymo et al, who failed to explain the abnormally low values of cross sections obtained for the $^{58}Ni/n,2n/^{57}Ni$ and $^{58}Ni/n,p/^{58}Co$ reactions. In order to support our decision we are going to perform a separate measurement for the ^{23}Na /n,2n/^{22}Na reaction at slightly higher neutron energies 17.4 MeV and 17.8 MeV. We expect that the new experiment will confirm the preliminary data presented above. If this is the case the excitation curve measured by Pualsen and Liskiem will turn out to be too high and can be disregarded. As a consequence the recommended curve will fall somewhere inbetween the LLL ENDL /1974/ and the KEDAK /1970/ evaluations in accordance with the lower cross section sets as well as in accordance with the single energy measurements near 14 MeV neutron energy. We are going also to complete this evaluation with the relative correlation matrices describing the correlation

between the uncertainties of the cross sections at different energies, according to the procedure developed by Tagesen and Vonach /18/, and to prepare the evaluated cross sections, their uncertainties and the correlation matrices in the ENDF/B format. The status of the data compiled for the ^{23}Na/n,2n/^{22}Na reaction, including our recent measurement, is presented in fig. 2.

Fast Neutron Cross Section Measurements

In addition to the evaluations described above excitation curves, requested in WRENDA 76/77 for fission reactor dosimetry purposes, have been measured in the energy range from 13 MeV to 18 MeV for the reactions ^{191}Ir/n,2n/$^{190g+m}$Ir and ^{193}Ir/n,2n/$^{192g+m}$Ir. The measured cross sections are listed in table III. These data agree with those obtained by Bayhurst et al /10/ providing a broad basis for the evaluation of the reactions discussed.

Quite recently a project has been started to measure neutron capture cross sections in the energy range 0.5 MeV to 2.0 MeV by activation method. Measurements have been accomplished for ^{108}Pd, ^{110}Pd, ^{114}Cd, ^{116}Cd, ^{190}Os, ^{192}Os, ^{191}Ir, ^{193}Ir, ^{196}Pt and ^{198}Pt. In order to account for the effects of low energy neutron background the measured cross sections were refered simultaneously to two different standard reactions, having excitation curves of opposite slope, namely the ^{115}In/n,n'/ and the ^{115}In/n,γ/ reactions. By this occasion the cross sections of the former reaction were remeasured in many runs and its excitation curve was reevaluated in the threshold region. The experimental works are complemented by programming the statistical model calculations based on the level density model accounting for pairing interaction in the frame of the superconductivity formalism. The preparation of a computer code, which is intended, among others, for future evaluational purposes, is now under way.

Table III

E_n/MeV/	$^{191}Ir/n,2n/^{190g+m}Ir$	$^{191}Ir/n,2n/^{190m2}Ir$	$^{193}Ir/n,2n/^{192g+m1}Ir$
	mb	mb	mb
13.04 ± 0.38	2133 ± 136	110.5 ± 9.5	2006 ± 232
13.36 ± 0.24	2145 ± 133	117.9 ± 8.0	1932 ± 121
13.87 ± 0.34	2092 ± 138	119.8 ± 7.8	1899 ± 115
14.49 ± 0.34	2139 ± 139	134.1 ± 8.2	1872 ± 115
15.04 ± 0.28	2277 ± 176	138.9 ± 9.1	1953 ± 148
15.40 ± 0.24	2029 ± 141	141.0 ± 9.0	1807 ± 122
15.94 ± 0.46	2155 ± 137	180.3 ± 12.9	1893 ± 219
16.59 ± 0.11	1830 ± 111	175.5 ± 19.6	1605 ± 141
17.42 ± 0.44	1442 ± 93	179.2 ± 18.7	1312 ± 115
17.86 ± 0.08	1216 ± 97	163.2 ± 13.3	1109 ± 138

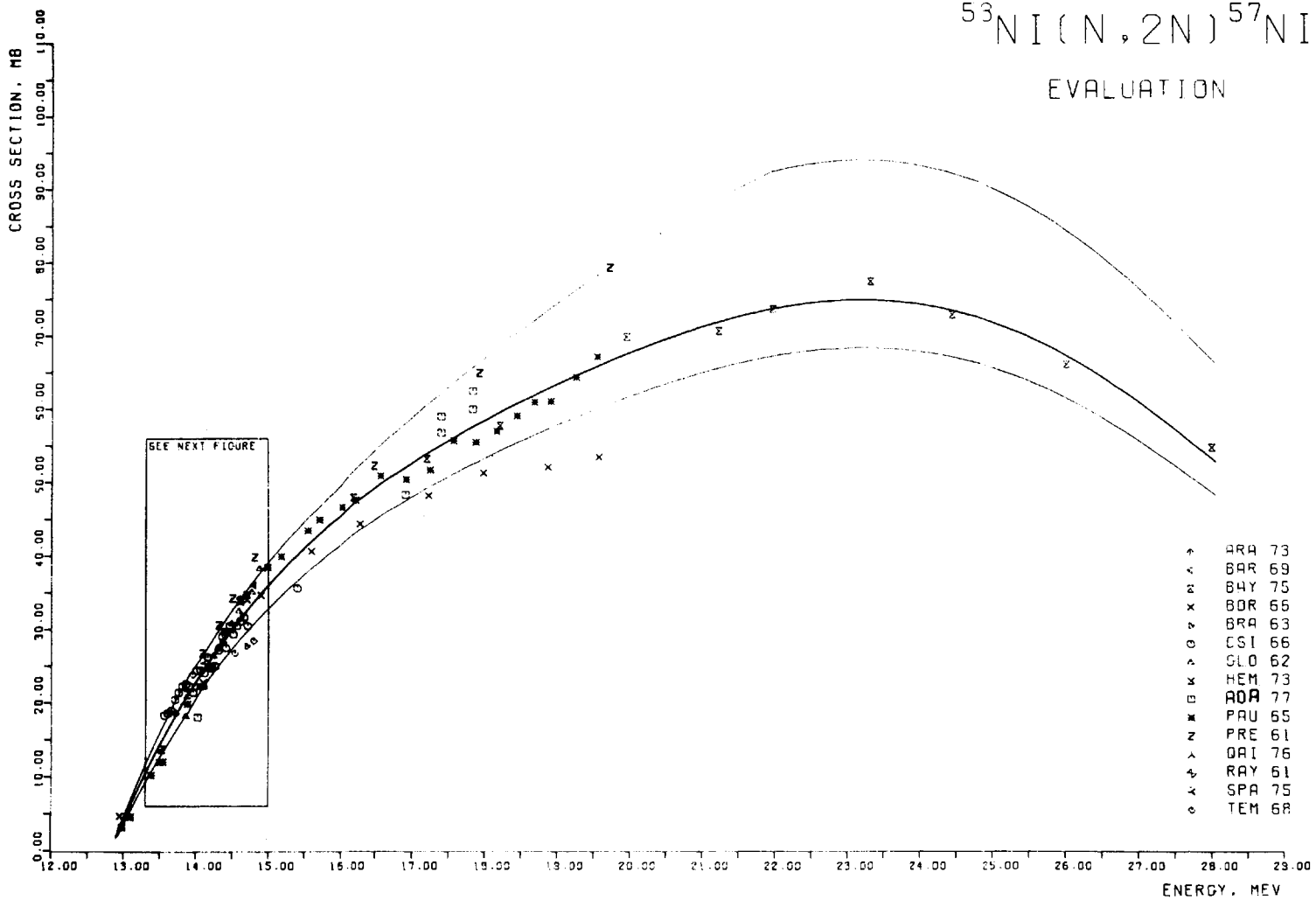

Fig. 1. Evaluated cross sections for the ^{58}Ni/n,2n/^{57}Ni reaction.

Fig. 2.
Comparison of $^{23}Na/n,2n/^{22}Na$ reaction cross-section measurements.

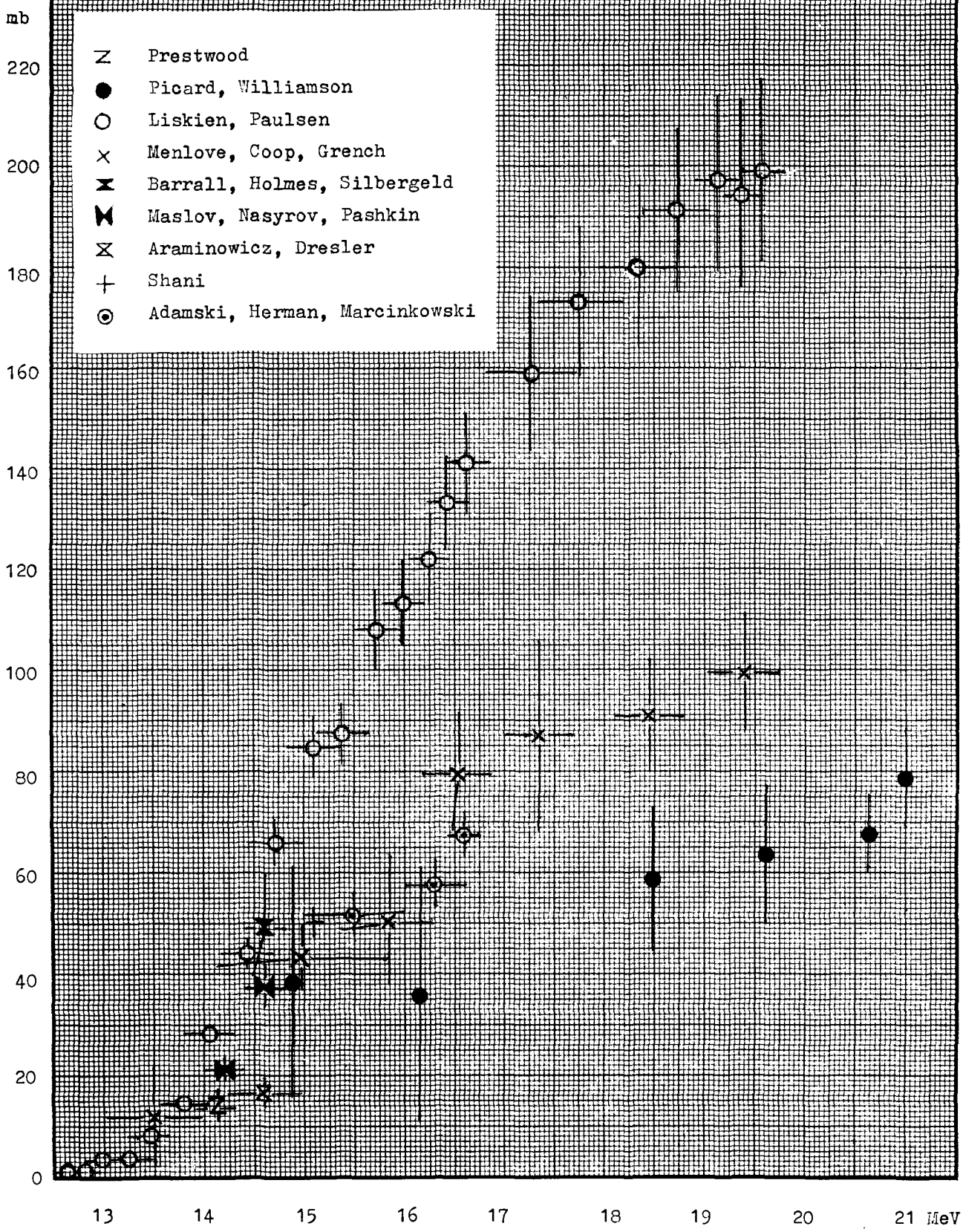

References

1. Proc. of the IAEA Consultants' Meeting on Nuclear Data for Reactor Neutron Dosimetry, Vienna 1973
2. Proc. of the IAEA Consultants' Meeting on Integral Cross Sections Measurements in Standard Neutron Fields, Vienna 1976 .
3. ENDF Summary Documentation BNL 17541 sec. Ed. of ENDF 201 compiled by B. Garber, Brookhaven 1975
4. Proc. of the First ASTM-Euratom Symposium on Reactor Dosimetry, Petten 1975
5. Status of Neutron Cross Sections for Reactor Dosimetry, INDC/NDS/-84/L+M
6. ANL/NDM-11 /1975/
7. R.J. Prestwood and B.P. Bayhurst, Phys. Rev. 121/1961/1438
8. A. Paulsen and H. Liskien, Nukleonik 7/1965/117
9. M. Bormann et al, EANDC/E/66U42
10. B.P. Bayhurst et al, Phys. Rev. C12/1975/451
11. J. Csikai, ATOMKI Közlemenyek 8/1966/79
12. L. Adamski, M. Herman and A. Marcinkowski, INR 1709/I/PL/A
13. C. Crouthamel, Gamma-Ray Spectroscopy, Pergamon Press 1960
14. R.J. Prestwood and B.P. Bayhurst, Phys. Rev. 121/1961/1438
15. A. Paulsen and H. Liskien, Nucl. Phys. 63/1965/393
16. H.O. Menlove, K.L.Coop and H.A. Grench, Phys. Rev. V163 /1967/1308
17. J.D. Picard and C.F. Williamson, Nucl. Phys. 63/1965/673
18. S. Tagesen and H. Vonach, RC-2047/RB, May 1978
19. N.D. Dudey, R. Kennerley, BNL-NCS-50446(75)80, ENDF/B-III(MAT. 6410)
20. P.G. Young and D.G. Foster, BNL-NCS-50446(75)24, ENDF/B-IV(MAT. 6193)

Summary Remarks and Recommended Reactions for An International Data File For Dosimetry Applications for LWR, FBR, and MFR Reactor Research, Development, and Testing Programs

W. N. McElroy and E. P. Lippincott (HEDL)

and J. A. Grundl (NBS), USA

A. Fabry

CEN/SCK, MOL, Belgium

R. Dierckx

JRC, ISPRA, Italy

U. Farinelli

CNEN-CSN, CASACCIA, Italy

November, 1978

For Inclusion in the Proceedings of the IAEA Advisory Group Meeting on "Nuclear Data for Reactor Dosimetry," November 13-17, 1978, Vienna, Austria.

This paper is based on work performed by Hanford Engineering Development Laboratory, Richland, Washington, operated by Westinghouse Hanford Company, a subsidiary of Westinghouse Electric Corporation for the United States Department of Energy and by the National Bureau of Standards, Washington, D. C.. The DOE Divisions of Reactor Research and Technology and Magnetic Fusion Energy and the Nuclear Regulatory Commission's Division of Reactor Safety Research sponsored parts of this work while other parts were sponsored by Euratom Research programs associated with the Euratom Working Group on Reactor Dosimetry (EWGRD).

I. Introduction

The need for the use of an internationally accepted data file for dosimetry applications for light water reactor (LWR), fast breeder reactor (FBR), and magnetic fusion reactor (MFR) research, development, and testing programs continues to exist for the Nuclear Industry.[1-11] The work of this IAEA meeting, therefore, will be another important step in achieving consensus agreement on an internationally recommended file and its purpose, content, structure, selected reactions, and associated uncertainy files.[1-18]

Summary remarks and a listing of recommended reactions for consideration in the formulation of an "International Data File for Dosimetry Applications" are presented in subsequent sections of this report.

II. Summary Remarks

A. An international data file should serve present dosimetry applications (fission reactor dosimetry) and future needs (fusion related applications and high energy neutron sources: D-T and D-Li). Therefore, the energy range in general should extend from thermal up to about 40 MeV. However, the upper energy limit for each dosimetry reaction will depend on the energy interval in which 90 to 95% of the reaction products are produced in representative benchmark neutron spectra.

B. Besides cross-sections as a function of energy, angular distributions of the reaction products and angular cross-sections should be included for a limited number of reactions. In particular, these are the reactions used in differential neutron spectrometry: $^{6}Li(n,\alpha)$, $^{3}He(n,p)$ and the (n,p) reaction for hydrogen.

C. Uncertainty data are essential* and should be of two types. The first should be more integral in nature and should be traceable to a selected number of permanent and well established "Standard" and "Reference" benchmark neutron fields. The second should be more differential in nature and should be traceable to a selected set of standard (Category I, p.30, reference 4) cross sections which are well known over their response range in a number of "Standard" benchmark neutron fields. The latter uncertainties should be in the form of covariance matrices. It must be determined, however, how extensive these covariance matrices can be and still be made true-to-fact, reasonable in size, and readily useable for standards, research, and applied problems.

D. With reference to the Second ASTM-Euratom Symposium and especially the work shop on computer codes for unfolding neutron spectra,[2] consideration should also be given to whether or not to include in the data file the integral and differential characteristics of the benchmark fields. These are the spectra, integral cross sections in these spectra, and the associated uncertainties and any covariance matrices that can be confidently established for these data. Having all of this information in the data file would facilitate the exploitation, with maxium efficiency, of the benchmark field results and uncertainty data.

E. In this regard, the subsequent requirements for data development and testing for data processing codes using various group structures must be given careful consideration. Especially since the use of a fixed

*Accuracy requirements are summarized in reference 4, p.3.

or single format for all standards, research, and applied problems dealing with neutron energies from thermal to about 40 MeV is not considered a realistic objective for an international data file.

From a practical point of view, the problems involved in establishing this international data file that should be considered and/or answered at this Advisory Meeting are:

- The identification of participating countries, agencies, and laboratories with their anticipated contributions and work completion schedules.
- The identification of IAEA sponsored work and completion schedules for activities not already supported by participating countries.
- What parts of the existing ENDF/B and other data systems are to be used?
- What format and what neutron energy range and benchmark neutron spectra are required and available for data development and testing? (II-A)
- Should angular data be required and included and in what format for a limited number of reactions? (II-B)
- What format and what uncertainty data are required? (II-C)
- What format and what standard cross sections are required? (II-C)
- What format and what benchmark neutron field data and documentation are required? (II-C and II-D)
- What format and what are the data processing codes and group structure requirements? (II-E)

III. Recommended Reactions

The more current listings and/or recommendations for neutron reactions for LWR, FBR, and MFR dosimetry applications are given in references 2, 4, 7, 10, 11, 14, 15, 16, and 18. The reader should consult these references for information on individual reactions, energy response ranges, evaluated cross sections, and uncertainty estimates based on the results of differential and integral data development and testing. Table I lists the reaction of interest in order of increasing proton number. The first part of the table contains the non-threshold reactions. The second part lists the threshold reactions. Reactions of interest for differential neutron spectrometry are identified with an asterisk. Angular as well as scaler cross section data are needed for these reactions. The tentative list of reactions in Table I form a more or less complete set of threshold and nonthreshold reactions from which a selection may be made for individual applications.

Table I

Non-threshold Reactions:

REACTION	LWR	FBR	MFR
$^{6}Li(n,total\,He)$	X	X	X
$^{6}Li(n,\alpha)^{3}H(*)$	X	X	X
$^{10}B(n,total\,He)$	X	X	X
(			
$^{13}C(n,\gamma)^{14}C$	X	X	X
$^{23}Na(n,\gamma)^{24}Na$	X	X	X
$^{30}Si(n,\gamma)^{31}Si$	X	X	X
$^{40}Ar(n,\gamma)^{41}Ar$	X	X	X
$^{45}Sc(n,\gamma)^{46}Sc$	X	X	X
$^{50}Cr(n,\gamma)^{51}Cr$	X	X	X
$^{51}V(n,\gamma)^{52}V$	X	X	X
$^{54}Fe(n,\gamma)^{55}Fe$	X	X	X
$^{55}Mn(n,\gamma)^{56}Mn$	X	X	X
$^{58}Fe(n,\gamma)^{59}Fe$	X	X	X
$^{58}Co^{m}(n,\gamma)^{59}Co$	X	(Burn-up correction)	
$^{58}Co(n,\gamma)^{59}Co$	X	X	X
$^{59}Co(n,\gamma)^{60}Co$	X	X	X
$^{63}Cu(n,\gamma)^{64}Cu$	X	X	X
$^{64}Ni(n,\gamma)^{65}Ni$	X	X	X
$^{71}Ga(n,\gamma)^{72}Ga$	X	X	X
$^{75}As(n,\gamma)^{76}As$	X	X	X
$^{80}Se(n,\gamma)^{81}Se$	X	X	X
$^{81}Br(n,\gamma)^{82}Br$	X	X	X
$^{93}Nb(n,\gamma)^{94}Nb$	X	X	X
$^{98}Mo(n,\gamma)^{99}Mo$	X	X	X
$^{100}Mo(n,\gamma)^{101}Mo$	X	X	X
$^{103}Rh(n,\gamma)^{104}Rh$	X	X	X
$^{108}Pd(n,\gamma)^{109}Pd$	X	X	X
$^{109}Ag(n,\gamma)^{110}Ag^{m}$	X	X	X
$^{114}Cd(n,\gamma)^{115}Cd$	X	X	X
$^{115}In(n,\gamma)^{116}In^{m}$	X	X	X
$^{121}Sb(n,\gamma)^{122}Sb$	X	X	X
$^{133}Cs(n,\gamma)^{134}Cs$	X	X	X

REACTION	LWR	FBR	MFR
$^{139}La(n,\gamma)^{140}La$	X	X	X
$^{152}Sm(n,\gamma)^{152}Sm^{m}$	X	X	X
$^{151}Eu(n,\gamma)^{152}Eu^{m}$	X		
$^{164}Dy(n,\gamma)^{165}Dy$	X		
$^{175}Lu(n,\gamma)^{176}Lu$	X		
$^{176}Lu(n,\gamma)^{177}Lu$	X		
$^{181}Ta(n,\gamma)^{182}Ta$	X		
$^{186}W(n,\gamma)^{187}W$	X		
$^{197}Au(n,\gamma)^{198}Au$	X	X	X
$^{232}Th(n,\gamma)^{233}Th$	X	X	X
$^{233}U(n,f)$ F.P.	X	X	X
$^{235}U(n,f)$ F.P.	X	X	X
$^{238}U(n,\gamma)^{239}U$	X	X	X
$^{239}Pu(n,f)$ F.P.	X	X	X

Table I (Continued)

Threshold Reactions:

REACTION	LWR	FBR	MFR
(m,p) (*)	X	X	X
$^{3}He(m,p)$ (*)	X	X	X
$^{14}N(m,p)^{14}C$	X	X	X
$^{19}F(m,2m)^{18}F$			X
$^{23}Na(m,2m)^{22}Na$			X
$^{24}Mg(m,p)^{24}Na$	X	X	X
Al(m,total He)	X	X	X
$^{27}Al(m,p)^{27}Mg$	X	X	X
$^{27}Al(m,\alpha)^{24}Na$	X	X	X
$^{28}Si(m,p)^{28}Al$	X	X	X
$^{31}P(m,p)^{31}Si$	X	X	X
S(m,total He)	X	X	X
$^{32}S(m,p)^{32}P$	X	X	X
$^{34}S(m,\alpha)^{31}Si$	X	X	X
$^{35}Cl(m,\alpha)^{32}P$	X	X	X
$^{45}Sc(m,2m)^{44}Sc^{m}$			X
Ti(m,total He)	X	X	X
$^{46}Ti(m,p)^{46}Sc$	X	X	X
$^{47}Ti(m,p)^{47}Sc$	X	X	X
$^{48}Ti(m,p)^{48}Sc$	X	X	X
Fe(m,total He)	X	X	X
$^{54}Fe(m,p)^{54}Mn$	X	X	X
$^{56}Fe(m,p)^{56}Mn$	X	X	X
$^{54}Fe(m,\alpha)^{51}Cr$	X	X	X
$^{55}Mn(m,2m)^{54}Mn$	X	X	X
$^{59}Co(m,p)^{59}Fe$	X	X	X
$^{59}Co(m,\alpha)^{56}Mn$	X	X	X
$^{59}Co(m,2m)^{58}Co$	X	X	X
Ni(m,total He)	X	X	X
$^{58}Ni(m,p)^{58}Co$	X	X	X
$^{58}Ni(m,\alpha)^{55}Fe$	X	X	X
$^{58}Ni(m,2m)^{57}Ni$	X	X	X
$^{60}Ni(m,p)^{60}Co$	X	X	X
Cu(m,total He)	X	X	X

REACTION	LWR	FBR	MFR
$^{63}Cu(m,\alpha)^{60}Co$	X	X	X
$^{63}Cu(m,2m)^{62}Cu$	X	X	X
$^{65}Cu(m,p)^{65}Ni$	X	X	X
$^{65}Cu(m,2m)^{64}Cu$	X	X	X
$^{64}Zn(m,p)^{64}Cu$	X	X	X
$^{64}Zn(m,2m)^{63}Zn$			X
$^{90}Zr(m,2m)^{89}Zr$			X
$^{93}Nb(m,m')^{93}Nb^{m}$	X	X	X
$^{93}Nb(m,2m)^{92}Nb$			X
$^{92}Mo(m,p)^{92}Nb$	X	X	X
$^{94}Mo(m,p)^{94}Nb$	X	X	X
$^{103}Rh(m,m')^{103}Rh^{m}$	X	X	X
$^{115}In(m,m')^{115}In^{m}$	X	X	X
$^{127}I(m,2m)^{126}I$	X	X	X
$^{197}Au(m,2m)^{196}Au$			X
$^{197}Au(m,3m)^{195}Au$			X
$^{197}Au(m,4m)^{194}Au$			X
Au (total He)	X	X	X
$^{199}Hg(m,m')^{199}Hg^{m}$	X	X	X
$^{232}Th(m,f)$ F.P	X	X	X
$^{238}U(m,f)$ F.P	X	X	X
$^{238}U(m,2m)$ F.P			X
$^{237}Np(m,f)$ F.P	X	X	X
$^{234}U(m,f)$ F.P	X	X	X
$^{236}U(m,f)$ F.P	X	X	X

References

(1) "Proceedings of the First ASTM-Euratom Symposium on Reactor Dosimetry," Petten, Netherlands, September 22-26, 1975. Report EUR 5667 elf, Parts I and II (1977).

(2) "Proceedings of the Second ASTM-Euratom Symposium on Reactor Dosimetry," Palo Alto, California, USA, October 3-7, 1977. Report NUREG/CP-0004, Volumes I, II, and III (1977).

(3) Proceedings of a "Consultants' Meeting on Nuclear Data for Reactor Dosimetry," Vienna, Austria, September 10-12, 1973. Compiled by M. F. Vlasov and C. L. Dunford, Report INDC (NDS)-56/U, IAEA (1973).

(4) Proceedings of a "Consultants' Meeting on Integral Cross-Section Measurements in Standard Neutron Fields for Reactor Dosimetry," Vienna, Austria, November 15-19, 1976. Compiled by M. F. Vlasov, Report IAEA-208 (1978).

(5) Proceedings of a meeting on "A Review of Radiation Energy Spectra Unfolding," compiled by D. K. Trubey, ORNL/RSIC-40 (1977).

(6) Proceedings of an "International Specialists' Symposium on Neutron Standards and Applications," National Bureau of Standards, March 28-31, 1977, NBS Special Publication 493, (1977).

(7) Proceedings of the "Symposium on Neutron Cross Sections 10-40 MeV," Brookhaven National Laboratory, May 3-5, 1977, BNL-NCS-50681, (1977).

(8) F.B.K. Kam, G. Guthrie, and B.F. Maskewitz, "Summary Report: Conclusions and Recommendations of the IAEA Technical Committee Meeting on Current Status of Neutron Spectrum Unfolding," Proceedings of the IAEA Technical Committee Meeting, Oct 10-12, 1977 Oak Ridge, Tennessee, USA.

(9) Proceedings of the Conference on Theory and Applications of Uncertainty Analysis, Oak Ridge, Tennessee, August 22-24, (1978).

(10) W. N. McElroy, et.al, Special Series, Nucl, Techn. 25, 177-422 (1975).

(11) W. L. Zijp and H. J. Nolthenius, "Progress Report: Intercomparison of Unfolding Procedures (Programs and Libraries)," in Reference 5.

(12) M.F. Vlasov, "Comments on Excitation Functions of Threshold Reactions Used in Reactor Neutron Dosimetry, in Reference 4, p.353 (1976).

(13) M. F. Vlasov, A. Fabry, and W. N. McElroy "Status of Neutron Cross Sections for Reactor Dosimetry,"in Proceedings of the International Conference on the Interactions of Neutrons with Nuclei, Lowell, Mass. USA, July 1976, 2, p.1187.

(14) B. A. Magurno, Editor, "ENDF/B-IV Dosimetry File." Report BNL-NCS-50446/NEACRP-L-145/ENDF-216 (1975).

(15) B. A. Magurno, "ENDF/B Dosimetry File for Version V," in Reference 4, p. 375 (1976).

(16) SAFE Subcommittee of the Cross Section Evaluation Working Group, Presented by L. Stewart, "Status of ENDF/B Special Applications Files," in Reference 2.

(17) F. G. Perey, "Uncertainty Analysis of Dosimetry Spectrum Unfolding," in Reference 2.

(18) 1978 Annual Book of ASTM Standards, Part 45, Nuclear Standards, American Society for Testing and Materials, 1916 Race St., Philadelphia, PA 19103, USA.

Neutron Fields available at the National Physical Laboratory and the need for Low Energy Neutron Standards.

E.J.AXTON and A.G.BARDELL
National Physical Laboratory, Teddington, Middlesex

The first part of this paper gives a brief description of the neutron standards facilities available at NPL. The facilities were described more fully at the 1966 and 1972 Symposia on Neutron Monitoring (1,2).

Fast neutrons are produced in a low scatter environment by means of 3.8 MV Van de Graaff and 150 kV SAMES accelerators which are used to bombard targets situated more than six metres from the floor, walls, or ceiling. Table 1 shows the neutron energies available, the methods of absolute measurement and the secondary standard instruments used to measure the fluence in calibration or intercomparison experiments, together with an estimate of the overall uncertainty at the 99% confidence level.

Another 150 kV accelerator has been installed recently to provide a collimated beam of 14MeV neutrons of high intensity suitable for the calibration of dosemeters used in neutron radiotherapy. Five circular beam sizes are available, the middle one of which is the standard treatment field size of 10 cm at 80 cm from the target. At this distance, with a target emmission rate of 10^{11} neutrons per second the dose rate will be about 5mGy (0.5 rads).min^{-1}. It will be possible to transport the beam from the Van de Graaff accelerator to the same target position in order to produce a change of spectrum in the collimated beam.

In addition to the fast neutron facilities, a number of moderating assemblies have been built for special purposes. The first of these, the standard thermal neutron flux (3), is a large graphite block containing two Be(d,n) neutron sources placed at about 50 cm. either side of the centre. The deuteron beam is servo-controlled by electrostatic deflector systems controlled by signals from neutron detectors in the moderator in such a way as to equalize the two neutron sources and to stabilize the neutron flux at the central measurement position to a level determined by a pre-set reference voltage (the demand level). The neutron field in the central 150 cm cavity has zero

gradient, is well thermalized, is reproducible to ± 0.1%, and is continuously variable from 10^4 to $3x10^7$ $n.cm^{-2}.s^{-1}$. The epithermal component of the neutron density amounts to about 1% of the total, and the spectrum is well described by the $E^{-1.05}$ law. The facility is suitable for the calibration of foils and small neutron detectors.

For the calibration of larger detectors such as long counters, moderating spheres, or rem-meters a thermal beam is used (the thermal column). Two layers of graphite are removed from the pile above one of the Be targets, and a cadmium lined cylindrical column is erected. The column, which is 1000 cm^2 in area, is closed at each end by aluminium windows 0.16 cm thick , and evacuated. The length is variable in steps of 50 cm from 150 cm to 300 cm. The thermal neutron fluence is found to obey the inverse square law, after correction for air attenuation above the top of the column, when the distance is measured from the bottom of the column. The flux level is continuously variable from 50 to 20000 $n.cm^{-2}.sec^{-1}$ at the window for a column length of 150 cm. The epithermal component of the neutron density amounts to about 2% of the total. Since cadmium difference measurements are required to obtain the thermal neutron response the facility is suitable only for those instruments which can be accurately read (eg digital output) in those cases where the small difference between two nearly equal measurements is involved. The spectrum of the fast neutron component of the beam is not known accurately at present, but it is reproducible, and contains neutron energies up to the mean source energy of about 3 MeV. A small component extends to 6MeV. The spectrum will be discussed in more detail in the second part of this paper.

The second moderating assembly consists of a cylindrical water tank two metres in diameter and two metres high with a single servo-controlled Be(d,n) neutron source at the centre. Foil samples can be irradiated in an intense slowing down flux close to the target on a rotating wheel, and compared with standard gold and manganese foils to measure resonance activation integrals. The spectrum of the slowing down neutrons is known to be accurately 1/E in shape at least over the energy range where activation integral measurements are possible (4).

The third moderating assembly is associated with the demand for low energy standards which are important in protection dosimetry. If the spectrum of neutrons leaking from a power reactor is taken to be 1/E in shape, then the spectrum is rectangular when plotted in logarithmic or lethargy units. There are 18 units of lethargy in the range from thermal to 2 MeV, the mean energy of the fission neutrons. Of these, 13.6 are

below 20 keV. Thus 75% of the flux is in an energy region where no calibration facilities are available. One method of producing neutrons in this energy region is to use the slowing down component of the beam from the thermal column described above. The thermal neutrons are first filtered out with cadmium, and the remaining neutrons successively attenuated with slabs of a 1/v absorber of known cross section. Boron-10 is suitable for this purpose. Figure 1 shows the difference spectra of the neutron flux for various combinations of absorber thickness, whilst figure 2 shows these spectra converted to neutron dose equivalent by means of the ICRU dose-fluence curve (5). The bumps towards the high energy end are due to the sharp rise in the dose fluence curve above 10 keV. To reduce these bumps a system is being constructed utilizing the Li(p,n) reaction to produce neutrons of energy up to about 100 keV which will be moderated by a small water bath from which a neutron beam may be extracted. An instrument can then be calibrated by making filter difference measurements with the instrument and with a calibrated BF_3 counter. The spectrum shape is calculated whilst the total neutron density is derived from the BF_3 counter response. With sufficient intensity in the slowing down spectrum the technique can be extended to other materials. For example, a gold absorber would give a difference spectrum of 4.9 eV neutrons due to the large principal gold resonance at this energy.

The second part of this paper deals with an assessment of the need for low energy neutron standards, by which is meant standards of fluence, dose or dose equivalent in the energy range between thermal and 30keV. There are two schools of thought on this subject. On the one hand, in a typical moderated fast neutron spectrum two thirds of the fluence might be expected to be in an energy range where no standards exist. Moreover there are circumstances in which metrologists attribute a significant proportion of the total neutron dose equivalent to the low energy region. Such results are usually obtained by subtracting a fast neutron contribution measured with one instrument from a total neutron contribution measured with another, and they indicate a rather unusual neutron spectrum! On the other hand it has been argued that no plausible neutron spectrum could be envisaged in which this situation would occur. In a 1/E shaped spectrum 70% of the neutron dose equivalent is due to neutrons of energy greater than 100keV, and 80% above 10keV. At a given point in a moderator or shield the low energy neutrons can only be generated by the remaining high energy neutrons, and the apparent low

energy contribution would have to be attributed to deficiencies in the instrument calibrations. In his summing up after the 1972 IAEA Conference on Neutron Monitoring (6) John Auxier said (of the albedo dosimeter) ' To me it seems fundamentally unsound to base a monitoring system on a detector system which has its greatest sensitivity in the energy range which contributes least to the dose and vice versa.' The question is, does this energy range always contribute least to the dose? It appeared that one needed low energy standards in order to determine whether one needed low energy standards.

For this reason the Li(p,n) reaction based moderating system described above was designed and built. However at this point a change of direction occurred and the Van de Graaff accelerator was closed down for conversion to optional pulsed operation. In the meantime, multi-sphere spectrometry was being developed as a means of assessing the dose equivalent likely to be received by a patient undergoing high energy X-radiotherapy as a result of unwanted neutrons in the beam (7). As it was likely to be some considerable time before the low energy source could be developed further it was decided to use the sphere technology to confirm or deny the need for the low energy source.

A typical site associated with the power station at Berkeley was selected by John Harvey of Berkeley Nuclear Laboratories as being likely, based on previous measurement, to have a significant low energy contribution to the neutron dose equivalent. Polyethylene spheres of diameter 2, 3, 5, 8, and 10 inches each containing a gold foil at the centre as a thermal neutron detector were irradiated at this site. Gold foils were chosen for the radiotherapy application rather than a dynamic counting device as they are completely stable and reproducible, independent of electronic drifts, and suitable for use in pulsed beams. Furthermore the response to photons is zero below the threshold for photoneutron production at 8MeV, and because of the small amount of gold present (100mg) almost so above this threshold. Even if a small amount of Au-196 is produced it can be separated out by its half life. Finally the half life of Au-198 is sufficiently long to allow the foils to be returned for measurement in the NPL low background anti-coincidence counter. The major drawback of these detectors for some applications is their low sensitivity. It was decided to use the same detectors for the current application.

Figure 3 shows the saturation counting rate recorded in the gold foils as a function of sphere size following irradiation at the Berkeley site. The curves are normalized to unity for the sphere giving the

maximum response. Also shown are similar curves obtained with various monoenergetic neutron fields, with Am-Be, Cf fission, and Sb-Be neutron sources, and with the NPL thermal column. It is immediately obvious even without knowing anything about the calibration factors of the spheres as a function of neutron energy, that the neutron spectrum at the Berkeley site is heavily weighted by low energy neutrons, softer even than the pseudo-monoenergetic 22.8keV antimony-beryllium spectrum, but with a suggestion of some higher energy neutrons in the tail.

Some attempts have been made to assess the neutron spectrum and hence the dose equivalent in some broad energy bands, but it should be emphasised that the results are not final as the work is still in progress. The sphere efficiency is defined as the saturation disintegration rate (equal to the neutron capture rate) per mg. of gold foil per unit fluence. Sphere efficiencies have been calculated by a Monte Carlo technique in which the energy scale is divided into logarithmic bins, five to a decade. The program also records, for each bin, the thermal neutron fluence and the Wescott epithermal flux parameter r, so that the relevant efficiencies can be determined when other thermal neutron detectors are placed at the centre of the spheres. The Monte Carlo calculations did not extend beyond 5MeV because the computing power available did not cater for the inelastic scattering in carbon. There are now several sets of efficiency computations published in the literature which show general agreement in the shapes above 5MeV, although there are wide differences at lower energies. These shapes were therefore used to extend the calibration by a further two bins. Figure 4 shows how the efficiency varies with sphere size. The spheres were calibrated with thermal neutrons from the NPL thermal column, with Sb-Be neutrons, and with some monoenergetic keV energies, the results indicating that the calculation could be 10 or in some cases even 15% too high.

Other calibrations in which the gold foil was replaced by an enriched Li-6 scintillator connected to a photomultiplier by a light pipe are less reliable. The detector is almost black and the Wescott formulation does not apply, which makes the conversion to equivalent gold foil activity suspect particularly for small sphere sizes. These calibration figures need further attention. Further work is required to finalize the efficiency matrix but for the purposes of the dosimetry which follows energy and sphere size dependent adjustments of up to 15% have been made to the efficiency matrix.

One way to derive fluence spectra is to solve a set of Fredholm equations such as:

$$\sum \psi_j \epsilon_{ij} = B_i$$

Where ψ_j is the neutron fluence in the $j^{th.}$ energy bin, ϵ_{ij} is the sphere efficiency for the $i^{th.}$ sphere for the mean energy of the $j^{th.}$ bin, and B_i is the saturation count rate for the $i^{th.}$ sphere. For the Berkeley spectrum i = 5 and 36 bins covered the energy range from the cadmium cut off energy to about 7.9MeV. With 5 equations and 36 unknown bin fluences the equations are under - determined and therefore have an infinite number of solutions. The task is to introduce constraints which lead to particular unique plausible solutions. By means of cadmium difference measurements with bare gold and manganese foils the fluence per unit lethargy at 4.9eV and 337eV (bins 4 and 14) was determined. The fact that the fluence is the same in these two bins is an indication that the shape may be close to 1/E in this energy region. It is convenient to normalize the results to unit fluence in these bins. A further constraint was that ψ_j should be non-negative.

Smoothing is introduced by minimizing an objective function by quadratic programming to achieve a unique solution. Figures 5 and 6 show this technique applied to the spectrum in the NPL thermal column. Function 1 minimizes the difference between the spectrum and an initial guess (F_j) as shown in tables 2 and 3. Function 2 minimizes the deviations from a straight line through any three consecutive points. Function 3 minimizes the deviation from a quadratic through any four consecutive points. It was found from experience that the equations should be re-written as inequalities so that the calculated gold count rates could deviate from the measured values by up to a certain specified tolerance, thereby allowing for errors in the measurements and uncertainties in the efficiency matrix. The near equality of the flux at the gold and manganese resonance energies suggests a 1/E shape up to about 400ev, so function 4 fits the data above bin 14 using an equally weighted combination of functions 2 and 3, with unity in bin 14 and below. Function 5 is similar to function 4 except that the constant in the lower bins, instead of being unity is allowed to float. It turns out to be 1.045, in good agreement with the expected value. Function 1 with F_j equal to 1 minimises the deviations from the 1/E shape. With zero tolerance this function gave an unlikely spectrum with lots of zeros and spikes. The spectrum with a tolerance of 6% is shown in figure 6. From

the calculated spectra the contributions to the dose-equivalent rate from three energy ranges were calculated. These are from the cadmium cut-off to 10keV where the dose-equivalent per unit flux is low and fairly constant, 10keV to 100keV where the curve is changing rapidly, and above 100keV where the curve is high and fairly constant. The normalized dose equivalent rates for various functions are shown in table 2 together with the rates expected from a spectrum with a 1/E shape up to 6MeV. It can be concluded that the spectrum behaves dosimetrically as if it were 1/E in shape.

Figures 6 and 7 show similar normalized results for the spectrum at the Berkeley site. Again, the flux per unit lethargy interval at the gold and manganese resonance energies were found to be nearly equal, and the results were normalized for convenience to unit flux in these two bins. Results for functions 2 and 3 are in reasonable agreement except where the tolerance is zero. Function 1 again gave spiky results with zero tolerance. The spectrum obtained with a tolerance of 6% is shown in figure 6. Function 4 results are unrealistic, and give zero contribution above 100 keV. The function 5 spectrum is good looking, but gives a flux at the gold and manganese resonance energies some 25% higher than measured. Table 3 shows the dose equivalent rates calculated from the various derived spectra. The fact that such different looking spectra produce a fairly uniform dosimetry pattern follows from the constancy of the dose-fluence conversion below bin 25. Neutrons may be moved around at will in this region without affecting the estimate of the dose-equivalent.

A common feature to these solutions is that they all show that about 60% of the dose equivalent is attributable to the region below 10keV as would be expected from the shapes shown in figure 3. No more than one third is contributed by neutrons with energies above 100keV. It is very unlikely that this conclusion could be changed by any plausible corrections to the efficiency matrix. It is not easy to understand how such a neutron spectrum comes to exist. It was suggested by John Williams of the University of London Reactor Centre that it may be described by an approximation to a 1/E spectrum arising from a low source energy determined by a window in a cross section such as iron. He also pointed out that it is very similar to the spectrum which we are attempting to produce with our Li(p,n) moderated source described in part one of this paper.

In conclusion, here at Berkeley is a situation where the neutron dose equivalent is undoubtedly determined predominantly by the low energy neutrons. Provided it is sufficiently accessible and reproducible, perhaps this site could be used as a ready made calibrated low energy standard until a more suitable one evolves.

Acknowledgements.

Our thanks are due to Dr.W.Murray and Ms.E.Long for their valuable help in suggesting the objective functions and in calculating the spectra, and to Dr.J.B.Hunt for the sphere calibrations with monoenergetic neutrons. We are grateful to Dr.J.Harvey for selecting the Berkeley site and undertaking the task of arranging the sphere irradiations at weekly intervals over a long period and returning the gold foils to us after each irradiation. Mr.S.J.Felgate measured the foil activities, and also spent many months running the Monte Carlo computations.

References.

1. E.J.Axton, J.C.Robertson, and T.B.Ryves. Neutron Monitoring, 669 - 678, I.A.E.A. Vienna 1967.

2. E.J.Axton, J.B.Hunt, J.C.Robertson, and T.B.Ryves. Neutron Monitoring for Radiation Protection Purposes, 431 - 439. I.A.E.A. Vienna, 1973.

3. T.B.Ryves, and E.B.Paul. Journal of Nuclear Energy. 22 759 - 775 1968.

4. T.B.Ryves, and K.J.Zieba. Journal of Physics A. Math. Nucl. Gen.7 2318 - 2332, 1974.

5. I.C.R.U. Report No. 20. Page 4. October 1971.

6. Reference 2. Page 497.

7. E.J.Axton, and A.G.Bardell. Physics in Medicine and Biology, 17 293 - 298, 1972.

8. T.B.Ryves, P.Kolkowski, and K.J.Zieba. Metrologia, 14, 127 - 135, 1978.

9. T.B.Ryves. Nuclear Instruments and Methods, 135, 455 - 458, 1976.

10. J.C.Robertson, T.B.Ryves, and J.B.Hunt. Journal of Nuclear Energy.26 507 - 515, 1972.

11. J.B.Hunt. N.P.L. Report RS5. April 1976.

12. J.B.Hunt, and R.A.Mercer. Absolute Calibration of the Long Counter by the Associated Activity Method. To be published in Nuclear Instruments and Methods.

13. J.C.Robertson, B.N.Audric, and P.Kolkowski. Journal of Nuclear Energy,27 139 - 149 1973.

Figure Captions.

1. Difference neutron flux spectra produced by 1/v absorbers in a 1/E shaped flux.

2. Difference neutron dose equivalent spectra produced by 1/v absorbers in a 1/E flux.

3. Gold foil count rates as a function of sphere diameter for different neutron spectra. Normalized to unity for the sphere with the highest response.

4. Monte Carlo calculations of sphere responses as a function of neutron energy.

5. Derived spectra for the N.P.L. thermal column with functions 2 - 5. Normalized to unit flux density per bin.

6. Derived spectra for the thermal column and the Berkeley site with function 1. Normalized to unit flux density per bin.

7. Derived spectra for the Berkeley site with functions 2 - 5. Normalized to unit flux density per bin.

TABLE 1.

Mono - Energetic Fast Neutron Standards.

Energy Range MeV	Reaction	Absolute Methods	Secondary Standards	Percentage Uncertainty at 99% Confidence	Additional References
0.03 - 0.60	$^{7}Li(p,n)$	Calibrated Radioactive Neutron Sources. Collimated Vanadium Bath. Hydrogen Proportional Counter.	Long Counter.	3.5	10 11
0.6 - 2.8	$^{3}H(p,n)$	Calibrated Radioactive Neutron Sources. Associated Activity. Hydrogen Proportional Counter.	Long Counter.	3.5	12
3.5 - 6.5	$^{2}H(d,n)$	Calibrated Radioactive Neutron Sources. Proton Telescope.	Long Counter.	4 - 5	
12 - 19	$^{3}H(d,n)$	Proton Telescope. Associated Particle Counter.	Fe(n,p) Reaction.	2.5 - 3.5	8 9 13

Table 2. Thermal Column Dose Equivalent Rate. mrem/hr. Normalised as described in the text.

	Function	Tol	Cd-10k	10-100k	>100k	TOTAL
1	$\Sigma(\Psi_j - F_j)^2$	6%	0.093	0.031	0.838	0.962
2	$\Sigma(\Psi_{j+1} - 2\Psi_j + \Psi_{j-1})^2$	0%	0.086	0	0.920	1.006
		3%	0.081	0.032	0.867	0.980
		6%	0.092	0.034	0.838	0.964
3	$\Sigma(\Psi_{j+2} - 3\Psi_{j+1} + 3\Psi_j - \Psi_{j-1})^2$	4%	0.083	0.040	0.841	0.964
		6%	0.092	0.035	0.831	0.958
4	2 + 3. Unity below bin 14	10%	0.094	0.041	0.655	0.790
5	2 + 3. Constant below bin 14	5%	0.094	0.017	0.866	0.977
		7%	0.096	0.030	0.829	0.955
		10%	0.092	0.038	0.782	0.912
	1/E to 6 MeV		0.088	0.040	0.826	0.954

Table 3. Berkeley Dose Equivalent Rate. mrem/hr. Normalised as described in the text.

	Function	Tol	Cd-10k	10-100k	>100k	TOTAL
1	$\Sigma(\Psi_j - F_j)^2$	6%	0.110	0.027	0.088	0.225
2	$\Sigma(\Psi_{j+1} - 2\Psi_j + \Psi_{j-1})^2$	0%	0.135	0.003	0.081	0.218
		3%	0.120	0.025	0.018	0.164
		6%	0.115	0.029	0.028	0.173
3	$\Sigma(\Psi_{j+2} - 3\Psi_{j+1} + 3\Psi_j - \Psi_{j-1})^2$	5%	0.121	0.034	0.028	0.183
		6%	0.120	0.036	0.039	0.195
4	2 + 3. Unity below bin 14	4%	0.129	0.001	0	0.130
5	2 + 3. Constant below bin 14	5%	0.117	0.020	0.038	0.175
		7%	0.114	0.029	0.059	0.202
		10%	0.110	0.024	0.095	0.229

FIGURE 1

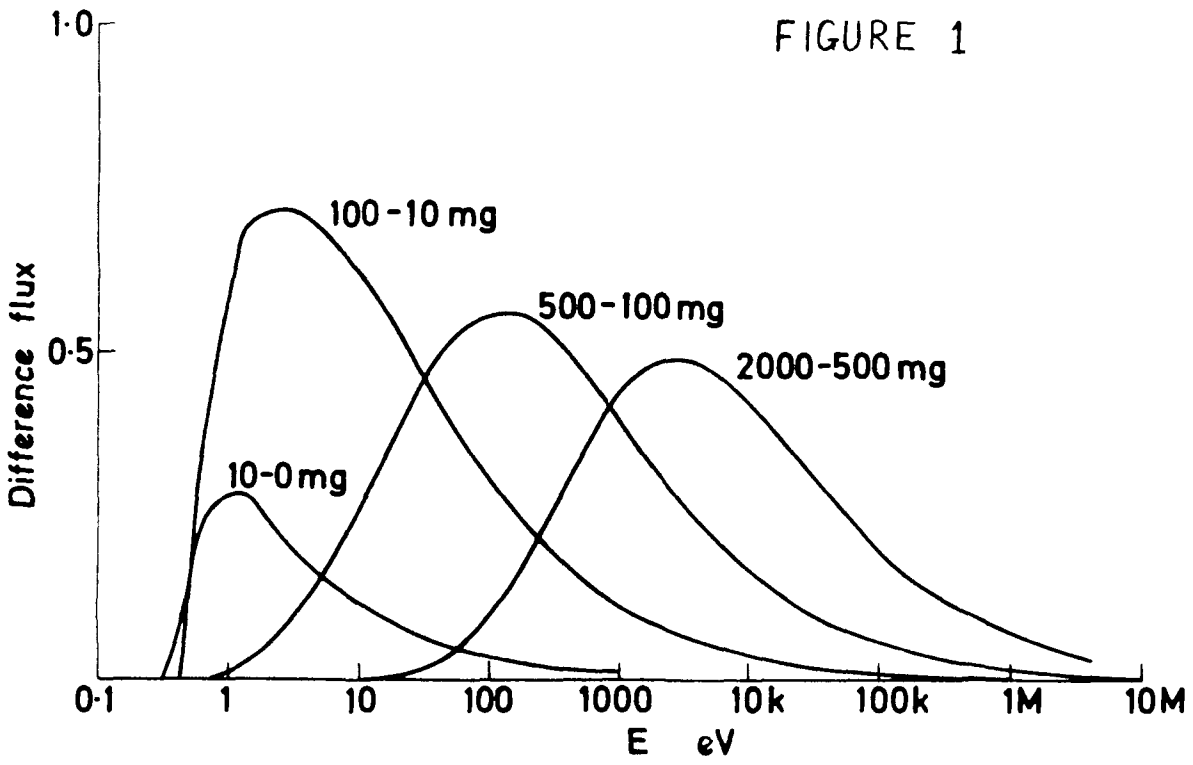

DIFFERENCE NEUTRON FLUX DENSITY SPECTRA FOR NEUTRONS ABSORBED IN SLABS OF ^{10}B

FIGURE 2

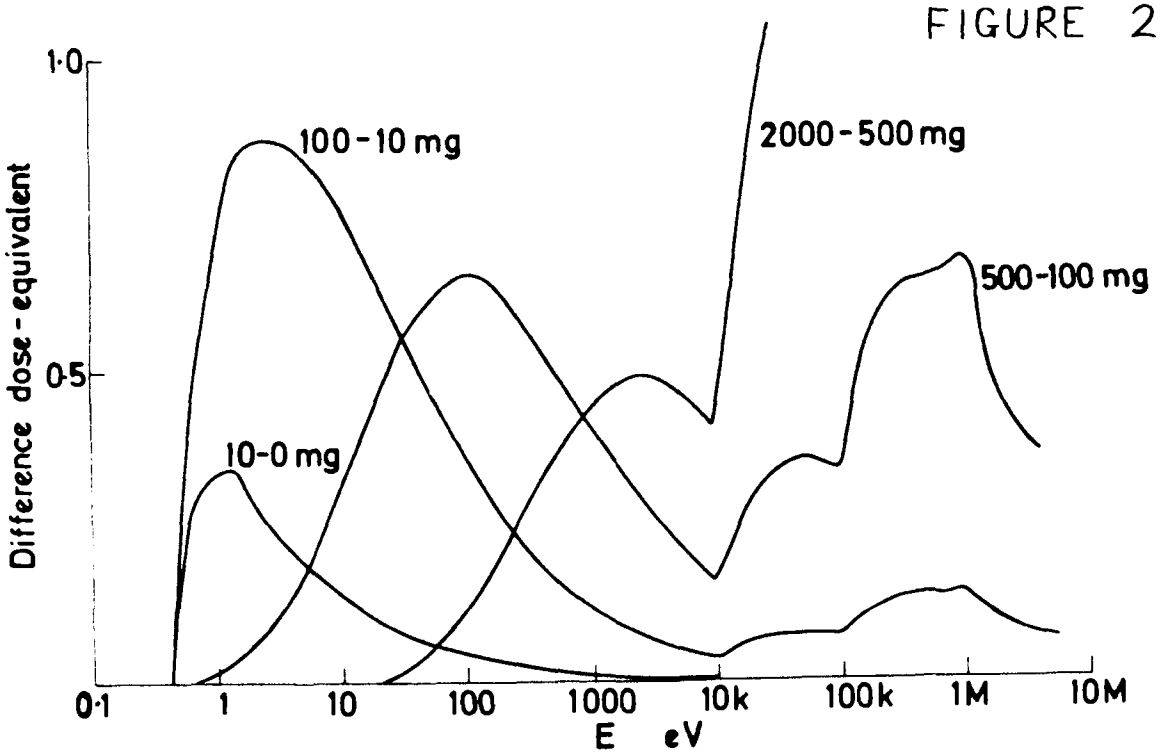

DIFFERENCE NEUTRON DOSE-EQUIVALENT SPECTRA FOR NEUTRONS ABSORBED IN SLABS OF ^{10}B

Figure 3.

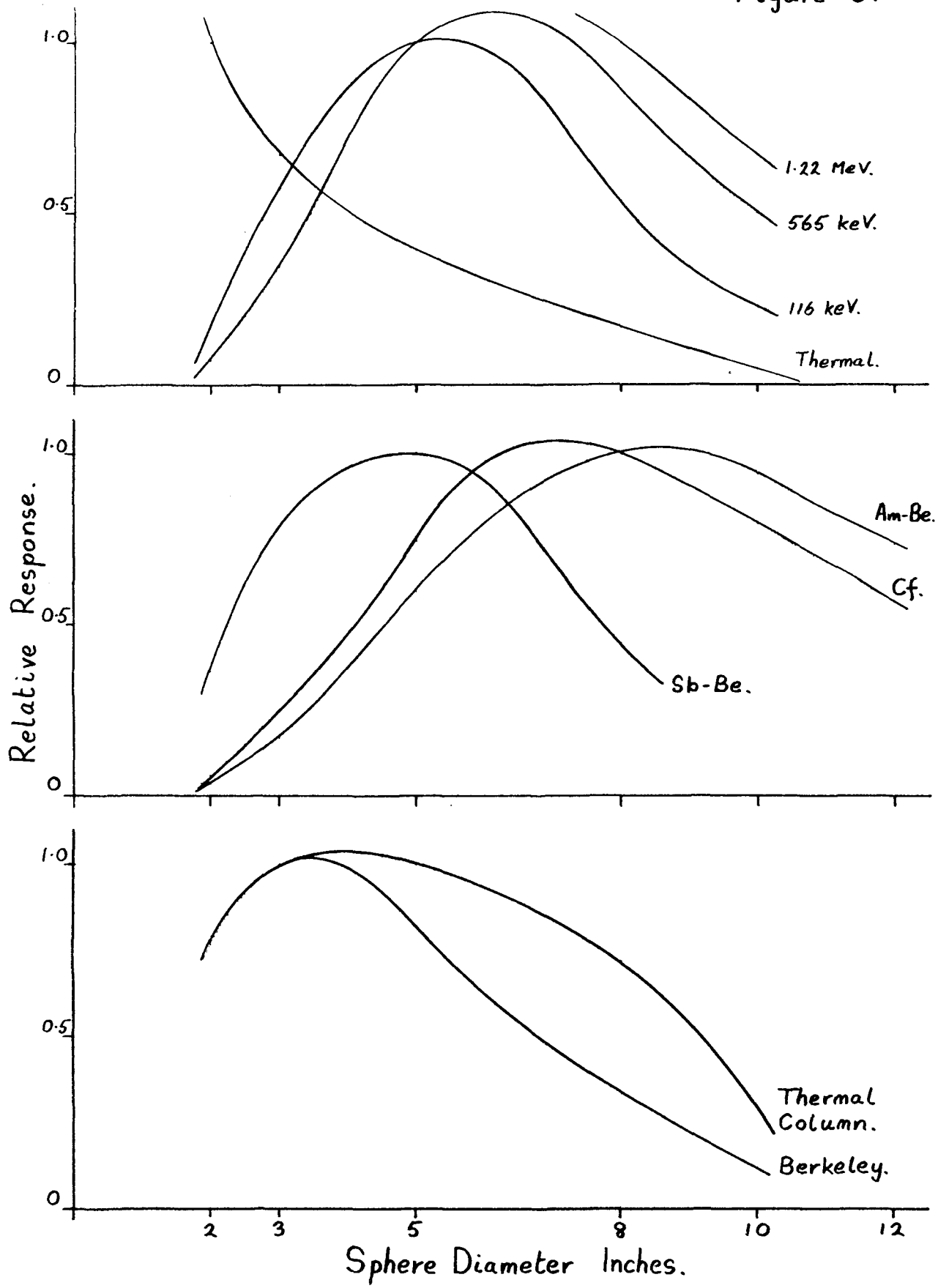
1·0
0·5
0
1·22 MeV.
565 keV.
116 keV.
Thermal.
Relative Response.
Am-Be.
Cf.
Sb-Be.
Thermal Column.
Berkeley.
2
3
5
8
10
12
Sphere Diameter Inches.

FIGURE 4

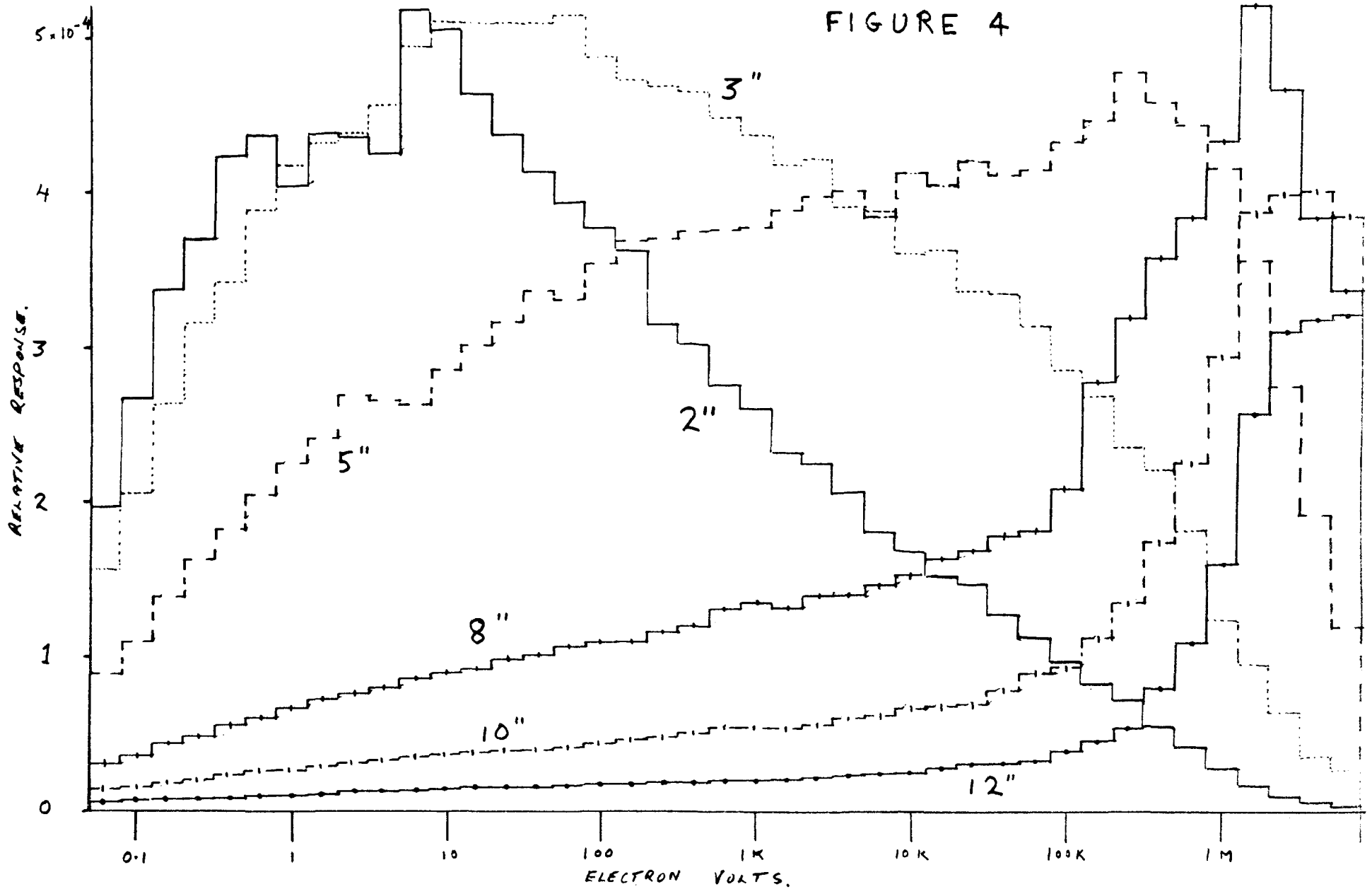
5 x 10⁻⁴
4
3
2
1
0
RELATIVE RESPONSE.
3"
2"
5"
8"
10"
12"
0.1
1
10
100
1K
10K
100K
1M
ELECTRON VOLTS.

FIGURE 5 THERMAL COLUMN SPECTRUM

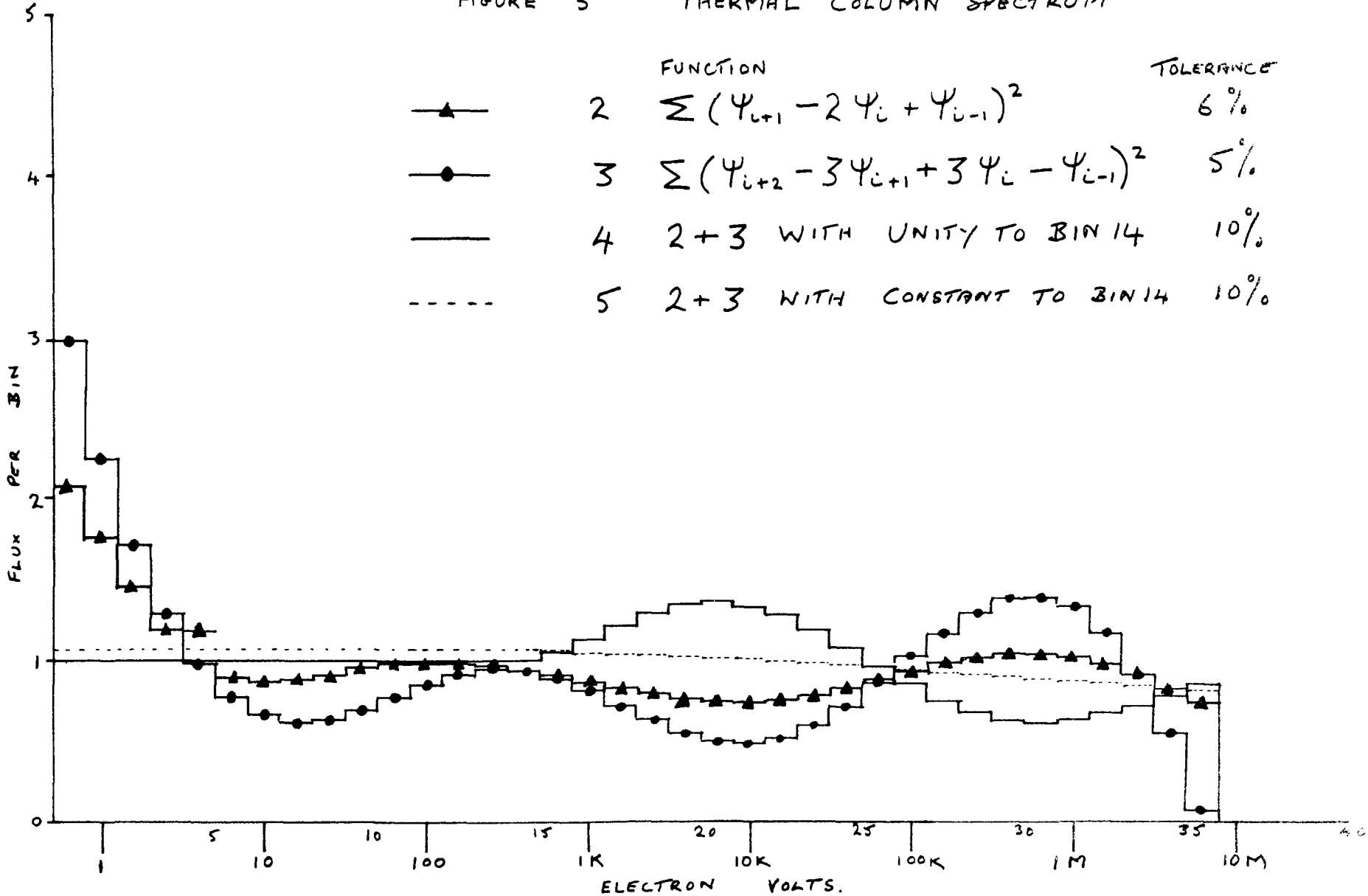

FIGURE 6

FUNCTION 1 $\Sigma (\Psi_j - 1)^2$

THERMAL COLUMN - - -

BERKELEY SITE ———

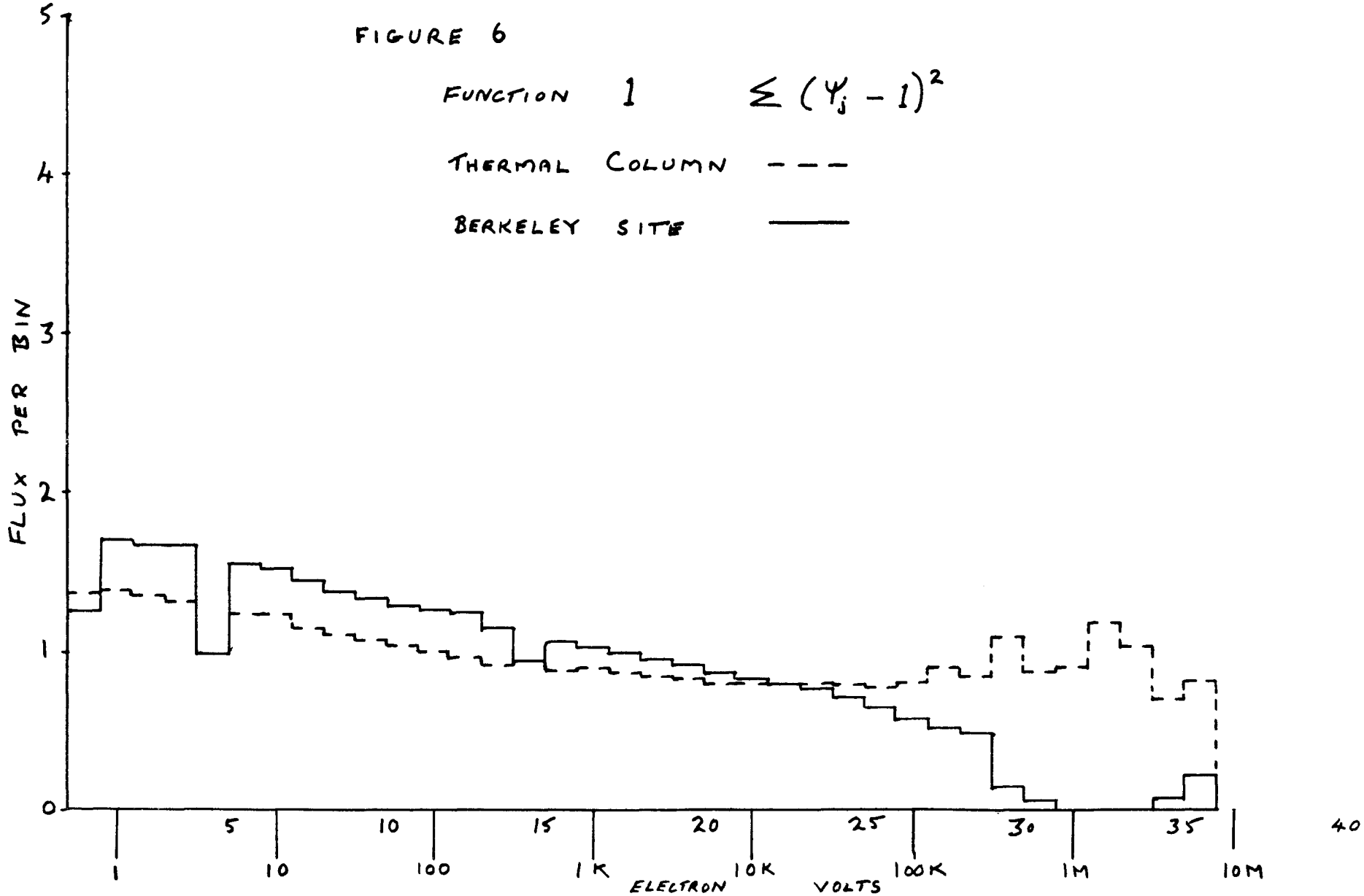

FIGURE 7 . SPECTRUM AT BERKELEY SITE

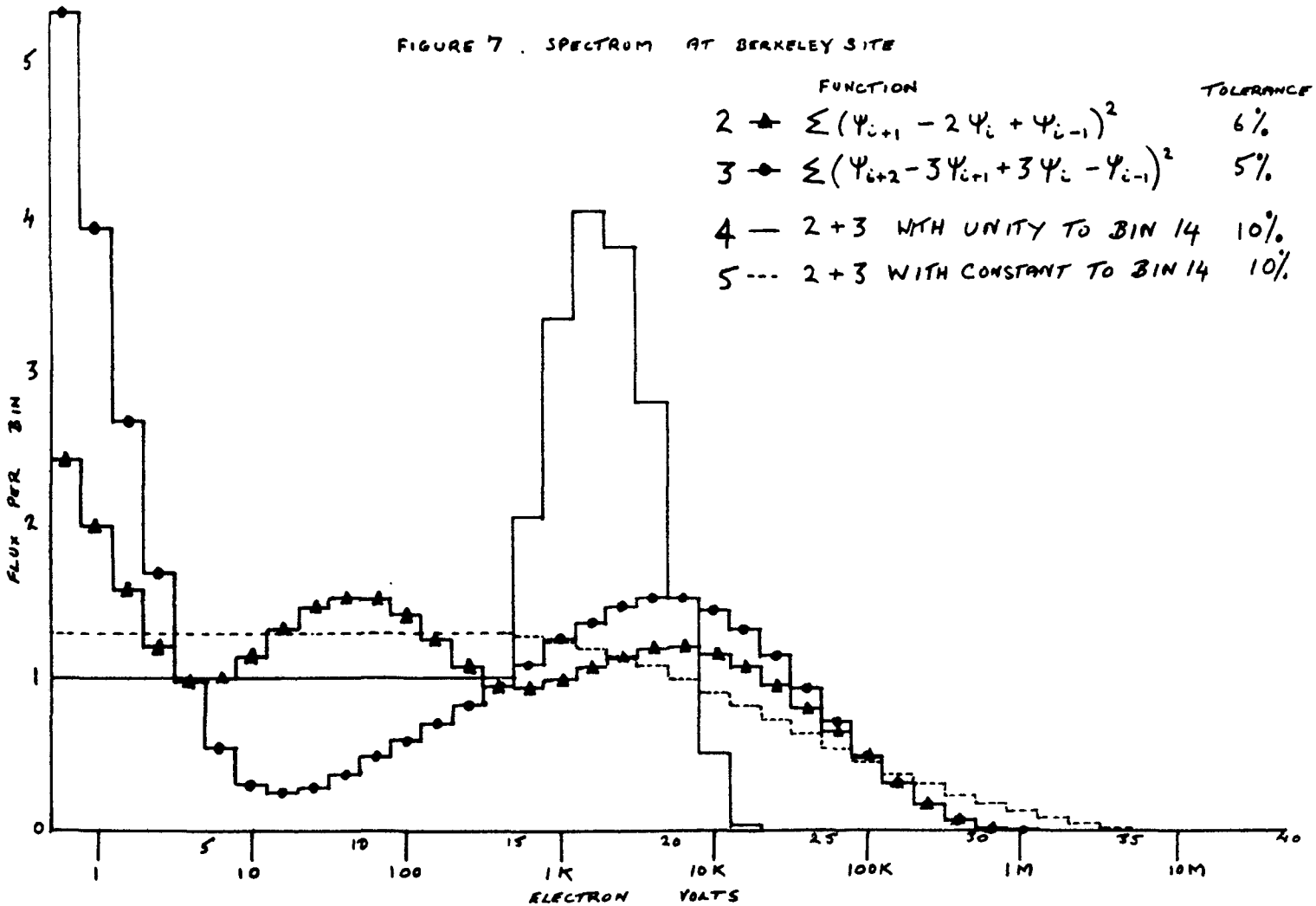

Fast Neutron Standard Fields at the Accelerators of the PTB

M. Cosack, H. Lesiecki, H. Klein, and R. Jahr

Physikalisch-Technische Bundesanstalt (PTB)
D-3300 Braunschweig

Abstract

The PTB techniques for 'monoenergetic' fast neutron standard field production at the Van de Graaff generator are described. Neutron background, photon background, and monitor problems are discussed.

1. General

Two PTB accelerators, a 3.75 MV Van de Graaff generator and a variable energy cyclotron, went into operation in 1975. Though since that time efforts have centered on the setting up of experimental devices and improving the characteristics of the accelerators, two major projects could be carried through. Firstly, we took part in an International Flux Density Intercomparison organized by the B.I.P.M. (ref [1]). Secondly, a 'Technical Seminar on Neutron Dosimetry in Radiation Protection', sponsored by the European Commission was held at the FMRB*) and the PTB's accelerator laboratory. In the course of this seminar, roughly 200 neutron dosimeters of various types from 15 different laboratories of the European Community were calibrated in the accelerator laboratory at neutron energies between 100 keV and 19.0 MeV. In both projects only the Van de Graaff generator was used.

So far, cross sections have not been measured in our laboratory. However, the greater part of our experience in neutron field standardization is also fundamental for cross section measurements.

The main features of our installation were described earlier [2]. A review of the techniques to be applied for measurement of neutron induced cross sections was given by D.L. Smith [3]. The scope of this contribution therefore is restricted to additional remarks on neutron standardization based on experience with our Van de Graaff generator.

---

*) Forschungs- und Meßreaktor Braunschweig

2. Concept of measurements

Two methods were used in order to irradiate a sample or a detector (both called "sample" in the following) with a known neutron fluence.

In the first method the sample was placed at 0° to the ion beam. Since in our case a simultaneous fluence measurement was not possible due to the large mass of the sample, the fluence of neutrons (with the reference energy E_n) was measured before and/or after the irradiation of the sample. Though this concept has obvious advantages [3], a serious problem is the provision of reliable fluence monitors. This is further discussed in sect. 6.

In the second method, the sample and the fluence meter were placed at symmetrical angles, for instance at $\pm$ 20° or $\pm$ 30° to the ion beam. The disadvantages of the stronger dependence of cross sections and neutron energies on angle, different distortions of the neutron field and different backgrounds, are compensated by the advantage of being independent of fluence monitors. This method was chosen for the International Flux Density Intercomparison [1]. Furthermore, this method was always used near the threshold of the reaction $^7Li(p,n)^7Be$, since two different neutron energies may be produced in the 0° direction [4].

3. Fluence meters

Neutron fluence measurements were carried out on the basis of the H(n,n)H cross section using a proportional counter [5] at energies of $E_n \lesssim 2$ MeV and a counter-telescope [6] at $E_n \gtrsim 1$ MeV. For $E_n \approx 1$ MeV both methods were in agreement to within 2 %. Both instruments have spectrometer properties to a certain extent and therefore simultaneously yield a rough information on the neutron spectrum in addition to the neutron fluence.

At present, several sources of systematic errors are being investigated in order to improve the accuracy of the fluence measurements with the proportional counter. Neutrons scattered from the walls of the counter into the sensitive volume cause an E_n-dependent correction

of < 2 % (ref.[7]). The E_n-dependent correction for the interaction of the neutrons with the surrounding air, i.e. attenuation of the neutron beam and scattering of the neutrons into the sensitive volume is being investigated [8]. Furthermore, information on the W_i-values, i.e. the energy expended by a recoil proton to produce one ion pair, is being extracted from the recoil proton spectra at low energies. Fig. 1 shows a pulse height spectrum at E_n = 24 keV. The Monte Carlo fit could possibly still be improved at lower pulse heights by incorporating neutron-gamma discrimination technique [5] into the experiment and including carbon recoil nuclei in the Monte Carlo calculation.

4. Neutron background

In particular when incident deuteron beams are used to produce neutrons, monoenergetic neutrons are not obtained. Fig. 2a shows an intersectional drawing through a Ti(T)-target on a silver backing. The broken lines indicate the ends of the range of deuterons of 0.436 MeV and 1.524 MeV which were used to bombard the target. Afterwards the target was bombarded with 2.587 MeV deuterons and the neutron time-of-flight spectrum was measured with a scintillation detector (fig. 2b). Besides neutrons from the unavoidable reaction Ti(d,n)V one observes the peaks 4 and 5 in fig. 2b which are due to $D(d,n)^3He$ reactions on deuterium self-targets from the previous deuteron irradiations. Even when a target not previously irradiated with deuterons is used, with increasing irradiation time the build-up of a neutron peak corresponding to an energy of 3.6 to 3.7 MeV is observed. This corresponds to $D(d,n)^3He$ reactions near the end of the range of the deuteron beam. Because of these self-target effects, the diameter of the evacuated flight tubes for the ion beam was chosen large enough (10 cm diam.) to prevent the deuterons from hitting the walls.

Though great care was taken to avoid residual hydrocarbon gases in the vacuum (metal seals, vac ion pumps and turbo-molecular pumps), neutrons from the $^{12}C(d,n)^{13}N$ reaction at the target were sometimes

observed. In rare cases, even a build-up of this background with increasing irradiation time was measured. Though the origin of the carbon has not yet been fully investigated, it is obvious, that all these effects require a continuous monitoring of the neutron spectrum from the target (see sect. 6).

Another important background is due to room scattered neutrons. The response of a 20 cm diam. polyethylene sphere detector [1] to these background neutrons was investigated in two different ways. Firstly, the unscattered radiation was absorbed by a shadow cone. Secondly, the deviation of the response from the $1/r^2$-law was measured. The background at a distance of 1.5 m from the target is given in the following table:

E_n	shadow cone	$1/r^2$-law
250 keV	9.3 %	6.4 %
565 keV	4.8 %	4.6 %
2.2 MeV	5.3 %	4.0 %
2.5 MeV	5.2 %	3.6 %

Monte Carlo calculations performed at E_n = 3-4 MeV (with a cut-off neutron energy at 0.5 MeV) predicted a total background of 2 % due to the concrete floor, the walls and the ceiling of the experimental hall and another 2 % due to the revolving gridded sector [11]. The sum of 4 % is in reasonable agreement with the data given above at E_n = 2.5 MeV. The calculated spectral fluence shows a distinct single scattering peak at an energy about 0.7 MeV below E_n.

5. Photon background

If the sample, the neutron fluence meter, or any neutron detector used for monitoring is also sensitive to photons, and if the photon response cannot be discriminated from the neutron response, then the photon fluence must be known for corrections.

There is always a photon background from the target produced by the incoming charged particles or the neutrons. Very high energy gamma rays may be obtained from nucleon capture or inelastic nucleon scattering reactions. For example, the $^{7}Li(p,\gamma)^{8}Be$ reaction yields gamma rays with energies of up to about 20 MeV [12,13].

Photon spectra from the target were measured by means of a Ge(Li) spectrometer. A time-of-flight technique was used to discriminate the photon events from the neutron events. Due to the strong decrease of the Ge(Li) sensitivity with increasing photon energy, the photon fluence at very high energies could not be evaluated quantitatively from the spectra. However, a rough estimation of this component could be obtained by using simultaneously an energy compensated Geiger-Müller counter [14-16], since the detection probability*) of this device increases with increasing photon energy. Results are given elsewhere [14,15].

An investigation of different target backings showed Ag and Ta to be suitable materials in order to achieve low photon yields [14,15].

6. Monitor problems

In general, monitors for at least the following three different quantities are required: The fluence of the reference neutron energy E_n, the neutron background spectrum from the target, and the photon field.

In many cases, the fluence meters described in sect. 3 are best suited as fluence monitors, too.

In other cases, however, if the sample is to be irradiated for a short time only, the uncertainty caused by the counting statistics is too large. The counter telescope, for instance, has a detection probability*) only about 10^{-7} to 10^{-8} at 20 cm from the target.

---

*) here defined as the number of counts divided by 4π times the differential quotient between the number of neutrons emitted from the target and the solid angle.

In these cases an NE 213 liquid scintillation counter is considered to be a good monitor. It has several advantages, e.g.

- good detection probability
- the capability of separating neutron and photon events by pulse shape discrimination
- fast signals which make simultaneous time-of-flight monitoring of the neutron background spectrum possible.

However, without special care the gain and therefore the detection efficiency is unstable. In particular, it depends strongly on the counting rates, and the time constant for adjustment of the gain may be as long as a few days.

The properties of such scintillation counters were therefore carefully investigated. The following results were achieved.

- The use of multiplier tubes with Cu-Be-dynodes (for instance Philips' XP 2000) reduces drifts of the gain due to changing counting rates to values < 1 %.
- A suitable design of the light guide avoids the dependence of the light collection on the locus of the light producing event. An energy resolution of 1 % as a high energy limit is achieved for a 5 cm (diam.) x 5 cm (height) NE 213 scintillator [17]. Such a good resolution improves the reproducibility of the threshold adjustment.
- A precise method of energy calibration by γ-rays was developed. The position of the Compton energy in the spectrum can be determined with uncertainties smaller than 1 % (see ref. [18]).

As mentioned above, the NE-213 liquid scintillator is also well suited to monitor the background spectrum of neutrons from the target if it is used in connection with the time-of-flight method.

For low energy neutrons, however , another fast detector such as a lithium glass scintillator or a "boron slab detector" (ref. [20]) may be necessary.

As a photon monitor, an energy-compensated Geiger-Müller counter[16] was routinely used. This is a simple and stable device with a low neutron sensitivity. The latter must be corrected for. The neutron sensitivity was recently measured in our laboratory for energies 0.1 MeV $\lesssim E_n \lesssim$ 19 MeV [14, 15, 19]. It should be mentioned that the Geiger-Müller counter is rather sensitive to the build-up of carbon layers mentioned in sect. 4, since it measures the 0.511 MeV annihilation γ-radiation produced in the decay of ^{13}N from the reaction $^{12}C(d,n)^{13}N$.

References

1. V.D. Huynh, "International Comparison of Flux Density Measurements for Monoenergetic Fast Neutrons", Proc. of International Specialists Symposium on Neutron Standards and Applications, Washington 28.-31.3.77. NBS Special Publication 493, p. 244.

2. S.R. Wagner in: "Neutron Cross Sections for Reactor Dosimetry", IAEA-208 (1978), Vol. II, p. 15

3. D.L. Smith, ibid., Vol. I, p. 321

4. J.H. Gibbons and H.W. Newson, in "Fast Neutron Physics" Part I, Edit. J.B. Marion and J.L. Fowler, Interscience Publ., New York, London 1960, p. 133

5. M. Cosack, M. Kutscha, and A. Paulsen in: "Proc. First Sympos. on Neutron Dosimetry in Biology and Medicine", Neuherberg/München 15.-19.5.1972, EUR 4896 d-f-e, Vol I, p. 267

6. S.J. Bame, E. Haddad, J.E. Perry, R.K. Smith, Rev. Sci. Instr. 28 (1957) 997

7. D. Schlegel-Bickmann, private communication

8. B. Siebert, private communication

9. W.G. Alberts, M. Cosack, G. Dietze, R. Jahr, H. Kluge, K. Knauf, H. Lesiecki, M. Matzke, H.J. Schuster, S. Wagner, H.W. Zill in "Internat. Sympos. on Advances in Radiation Protection Monitoring", IAEA, Stockholm 26.-30.6.1978 (to be published)

10. W.G. Alberts, Report PTB-FMRB-70 (1978)
Physikalisch-Technische Bundesanstalt

11. G. Dietze, R. Jahr and H. Schölermann, Proc. First Sympos. on Neutron Dosimetry in Biology and Medicine, Neuherberg/München, May 15-19, 1972, EUR 4896 d-e-f, p. 915

12. T. Lauritsen and F. Ajzenberg-Selove, Nucl.Phys. 78 (1966) 1

13. G.A. Fisher, P. Paul, F. Riess, and S.S. Hanna,
Phys.Rev. C 14 (1976) 28

14. S. Guldbakke, R. Jahr, M. Cosack, H. Klein and H. Schölermann, Proc. Third Sympos. on Neutron Dosimetry in Biology and Medicine, Neuherberg/München, May 23-27, 1977, EUR 5848 DE/EN/FR, p. 821

15. R. Jahr, S. Guldbakke, M. Cosack, G. Dietze und H. Klein,
Report PTB-ND-10 (1978), Physikalisch-Technische Bundesanstalt

16. E.B. Wagner and G.S. Hurst, Health Phys. 5 (1961) 20

17. H. Klein and H. Schölermann,
Contribution to the Nuclear Science Symposium on Semiconductor and Scintillation Counters, Oct. 18 - 20, 1978, Washington
(to be published in IEEE-Transactions on Nuclear Science)

18. G. Dietze, ibid. (to be published)

19. H. Klein, S. Guldbakke, R. Jahr, H. Lesiecki
(submitted to Phys. in Med. and Biology)

20. H. Liskien and E. Wattecamps,
Nucl. Sci. and Technology, 68 (1978) 132

Figures

Fig. 1: Curve (1): Recoil proton spectrum from a proportional counter, measured in a 24 keV neutron beam [9,10].

Curve (2): Monte Carlo fit.

Fig. 2: a) Intersectional drawing of a Ti(T)-target on silver backing.

b) Neutron time of flight spectrum from the pre-irradiated target (see text; flight path 7 m; time calibration 0.4 ns/channel).
1: Prompt gamma peak;
1': Uncorrelated gamma background;
2: 19 MeV neutrons from $T(d,n)^3He$;
3: Neutrons from Ti(d,n)V;
4 and 5: Neutrons from $D(d,n)^3He$ from deuterium self-targets.

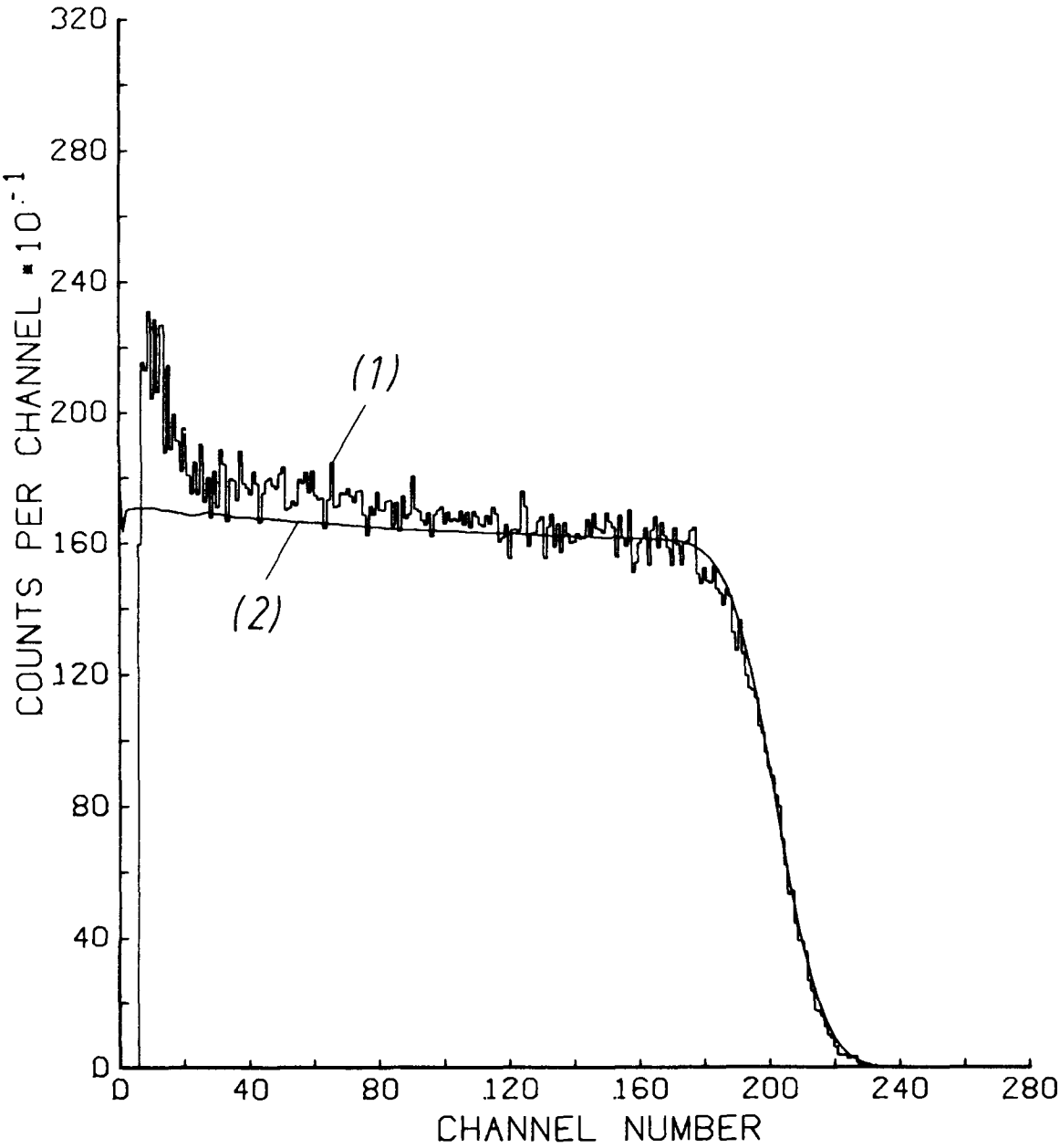
320
280
240
200
160
120
80
40
0
COUNTS PER CHANNEL *10⁻¹
(1)
(2)
0
40
80
120
160
200
240
280
CHANNEL NUMBER

fig. 1

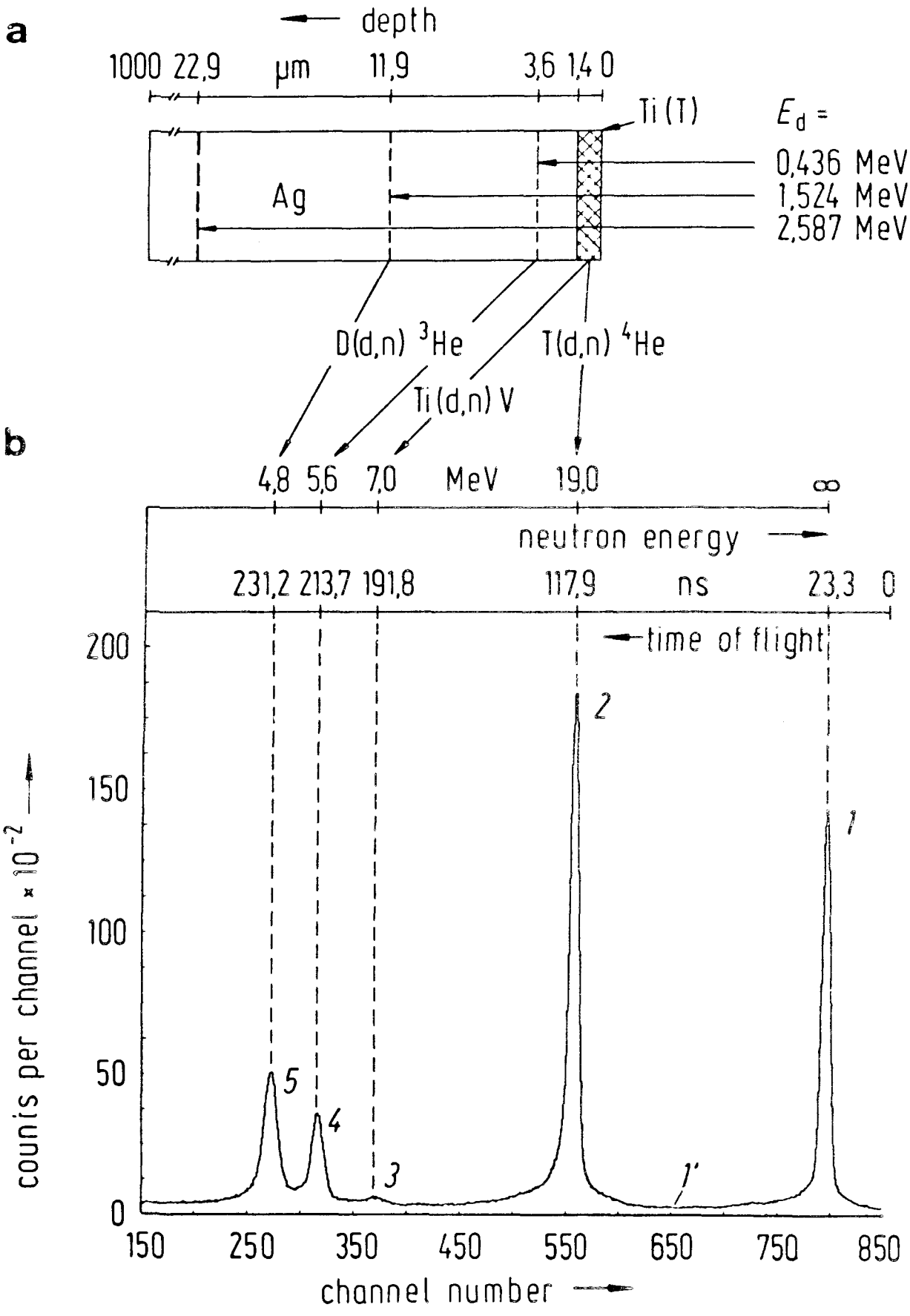
a
depth
1000 22,9 µm 11,9 3,6 1,4 0
Ti (T)
E_d =
0,436 MeV
1,524 MeV
2,587 MeV
Ag
D(d,n) ^{3}He
T(d,n) ^{4}He
Ti(d,n) V
b
4,8 5,6 7,0 MeV 19,0 ∞
neutron energy
231,2 213,7 191,8 117,9 ns 23,3 0
time of flight
counts per channel × 10^{-2}
200
150
100
50
0
1
2
3
4
5
1'
150 250 350 450 550 650 750 850
channel number

fig. 2

AG/160-11

October 18, 1978

ACCELERATOR-BASED DOSIMETRY BENCHMARKS

R.DIERCKX

JRC ISPRA,
Italy

ADVISORY GROUP MEETING ON NUCLEAR
DATA FOR REACTOR DOSIMETRY

VIENNA, 13-17 NOVEMBER 1978

ABSTRACT

Accelerator-based neutron dosimetry Benchmarks are a necessary step, to relate neutron dosimetry in first-wall fusion reactor spectra and in high energy neutron sources to the fission reactor dosimetry.

A 14 MeV (D-T) source should be adopted to generate a STANDARD FIELD, complemented with some other REFERENCE FIELDS, such as a D-Be or D-Li source, and a D-T-blanket source (first-wall fusion reactor spectrum). A large effort for spectrum characterization is necessary in the REFERENCE FIELDS.

---

1. INTRODUCTION

The accelerator-based neutron dosimetry benchmarks are a new generation of benchmarks, necessary for fusion applications. A fusion reactor, even power sustained, is far from being realized but radiation damage in fusion reactor environments is one of the primary problems to be solved. Accelerator-based neutron sources are projected and will be built in the near future to study the effect of high energy neutron irradiation on the materials, especially first-wall materials. Dosimetry in these neutron fields is of primary concern to permit a correlation and extrapolation of radiation damage results to fusion reactor first-wall irradiation conditions. [1-4]

The intense high-energy neutron sources will be of two types. (D-T)n and (D-Li)n. Examples of the D-T sources are the Rotating Target Neutron Source, RTNS-II,[5] with a 14 MeV neutron source strength of 5.10^{13} n/s, and the projected Intense Neutron Source, INS, [6] with a source strength of 3×10^{15} n/s. For the latter a multiplying blanket is proposed creating in the enclosed irradiation volume, fusion reactor first-wall neutron spectra.[7] At HEDL (Richland, USA) and at GFK Karlsruhe (Germany) in cooperation with the JRC Ispra a D-Li source is studied.

The irradiation damage experiments to be executed in these sources have to be monitored for neutron spectrum and neutron fluence. As for the fission reactor experiments dosimetry benchmarks will be of great importance and help in the development and calibration of dosimetry techniques for the intense high energy neutron sources and for cross section adjustments.

2. STANDARD FIELD

The list of standard neutron fields for reactor dosimetry[8] does not yet include an accelerator-based neutron field. For fusion applications it is necessary to include in this list a (D-T) source as an absolute standard for 14 MeV neutrons (the exact energy depends on ion bombarding energy and emitting angle). The D-T reaction is very well known and is already used as standard in different laboratories.[9-11]
Special counting techniques, as the associated charged particle technique, and the well known characteristics of the source spectrum does make the D-T source a reliable STANDARD for the fusion field.
A standard 14 MeV source is necessary to correlate fission reactor dosimetry, D-Li neutron source dosimetry, 14 MeV neutron source dosimetry and fusion reactor first-wall dosimetry.

3. REFERENCE FIELDS

In the IAEA list of reference fields [8] the D-Be source is already included with stated accuracy for the knowledge of the spectrum of about 30%. Fig.1 gives the neutron spectrum for 30 MeV deuterons in the 0° direction as measured with foils.[12] Fig.2 gives a time of flight (TOF) spectrum for 40 MeV deuterons in the 0° and 90° directions.[13] It shows the big uncertainty in the spectrum.
Especially the lower energy part($E < 2$MeV) is very inaccurately known. No time of flight measurements of these spectra are available for neutron energies below 2 MeV.
A difficulty is to relate the TOF measurements of the leakage spectra with the neutron spectrum existing nearby the source. The use of a neutron multiplying booster to tailor the neutron spectrum of a D-Li source, in order to obtain similar primary knock on (PKA) spectra as in a fusion reactor first-wall environment, requires additional experimental and theoretical investigations.
Much more effort for the spectrum characterization is necessary in case a D+Be or D-Li source is adopted as a reference field.

However such a reference field is needed urgently to solve the problems of neutron dosimetry for the high energy neutron sources for exemple the proposed Fusion Materials Irradiation Test Facility (FMIT) to be built at HEDL Richland or an European D-Li source.

A second reference field, needed in the fusion materials program should be a real first-wall-fusion-reactor neutron spectrum. Such a spectrum is available in the blanket facility, studied and developed for the INS.[7] Fig.3 gives the neutron spectra in the irradiation volume of the INS blanket and the first-wall neutron spectrum of a TOKAMAK reactor. Such a blanket facility could also be build around each D-T source. The only difference would be a smaller flux intensity depending on the source strength . Naturally this spectrum has to be calculated and measured with different techniques including TOF techniques.[14]
For the fusion materials programmes such a high intensity source with high fluxes ($\phi > 10^{14}$ n/cm^2 s) in a reasonable volume is needed to correlate damage data obtained in fission reactors, D-Li sources and charged particle accelerators to first-wall fusion reactor conditions.

4. CONTROLLED ENVIRONMENTS

The radiation fields in the different high energy neutron sources can all be classified and used as controlled environments. These are the existing D-T source, RTNS II, and proposed sources (INS, FMIT and D-Li-neutron booster), and similar future sources in the rest of the world (Japan, Canada, Europe, USSR, etc.).

In the controlled environments an extensive experimental dosimetry programme, backed by theoretical calculations has to be executed. These dosimetry measurements have to be correlated with the reference fields and the standard field.

5. CONCLUSIONS

Accelerator-based dosimetry benchmark facilities do not exist at present. Some experimental activities are carried out but a much more systematic study of these neutron environments should be executed.
The first fusion dedicated facilities will be the controlled environments at RTNS II, and FMIT in the USA on which extended dosimetry measurements will be executed. These dosimetry measurements need at least one STANDARD FIELD, a pure 14 MeV (D-T) source, in order to correlate and calibrate the high energy neutron source dosimetry to the fission reactor dosimetry. Further some reference fields, a D-Be or D-Li source and a D-T-blanket source (first wall fusion reactor spectrum) would help to test, to develop, and to compare dosimetry methods in the fusion field.

REFERENCES

1. W.M. McELROY et al.
Standardization of dosimetry and damage analysis work for U.S.LWR, FBR, and MFR Development programs.
NUREG/CP-0004 p.17 vol I, 1977

2. R.R.HEINRICH, L.R.GREENWOOD, G.R.ODETTE, H.FARRAR IV, R.DIERCKX and R.GOLD
Dosimetry needs for magnetic fusion materials program.
NUREG/CP-0004, 1017 vol.III, 1977

3. R.DIERCKX, C.R.EMIGH and D.PARKIN
Correlation of radiation damage results in different neutron spectra.
ASTM 9° Intern.Symp. on Effects of Radiation on Structural Materials, Richland, Wash. 1978

4. R.DIERCKX and C.R.EMIGH
Application of the INS facility as a high-flux benchmark for neutron dosimetry and for radiation damage studies in D-T fusion spectra
NUREG/CP-0004, 1031 vol.III, 1977

5. R.BOOTH, J.C.DAVIS, C.L.HANSON, J.L.HELD, C.M.LOGAN, J.E.OSHER, R.A.NICKERSON, B.A.POHL, B.J.SCHUMACHER
Rotating target neutron generators.
Nucl.Instr. and Meth. 145, 25 (1977)

6. D.D.ARMSTRONG, C.R.EMIGH, K.L.MEIER, E.A.MEYER and J.D.SCHNEIDER
A 14-MeV intense neutron source facility.
Nucl.Instr. and Meth. 145, 127-148 (1977)

7. M.E.BATTAT,R.DIERCKX, C.R.EMIGH
Feasibility study to produce first-wall neutron fusion reactor spectra around a 14 MeV point source.
to be published in Nucl. Technology

8. Summary report of a specialists'meeting, Vienna Nov.1976 on : Neutron cross-sections for reactor dosimetry.
IAEA-208, p.1 vol I, 1978

9. O.A.WASSON,
NBS facilities for standardization of neutron dosimetry from 0.001 to 14 MeV .
NBS-SP-493 p.115, 1977

10. M.M.MEIER
Associated particle methods.
NBS-SP-493, p.221, 1977

11. V.M.ADAMOV et al.
Absolute 235U, 238U, 237Np fast neutron fission cross section measurements.
NBS-SP-493, p.313, 1977

12. D.R.NETHAWAY, R.A.VAN KONYNENBURG, M.W.GUINAN, L.R.GREENWOOD
Neutron spectra from 30 MeV deuterons on a thick beryllium target
BNL-NCS-50681, p. 135, 1977

13. M.J.SALTMARCH, C.A.LUDEMANN, C.B.FULMER
Nucl. Inst. & Meth. (1977)

14. R.DIERCKX
Neutron monitoring and neutron measurements; Experimental possibilities at the INS source
LA-6792-MS and BNL-NCS-50681, p 351, 1977

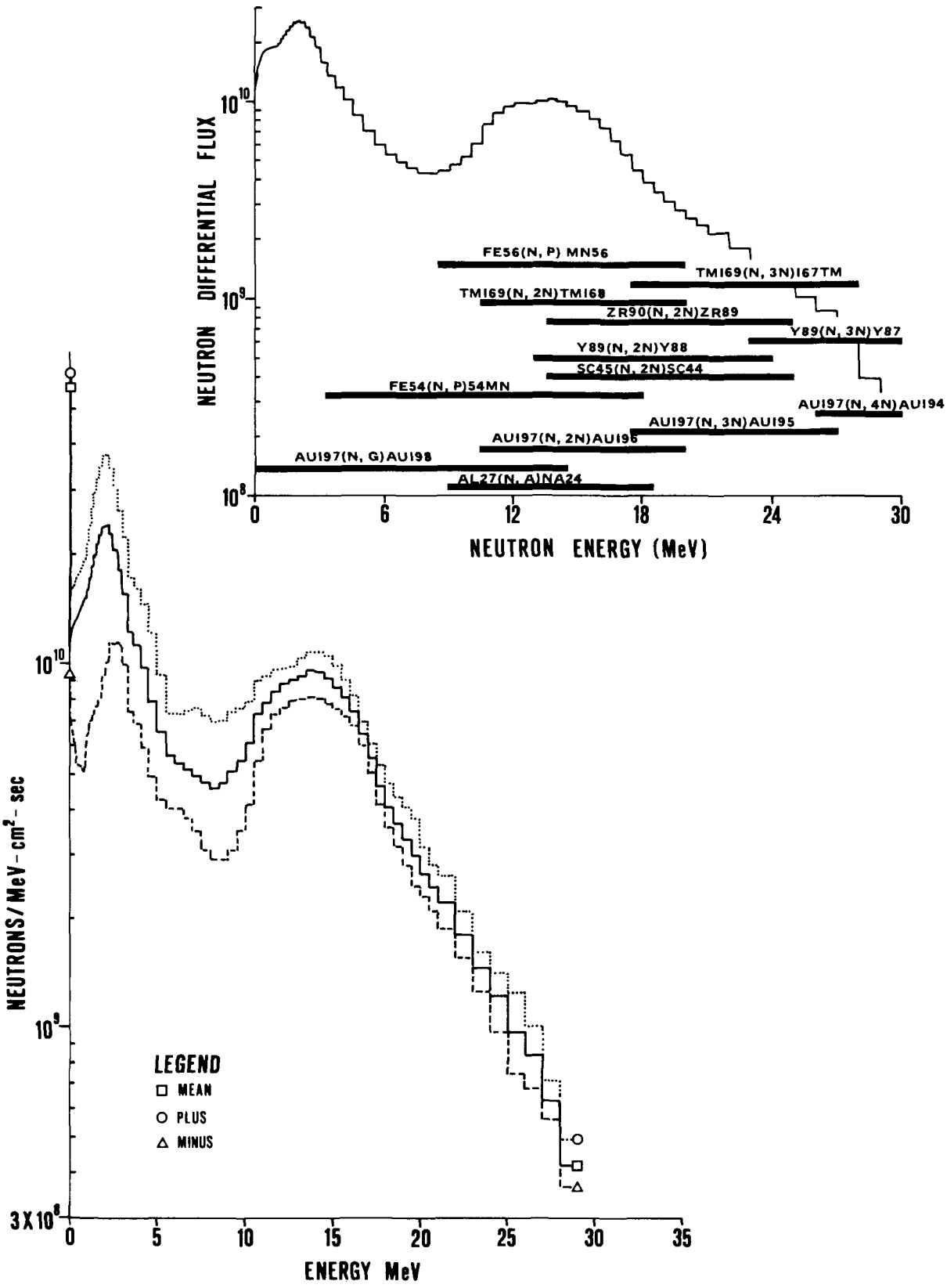

Fig. 1 Unfolded spectrum (neutron/cm² - sec - MeV)at 44 mm from midrange of 30 MeV deuterons in Be target. The horizontal bars indicate the 95 % sensitivity range for the reactions used in the unfolding. The mean spectrum and those corresponding to plus or minus one standard deviation are shown (ref. 12).

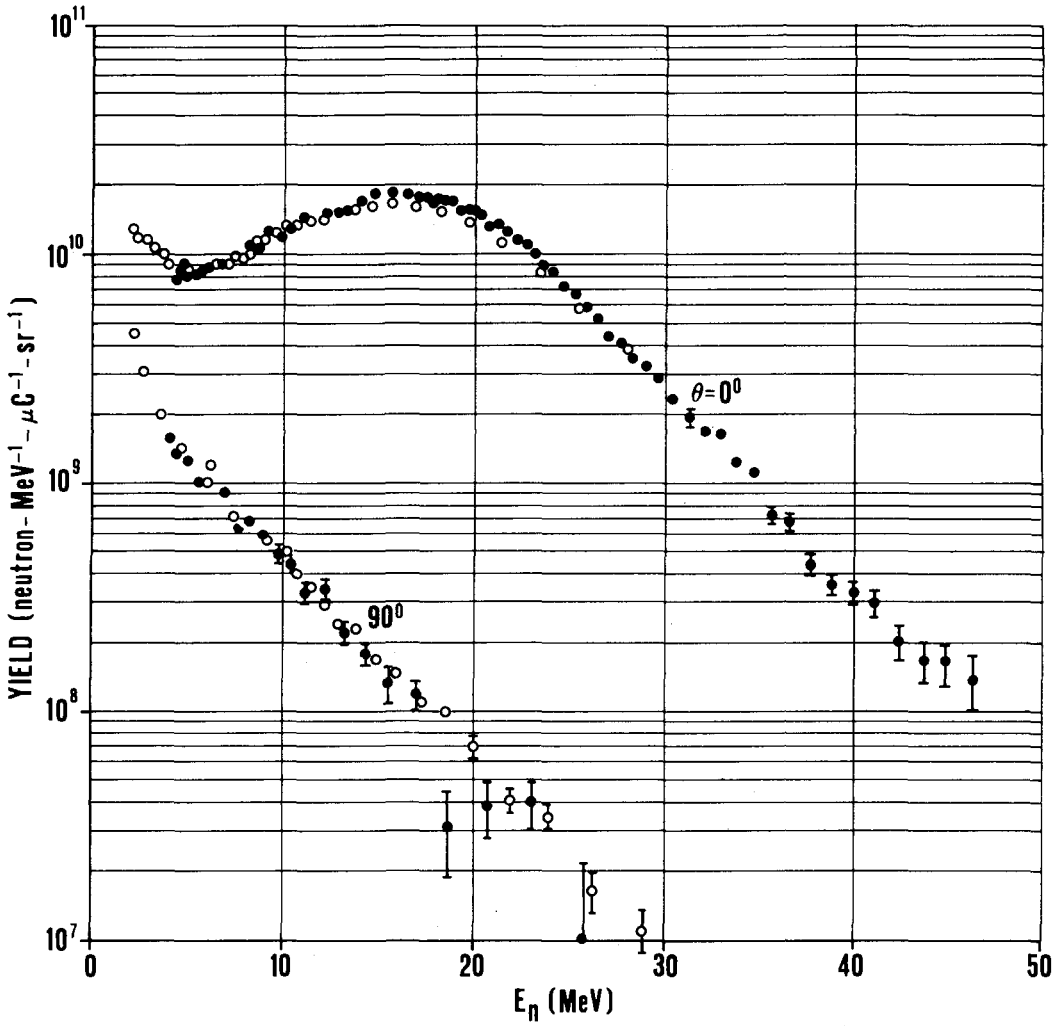

Fig. 2 Neutron spectral distributions from 40 MeV deuterons on a thick Be target (ref. 13)

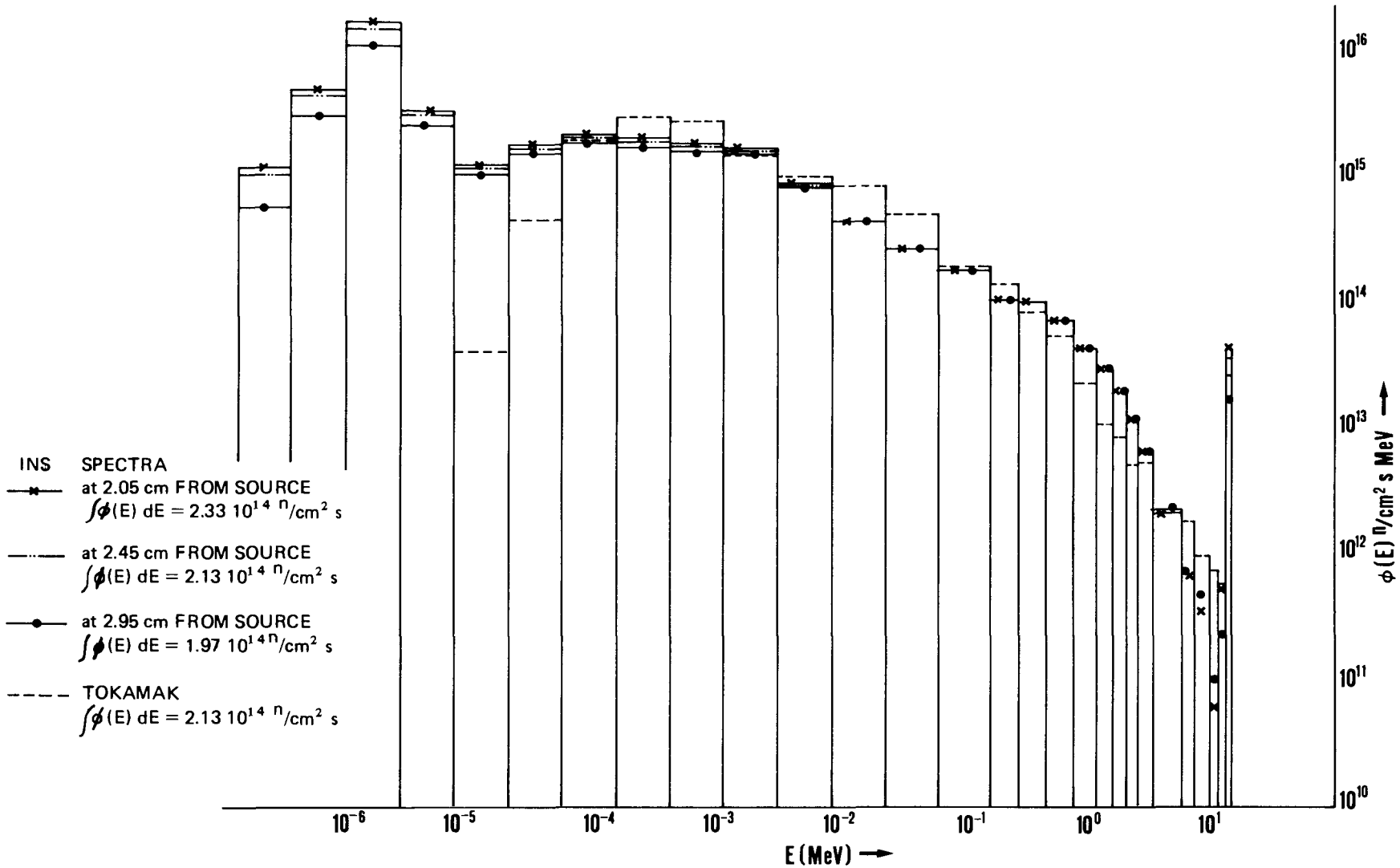

Fig. 3 Neutron Spectra around point D-T source with a blanket

AG/160-12A

IAEA ADVISORY GROUP MEETING ON
"NUCLEAR DATA FOR REACTOR DOSIMETRY"

Vienna 13-17 November 1978

Iteration Acceleration in the ITER-2 Unfolding Code

M.Pauko and M.Najžer

University of Ljubljana
J.Stefan Institute

Abstract

Program ITER-2 used previously for neutron activation detectors data unfolding was made capable of pulse height spectra unfolding also. The rather slow convergence rate was improved by two simple routines incorporated into the program. Their effects were examined in the case of unfolding the single crystal scintillation spectrometer data.

1. Introduction

Program ITER-2 was previously designated for neutron activation detectors data unfolding /1-4/. Subsequently the program was made capable to unfold pulse height spectra also /5/. A number of computer simulated experiments using single crystal NE-213 and NaI spectrometers data were undertaken in order to check the abilities of the iterative method /5,6/. Further, the iterative method was successfully applied for multispectrometer unfolding /7/.

It was observed that the rate of convergence of the ITER-2 was not satisfactory. To accelerate the iterative process two simple routines were incorporated into the program. In the following these routines and their effects on the unfolding of data from single crystal scintillation spectrometer are described.

2. Unfolding by ITER-2 program

In the neutron activation detectors data unfolding one seeks for an appropriate soultion of the following equations

$$a_j+\delta a_j = \int_{E_{min}}^{E_{max}} \sigma_j(E)\ \Phi(E)\ dE \qquad j=1,\ldots,N \qquad (1)$$

were a, δa, σ and Φ denote: measured reaction rates, their estimated errors, neutron cross section and neutron energy spectrum, respectively.

ITER-2 program adopts an iterative procedure to obtain the estimate of $\Phi(E)$. Assuming the k-th iterate, $\Phi^{(k)}(E)$, is known the (k+1)-th is calculated as follows /1,5/:

$$\Phi^{(k+1)}(E)=\Phi^{(k)}(E)\ \frac{\sum_{j=1}^{N} \dfrac{a_j\ \sigma_j(E)/\delta a_j}{\left[\int_{E_{min}}^{E_{max}} \sigma_j(E)\ \Phi^{(k)}(E)\ dE\right]^2}}{\sum_{j=1}^{N} \dfrac{\sigma_j(E)/\delta a_j}{\int_{E_{min}}^{E_{max}} \sigma_j(E)\ \Phi^{(k)}(E)\ dE}} \qquad (2)$$

All the a priori information about the seeked-for spectrum is introduced through guess spectrum $\Phi^{(0)}$. Then an acceptable estimate of $\Phi(E)$ is thought to be obtained when a prescribed number of iterations is achieved or the following condition is met:

$$\left| a_j - \int_{E_{min}}^{E_{max}} \sigma_j(E)\ \Phi^{(k)}(E)\ dE \right| \leq \delta a_j \qquad j=1,\ldots,N \qquad (3)$$

When going over to pulse height spectra unfolding, the formulation of the problem and its ITER-2 algorithm solution can be retained /5/. Now, the symbol a_j stands for bin values, as measured with multichannel spectrometer, δa_j for the appertaining estimated error and σ corresponds to response surface of the spectrometer. Usually the Eq.(1) is solved in its discretized form

$$a_j + \delta a_j = \sum_{i=1}^{M} \sigma_{ji}\ \Phi_i \qquad \begin{matrix} j=1,2,\ldots,N \\ i=1,2,\ldots,M \end{matrix} \qquad (4)$$

Here, the symbols σ_{ij} and Φ_i stand for the integrals of $\sigma_j(E)$ and $\Phi(E)$ over the limited number of energy intervals. However, it is very important to choose both the number and widths of bins and energy groups appropriately in order to keep the problem from beeing ill-conditioned.

Using the notations introduced in Eq.(4) the ITER-2 algorithm takes a very simple form:

$$\Phi_i^{(k+1)} = \Phi_i^{(k)} \frac{\sum_{j=1}^{N} W_{ij}^{(k)} \frac{a_j}{a_j^{(k)}}}{\sum_{j=1}^{N} W_{ij}^{(k)}} \qquad i=1,\ldots,M \qquad (5)$$

where "calculated"bin value is defined as follows

$$a_j^{(k)} = \sum_{i=1}^{M} \sigma_{ji}\ \Phi_i^{(k)} \qquad (6)$$

and the weight $W_{ij}^{(k)}$ is computed according to the formula

$$W_{ij}^{(k)} = \frac{a_j}{\delta a_j} \quad \frac{\sigma_{ji}\, \Phi_i^{(k)}}{a_j^{(k)}} \tag{7}$$

where the first and the second factors are the inverse value of the relative error in the j-th bin and the relative sensitivity of the j-th bin to neutron of i-th energy. According to Eq.5 the neutron flux is obtained as an weighted average over all N bin values.

3. Modifications of ITER-2 iterative method

ITER-2 program when applied for the unfolding of 10 - 15 reaction rates yields satisfactory results after about 10 - 20 iterations. Roughly 100 of iterations are required when the same method is used for the multichannel spectrometer data unfolding. Additionally, after first twenty iterations where the calculated bin values are on the average very rapidly adjusted to the measured ones, rather a slow convergence was observed. To remedy such a situation simple modifications of the original ITER-2 algorithm are considered with the aim to improve the rate of convergence. Confinement of the averaging only to significant bins as well as a method of the accelerating the iterative process similar to SOR scheme were tried.

3.1. Confinement of the averaging to significant bins

The response functions often extend over considerable number of bins. In the limiting case the sums in

Eq.(5) may include even all of them with no respect to the position of σ_{ij} in the j-th row of the response matrix. It seems reasonable to limit the averaging to bins having a significant sensitivity to neutrons of the i-th energy.

This restriction, determining the lower and the upper bound of index j at i selected, may be formulated as follows:

$$jmin_i = \min_j \left\{ \sum_{m=1}^{i} \sigma_{jm} \Phi_m^{(k)} \leq G \sum_{m=1}^{M} \sigma_{jm} \Phi_m^{(k)} \right\} \qquad (8)$$

$$jmax_i = \max_j \left\{ \sum_{m=1}^{i} \sigma_{jm} \Phi_m^{(k)} \geq F \sum_{m=1}^{M} \sigma_{jm} \Phi_m^{(k)} \right\} \qquad (9)$$

where the two auxiliary parameters F and G are subject to the condition $0 \leq F < G \leq 1$. Evidently, the choice of $(F,G) = (0,1)$ poses no restriction on the averaging, thus leaving the original algorithm unchanged. The interval $(F,G) \neq (0,1)$ should not be selected without paying attention to the shape of the response functions, actually dealt with in an unfolding problem. Further, the interplay between the order of relative estimated errors, $\delta a/a$, and the extent of the averaging determined with (F,G) should be taken into account.

The algorithm takes then the following form:

$$\Phi_i^{(k+1)} = \Phi_i^{(k)} \frac{\sum_{j=jmin_i}^{jmax_i} W_{ij}^{(k)} \frac{a_j}{a_j^{(k)}}}{\sum_{j=jmin_i}^{jmax_i} W_{ij}^{(k)}} \qquad (10)$$

3.2. The acceleration of the iterative process similar to SOR technique

In resemblance with SOR iteration scheme widely used for solving linear systems /8/ the following modification of the ITER-2 algorithm is made:

$$\tilde{\Phi}_i^{(k+1)} = \Phi_i^{(k)} + \omega \left(\Phi_i^{(k+1)} - \Phi_i^{(k)} \right) \tag{11}$$

thus, the iteration process continues at the (k+1)-th step with the corrected estimated spectrum, namely with $\tilde{\Phi}^{(k+1)}$. The parameter ω was selected to depend on the ratio:

$$m = \frac{\chi^{2(k)}}{\chi^{2(k-1)}} \tag{12}$$

where $\chi^{2(k)}$ is defined by the expression:

$$\chi^{2(k)} = \frac{1}{N-M-1} \sum_{j=1}^{N} \left[\frac{a_j - \sum_{i=1}^{M} \sigma_{ji} \Phi_i^{(k)}}{\delta a_j} \right]^2 \tag{13}$$

and then ω is computed according to the formula

$$\omega = \frac{2}{1 + \sqrt{1-m}} \tag{14}$$

Besides these two modifications the third one is defined as a combination of the first two. For later referencing let us assing following labels to the original and to modified iterative algorithms:

- original ITER-2 algorithm,	Eq.(5)	A
- modified	Eq.(8)	B
- modified	Eq.(9)	C
- combination of B and C		D

4. Pulse height spectra unfolding with ITER-2 algorithms

The unfolding of the organic scintillator data is known to be often far from trivial. Thus, the verification of the iteration schemes on the NE-213 type of multichannel spectrometer was thought to be reliable enough. The use was made of single crystal response function as measured at Oak Ridge and given in the FERDOR-COOLC program package /9/. According to this data the number of bins is equal to 113 and the number of neutron energy groups is set to 77, covering the neutron energy region between 0.2 and 18 MeV approximately.

In the work presented the unfolding of three test examples is undertaken in order to prove the abilities and adequacy of different iteration schemes based on ITER-2 algorithm. Two test spectra are synthetical. The first one consists of two Gaussian peaks at 5 and 10 MeV, superimposed on an exponentially decreasing background. The spectrum of the test case II has valleys instead of peaks on the same background. By multiplying the response matrix with these test spectra two simulated pulse height distributions were generated readily.

An actually measured Po-Be neutron spectrum is considered an excellent test example. The data needed

are attached to the FERDOR program as its test case together with the FERDOR's constrained minimization estimate of the neutron spectrum.

In the case of the synthetic test spectra the estimated errors δa_j are set equal to $\sqrt{a_j}$ while in the experimental test case they are compiled from the program package mentioned above. An important difference between the first two cases and the third case must be kept in mind: computer simulated pulse height distributions are not statistically scattered as it is the case with the experimental test distribution.

5. Results and discussion

In Figs. 1-3 test neutron spectra and the iterative estimates after 100 iterations are presented. A simple guess spectrum in the form $\phi^{(0)}(E)=1$ was used in all calculations. "True" synthetic spectra are drawn by dashed lines while in the third test case FERDOR's confidence interval is given. It has to be emphasized that all the spectra shown in Fig. 3, are smoothed as prescribed by FERDOR program since its unsmoothed estimate does not appear in the printout of the test case.

The benefit of introducing the modifications into the original algorithm can be clearly realized comparing the solutions using different algorithms (the correspondence of labels A, B, C and D is established in the par. 3). Variants B and D are obtained through limiting the averaging over bin value ratios with interval (F,G) = (0.1, 0.9) chosen.

As shown by Figs. 1 and 2 the peaks and valleys are rather well reproduced though the latter slightly broader. In the third test case, a good agreement of iterative estimates with FERDOR's confidence interval was achieved. There are still differences, especially below 0.4 MeV and above 11 MeV where FERDOR's confidence interval significantly widens and extends even to the negative flux values. The solution according to the algorithm D seems to be the best one. For clearness only, the variants B and C are omitted in the Fig. 3.

Besides the smoothed iterative estimates presented in Fig. 3 it is very interesting to compare the unsmoothed energy spectra with the FERDOR's estimate. This is done in Fig. 4. Evidently, unsmoothed estimate obtained by the algorithm D, requires smoothing after the 100^{th} iteration step.

In Table I the ratios of iterative solutions with true spectra are given. In the case of Po-Be spectrum the middle of the FERDOR's confidence interval was taken for the "true" spectrum. Clearly, the ratios are improved almost without exception when going from the original algorithm over to the modified ones. From these data a simple conclusion can be drawn: the effects of versions B and C seem to be nearly additive.

In the algorithms B and D the conditions of Eq.(8) and Eq.(9) are built in what forces the response matrix to be "seen" somewhat distorted. Immediate consequence of the choice F = 0.1 in the case of proton recoil spectrometer is the slight shift of peaks and valleys to higher energies in first ten or twenty

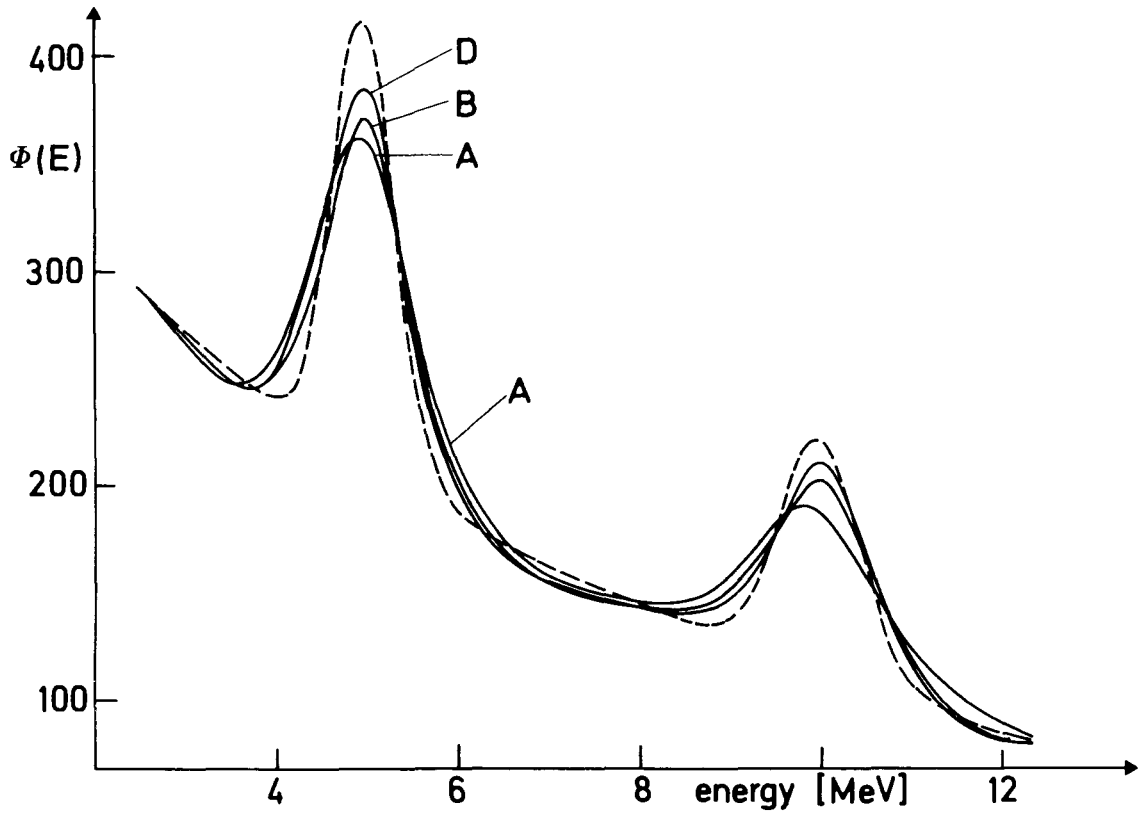

Fig.1. Test case I

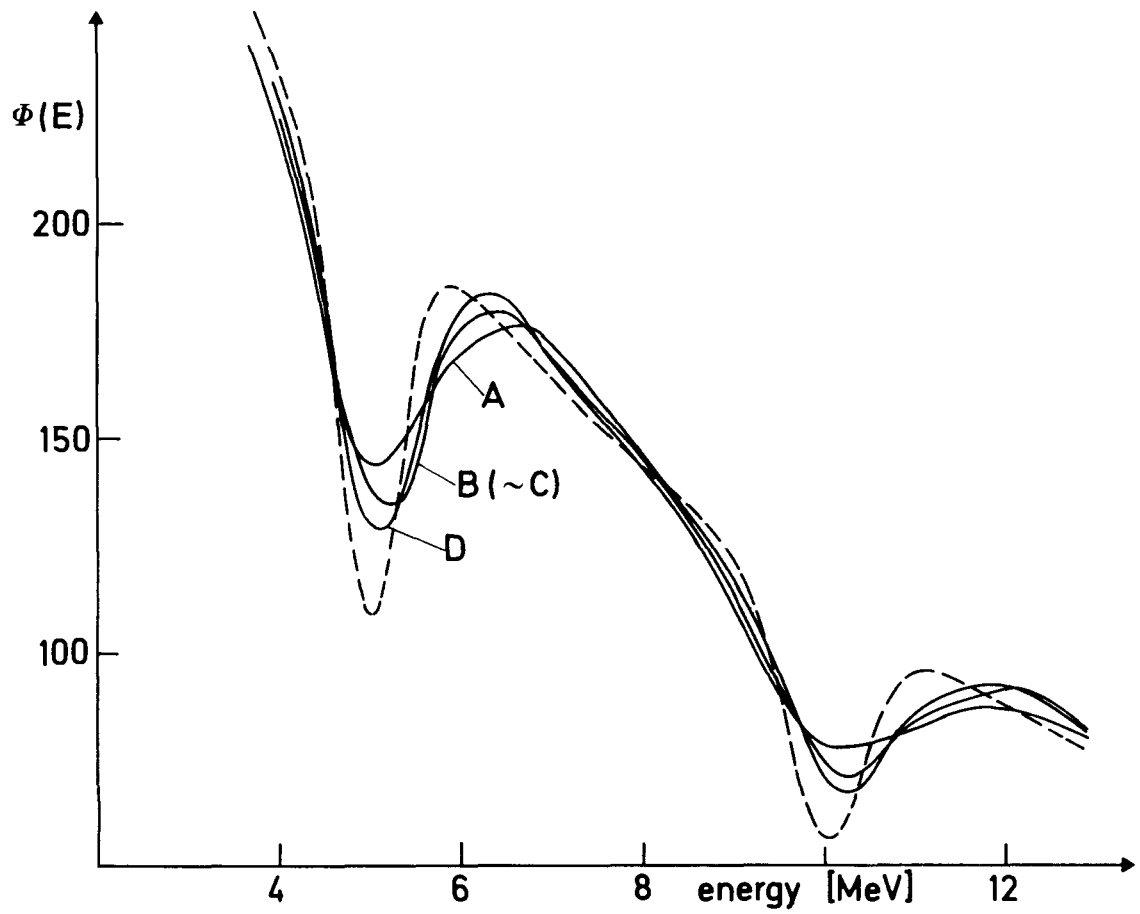

Fig. 2 Test case II

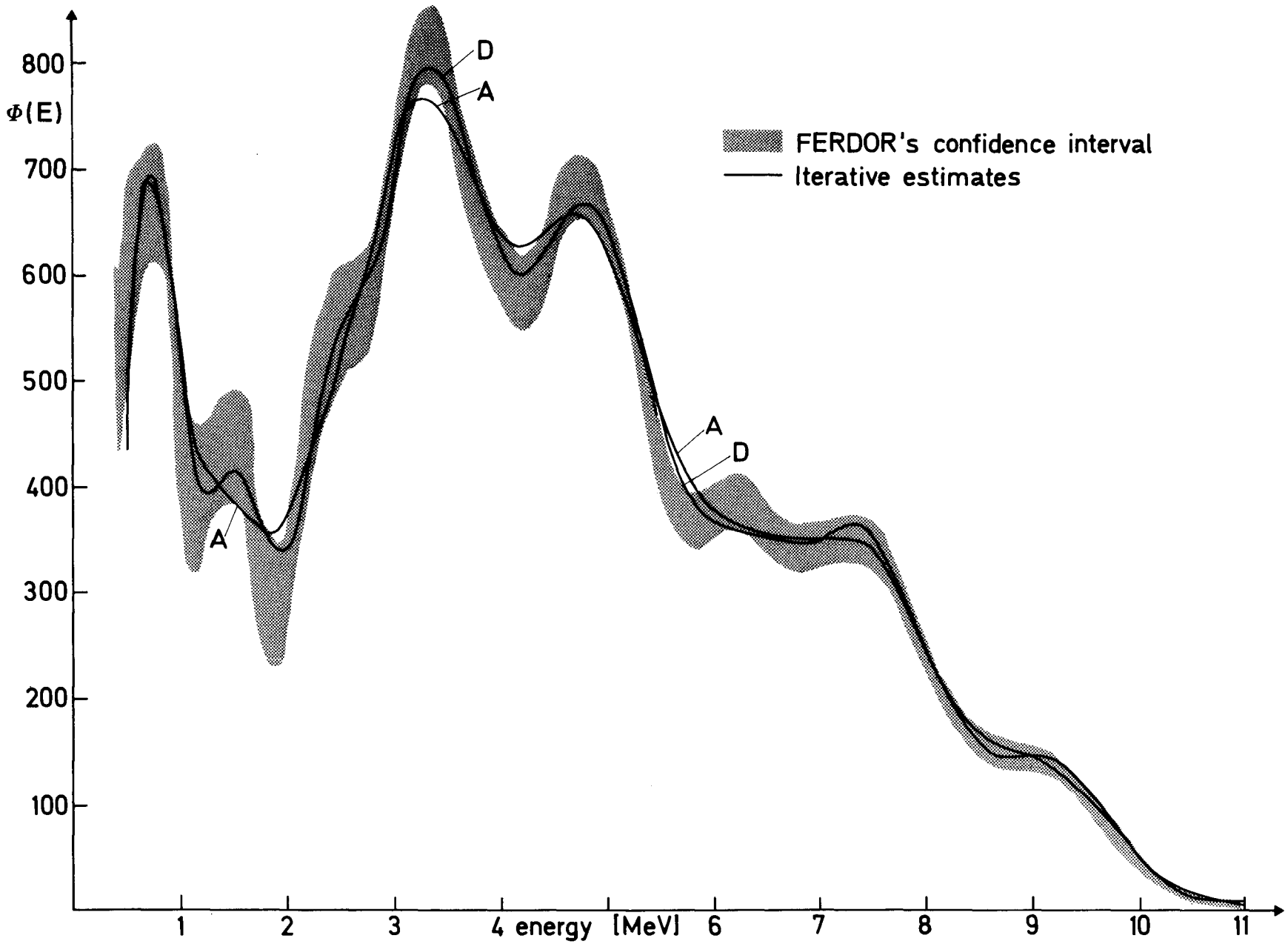

Fig. 3 Test spectrum III (smoothed)

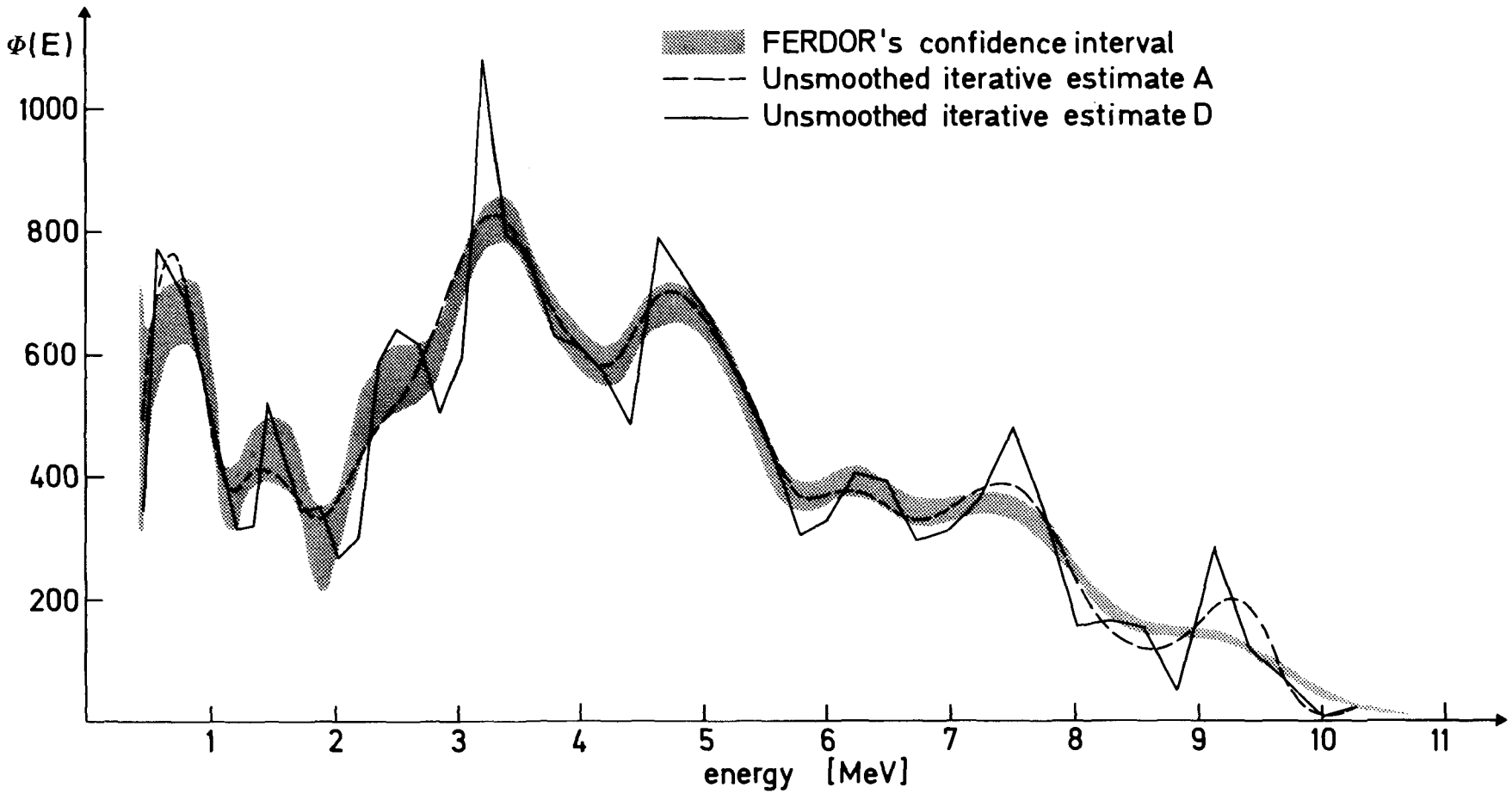

Fig. 4 Test spectrum III (iterative estimates unsmooted)

iterations. Later on they shift in the reversed direction monotonically toward the "true" positions. The relative distances between the calculated and true positions after 100 iterations are given in the Table II.

Besides the number χ^2, defined by Eq.(13), additional quantity S is calculated after each iteration according to the formula:

$$S^{(k)} = \frac{1}{M} \sum_{i=1}^{M} \frac{\left| \Phi_i^{(k)} - \Phi_i^{TRUE} \right|}{\Phi_i^{TRUE}} \qquad (15)$$

It serves as a measure of the distance between the calculated and the true spectrum. In Figs. 5 and 6 the numbers χ^2 and S are presented in dependance on the iteration counter when different iterative algorithms are applied. On the basis of these two diagrams the number of iterations required for attaining preselected values of χ^2 and S can be found. This is shown on Fig. 7 for test cases I and III.

With respect to χ^2 and S one chould conclude that the modificated algorithm is faster than the algorithm A for a factor of about 2.

It is also of great interest how well the integral over the neutron spectrum is reproduced by the unfolding procedure. Consequently, the integrals of the unfolded test spectra are compared with the integrals of the "true" test spectra. The relative differences in percents after the 100^{th} iteration are given in the Table III. The integrals are performed over the whole energy interval, except for the case III where

Table I. Ratias $\Phi^{(100)}_{CALC}/\Phi_{TRUE}$

Test case	Neutron Energy x(MeV)	ALGORITHM A peak	A vall.	B peak	B vall.	C peak	C vall.	D peak	D vall.
I	5	0.865		0.900		0.899		0.945	
	10	0.848		0.890		0.883		0.940	
II	5		1.311		1.248		1.258		1.185
	10		1.372		1.342		1.316		1.287
III	1.9		1.261		1.258		1.233		1.195
	3.4	0.934		0.952		0.952		0.972	
	4.2		1.081		1.060		1.081		1.032
	4.8	0.954		0.952		0.975		0.977	

Table II. Relative distance between the calculated and true positions (in %)

Test case	Neutron Energy (MeV)	ALGORITHM A peak	A vall.	B peak	B vall.	C peak	C vall.	D peak	D vall
I	5	-1.1		+1.4		-0.8		+1	
	10	-0.54		+1.0		-0.3		+1	
II	5		-1.2		-1.0		+1.9		+1.9
	10		-1.0		-0.8		+1.1		+2.4
III	1.9		-4.7		+2		-3.4		+2.9
	3.4	-1.2		+0.4		-1.2		+0.2	
	4.2		+0.3		+5		-0.5		+0.4
	4.8	-1.3		+1.5		-0.1		+0.7	

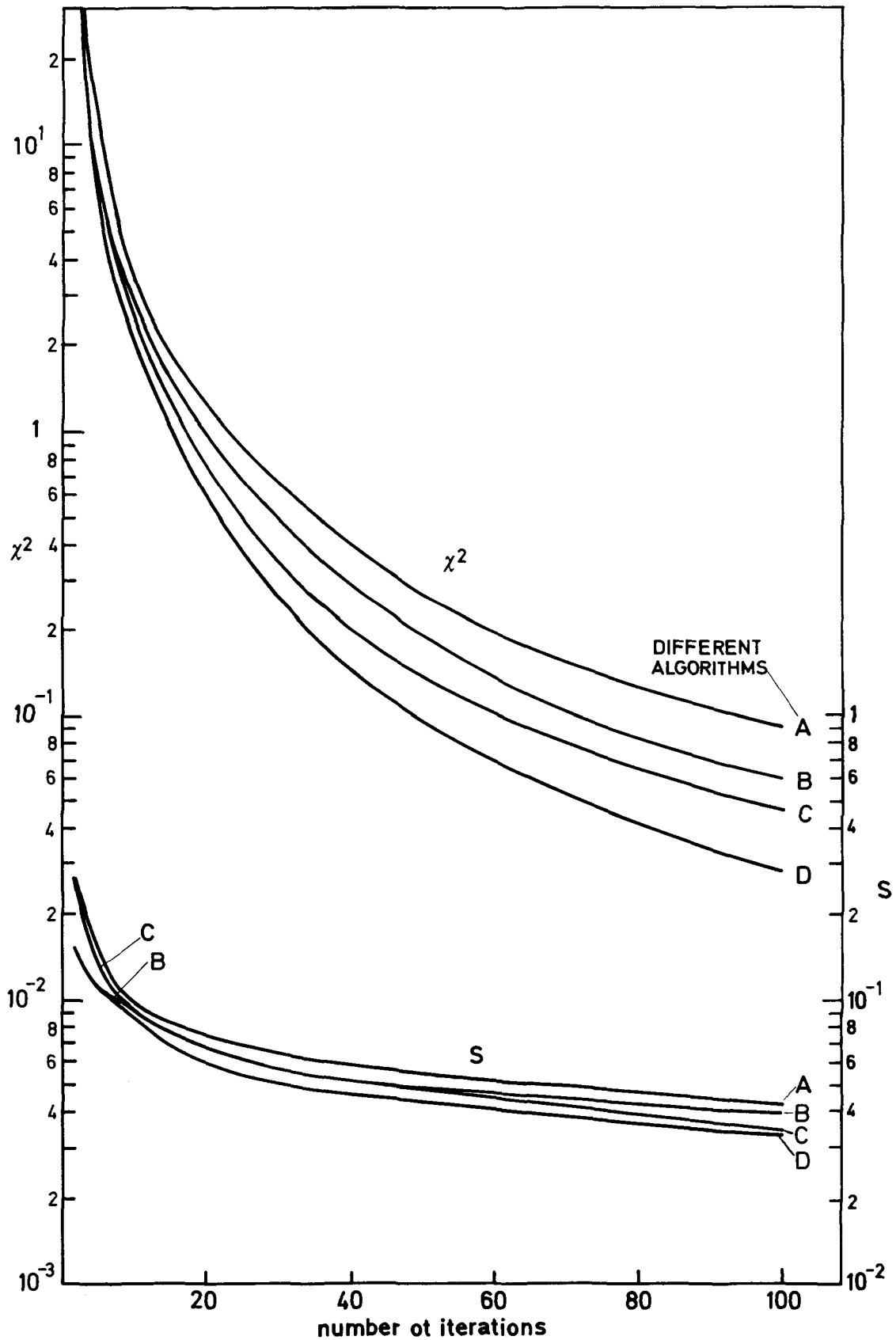

Fig. 5 Numbers χ^2 and S in the test case I

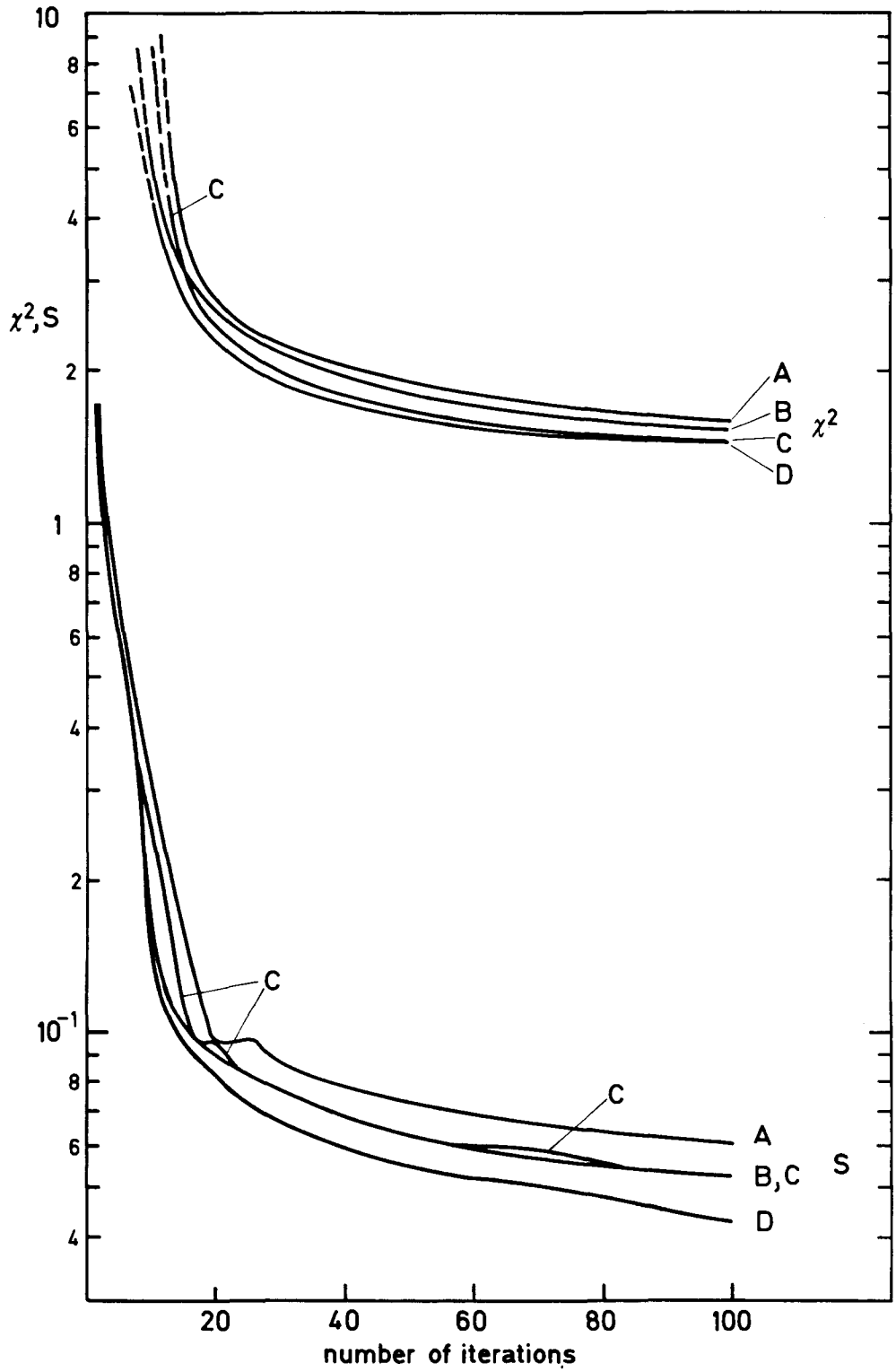

Fig. 6 Numbers χ^2 and S in the test case III

Test case I

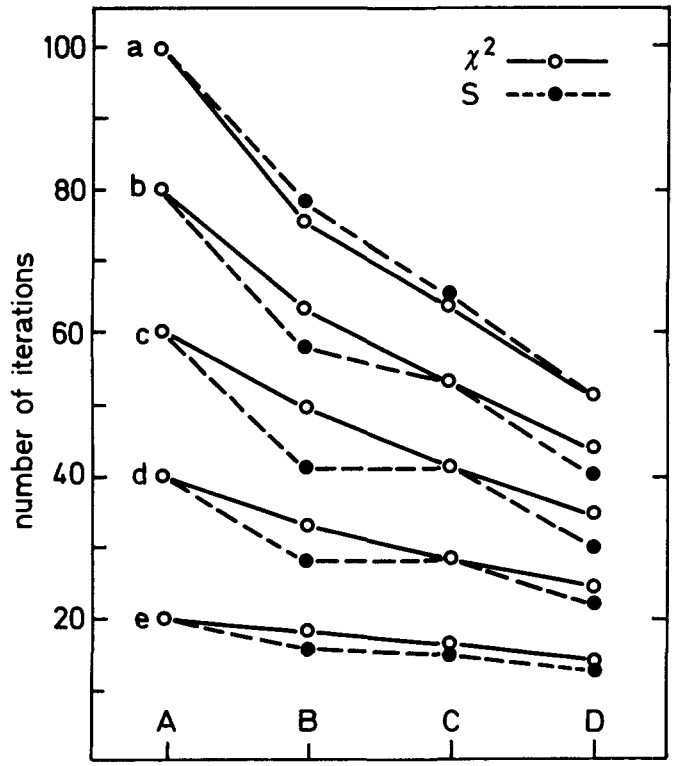

	χ^2	S
a	0.092	0.044
b	0.13	0.048
c	0.20	0.052
d	0.40	0.058
e	1.22	0.076

Test case III

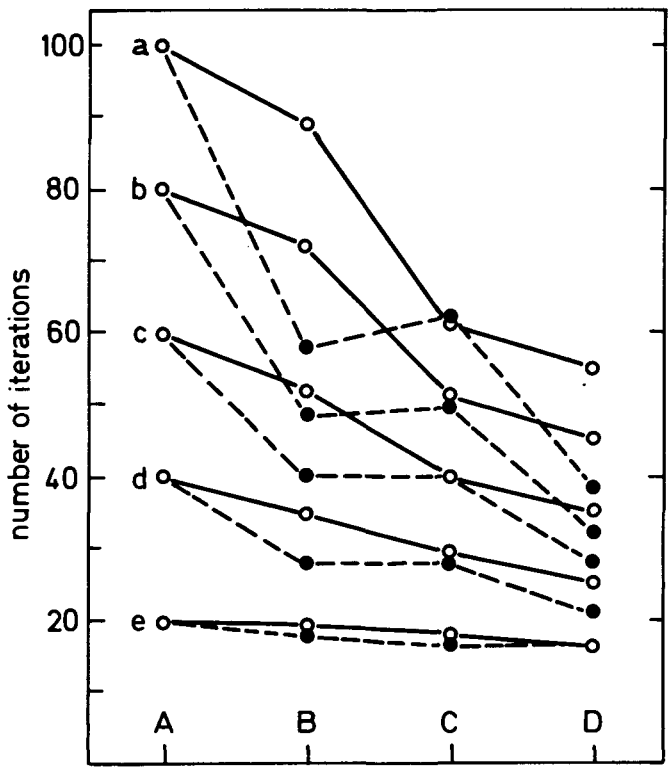

	χ^2	S
a	1.57	0.061
b	1.65	0.065
c	1.78	0.070
d	2.03	0.079
e	2.80	0.097

Fig. 7 Number of iterations required for attaining preselected values of χ^2 and S

only the energy region betweem 0.45 and 11.2 MeV is taken into account.

Table III. Difference between the integrals of calculated spectrum and the integrals of true spectra (in %)

Test case	ALGORITHM A	B	C	D
I	0.18	0.15	0.15	0.15
II	0.18	0.18	0.18	0.18
III	-0.32	-0.31	-0.35	-0.29

It is worth to mention that the integrals of calculated test spectra achieve the 99 % of their value after the 100^{th} iteration before the 20^{th} iteration.

References

/1/ Najžer, M. et al., Proceedings of the XIVth Conference on Electronics, Telecommunications, Automation and Nuclear Engineering, Sarajevo, June 1970.

/2/ Fisher, A., "International Intercomparison of Neutron Spectra Evaluating Methods Using Activation Detectors", Berichte der Kernforschungsanlage Jülich - Nr. 1196, (Nov. 1974) 138-154.

/3/ Čopič, M., Rant, J., Supplement to "Measurements of Fast Neutron Spectra in the Experimental Beam Ports of Reactor TRIGA Mark II", IJS Report 528, Nov.1972, J.Stefan Institute, University of Ljubljana.

/4/ Najžer, M., Pauko, M., "Fast Neutron Spectra in Standard Seed Irradiation Facilities for TRIGA Reactors", Symp. on the Effects of Neutron Irradiation upon Cell Function, Neuherberg 1973.

/5/ Najžer, M., Pauko, M., "A New Method for the Unfolding of Pulse Height Distributions from Continuous Energy Spectra", 1st ASTM-EURATOM Symposium on Reactor Dosimetry, Petten 22.-26.Sept.1975.

/6/ Pauko, M., "Unfolding of Pulse Height Spectra using the ITER-2 Method", Master Thesis, University of Ljubljana (1977).

/7/ Najžer, M., et al., "Present Development and the Use of the ITER-2 Based Unfolding Programs, Proc. 5thEuropean Conference of TRIGA Users, Portorož (Sept. 1978), Yugoslavia.

/8/ Wachspress, E.L., "Iterative Solution of Elliptic Systems". Prentice Hall, Inc., New York 1966.

/9/ ORNL, PSR-17, PSR-18, COOLC and FERDOR Spectra Unfolding Codes.

Multispectrometer Unfolding by ITER Code

B. Glumac and M. Najzer

University of Ljubljana
J. Stefan Institute

Abstract

Multispectrometer unfolding by a SAND II type iterative code is tested on seven typical neutron spectra by a numerical experiment. The influence of the initial spectrum on the solution is discused. A method is described which can correct for an error in the renormalization of data from the spectrometers to the common neutron flux intensity.

1. Introduction

The raw data of a neutron spectrum measurement may consist of the output of several different detector types, such as proportional counters, activation detectors, scintillation spectrometers etc. Attempts are being made to unfold the spectral data of each detector separately and to seek consensus of thus obtained solutions, which may be subject to inconsistencies. Multispectrometer unfolding, i.e. simultaneous unfolding of all spectral data available and thus obtaining the neutron spectrum in one single step, has been tried and proved possible by the RADAK program /1/. The ability of the SAND-II type iterative codes to perform the same has been discussed /2/ and recently proven with the machine-simulated expe-

riments, conducted by the use of our ITER unfolding code. Description of its functioning is given by /3/, which is also a contribution to this meeting.

To summarize briefly the multispectrometer unfolding problem we observe the set of equations (1):

$$a_i \pm \delta a_i = \int \Phi(E)\, R_i(E)\, dE \qquad (1)$$

$$i = 1 \ldots N_1;\ N_1 + 1, \ldots N_2;\ N_2 + 1, \ldots N_3; \ldots .$$

where a_i and δa_i are the experimental data (i.e. the measured bin values or reaction rates) and their absolute errors, $\Phi(E)$ is the neutron spectrum being measured and $R_i(E)$ the response function of each bin. Index i goes from 1 to N_1 for the first detector applied, from $N_1 + 1$ to N_2 for the second detector, etc. In general we have to deal with a rather big system of equations (1).

2. Preparation of the Response Functions

Energy interval of interest for our calculations ranges from 10^{-10} MeV up to 18 MeV. We made use of the SAND-II energy group structure, but condensing it to only 107 energy groups. In the energy region from 10^{-10} MeV to 1.1 MeV the lethargy intervals are constant being approx. 0.78, while above 1.1 MeV the energy intervals are 0.2 MeV.

The detectors used in the above mentioned simulated experiment were three proportional counters, one scintillation spectrometer and a set of fifteen activation detectors.

The response functions of the proportional counters were calculated /4,5/ for 4 cm diameter spherical counter with no dead regions and with following gas fillings at 15 ^{o}C:

- 4.58 atm of hydrogen, 0.48 atm of methane and 4.58 atm of argon with useful range from 0.4 to 2.0 MeV;
- 9.63 atm of hydrogen with useful range from 0.2 to 1.2 MeV;
- 0.488 atm of hydrogen with useful range from 0.02 to 0.15 MeV.

For each spectrometer the responses were calculated for 30, 50 and 55 bins respectively and spanning the above mentioned energy intervals. Bin widths are such that (i+1)-th bin width is 5 % wider than i-th bin width.

The response surface of the NE-213 liquid organic scintillator is taken from the COOLC-FERDOR program package /6/. We have prepared response functions for 100 bins.

The neutron cross-sections data for activation detectors were taken from the SAND-II program library /7/ and were renormalized, using the recent evaluation of fission spectrum averaged cross-sections /8/. The fifteen detectors applied were:

^{237}Np(n,f), ^{32}S(n,p), ^{19}F(n,2n), ^{63}Cu(n,gamma), ^{197}Au(n,gamma), ^{23}Na(n,gamma), ^{235}U(n,f), ^{55}Mn(n,gamma), ^{103}Rh(n,n'), ^{56}Fe(n,p), ^{27}Al(n,alpha), ^{64}Zn(n,p), ^{115}In(n,n'), ^{27}Al(n,p) and ^{24}Mg(n,p).

The confidence interval of all the response function was taken to be constant for all bins and being about one percent.

The size of the response matrix is therefore 250 bins x 107 energy groups.

3. Description of the Numerical Experiment

At first the pulse height spectra bin values or the reaction rates a_i were calculated by a separate program, using

$$a_i \rightarrow \int_{E_1}^{E_2} \phi_t(E)\, R_i(E)\, dE \qquad (2)$$

where $\phi_t(E)$ is the neutron spectrum being tested and $R_i(E)$ is the response of i-th bin. This was done for all the detectors applied, that is for 250 bins and reaction rates.

In order to simulate the experimental conditions, all values a_i were additionaly randomly scattered according to the Gaussian distribution arround the calculated value a_i. Standard deviation of the distribution was taken to be the error δa_i. Relative error $\delta a_i/a_i$ was determined for each spectrometer type separately. It was taken to be 10 % for the minimal bin value and proportionally less for other bin values of the same spectrometer. Errors of the activation

detectors were taken to be few percent, according to our previous experience.

With all this data available we could proceed with the unfolding. Typical running time of our ITER routine was about 120 seconds and using some 40 K words of a CYBER 72 computer core.

4. Results

In these computer-simulated experiments we have investigated the following standard neutron spectra:

- Watt fission spectrum /7/
- Thermal reactor spectrum /7/
- $\Sigma\Sigma$ spectrum /9/
- fusion reference blanket spectrum /10/
- STEK-400, STEK-1000 and STEK-500 spectra /11/

All these spectra were unfolded using the whole 250 bins and three different initial spectrum approximations, namely a Watt fission spectrum, 1/E spectrum and constant.

Our expectation, that the influence of the initial approximation on the solution is negligible in the energy region well-covered by the detector responses (in our case from approx. 20 KeV to 14 MeV), was confirmed.

Fig. 1 and Fig. 2 present ratios ϕ_c/ϕ_t (i.e. unfolded spectrum ϕ_c versus tested spectrum ϕ_t) for the $\Sigma\Sigma$ and the thermal reactor spectrum in the energy region from 20 KeV to 14 MeV, as obtained with all three initial approximations. It can be seen that this

ratio is close to one within few percent deviation. This deviation can be explained as a consequence of random scattering of the input bin values a_i, since almost no deviation was observed for the spectra using non-scattered input bin values a_i.

As it can be expected, the ratio ϕ_c/ϕ_t will not be so close to one outside of the well-covered energy region. This can be seen in the Fig. 3, which depicts this ratio for the ΣΣ spectrum and all three initial spectrum approximations.

Tab. I presents the results of a thorough testing of the influence of the initial spectrum approximation upon the solution spectrum. All seven spectra were tested using all three initial spectra, in each case the same number of iterations was applied for the unfolding and the input bin values were randomly scattered. At the end the expression:

$$\xi = \sqrt{\sum_i \left(\frac{\phi_c^i - \phi_t^i}{\phi_c^i} \right)^2} \qquad (3)$$

was calculated for each solution spectrum within the energy region from 20 KeV to 14 MeV. One can conclude that the expression (3) varies very little with the initial approx. applied. Tab. I also presents the integral values of the tested spectra and of all unfolded spectra for the above menioned energy interval.

Measurements of a certain neutron spectrum are usually done at different neutron flux levels for different detectors. The error in renormalization of data to the same flux level may lead to the case in which all the pulse height data of a certain detector

or all reaction rates of activation detectors are wrong for the same fractional value. This leads to an erroneous solution spectrum. This was overcome by the following procedure:

a) Let us calculate the quantity:

$$f_i = \frac{1}{N_i} \sum_{j=N_{i-1}+1}^{N_{i-1}+N_i} \frac{a_j}{a_j^c} \qquad i=1,2,..,n \quad (4)$$

where a_j^c is i-th reaction rate or i-th bin value calculated from the known response function and the unfolded neutron spectrum, N_i is the number of bins of the i-th detector and n is the number of detectors. The expression (4) represents the average ratio of measured and calculated bin values for the i-th detector. All f_i should be close to one if the renormalization has been done correctly. If there is an renormalization error, the f_i will more or less deviate from one for all detectors. This is true also if only one detector is in error.

b) To find the wrong detector the following quantity is calculated

$$M_i = N_i \mid 1 - f_i \mid \qquad i=1,2,..,n \quad (5)$$

The erroneous detector belongs to the largest of M_i.

c) All of its bin values are multiplied by f^{-1} and the unfolding is repeated.

d) The procedure is iterated until the correction is smaller than a prescribed value.

Tab. II presents results of a thorough testing of the ΣΣ spectrum. Initial spectrum was constant and all bin values randomly scattered. To simulate the renormalization error all bin values for the three proportional counters and the scintillation spectrometer were one at the time increased and decreased for 5 and 15 %. In each case our routine, based upon expression (5), could detect the renormalization error and could compensate for it within the range of the pre-requested precision.

In Fig. 4 and Fig. 5 is shown the effect upon the unfolded ΣΣ spectrum of a 15 % renormalization error in 9.63 atm hydrogen filled proportional counter bin values. After the application of the correction routine the solution spectrum changed to its normal shape. The ratios a_j/a_j^c were appreciably below one and become one after application of the corrective routine, what indicates a much better fit to the experimental data.

5. Conclusions

The possibility of multispectrometer unfolding by a SAND-II type iterative code was demonstrated on seven typical neutron spectra. It was shown that the influence of the initial approximation on the solution is negligible in the energy region covered by the spectrometers used. A subroutine was developed which can correct for a possible error in the renormalization of the data from one spectrometer to the common neutron flux intensity.

References:

1. A.K.McCracken, M.J.Grimstone, The Experimental Data Processing Program RADAK; 1st ASTM-EURATON Symposium on Reactor Dosimetry, Petterm 1975.

2. M.Najžer, On the Possibility of Unfolding Simultaneously Data from Multiple Foil Proton Recoil and Other Neutron Spectrometers by the SAND-II Type Unfolding Codes, IAEA Consultants' Meeting, Vienna, Nov. 1976.

3. M.Pauko, M.Najžer, Iteration Acceleration in the ITER Unfolding Code,(on this conference).

4. N.L.Snidow, H.D.Warren, Wall Effect Corrections in Proportional Counter Spectrometers, Nucl. Inst. Meth. 51(1967).

5. J.B.Parker et al., The Interpretation of Recoil Proton Spectra, Nucl. Instr. Meth. 23(1963).

6. Oak Ridge National Lab. PSR17 and PSR18 - COOLC and FERDOR Spectra Unfolding Codes.

7. W.N.McElroy et al., A Computer Automated Iterative Method for Neutron Flux Spectra Determination by Foil Activation, RSIC Report AFWL-TR-67-41, Sept. 1967.

8. A.Fabry et al., Reaction Dosimetry Integral Reaction Rate Data in LMFBR Benchmark and Standard Neutron Field, Status, Accuracy and Implications, 1st ASTM--EURATOM Symposium on Reactor Dosimetry, Petten,1975.

9. G.De Leeuw et al., Neutron Spectrometry Data in LMFBR Benchmark and Standard Neutron Fields, 1st ASTM--EURATOM Symposium on Reactor Dosimetry, Petten 1975.

10. L.Y.M.Kuijpers, Experimental Model Studies for a Fusion Reactor Blanket, Eindhoven, 1976.

11. A.Fisher et al., Comparison of SAND-II and RFSP Spectrum Unfolding Codes for Several Neutron Spectra in the STEK Facility, RCN-75-115, Petten,1975.

Tab. I : Value ξ (Eq.3) and integral spectral values for different initial approximations, evaluated between 20 KeV and 14 MeV for seven tested spectra

spectrum	test sp. int.val.	1		1/E		fission	
		ξ	int.val.	ξ	int.val.	ξ	int.val.
$\Sigma\Sigma$	9.873E-4	0.173	9.817E-4	0.139	9.817E-4	0.288	9.817E-4
therm.react.	4.2	0.243	4.22	0.128	4.22	0.240	4.22
Watt fission	1.028	0.239	1.027	0.292	1.027	0.175	1.027
fusion[+]	1.611	2.464	1.598	2.404	1.598	1.872	1.598
STEK-4000	1.349E12	0.293	1.348E12	0.246	1.348E12	0.369	1.348E12
STEK-2000	1.144E12	0.302	1.174E12	0.259	1.174E12	0.369	1.174E12
STEK-500	1.036E12	0.278	1.036E12	0.278	1.036E12	0.330	1.036E12

[+]integral values calculated between 20 KeV and 17 MeV because of the peak at 14.1 MeV

Tab.II : Results obtained with the renormalisation routine
($\Sigma\Sigma$ spectrum with constant initial approximation)

a	figure of merit Mi					n	b
	P1	P2	P3	SC	AD		
Energy range 0.4 MeV - 2.0 MeV (proportional counter P1)							
1.05	0.688	0.440	0.070	0.460	0.123	3	1.008
0.95	0.722	0.600	0.027	0.570	0.003	3	0.991
1.15	1.953	1.385	0.103	1.380	0.254	5	1.007
0.85	2.306	1.760	0.005	1.760	0.155	5	0.996
Energy range 0.2 MeV - 1.2 MeV (proportional counter P2)							
1.05	0.391	1.090	0.383	0.270	0.108	3	1.007
0.95	0.397	0.985	0.297	0.360	0.023	3	0.990
1.15	1.110	2.985	1.015	0.830	0.186	5	1.007
0.85	1.234	3.251	1.037	1.060	0.072	5	0.984
Energy range 0.02 MeV - 0.15 MeV (proportional counter P3)							
1.05	0.012	0.195	0.340	0.030	0.098	2	1.020
0.95	0.012	0.345	0.459	0.050	0.036	4	0.980
1.15	0.028	0.670	1.048	0.010	0.152	9	1.038
0.85	0.040	0.965	1.382	0.080	0.024	5	0.963
Energy range 0.2 MeV - 16.0 MeV (scintillation spectrometer SC)							
1.05	0.260	0.140	0.059	1.260	0.384	4	1.010
0.95	0.260	0.275	0.038	1.210	0.273	4	0.985
1.15	0.775	0.550	0.081	3.590	0.945	5	1.032
0.85	0.794	0.705	0.016	3.860	1.043	5	0.965

a - multiplication factor for bin values a_i in order to simulate miscalibrated data
n - number of iterative steps for the renormalisation routine
b - factor for which the bin values still differ from one after the correction
M_i - figure of merit (Eq. 5)
AD- activation detectors

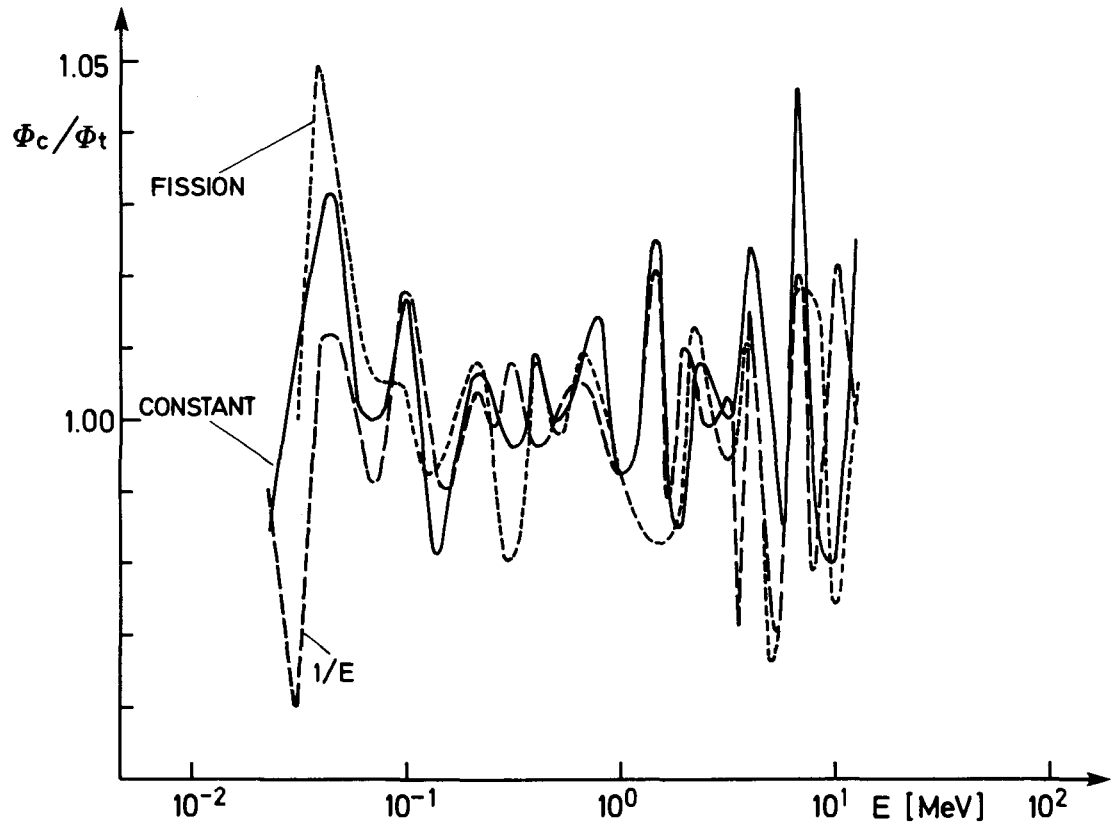

Fig.1 Ratios Φ_c/Φ_t for the $\Sigma\Sigma$ spectrum and three initial approximations

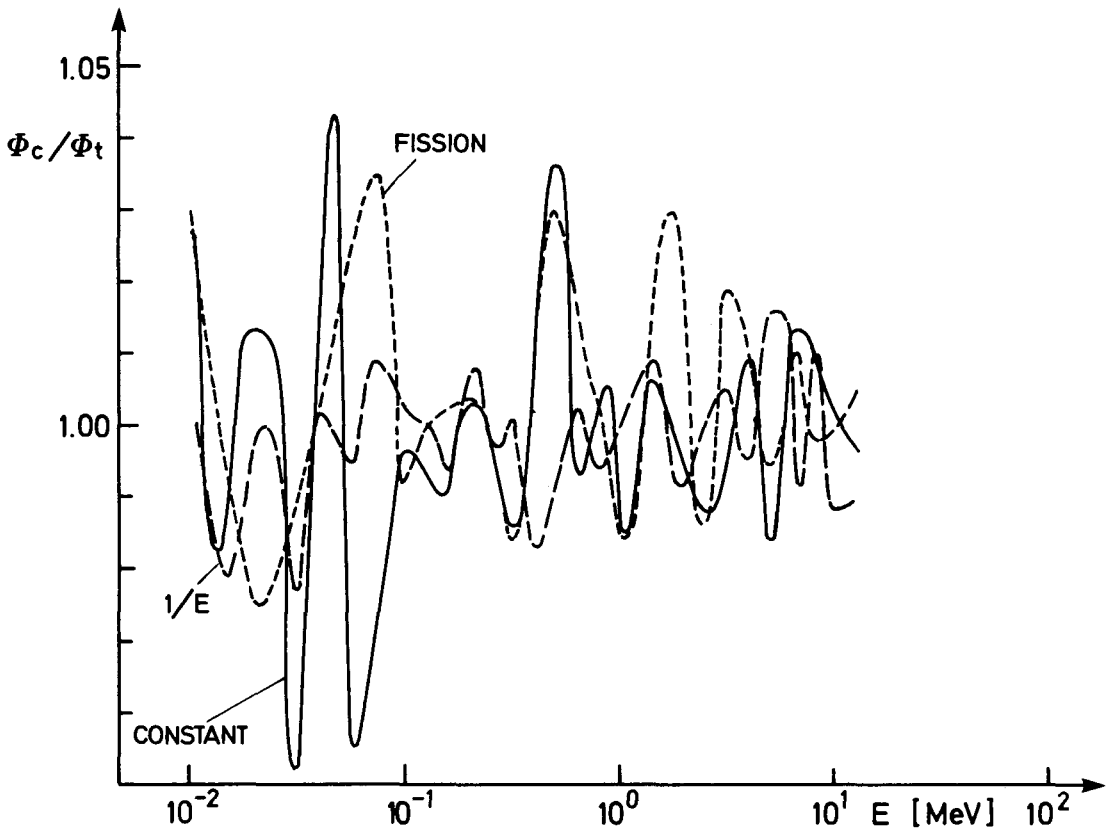

Fig.2 Ratios Φ_c/Φ_t for thermal reactor spectrum and three intial aproximations

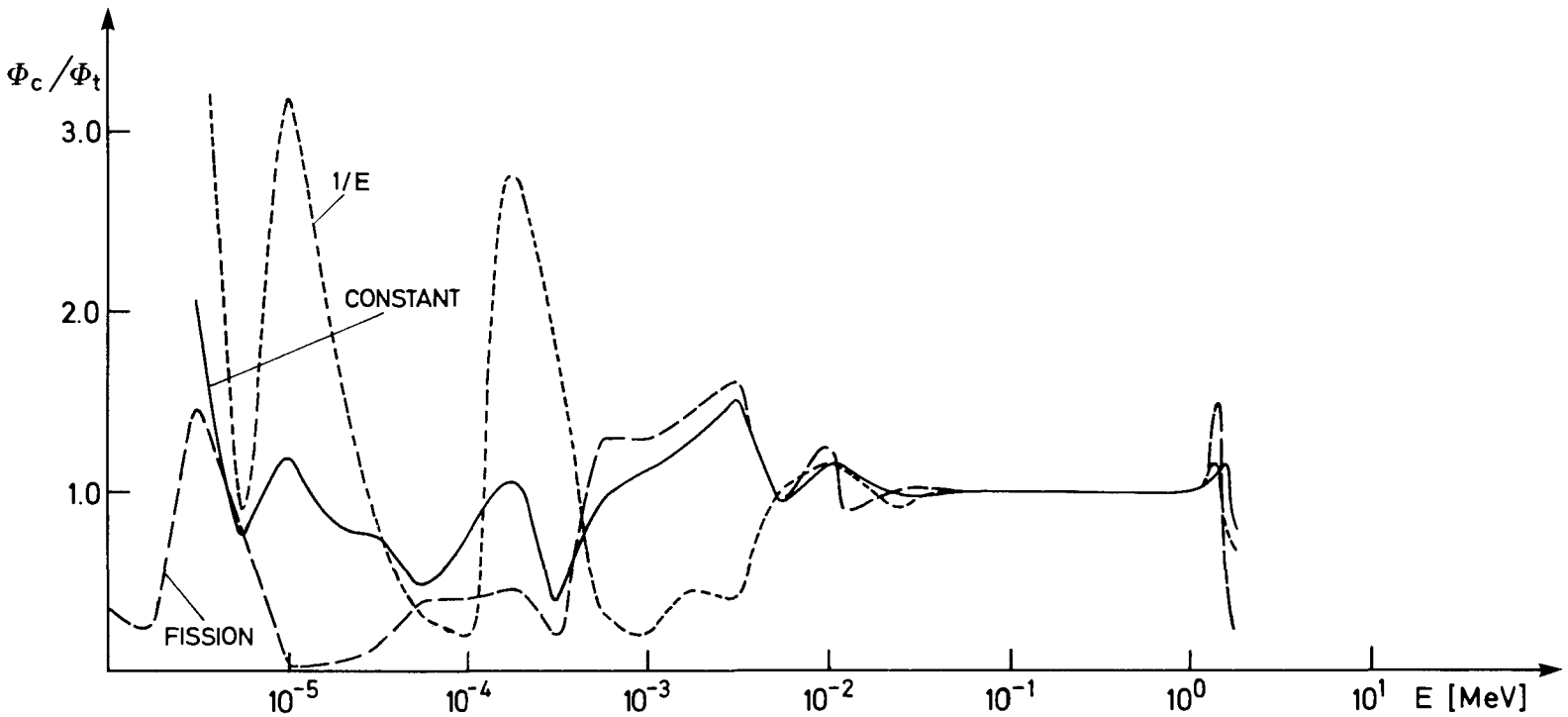

Fig. 3 Ratios Φ_c/Φ_t for $\Sigma\Sigma$ spectrum for three initial approximations

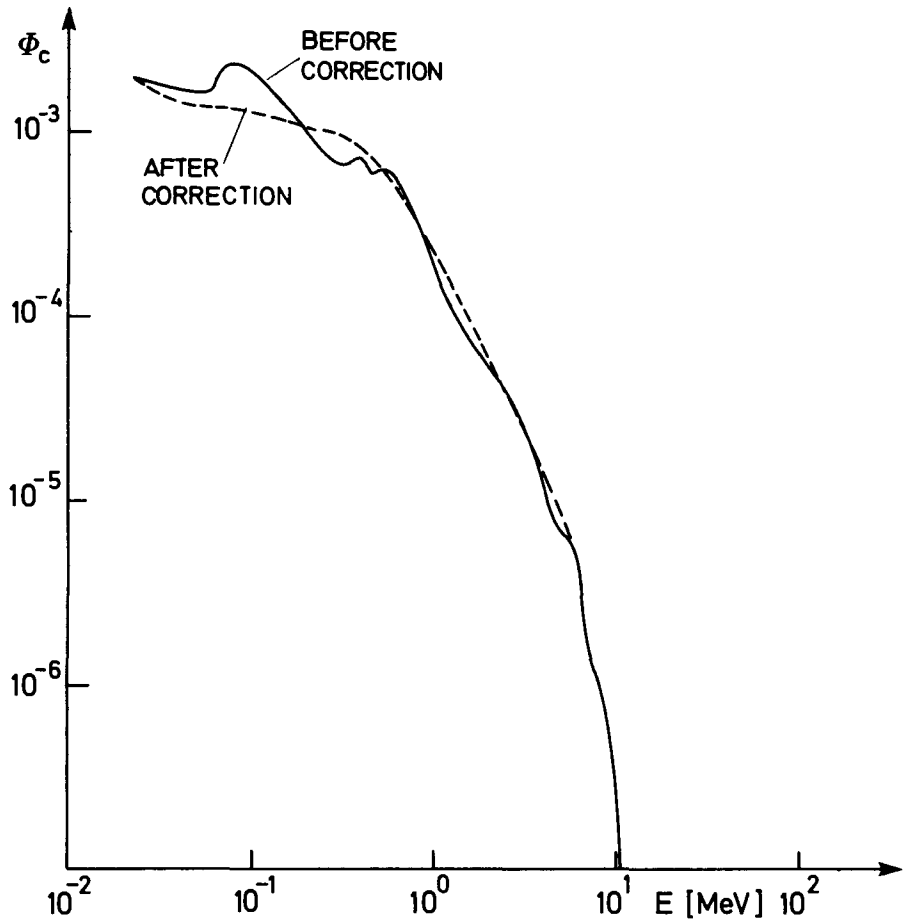

Fig. 4 $\Sigma\Sigma$ spectrum before and after correction of the shifted detector

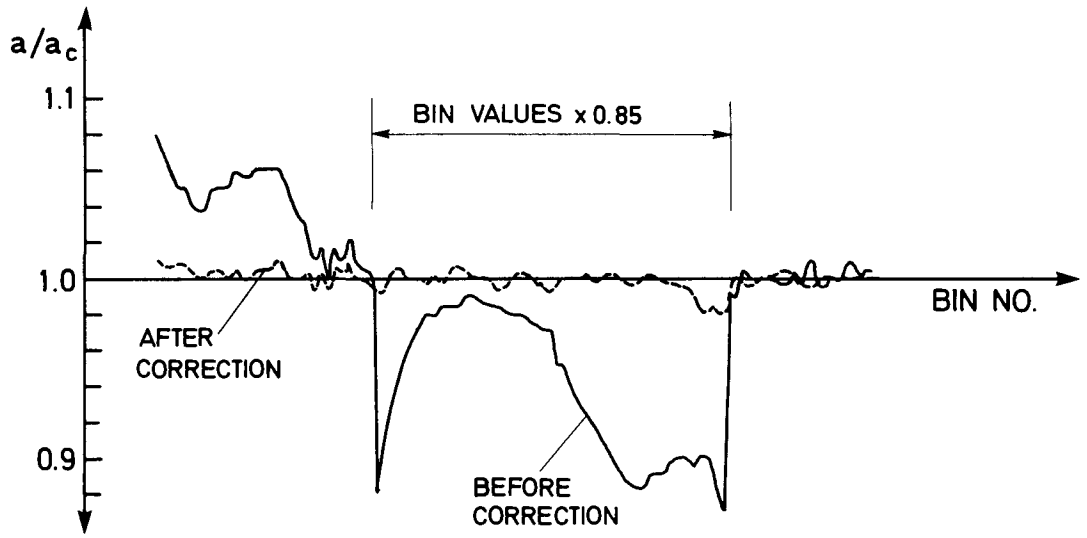

Fig. 5 Ratios a/a_c before and after correction ($\Sigma\Sigma$ spectrum)

Progress Report on the IAEA programme on the Standardization of Reactor Dosimetry Measurements

C. Ertek, B. Cross and V. Chernyshev

International Atomic Energy Agency
Vienna, Austria

Abstract

This report briefly summarizes present activities, current status and procedures associated with neutron spectrum unfolding by activation technique within the IAEA programme on standardization of reactor radiation measurements.

Experimental efforts and calculations related to unfolding are critically analyzed including the most recent techniques, interlaboratory cooperation, direct influence of recently measured cross-sections on the unfolded neutron flux density spectrum, re-evaluation of some cross-sections, neutron self-shielding factors and scattering effects.

This work has been performed within the IAEA programme on standardization of reactor radiation measurements, one of the important objectives of which is assistance to laboratories in the Member States to implement the multiple foil activation technique for neutron spectra unfolding, an especially useful technique for in-pile neutron measurements. The programme was initiated by the Metrology Section of the Seibersdorf Laboratory in cooperation with the Nuclear Data Section, the Reactor Physics Section of the Division of Nuclear Power and Reactors and with the support of the Computer Section.

Investigation of relevant problems, such as intercomparisons, influence of cross-section structure on unfolded neutron spectra, implementation of new codes, distribution of calibration source and foils, multigroup scheme, neutron self shielding factors, compilation work, critical evaluation of unfolding codes and application of recently evaluated cross-sections are briefly summarized.

1. Seibersdorf-Helsinki Intercomparison

We are grateful to laboratories of Member States for the concern they have shown to our IAEA programme on standardization of reactor radiation measurements especially to Helsinki University of Technology, Finland for their close cooperation under the leadership of Prof. Dr. Routti. In that particular work, a new generalized least squares unfolding method, LOUHI, (1) is directly compared with the SAND-II programme (2) by solving three different problems. In two of these problems, light water type reactor (LWR) neutron flux density spectra are considered. For the third problem, a betatron associated neutron flux spectrum is taken into consideration. In both calculation techniques, the LOUHI and the SAND-II, the same cross-section library ENDF/B-IV is used. For the first two LWR problems the same input spectrum and the reaction rates are used for calculation. As a result, through a series of procedures which are explicitly explained in Ref. (3-5), the solution reaction rates and neutron flux density spectra are compared. Very interestingly by this effort we almost find the same problematic reaction rates as found by the SAND-II using entirely different computer technique. The reaction rates giving the large differences between input and output values are tabulated in Table 1. Other values of reaction rates obtained by the LOU HI and SAND-II are shown in Table 2. Previously we presented 90% response intervals of these reactions (Ref 4). The overall differences in the neutron flux density spectra and more detailed results are presented in Ref.6. More detailed investigations on the physical as well as the mathematical aspects of the results will be further performed by Prof. Dr. J.T. Routti, Dr. J. Sandberg and co-workers.

Reaction	LOUHI	Δ_1 (%)	SAND-II	Δ_2 (%)
$^{27}Al(n,\alpha)^{24}Na$	1.402E-28	+ 9.45	1.366E-28	+ 6.64
$^{48}Ti(n,p)^{48}Sc$	4.816E-29	- 8.32	4.828E-29	+ 8.59
$^{115}In(n,n')^{115}In^{m}$	5.644E-26	+14.5	4.949E-26	+ 2.59
$^{127}I(n,2n)^{126}I$	1.928E-28	+33.9	1.331E-28	- 7.50
$^{232}Th(n,f)$	1.887E-26	+ 9.26	1.786E-26	+ 3.42

TABLE 1. Problematic reaction rates obtained by the LOUHI and the SAND-II

Reaction	LOUHI	Δ_1 (%)	SAND-II	Δ_2 (%)
$^{27}Al(n,p)^{27}Mg$	9.127E-28	+ 3.10	8.673E-28	- 2.03
$^{32}S(n,p)^{32}P$	1.455E-26	- 1.29	1.386E-26	- 5.97
$^{46}Ti(n,p)^{46}Sc$	2.651E-27	- 0.04	2.654E-27	+ 0.075
$^{47}Ti(n,p)^{47}Sc$	4.010E-27	- 1.26	4.206E-27	+ 3.57
$^{54}Fe(n,p)^{54}Mn$	1.832E-26	+ 0.38	1.754E-26	- 3.89
$^{56}Fe(n,p)^{56}Mn$	2.371E-28	+ 0.21	2.403E-28	+ 1.56
$^{58}Ni(n,p)^{58}Co$	2.414E-26	- 0.78	2.360E-26	- 3.00
$^{63}Cu(n,2n)^{62}Cu$	2.075E-29	+ 3.29	2.031E-29	+ 1.095
$^{103}Rh(n,n')^{103}Rh^{m}$	2.125E-25	- 5.64	2.180E-25	- 3.20
$^{237}Np(n,f)$	4.257E-25	- 1.69	4.279E-25	- 1.18
$^{238}U(n,f)$	6.791E-26	- 2.65	6.984E-26	+ 0.11

TABLE 2. Reaction rates obtained by the LOUHI and the SAND-II

2. Seibersdorf-CESNEF Cooperator

In CESNEF-politecnico di Milano, they have installed near the core of a water boiler of 50 kw, a neutron filter made of B_4C, in order to obtain a neutron flux density spectral shape that could be of utility in intercalibration problems connected with irradiations in fast assemblies. Dr. V. Sangiust kindly sent the input guess flux spectrum and a series of measured reaction rates to be treated by IAEA using the SAND-II and the CRYSTALL BALL (7) programmes. The meaningful comparison using the same ENDF/B-IV cross-section data is in progress. There are some refinement questions on the values of $^{27}Al(n.p)^{27}Mg$ and $^{54}Fe(n,p)^{54}Mn$ reaction rates.

3. Influence of cross-section structure on unfolded neutron spectra

The influence of cross-section structure on neutron spectra unfolded by multiple foil activation technique has been studied for the SAND-II case. For three reactions with evident structure in neutron cross-section above threshold: 27Al(n,α)24Na, 31P(n,p)31Si and 32S(n,p)32P, two remarkably different sets of evaluated data were selected from the available evaluations; one set of data was "smooth", the structure having been averaged over by a smooth curve; the other set was "sharp" with structure given in detail. These data were used in unfolding procedure together with other reactions, the same in both cases (as well as input spectra and measured reaction rates). It was found that during unfolding calculations less iteration steps were needed to unfold the neutron flux spectrum with the set of "sharp" data. In case of "smooth" data it was difficult to obtain an agreement between measured and calculated activity values even by increasing the number of iteration steps. Contrary to expectations, considerable deformation of unfolded neutron flux spectrum has been observed in the case of the "smooth" data set. These results are presented in the RSIC seminar-workshop or the "The ory and Application of Sensitivity and Uncertainty Analysis" held in Oak Ridge, Tennessee, August 22-24, 1978.

4. Implementation of the CRYSTAL BALL Programme

The implementation of the CRYSTAL BALL programme (7) is successfully achieved in the IAEA Seibersdorf Laboratory with the support of the IAEA Computer Section. But, unfortunately, the calculations showed that, from the computation time point of view, we found it 30 times more expensive than the code (2) SAND-II

for a particular problem. That was a drawback as one considers the implementation of this code in the laboratories of the Member States. But recently, Drs. F.B.K. Kam and F.W. Stallman, Oak Ridge National Laboratory, have incorporated a linear programme technique to obtain upper and lower bounds for integral responses of activation foils. They have now decided to replace the CRYSTAL BALL by the new code WINDOWS (8). They kindly informed us that the CRYSTAL BALL option in WINDOWS is executing approximately five times faster than the version we have in the IAEA Seibersdorf Laboratory. The documentation for WINDOWS is completed, however, the authors did not obtain approval to release the code. They predict that the WINDOWS will be available through RSIC before the end of the year, 1978. Preparations for the implementation of the WINDOWS has started in the IAEA Seibersdorf Laboratory.

5. Distribution of calibration source and foils

The reaction $^{103}Rh(n, n^1)^{103}Rh^m$ is, because of its low neutron energy threshold, very useful for the determination of the low energy part of fast neutron fluences in reactors or accelerators. Because of the short half-life (56 min) of the activation product 103-Rh-m, no activity standards of this nuclide can be procured from elsewhere. Relatively long-lived standards can be supplied, however, in the form of 103-Pd sources; this nuclide has a more convenient half-life of 17 days and emits the same K-X-rays or the 103-Rh-m.

The International Atomic Energy Agency's Seibersdorf Laboratory offered, as a part of its programme on the standardization of reactor radiation measurements, a limited number of kits which enabled a number of institutes to perform the necessary 103-Rh-m activity determinations for which only a suitable x-ray detector (e.g. a thin NaI(TI) detector with a Be-window) is needed.

One kit 103-Rh-m-11 was consisting of:

(a) 3 pure rhodium discs, diameter 10 mm, thickness 0.10 mm;
(b) 2 discs, diameter 10 mm, thickness 0.15 mm, consiting of aluminium and (4.00±0.01)% rhodium.
(c) One 103-palladium source with a nominal activity of about 74 kBg (2μCi). The radioactive material is sealed by heat between two

polystyrene foils; the diameter is 20 mm, the total thickness 0.5 mm.

More than 40 laboratories showed interest of having IAEA special standard foils and/or sources have been informed and a very good response received. Relevant information is given in Appendix 1. 14 kits to 13 laboratories of Member States have been supplied by IAEA, Seibersdorf Laboratory. Researchers, institutions and countries are shown in Table 3.

It is a great pleasure to acknowledge the interest and close cooperation of laboratories of the Member States with the IAEA Seibersdorf Laboratory.

The inclusion or exclusion of this $^{103}Rh(n,n^{1})^{103}Rh^{m}$ reaction to the neutron flux spectra unfolding may yield different results and these must be further investigated. We are kindly informed of some discrepancies from few of the laboratories of the Member States and this new information will provide further challenges to the understanding of unfolding and/or to the "best" set of reaction rates.

6. Multigroup scheme

As it is emphasized by U. Farinelli (9) it is important to optimize the subdivision of energy groups for a particular problem. For example 621 groups of SAND-II are too many for comfortable processing with space-dependent codes and too few to take into account the detailed resonance structure in a condensation procedure. There are improvements in this direction using e.g., 100 neutrons and 17 gamma groups (12). A standard scheme compatible with those set up in reactor physics and in shielding could have many advantages (9). The number of neutron energy groups may be decreased on the high energy tail of the flux spectrum and number of groups on the resonance energy may be increased. In cooperation with IAEA Seibersdorf Laboratory, CESNEF is working for preliminary unfolding on a MINISAND programme using smaller number of neutron energy groups. It will be interesting to calculate the influence of less neutron energy groups on unfolding. In order to see the interpolation and extrapolation errors in neutron spectra folding and unfolding a detailed report (13) is presented.

Researchers	Institutions	Countries
1. Doc. Dr. F. Bensch	Atominstitut d. Österr. Universitäten, Vienna	Austria
2. Dr. J.T. Gutierrez	Instituto de Asuntos Nucleares, Bogotá	Colombia
3. Prof. Dr. D. Seeliger	Technische Universität Dresden, Dresden	German Democratic Republic
4. Dr. M. Bricka	Centre d'Etudes Nucléaires de Cadarache, Cadarache	France
5. Dr. J.T. Nerurkar	Department of Atomic Energy, Bombay	India
6. Dr. R.A. Al-Kital	Iraqi Atomic Energy Commission, Baghdad	Iraq
7. Dr. N. Abdullah	Badan Tenaga Atom Nasoonal, Jakarta	Indonesia
8. Dr. M. Najzer	Institut "Jozef Stefan", Ljubljana	Yugoslavia
9. Dr. J. Spaans	Hoofd Bureau Commerciele Zaken Research Center, Petten	The Netherlands
10. —	University of Witwatersrand, Johannesburg	South Africa
11. Dr. G.W. Burholt	Univ. of London Reactor Center, Ascot, Berkshire	U.K.
12. Dr. W.H. Taylor	U.K. Atomic Energy Authority, Winfrith, Dorchester	U.K.
13. Dr. M.K. Kozlowski	Argonne National Laboratory, Argonne, Illinois	U.S.A.

Table 3

In this work, we first took an input spectrum for LWR type reactor, ENDF/B-IV cross-section data and a set of given saturation activities as indicated in reference (3). In order to find the energy spectrum of neutrons we ran the SAND-II programme on iteration mode and then activation mode is applied to find the same saturation activities. Then using the same cross-section data we recalculated the neutron flux spectrum. Two spectra are compared through the quantity called F (13) for 621 groups of neutron energy. In most of the points an agreement of the order of 0.02% has been achieved (13). That particular procedure can be an efficient check-up for the errors involved in the decrease of neutron energy groups at reasonably high energies.

7. Neutron self-shielding factors

As discussed in reference (3) in the determination of neutron self-shielding factors there are many discrepancies between calculations and experimental results (14-17). Especially, if one takes the case of self-shielding of ^{59}Co in the CFRMF neutron spectrum (18, 19) and 1/E neutron spectrum, the discrepancies are high (Table 8 and Fig. 7 of Ref. 14). With the CFRMF spectra and 1/E neutron spectrum, the use of total cross-sections from the ENDF/B-IV file yield much too low G values, especially at the resonance region.

For ^{55}Mn, both the ENDF/B-III without scattering and the ENDF/B-IV with total cross-sections give 6 values much lower than "expected" (Table 10 and Fig. 9 of Ref. 14). With the CFRMF spectra and 1/E neutron spectrum, the use of total cross sections from the ENDF/B-IV file yield much too low self-shielding G values, especially at the resonance peak region. For ^{55}Mn, both the ENDF/B-III without scattering and the ENDF/B-IV with total cross sections give G values much lower than "expected" for the resonance peaks at energies of a few hundred eV (Table 10 and Fig.9 of Ref.14).

Seibersdorf Laboratory has close contact with JAERI, Japan through Dr. I. Kondo on the compilation and selfshielding corrections of the cross-sections for resonance activation detectors. Up to now, the total or the absorption cross-section of the foil material is insufficiently considered

as far as the contribution to the selfshielding is concerned. As a matter of fact, the effect of scattering in the foil is often considered to be negligible. Sometimes it is considered to increase the chance of activations of the neutrons in the thermal energy region, and often to decrease the chances greatly at the resonance regions. However, in some cases, even in a resonance energy region, the energy loss of the neutron scattered by the foil nucleus is not large enough to be removed from the energy region under consideration. We are fully in agreement with JAERI and Petten that when the scattering to capture ratio is large or is found in cases of ^{55}Mn and ^{63}Cu it is not clear how to handle the situation. The decision should be made in the process of the neutron spectra computations with several combinations of the foil activities and the corresponding cross-section data. This problem together with streaming problems (20, 21) should be considered for each experimental set-up. We will repeat the need of having a special study group working only on these effects in specific irradiation arrangements for neutron dosimetry and damage determinations in reactor and CTR materials.

There are recent indications (22) that the determination of resonance parameters by area analysis give different scattering widths than the shape analysis of transmission. The evaluated parameters are not able to explain various integral experiments in thermal-neutron reactor fuel lattices. The effective or shielded resonance integrals, which are largely dependent (23) on the capture width of the 6.67eV resonance of e.g. ^{238}U are especially overpredicted by the evaluated resonance parameters. There is a spread on Γ_γ which we find very important.

Finally, a recent work (24) has indicated some important differences between the measured cross-section values and the values operated in the foil media. There is a systematic difference between the way for finding total cross-sections and the way of application of self-shielding factors. The determination of some self-shielding factors at Seibersdorf Laboratory with cooperation with Dr. F. Bensch from the Austrian Atomic Institut has started for on-resonance and off-resonance regions for neutron activation detectors.

8. $^{115}In(n,\gamma)^{116}In^m$ Reaction

An extensive report by the principal author (25) is issued on the penetration of mono-energetic neutrons inside the detector foils and related problems.

9. Reaction rate and neutron flux spectra compilation work

Compilation work of spectra obtained by calculation and/or by direct spectrometry and corresponding measured reaction rates for 1/E, LWR core and pressure vessel, CTR first wall and blanket have been completed. Unfortunately requests for LMFBR core and blanket and HTGCR moderator and iron block have not yet been supplied. Following the IWGRRM recommendations, the compilation of reaction rates have already yielded ways of finding biased reaction rates measured in some laboratories of Member STates and information exchange is in progress.

Reports on investigation of the neutron spectrum in the SCHERZO System BFS-35 by means of proton recoil proportional spectrometers and on measurements of neutron spectra behind iron-water and iron-shielding-configurations at the University Budapest by means of the Rossendorf proton recoil proportional counter spectrometer have been kindly sent by Dr. D. Albert and it is gratefully acknowledged.

10. Critical evaluation of unfolding codes

The merits of three neutron spectrum unfolding programmes are under investigation by Dr. W.L. Zijp (26). These unfolding programmes are: CRYSTAL BALL (7), RFSP-JÜL (27) and SAND-II (2). Recently a new neutron spectrum unfolding code STAY'SL became available (28). A sample problem for the intercomparison of these four existing programmes was also applied (29). It is found that (Fig. 1 of ref. 26) solution spectra and their ratio to the input spectrum introduces largest modifications and also the smoothest spectrum structure in the case of CRYSTAL BALL. The modifications of RFSP-JÜL and SAND-II are different and they have the same order of magnitude. We have only vague ideas about the origin of these modifications. In order to investigate them a systematic selection of activation detector (foils) sets seems important. In the test problem explained in Ref. 29, a set of only nine reaction rates was applied. They were eight activation reactions and one fission reaction. From the uncertainty data of the output spectrum of STAY'SL, it is found that the modifications are small in respect to their standard deviation. Under this condition no meaning can be given to the modifications and the reasons of these modifications are not known. The situation may not be the same for another

sets of reaction rates. The interference of the response functions must be carefully investigated. Fluctuations on the output spectra have been obtained for a number of set of reaction rates (3-6). For example, in Ref. 3, Fig.6, exclusion of $^{27}Al(n,\alpha)^{24}Na$ reaction has made significant changes in the betatron associated neutron flux spectrum. However 10% decrease in the value of this reaction rate did not make any substantial change. We do not know to what extent the systematic errors in cross-section data and activity values can contribute to unjustified modifications in different sets of reaction rates (29). The selection of suitable set or sets of reaction rates, neutron spectrum shape found by SAND-II unfolding code, 10 reaction rates from the second set (Ref. 3, Table 4) was almost identical with the spectrum obtained by the second set of 17 reaction rates. In addition, for the LWR input spectra (Ref.5 page 4), the prediction of saturation activities by SAND-II unfolding code show larger uncertainties for the following reactions:

$$^{238}U(n,\gamma)^{239}U,\quad ^{48}Ti(n,p)^{48}Sc,\quad ^{115}In(n,\gamma)^{116m}In,\quad ^{27}Al(n,\alpha)^{24}Na$$

$$\text{and}\quad ^{127}I(n,2n)^{126}I.$$

We need more solid justification criteria for the modifications which seems to be reliable. More comparisons with the direct spectrografic measurements and analytical calculations are needed using the F factor criteria which introduced in Ref. (3, 13).

Another difficulty is that the four unfolding codes have different methods to check whether the results after a modification step fulfil the required agreement with the input data. Additional difficulty is the difference in the number of energy groups. The programme STAY'SL does not need an external convergence criterium and it has a unique solution character. But it depends on the uncertainties given in the form of covariance matrices of the input spectrum, the activation data and the cross-sections. In addition, it is assumed that the three sets of input data (activation, cross-section and input neutron spectrum data) show no correlation of uncertainties between the sets (28). The input spectrum may be inadequate to obtain optimal results and in many cases plays a dominant role. The results presented in Ref.29 clearly supports

the conclusions of B. Arcipiani and M. Marsequerra (30) on the influence of the input spectrum dependency and the physical meaning of the modifications of the codes. The programme STAY'SL needs also input flux density with covariance data. In Ref. 29, 3% normalization uncertainty was applied and a purely diagonal component with a constant relative standard deviation of 24%. Questions like, why it is constant and why the value is 24%, remain for further discussion. The intercomparison between the codes should be made also in the energy ranges less than 1Mev with the F factor analysis protocol using a well-known cold, clean reactor reference spectrum (3, 13). The impact of unjustified modifications of different codes to the damage cross-section evaluations needs to be investigated.

The unfolded spectra for the ANL 16-Mev system (32) indicate that the neutron flux must be very small below 1 Mev. In order to make the calculated (n,γ) activation integrals agree with measurements, it was necessary to drop the lux sharply below the lowest measured flux at about 800 keV. The shape of the low energy portion of the spectrum cannot be precisely determined since the (n,γ) and $^{235}U(n,f)F.P.$ reactions have energy responses that are much too broad to unfold fine structure. Some of the (n,γ) reactions may have large errors in the Mev region as was seen for $^{197}Au(n,\gamma)$ at the recent NBS Symposium (31). Reducing the fast neutron cross sections would of course allow more flux at low energies (32).

11. Applications of new Titanium cross-sections

P. Smith, from the IAEA Nuclear Data Section has converted the point wise data of C. Philis et al. (33) to 621 groups for the $^{46}Ti(n,p)$, $^{47}Ti(n,p)$ and $^{48}Ti(n,p)$ reactions. Substantial changes in the neutron flux shape have been obtained and evaluations are in progress. Contributions from higher mass isotopes via (n,d) or (n,t) type reactions have been taken into account. Application of new digital values of ^{103}Rh by E. Barnard and D. Reitmann (34) is in consideration.

Final Remark

The success of the programme depends on the continuous and active interest of the laboratories of the Member States.

Acknowledgement

The authors are grateful to C.Z. Serpan, Jr. (NRC), W.N. McElroy (HEDL), U. Farinelli (CNEN, CSN), A. Fabry (CEN-SCK), J.A. Grundl (NBS), S. Pearlstein (BNL), W.L. Zijp (ECN), A.K. McCracken (AEEW), S.B. Wright (UKAEA), P. Mas (CEA), I. Kimura (Osaka), V. Benzi (Centro di Calcolo, Bologna) and J.T. Routti and J. Sandberg (Helsinki Uiversity of Technology) for their guidance, interest in, and valuable and continued support of this programme.

The authors thank J.J. Schmidt, A. Lorenz, H. Houtermans, J.A. Phillips, M. Vlasov and K. Okamoto for support and valuable comments on this programme.

We are indebt to F.B.K. Kam and B.F. Maskewitz (ORNL) for their cooperation.

Final note of appreciation goes to K. Schärf, N. Haselberger, F. Reichel, O. Milosevic and E. Ettel from Seibersdorf Laboratory for their many technical contributions.

REFERENCES

1. E. Rantanen, J. J. Routti, B. Bärs, Threshold detector measurements of fast neutron spectra on a Triga reactor with application of a new unfolding method, Atomkernergie (ATKE) Bd. 26 (1975) Lfg 2.

2. W. N. McElroy, et. al., "SAND-II, Neutron Flux Spectra Determination by Multiple Foil Activation Interative Method", RSIC Computer Code Collection CCC112, ORNL, (May 1969).

3. C. Ertek, et al., "Progress Report on the IAEA Activity on Neutron Spectra Unfolding by Activation Technique", 2nd ASTM-EURATOM Symposium on Reactor Dosimetry NUREG/CP-0004 Vol 3. p. 1385-1410, Oct. 1977.

4. C. Ertek, "Report on Some Interlaboratory IAEA Activities on Neutron Spectra Unfolding by Activation Technique" IAEA/RL/47, May,1978.

5. C. Ertek, "Prediction of Subgroup Saturation Activities Using Same Input Spectrum with Different Sets of Reaction Rates and Related Nuetron Spectra Unfolding Problems, IAEA/RL/49, June, 1978.

6. C. Ertek, Seibersdorf-Helsinki Intercomparison of Neutron Flux Density Spectra

7. F.B.K. Kam, F.W. Stallman, CRYSTAL BALL, Report ORNL-TM-4601, (June 1974).

8. F.B.K. Kam, private communication, Oct., 1978

9. U. Farinelli, 2nd ASTM-EURATOM Symposium on Reactor Dosimetry NUREG/CP-0004 Vol.1, p. 10, Oct. 1977.

10. E. Caglioti, M. Mattes, R. Nicks, H. Penkuhn, G. Hehn and V. Herrnberger "Generation and Testing of Shielding Data Libraries for Fission and Fusion Technology" 5th Int. Conf. on Reactor Shielding (Knoxville, 18-22 April 1977) paper C/6.

11. J. Schriever, G. Hehn, M. Mattes, G. Pfister and J. Keinert, "Integral Tests of Coupled Multigroup Neutron and Gamma Cross Sectons with Fission and Fusion Sources" ibid. paper TC84/12.

12. C.R. Weisbin, R.W. Roussin, E.M. Oblow, D.E. Cullen, J.E. White and R.Q.Wright "The Role of "Standard" Fine-Group Cross Section Libraries in Shielding Analysis" ibid. paper C/5.

13. C.Ertek, Errors Involved in the Folding and the Unfolding of Neutron Spectrum by SAND-II, IAEA/RL/51, August 1978.

14. A.M. Barsky, H.J. Nolthenius "Neutron Self-Shielding of Activation Detectors using Total Cross Section Values from the ENDF/B-IV Library, RCN-75-156 (Nov. 1976).

15. T.H.R. Skyrme, "Reduction in Neutron Density caused by an Absorbing Disc", UKAEA-MS (1961).

16. W.N. McElroy, "LMFBR Reaction Rate and Dosimetry 8th Progress Report for period March-September 1973", HEDL-TME-73-54, Hanford Engineering Dev. Lab., Richland, Washington, USA, February 1974.

17. A. Fabry, G. De Leeuw, S. De Leeuw, "The Secondary Intermediate Energy Standard Neutron Field at the Mol-Sigma Facility". Nuclear Technology, Vol. 25 (349-375),

18. G. De Leeuw-Gierts, S. De Leeuw, H.H. Helmick, J.W. Rogers, "Neutron Spectrometry Data in LMFBR Benchmark and Standard Neutron Fields", 1st ASTM-EURATOM Symposium on Reactor Dosimetry, Petten, Netherlands, EUR 5667 eff parts I and II (September 1975).

19. J.W. Rogers, Y.D. Harker, D.A. Millsop, "Fast Neutron Spectrum and Dosimetry Studies in the Coupled Fast Reactivity Measurements Facility, 1st ASTM-EURATOM Symposium on Reactor Dosimetry, Petten, Netherlands, EUR5667 eff parts I, II (September 1975).

20. G.P. Beer, "Differential Neutron Albedos for Cylindrical Water Surfaces", Nuc. Eng. and Design 33, 435-442 (1975).

21. G.P. Beer, "Neutron Streming through Conical Ducts in Water Shield", Nuc. Eng. and Design 33, 435-442 (1975).

22. P. Staveloz and E. Cornelis, "Precise measuremnt of the capture width of the 6.67 ev neutron resonance of Uranium-238, Nuc. Science and Eng. 66, 349-353 (1978).

23. M.R. Bhat, Proc. Sem. ^{238}U Resonance Capture, March 18-20, 1975, BNL-NCS-50451, p. 255, S. Pearlstein, Ed., Brookhaven National Laboratory (1975).

24. C. Ertek, An Investigation on the thickness dependence of the total cross-section determination, submitted to Nuclear Technology, 1978.

25. C. Ertek, On the penetration of mono-energetic neutrons inside the detector foils and related problems, IAEA RL-44, February 1977.

26. W.L. Zijp, Nico J.C.M. van der Borg and H.J. Nolthenius, Comparison of neutron spectrum unfolding codes, ECN-78-033, March 1978.

27. A. Fischer, "RFSP-TÜL: A programme for Unfolding Neutron Spectra from Activation Data", Jül-1475 (December 1977).

28. F.G. Perey, Least-Squares Dosimetry Unfolding: The Program STAY'SL ORNL/TM-6062, ENDF-254, October 1977.

29. W.L. Zijp, Nico J.C.M. van der Borg and H.J. Nolthenius, Comparison of neutron spectrum unfolding codes for the L54 Spectrum, ECN-78-125, August 1978.

30. B. Arcipiani and M. Marseguerra. Nuc. Inst. and Meth. 108 (1973) 301-307.

31. C.D.Bowman, A.D. Carlson, H.O. Liskien, eds. NBS, Special Publication 493 (October 1977).

32. R.R. Heinrich, L.R. Greenwood et al., Dosimetry needs for the magnetic fusion materials program, 2nd ASTM-EURATOM Symposium on Reactor Dosimetry, Palo Alto, California, USA, NUREG/CP-0004 p. 1017 (October 1977).

33. C. Philis, O. Bersillon, D. Smith, A. Smith, ANL/NDM-27, February 1977.

34. E. Barnard and D. Reitmann, Scattering of fast neutrons from ^{103}Rh, Nuclear Physics A303 (1978) 27-50.

APPENDIX 1

Vienna, 1978-02-20

Information

Kit 103-Rh-m-11

Some references on the excitation function of the reaction 103-Rh(n,n')103-Rh-m are given below (1)(2)(3).

103-Pd reference source

103-Pd decays, with a half-life of (16.96 ± 0.06 days) (4), in 99.97% of the electron capture transformations to 103-Rh-m. The conversion factor of 103-Rh-m being very large (α_K = 126), both nuclides emit essentially the same K-X-rays of about 20 keV only, with probabilities of 78% and 8.3% resp. The K-X-ray emission of the 103-Pd source (c) will therefore correspond to that from a 103-Rh-m source of about 1 MBq. This value, i.e. the equivalent 103-Rh-m activity (decaying with a half-life of 17 days), will be stated in the certificate.

Use of the Al-Rh discs

The 103-Rh-m activity in an irradiated Al-Rh foil (b) can easily be determined by comparing the X-ray emission with that from the 103-Pd source (c), measuring both in about 2 cm from a NaI(Tl) detector with Be-window. For the Al-Rh foils, the self-absorption is of the order of 1% only and can be calculated if better precision is desired.

Use of the pure Rh discs

The activity of the Al-Rh discs may, however, be too low for the measurements, if the neutron fluence is to be determined at places where the neutron flux density is low. The pure Rh discs (a) contain about 80 times more Rh than the Al-Rh discs and should be used in these cases.

Unfortunately, the self-absorption of the Rh discs when measuring K-X-rays is of the order of 50%. Some typical experimental values are given in (4), but whenever possible, the measurement of the self-absorption should be made for the source-detector set-up used. This can be done relatively easily, if Rh and Al-Rh can be irradiated simultaneously at some other place where the flux density is high enough to give convenient counting rates for both discs.

Multiple use of the Rh detectors

A half-life of (56.116 ± 0.009) min has been published for 103-Rh-m. The discs can therefore be used for several activations if the main activity is allowed to decay. Some long-lived activities, mainly 192-Ir, may build up, but their contribution to the counting rate may be subtracted if the disc is measured a second time after a day or so.

References

(1) Butler, J.P., Santry D.C., Conf. on Neutron Cross Section Technology, Proceedings, Washington (1968) Vol. 2, p. 803

(2) Kimura, I. et al., Nucl. Sci. Technology, 6, 485 (1969)

(3) Nagel, W., Aten Jr., A.h.W., J. Nuc. Energy 10, 475 (1966)

(4) Czock, K.H., Haselberger, N., Reichel, F., Int. J. Appl. Radiat. Isotopes 26, 417 (1975)

(5) Günther, E.R., Knauf, K., Walz, K.F., Int. J. Appl. Radiat. Isotopes 24, 87 (1973)

INFLUENCE OF CROSS-SECTION STRUCTURE ON UNFOLDED NEUTRON SPECTRA

C. Ertek, M.F. Vlasov, B. Cross, P.M. Smith
International Atomic Energy Agency
Vienna, Austria

ABSTRACT

The influence of cross-section structure on neutron spectra unfolded by multiple foil activation technique, SAND-II case, has been studied. For three reactions with evident structure in neutron cross-section above threshold: $^{27}Al(n,\alpha)^{24}Na$, $^{31}P(n,p)^{31}Si$ and $^{32}S(n,p)^{32}P$, two remarkably different sets of evaluated data were selected from the available evaluations; one set of data was "smooth", the structure having been averaged over by a smooth curve; the other set was "sharp" with structure given in detail. These data were used in unfolding procedure together with other reactions, the same in both cases (as well as input spectra and measured reaction rates). It was found that during unfolding calculations less iteration steps were needed to unfold the neutron flux spectrum with the set of "sharp" data. In case of "smooth" data it was difficult to obtain an agreement between measured and calculated activity values even by increasing the number of iteration steps. Contrary to expectations, considerable deformation of unfolded neutron flux spectrum has been observed in the case of the "smooth" data set.

This work has been performed within the IAEA programme on standardization of reactor radiation measurements, one of the important objectives of which is assistance to laboratories in member states to implement the multiple foil activation technique for neutron spectra unfolding, an especially useful technique for in-pile neutron measurements. The importance of this method, e.g. for radiation damage studies is well recognized [1,2].

In order to unfold a neutron spectrum, the following information is required:

a) measured saturation activities of the irradiated detector foils;

b) a set of energy-dependent neutron cross-sections for each foil;

c) a computer programme for unfolding spectra using an input spectrum and data noted in (a) and (b).

The ENDF/B Dosimetry File is finding increasing use as a reference cross-section data set; however, it does not include some important dosimetry reactions. Therefore, the IAEA Nuclear Data Section has initiated an

activity to evaluate these additional reactions. It is hoped that this expanded file will form a basis for an internationally recommended data set for neutron dosimetry applications.

The IAEA Seibersdorf Laboratory, with the support of the IAEA Computer Section, is currently involved in the intercomparison of available computer programmes for spectrum unfolding to recommend the best one (or a few) for general use. For the time being, the SAND-II [3] and CRYSTAL BALL [4] programmes have been implemented [5-7]. The RFSP-Jül [8] programme is under consideration and preparation have been started to implement the STAY'SL[9] unfolding code. The SAND-II programme has been compared with a new generalized least squares method by J.T. Routti [10].

As a part of these activities, we plan to investigate related problems such as the influence of input spectra on the solution spectrum, consistency of measured reaction rates, effects of structure in the energy-dependent neutron cross sections on the shape of the unfolded spectrum, etc. As the first step, we have studied the influence of cross-section structure on spectra unfolded with the SAND-II programme. The pressurized water reactor (PWR) type spectrum was chosen.

Three reactions ($^{27}Al(n,\alpha)^{24}Na$, $^{31}P(n,p)^{31}Si$ and $^{32}S(n,p)^{32}P$) with evident energy dependent cross-section structure were selected. For each reaction two sets of the evaluated data, "smooth" (structure averaged by smooth curve) and "sharp" (structure given in detail), were taken from the available evaluations and converted, where necessary, into SAND-II format. The cross sections together with the response functions in a Watt neutron spectrum are given in Fig. 1-6. In addition to these three reactions, seven other reactions, with identical evaluations in both "smooth" and "sharp" cases, were used to unfold the PWR type neutron spectrum. The saturation activities calculated with this spectrum were compared with the measured ones. This comparison is given in Table 1, from which it can be seen, that for the $^{31}P(n,p)^{31}Si$ reaction, the deviation of the measured from the calculated activity is ~7% in the "smooth" case, while it is only 0.5% in the "sharp" case.

For the $^{32}S(n,p)^{32}P$ reaction this deviation is ~-6% and -3% respectively. Less than 0.1% deviation is observed in both cases for $^{27}Al(n,\alpha)^{24}Na$ reaction. The overall standard deviation of the measured activities is ~3% in the "smooth" case as compared to 1.5% in the case of "sharp" data. Increasing the number of the iteration steps in the case of "smooth" data does not decrease the final deviation of the measured from calculated activity.

At first, one might expect that sharp structure in the cross-section would perturb the smooth shape of the unfolded spectrum; however, contrary to expectations, considerable deformation of the unfolded neutron flux spectrum has been observed in the case of the "smooth" data set in the energy range from 2.2 MeV up to ~6 MeV as shown in Fig. 8. It is difficult to explain in detail the observed results. However, it is clear that the "sharp" data, which more accurately represent the measured neutron cross sections, are preferable. At the same time these results suggest, that

smoothing of the input cross-section data should be done very carefully in order to avoid introducing distortions of the type seen in this work.

ACKNOWLEDGEMENTS

The authors would like to thank Dr. D.W. Muir for useful discussions and Mr. K. McLaughlin for assistance with computer plotting programmes.

REFERENCES

[1] 1st ASTM-EURATOM Symposium on Reactor Dosimetry, Petten, Netherlands, EUR 5667 e/f parts I and II (September 1975).

[2] 2nd ASTM-EURATOM Symposium on Reactor Dosimetry, Palo Alto, Calif., USA (October 1977) to be published.

[3] W.N. McElroy et al., "SAND-II, Neutron Flux Spectra Determinations by Multiple Foil Activation Iterative Method", RSIC Computer Code Collection CCC112, ORNL, (May 1969).

[4] F.B.K. Kam, F.W. Stallman, CRYSTAL BALL, Report ORNL-TM-4601 (June 1974).

[5] C. Ertek, "On the Penetration of Mono-energetic Neutrons Inside the Detector Foils and Related Problems", IAEA/RL/44 (February 1977).

[6] C. Ertek, et al. "Progress Report on the IAEA Activity on Neutron Spectra Unfolding by Activation Technique", paper presented at the Second ASTM-EURATOM symposium on Reactor Dosimetry, Palo Alto, Calif., USA (October 1977).

[7] C. Ertek, "Report on Some Interlaboratory IAEA Activities on Neutron Spectra Unfolding by Activation Technique", IAEA/RL/47 (May 1978).

[8] A. Fischer, "RESP-JÜL: A Programme for Unfolding Neutron Spectra from Activation Data", Jül-1475 (December 1977).

[9]. F.G. Perey, "Least-Squares Dosimetry Unfolding: The Programme STAY'SL", ORNL/TM-6062 (October 1977).

[10] J.T. Routti et al. "Threshold Detector Measurements of Fast Neutron Spectra in TRIGA Reactor with Application of a New Unfolding Method", Atomkernenergie (ATKE) Bd. 26(1975), Lfg. 2.

Table 1

RESULTS OBTAINED AFTER 12 ITERATIONS ("SMOOTH")

Foil Reaction	Saturated Measured Activity (DPS/Nucleus)	Saturated Calculated Activity (DPS/Nucleus)	Ratio Measured to Calculated Activities	Deviation of Measured from Calculated Activity (Percent)
$Sc45(n,\gamma)Sc46$	1.713E-24	1.734E-24	0.9880	-1.20
$Na23(n,\gamma)Na24$	3.997E-26	3.974E-26	1.0057	0.57
$Au197(n,\gamma)Au198$	6.836E-23	6.839E-23	0.9996	-0.04
$Co59(n,\gamma)Co60$	4.936E-24	4.936E-24	1.0001	0.01
$Th232(n,f)FP$	1.727E-26	1.749E-26	0.9877	-1.23
$Fe54(n,p)Mn54$	1.825E-26	1.822E-26	1.0019	0.19
$U235(n,f)FP$	4.084E-23	4.065E-23	1.0047	0.47
$Al27(n,\alpha)Na24$	1.281E-28	1.281E-28	1.0000	0.00
$P31(n,p)Si31$	7.836E-27	7.324E-27	1.0699	6.99
$S32(n,p)P32$	1.474E-26	1.564E-26	0.9425	-5.75
		Standard Deviation of Measured Activities (Percent)		3.08

RESULTS OBTAINED AFTER 12 ITERATIONS ("SHARP")

$Sc45(n,\gamma)Sc46$	1.713E-24	1.733E-24	0.9883	-1.17
$Na23(n,\gamma)Na24$	3.997E-26	3.973E-26	1.0061	0.61
$Au197(n,\gamma)Au198$	6.836E-23	6.837E-23	0.9999	-0.01
$Co59(n,\gamma)Co60$	4.936E-24	4.934E-24	1.0004	0.04
$Th232(n,p)FP$	1.727E-26	1.738E-26	0.9938	-0.62
$Fe54(n,p)Mn54$	1.825E-26	1.771E-26	1.0305	3.05
$U235(n,f)FP$	4.084E-23	4.064E-23	1.0049	0.49
$S32(n,p)P32$	1.474E-26	1.515E-26	0.9727	-2.73
$P31(n,p)Si31$	7.836E-27	7.796E-27	1.0052	0.52
$Al27(n,\alpha)Na24$	1.281E-28	1.283E-28	0.9981	-0.19
		Standard Deviation of Measured Activities (Percent)		1.47

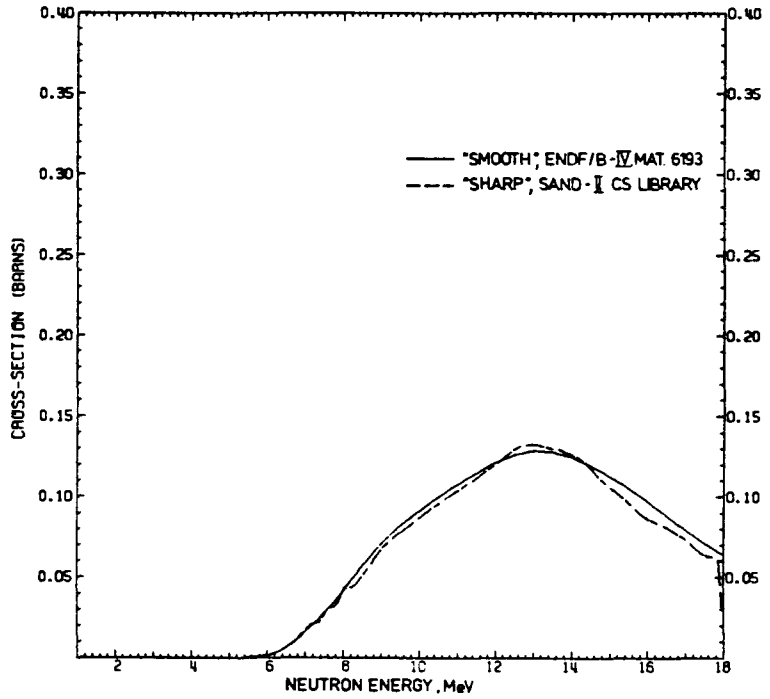

Fig. 1. 27Al(n,α)24Na neutron cross section.

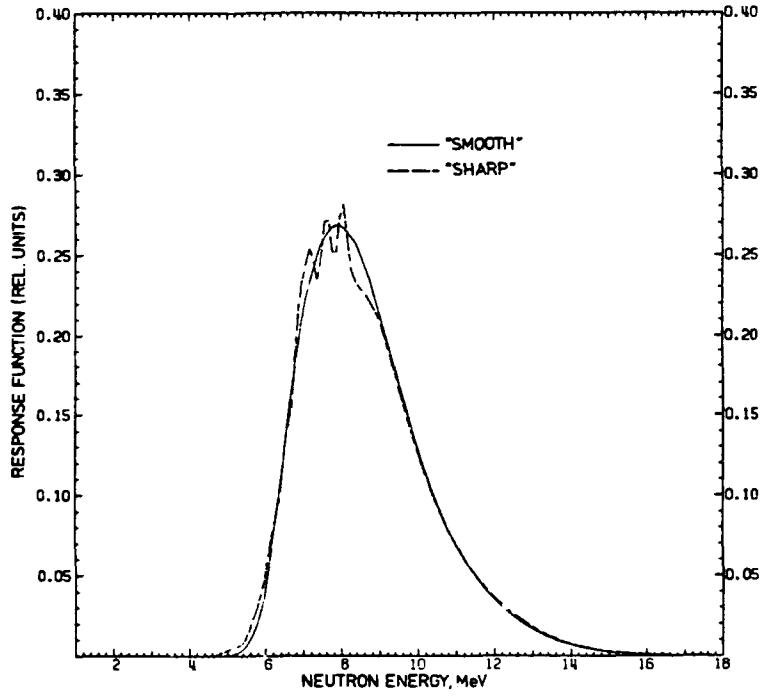

Fig. 2. 27Al(n,α)24Na response in Watt spectrum.

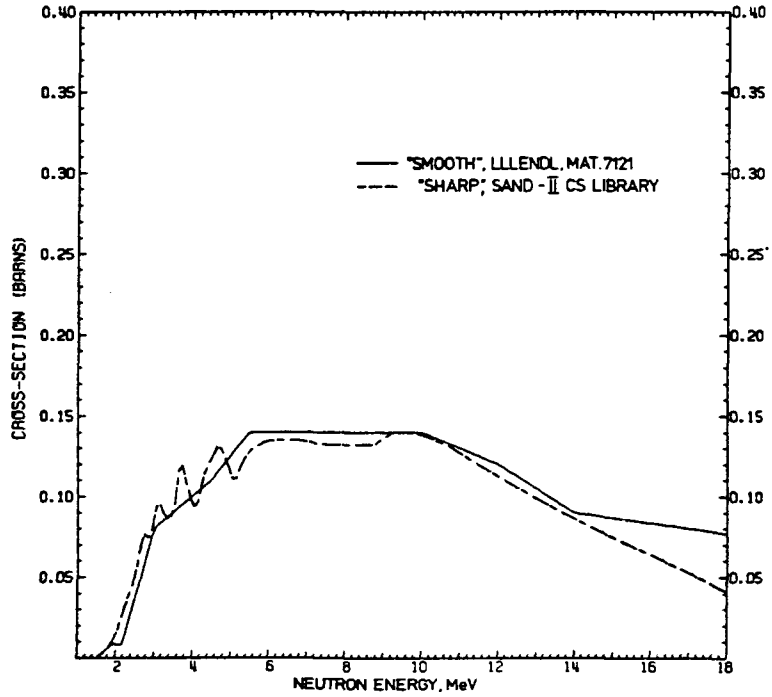

Fig. 3. 31P(n,p)31Si neutron cross section.

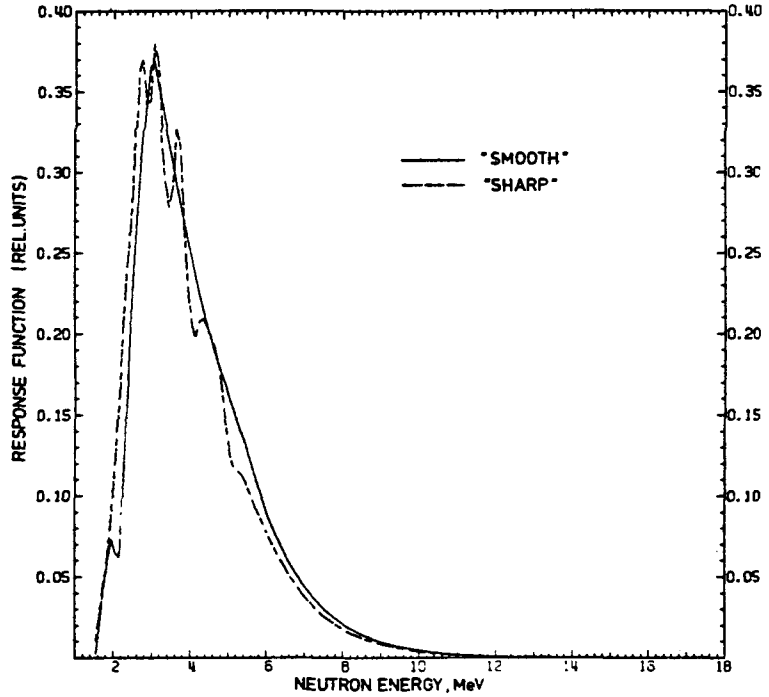

Fig. 4. 31P(n,p)31Si response in Watt spectrum.

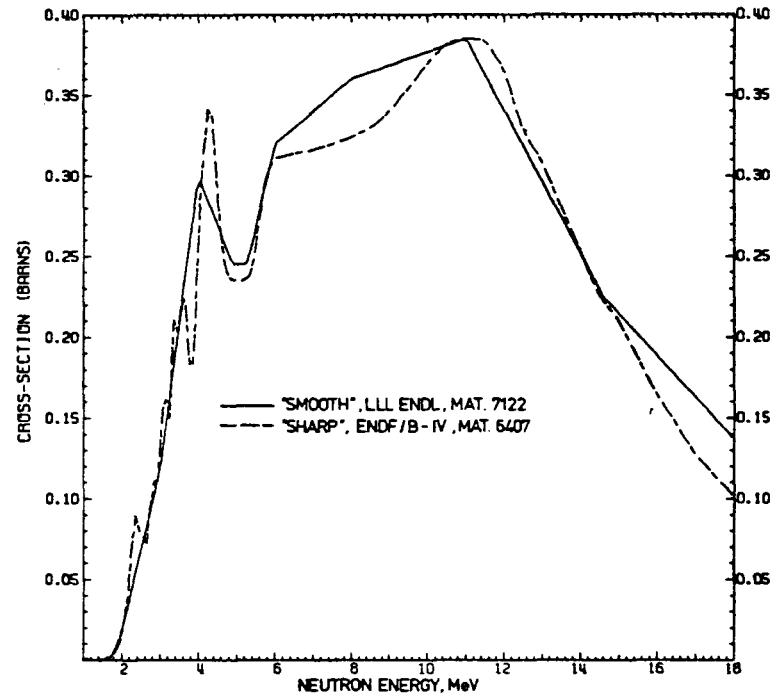

Fig. 5. 32S(n,p)32P neutron cross section.

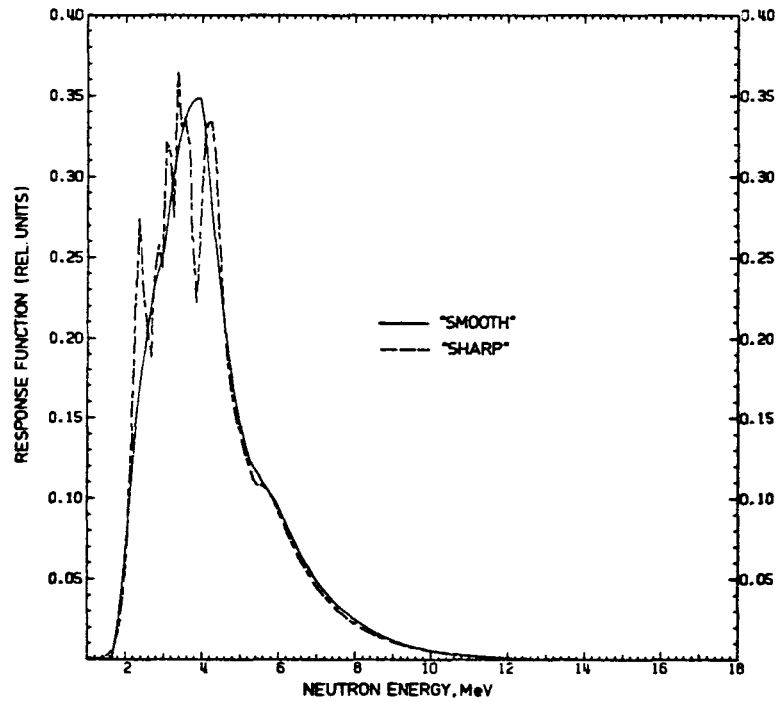

Fig. 6. 32S(n,p)32P response in Watt spectrum.

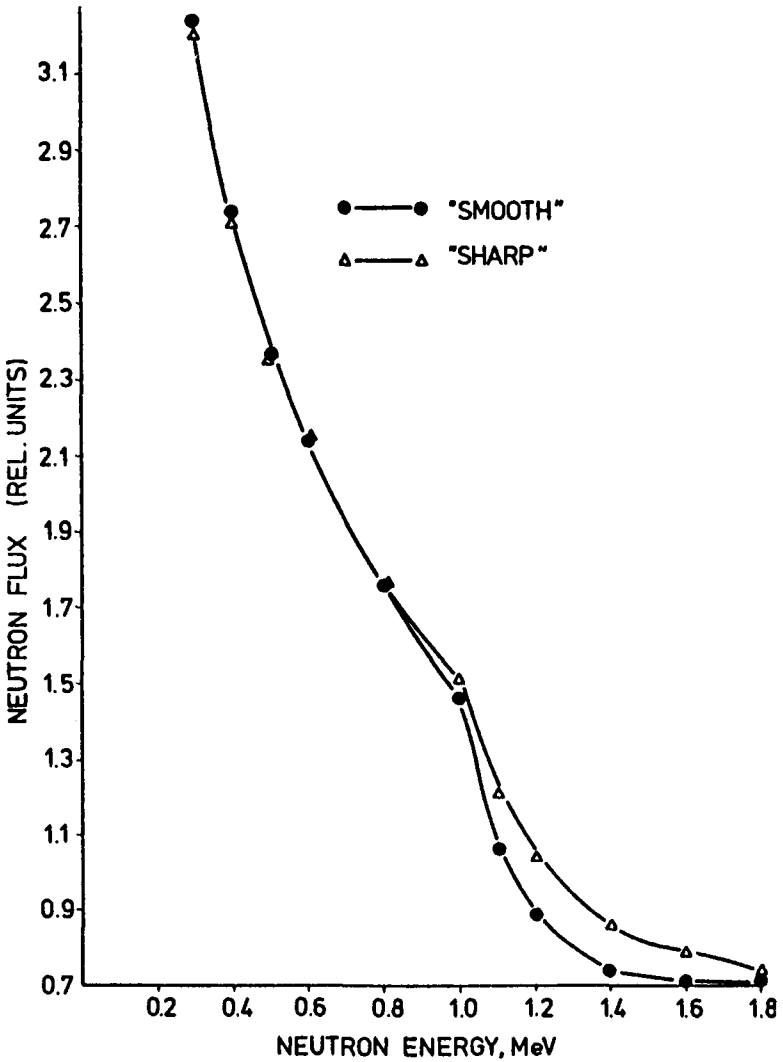

Fig. 7. PWR unfolded flux spectrum.

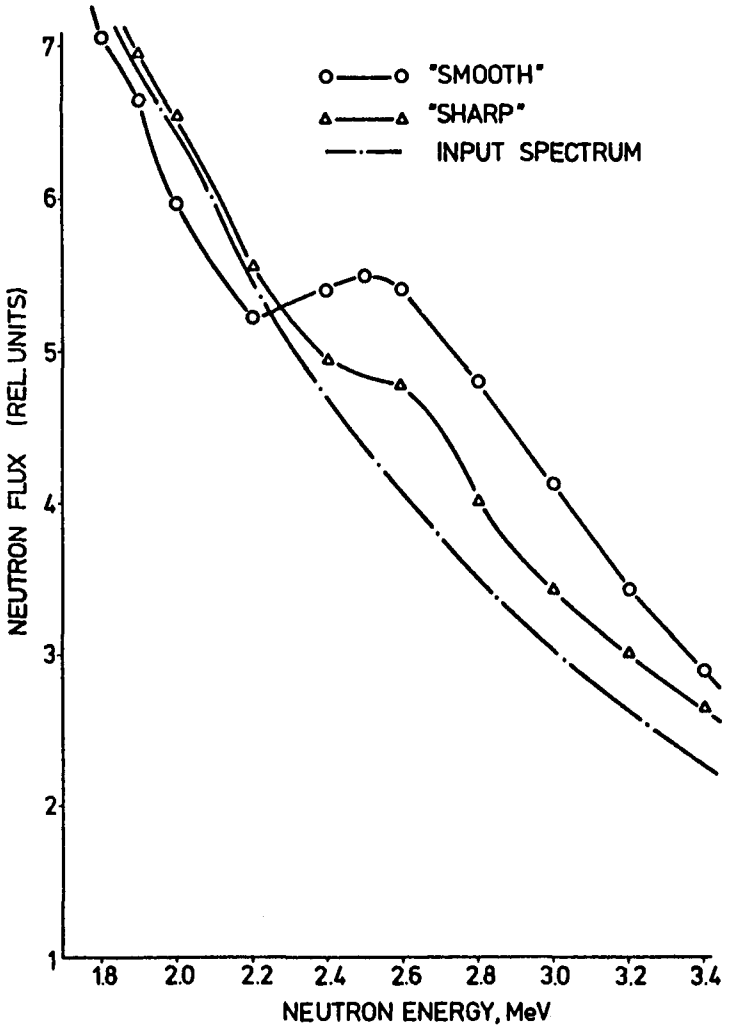

Fig. 8. PWR unfolded flux spectrum.

INTEGRAL CROSS SECTION MEASUREMENTS IN THE REFERENCE FIELD NISUS

G.D. Burholt, G.P. Dixon, S. Ghanbarzadeh,

M. Rahbar[+] and J.G. Williams

University of London Reactor Centre,
Imperial College,
Silwood Park, Sunninghill,
Ascot, Berkshire, SL5 7PY
U.K.

1. INTRODUCTION

The reference neutron field NISUS[1] at ULRC is one of a family of similar fields including also Mol-ΣΣ[2] and ITN-ΣΣ[3] generated by spherical natural uranium shells situated in reactor thermal columns.

Reaction rates measured in NISUS were reported at a previous IAEA meeting [2,3] two years ago. New measurements have been made since then with the objectives of comparing new techniques with results previously obtained, of providing data for reactions not previously studied and of confirming or improving previous data. Some of the measurements reported here were done as the starting point for a series of spherical shell transmission measurements to be done in the NISUS field. Transmission measurements in ^{238}U shells have been completed[4], and will be reported elsewhere.

The techniques used in this work were:

(i) absolute fission chamber measurements for five isotopes, including ^{236}U which has not previously been used in NISUS,

(ii) solid state track recorders (SSTR) for fission rate measurements in the same isotopes as (i) and for $^{10}B(n,\alpha)$ reaction rate, which has only previously been measured in benchmark fields by the total helium production technique[5],

(iii) activation foil measurements by calibrated gamma spectrometry for a number of threshold reactions, including $^{103}Rh(n,n')$ not previously measured in NISUS.

In this paper the experimental methods are reviewed and the new data are compared with previous ones. A revised set of recommended average cross-sections is presented. These are compared with values calculated from multi group dosimetry cross section data using the recommended NISUS spectrum[6].

[+]University of Tehran, P.O. Box 2989,
Tehran, Iran.

2. MONITORING PROCEDURES

A precise and stable flux monitoring system is a cardinal requirement for the operation of any standard or reference benchmark field. In NISUS this is achieved by means of gold foils and pulse fission chambers exposed to thermal neutrons in the thermal column in which the NISUS assembly is situated. The gold foil monitoring positions and the specification of the gold foils themselves have remained unchanged for experiments performed during the last four years. Since these monitors do not depend on any particular instrument they are considered to be the primary means of assuring long term reproducibility of the flux scale. The precision provided by these foil measurements, however, approaching ± 1% (1 standard deviation) on a single measurement, is inferior to that obtainable from the fission chamber monitors. The principal fission chamber monitor is a parallel plate pulse ionization chamber containing a ^{235}U deposit 20 mm in diameter. The secondary fission chamber monitor is a miniature cylindrical one also containing ^{235}U. The principal monitor which was installed early in 1977 provides a precision of ± 0.35% (1 s.d.).

All reaction rate data are reported here as reactions per principal monitor count, and the appropriate conversion to this scale has been made for all data taken prior to the installation of the present principal fission chamber monitor. The principal gold monitor (designated as position A in some reports) gives a saturated activity of 2.770×10^{-19} ± 0.6% disintegrations per target nucleus per principal fission monitor count.

3. ABSOLUTE FISSION CHAMBER MEASUREMENTS

Absolute fission chamber measurements previously reported for NISUS[3] were done with NBS-type, double gas-flow ionization pulse counters previously exposed in Mol-ΣΣ and ITN-ΣΣ. The measurements reported here were made with a new double fission chamber constructed at ULRC having electronic and neutronic specifications similar to the NBS type, but capable of taking a larger diameter of fission source. The sources consist of 20.0 mm diameter fissionable oxides prepared by vacuum evaporation on 32.0 mm diameter polished platinum discs 0.127 mm thick. These deposits were fabricated by the Chemistry Division of AERE Harwell under the supervision of Mrs. K. Glover[8,9].

Specifications of the deposits used in this work including values of the principal isotope masses are shown in Table 1. For ^{235}U and ^{238}U these masses were obtained by intercomparison with the NBS deposits used in earlier NISUS measurements[10]. For ^{239}Pu, ^{237}Np and ^{236}U the masses used were those measured at AERE Harwell by low geometry α assay[9]. Also shown in table 1 are the impurity fission corrections applied to each deposit for NISUS and corrections for fission fragment absorption in each deposit.

The chamber was operated in the way recommended by Grundl et al[7] for the NBS chambers. Three discriminators and scalers were used for each side of the double chamber. The setting of these discriminators were 0.36 Vp, 0.54 Vp and 1.4Vp, where Vp is the pulse height of the peak in the height distribution, and the counts in each scaler were denoted by S_L, S_U and S_{GC} respectively. The difference in counts S_L and S_U is used to infer the number of valid fission counts between 0.36Vp and zero pulse height, and hence the extrapolation to zero (ETZ) correction to be applied to the recorded counts, S_L. The needed correction is assumed to be $2(1 - S_V/S_L)$, on the basis that the pulse height distribution for valid fission pulses is flat for $0 < V < 0.54Vp$. This correction was found to vary in a nearly linear way with deposit thickness, with a near zero intercept for zero deposit thickness (Fig. 1). The close similarity of Fig. 1 with Fig. 4 of reference 7 is very gratifying as it proves that despite its larger diameter and other slight differences our chamber is performing in an almost identical way as the NBS chambers, and the deposits also must be of similar uniform quality. Although Fig. 1 shows the result obtained for a deposit of nearly 1000 $\mu g/cm^2$ the thickest deposit used for fission rate determinations in the chamber was less than 250 $\mu g/cm^2$.

In addition to providing the necessary ETZ corrections the ratio S_U/S_L and also S_{GC}/S_L provide sensitive checks on the performance of the chamber during each measurement. During some of the early runs some departures from the expected ratios were noticed. These were later found to be due to a lack of earth continuity to the chamber body, resulting in enhanced interference pick-up. This effect was eliminated and subsequent runs always produced ETZ corrections very close to the values shown in Fig. 1. Data from runs containing anomalous S_U/S_L ratios were always rejected.

3.2 MOUNTING ARRANGEMENTS AND FIELD PERTURBATION CORRECTIONS

The chamber was mounted in NISUS in the manner shown in Fig. 2. This mounting is neutronically equivalent to mountings previously employed in the Mol-ΣΣ facility[11] and is almost the same as that previously used in NISUS[3] except that the 45 mm diameter access hole in the boron carbide shell is now almost completely filled with boron carbide, instead of only cadmium. The same correction factor (0.995 ± 0.005) as previously used in Mol-ΣΣ and NISUS for epicadmium neutron leakage along the remaining cylindrical hole was applied to the present data for ^{235}U and ^{239}Pu fission rates. No correction is needed for subcadmium neutron leakage because the solid angle containing paths not covered by cadmium pieces is extremely small. The same correction factors as previously used in Mol-ΣΣ and NISUS for neutron scattering and absorption in the NBS fission chamber components were also applied to the new ULRC fission chamber results reported here, because of the similarity in materials and geometry of the new chamber to the NBS one (the only significant change is in the diameter). These correction factors[3] were 1.006 ± 0.003 for threshold detectors and $1.000 \pm .001$ for ^{235}U and ^{239}Pu.

3.3 FISSION RATES

Raw fission count rates for each of the five isotopes and for the two fission chamber monitors were recorded in several runs with different combinations of pairs of deposits used back-to-back. Corrections were applied for impurity fissions and absorption of fission fragments (Table 1), and ETZ (Fig. 1). Dead time losses were negligible.

Reaction rates obtained per principal fission monitor count are shown in Table 2. Also shown are fission cross section ratios relative to ^{235}U for the present work and previous measurements done with the NBS chambers. The agreement is very satisfactory and demonstrates, among other things, that the mass assays done at Harwell for the ^{237}Np and ^{239}Pu deposits are consistent with NBS masses. (The ^{235}U and ^{238}U deposit masses used here were obtained from back-to-back intercomparisons with NBS deposits).

4. SSTR FISSION RATE MEASUREMENTS

The use of SSTR for absolute fission rate measurements was considered by Grundl et al[7] to have the status of a secondary method, while fission chamber measurements were the primary and reference method. This point of view has been deprecated by Gold[12] who cites earlier work in which the accuracy obtainable with SSTR is documented and points to the undeniable advantages of having two techniques. This discussion concerned the merits of track recorder measurements made in 2π geometry, i.e. with the detector in contact with a fissionable source.

Two of the present authors (G.P. Dixon and J.G. Williams) have studied this question and consider that etched track recorders exposed to fission fragments in 2π geometry can never routinely provide performance comparable with fission chambers because of the nature of the process whereby tracks are revealed by etching. Tracks incident at angles less than a critical angle, θ_c, with the surface of an SSTR are not revealed because of the removal of bulk material from the surface. The criterion is usually stated as $\sin\theta_c = V_B/V_T$, where V_B and V_T are the bulk and track etching rates respectively. The matter is not so simple as might appear from this, however, for two reasons. The first is that the track etch rate V_T is not constant along the length of a track, because of energy loss, and also differs from one fission fragment to another. Thus the effective value of θ_c depends on a variety of factors including the thickness of the source and the etching conditions employed. The second problem is that while particles incident on the film at angles greater than θ_c to the surface can produce etch pits, the depth of these tends to zero as the critical angle is approached. Obviously a track can only be seen if it has some minimum depth, but what this minimum is will depend on a number of factors which are very difficult to control. These include the illumination conditions in the

microscope, the visual acuity of the observer and the number and nature of the extraneous features invariably found in SSTR materials. The results of Gold[12] and his group do suggest that these problems can be overcome with sufficient effort and determination, but the claim that the task of correcting for undetected fissions in SSTR is analogous to the ETZ corrections needed in fission chamber measurements will not stand close examination, because the proportion of events falling below and near the registration threshold is much larger in SSTR (5-6%) than is normally tolerated in fission chamber work, and furthermore this proportion does not tend to zero as the source thickness is reduced. A further complication, easily overlooked, is that the corrections for SSTR optical efficiency and for fission fragments stopped in a deposit are not independent of one another since the same low angle events are involved in each case.

The above mentioned problems are all associated with detection of tracks at low angles to the detector surface, and can therefore be eliminated if 2π geometry is abandoned. This was done by Gilliam and Knoll[13] in their fission cross-section measurements using monoenergetic neutron sources, and in the work reported here. The introduction of a space between the fission fragment source and the detector means relinquishing some of the usual advantages of the SSTR technique in terms of size and convenience, and also introduces an error due to solid angle determinations, but the gain in ease of track counting is very great and the assumption can be safely made that every fission fragment incident on the detector will leave an identifiable track.

4.1 IRRADIATION CONDITIONS

The track recorder measurements reported here were made in an evacuated chamber in which pairs of fissionable deposits were exposed back-to-back in NISUS. The detectors were positioned behind circular apertures 20 mm in diameter (the same as the diameter of the deposits) spaced at 10 mm from the face of each deposit. The chamber containing the deposits was held on a long pumping stem similar to the stem of the fission chamber and the construction and mounting arrangements were made as similar as possible to those used for the fission chamber work so that the same instrumental and field perturbation corrections could be applied. Irradiation times were controlled by means of the NISUS shutter and the two fission chamber monitors were used. The deposits used were from the same set as used for the fission chamber experiments (Table 1).

4.2 TRACK ETCHING AND COUNTING

The track recorders used were cut from sheets of Cronar (Dupont trade name for polyethylene tetraphthalate) 94 mm thick, washed in demineralised water and dried before irradiation. Etching was done in 6.25N NaOH at 50°C for five hours without agitation. This treatment caused a change in thickness of 9 μm (4.5 μm from each side) and resulted in circular or oval fission tracks 6-8 μm across the minor axis. The tracks were very easily identifiable at 400X magnification in transmitted light and no background tracks were seen on the reverse of the film or in the unexposed portion around the edges. A few surface defects in the film were noticeable but these were easily distinguishable as such. Overlapping tracks could also be readily identified, even the rare events where more than two tracks intersected were usually easily resolved.

The whole exposed area of each recorder was scanned. The exposure time of each deposit were chosen to provide a suitable total number of tracks, between 9,000 and 23,000, in each case. Counting these took between 2½ and 6 hours, in sessions of not more than 1 hour.

4.3 SSTR RESULTS

Track counts were corrected for impurity fissions and for field perturbations, using the same values as for fission chamber measurements. The geometry factor was calculated using the formula of Jaffey[14]:

$$g = \tfrac{1}{2}\left[1 - \frac{D}{T}\right] - \frac{3}{16} A^2\left[\frac{B^2 D}{T^5}\right] + \frac{5}{32} A^4\left[\frac{B^2 D}{T^9}\right] \times \left[D^2 - \frac{3}{4} B^2\right]$$

where D = distance from source to detector aperture
A = source radius
B = aperture radius
T = $(D^2 + B^2)^{\frac{1}{2}}$

The efficiency is obtained by doubling the result to account for both fission fragments. No correction for fission fragment scattering has been considered necessary.

The results for each isotope are shown in Table 3, where the fission chamber values are also given for comparison and the ratio of the two results. The agreement between the two techniques is disappointing, even granted the modest statistical precision of the SSTR results (∿ 1%), and it seems that the SSTR values must be to blame. The only cause which seems plausible is that the geometry was not well enough controlled because of a lack of flatness of the deposit backings. The

irradiation rig was deliberately miniaturised so that back-to-back irradiations could be performed in a chamber comparable in size with a double fission chamber. It now appears that this was a mistake and that a larger rig is necessary. The track counting errors were certainly very much less than the statistical errors as consistency between two observers showed.

Despite the above remarks the comparison has been a useful one and the method does seem worth persevering with and still seems potentially superior to 2π geometry methods.

5. SSTR $^{10}B(n,\alpha)$ MEASUREMENTS

The need for an alternative technique for (n,α) reaction rate measurements to supplement the helium accumulation method was pointed out at the previous IAEA meeting on cross sections for reactor dosimetry[15].

Among plastics which have been used as SSTR are a few which can record α particles, including cellulose nitrate (C.N), cellulose acetate (C.A) and cellulose acetate butyrate (C.A.B). Cellulose nitrate film CA80-15 (Kodak Pathe) was chosen for $^{10}B(n,\alpha)^{7}Li$ reaction rate measurements in NISUS. This material will record both the ^{7}Li and alpha particles at least up to 4 MeV[16]. High energy alpha particles are also recorded but these are only revealed by etching if the etching time is long enough to remove the surface by bulk etching down to the point where the particles have slowed to approximately 4 MeV. On the other hand very long etching will also remove some etch pits due to shorter range particles and those at small angles with the surface. In NISUS irradiations the fraction of alpha particles from $^{10}B(n,\alpha)$ reactions with energies above 4 MeV is much less than one percent and can be neglected, but this may not be the case in a harder neutron spectrum.

In addition to the need to record α particles up to 4 MeV the following desirable characteristics were sought:

(i) The detector should be free of inherent faults and background tracks.

(ii) The detector should be insensitive to particles from $^{14}N(n,\alpha)^{11}B$, $^{14}N(n,p)^{14}C$ and $^{17}O(n,\alpha)^{14}C$ reactions occurring in the detector material.

(iii) The detector should be insensitive to recoil particles such as hydrogen, carbon and oxygen produced by elastic collisions of fast neutrons.

Unfortunately all the above requirements could not be met by any detector tried. In particular a material without nitrogen was not found which had adequate sensitivity to α particles and was able to satisfy (i). CA80-15 is of good enough quality but also records recoil tracks including protons and contains a lot of nitrogen. The proton tracks are only etchable when their energy falls below 100 keV and so produce only very short tracks ($\sim$ 0.5 μm). All films exposed in the fast neutron field were found to be peppered liberally with small dark dots which were attributed to recoil protons. These could be distinguished

from α and ^{7}Li tracks because of their small size. More troublesome were longer tracks attributed mainly to $^{14}N(n,\alpha)$ reactions and carbon and oxygen recoils. These could not be distinguished in any systematic way from the wanted tracks, and therefore had to be treated by means of a background correction obtained by counting tracks on the reverse side of the detectors.

5.1 EXPERIMENTAL PROCEDURE

It had been hoped initially to conduct the $^{10}B(n,\alpha)$ measurements not in 2π geometry, but in the same way as the fission rate measurements already described. This was not possible because of the problem of background tracks which made the signal to background ratio an overriding consideration. Therefore the detectors were placed in contact with the source in the usual way.

The source consisted of a natural boron evaporated deposit of approximately 20 $\mu g/cm^2$ on an aluminium backing 0.5 mm thick. Since the mass of this was not well known and nor was the registration efficiency of the detector, a calibration experiment using thermal neutrons was done. For this a gold foil 5 μm thick was irradiated in contact with the deposit backing in a cavity in a very well thermalised flux. The activity of the foil was found using the $4\pi\beta$-γ coincidence method. It was not possible, because of the high sensitivity of the track recorder to count the tracks formed in this irradiation, so a second irradiation was done under the same conditions but at a lower flux and fission chamber monitors were used to provide the appropriate normalisation. The effective mass per unit area (actually the product of the true mass per unit area and the registration efficiency) of the deposit could thus be found.

The recorders were etched at 18°C in 2.5N NaOH solutions for 28 hours. Previous trials had established that the track density found after 21 hours of etching did not change after a further 7 hours, but the tracks became larger and easier to count. Films exposed in the thermal flux and in NISUS were counted on both sides but only a negligible number of background tracks were found for the thermal irradiations. For the NISUS irradiation the count on the back of the detector was 16% of that on the front. Apart from this the presence on the film exposed in NISUS of large numbers of small proton tracks not included in the count made counting rather difficult and subject to a possible systematic error estimated at ± 5%.

5.2 $^{10}B(n,\alpha)$ RESULT

The 5% systematic error in counting the SSTR irradiated in NISUS dominates the overall uncertainty in the reaction rate measurement. Taking into account statistical errors on both films and errors in gold foil activity measurements and monitoring this came to ± 6.2%.

The result for the $^{10}B(n,\alpha)^{7}Li$ reaction rate in NISUS was $6.13 \times 10^{-20} \pm 0.38 \times 10^{-20}$ reactions per principal fission monitor count.

The quoted accuracy of this result is less good than those cited for the helium accumulation method used in other facilities, but the technique reported here does seem a useful one. The use of enriched boron in the source is the main way in which the method could be improved, since this would give an improvement in the signal to background ratio of up to a factor of 5 without increasing the source thickness. The background from small tracks would still be troublesome but the counting errors would definitely be less. In other facilities one could expect a great improvement in softer spectra, but a measurement in a fission spectrum would be much more difficult.

6. ACTIVATION MEASUREMENTS

Previous activation measurements in NISUS have been reported[2] and compared with data obtained in Mol-ΣΣ. A number of threshold reactions previously used have been selected, together with some fission reactions, for use in spherical shell transmission measurements in NISUS and the measurements therefore have been recently repeated[5]. In addition $^{103}Rh(n,n')^{103m}Rh$ has been used. Apart from the last mentioned these reaction rates have been measured by the same method as described previously, using a calibrated Ge(Li) gamma spectrometer, so the details need not be repeated here.

6.1 $^{103}Rh(n,n')^{103m}Rh$ MEASUREMENTS

^{103m}Rh activity was measured using a 200 mm^2 planar intrinsic Ge detector to record the 20 keV K_α peak. Efficiency calibration was done with an IAEA ^{103}Pd source used as a standard for ^{103m}Rh with an equivalent activity of 1059 KBq ± 2.2%. This source was used to obtain the detector efficiency relative to ^{57}Co(14 keV) and ^{241}Am(26 keV) sources which were used at the time of each ^{103m}Rh measurement. Peak areas were found by subtraction of linear background under the peaks, measured in a consistent way in all measurements. 0.05 mm thick rhodium metal foils 7.6 mm in diameter were used for the measurements in NISUS. Because of the large corrections required for photon self absorption in these foils, they were individually calibrated against 4% Rh - Al foils 0.15 mm thick supplied by IAEA. These have small and easily calculated self absorption corrections, but could not be used in NISUS because of insufficient sensitivity. The attenuation found for the 0.05 mm Rh foils was approximately 0.625 for each foil.

^{103m}Rh activity was always measured 1 to 2 hours after the end of irradiation.

6.2 ACTIVATION REACTION RATE RESULTS

Results of the activation measurements are shown in Table 4 and compared with previous values. Agreement is very good in all cases and the $^{27}Al(n,\alpha)^{24}Na$ result confirms the previous value which had been noticed to be discrepant with the Mol-ΣΣ value measured by the Mol experts[17].

7. INTEGRAL CROSS SECTIONS

In order to derive cross sections from the measured reaction rates it is necessary to know the total flux. Various methods are available and have been discussed at the previous IAEA meeting[17,18]. In this work the $^{239}Pu(n,F)$ flux transfer method proposed by Grundl and Eisenhauer[18] has been chosen since this offers the best prospects of consistency between laboratories. To apply this method in NISUS it is necessary to take the following steps:

(i) The average $^{239}Pu(n,F)$ cross-section in NISUS and the average cross-section in ^{252}Cf fission spectrum are calculated using consistent dosimetry cross sections, in this case the ENDF/BIV file, and the recommended evaluated spectra for each. In this way the ratio of cross sections in the two fields is found.

(ii) The measured cross section in the NBS ^{252}Cf spectrum, 1804mb[17], is used to find a bias factor, 1.008, relative to the calculated value for that field.

(iii) The same bias factor, relative to ENDF/BIV data, is assumed in NISUS to obtain an average cross section consistent with the value of 1804mb in the ^{252}Cf spectrum.

(iv) The NISUS flux is deduced from this value using the $^{239}Pu(n,F)$ reaction rate measured with one of the NBS series of deposits[3].

Evaluated cross sections deduced from the flux transfer derived are shown in Table 5 where all the measurements reported here and the previous measurements have been taken into account. Also shown are values calculated using ENDF/BIV data, where available, or other data sets. Ratios of measurement to calculation are also given. The spectrum used for the calculated values is that reported in reference 6, in which $^{197}Au(n,\gamma)$, $^{239}Pu(n,F)$, $^{237}Np(n,F)$, $^{238}U(n,F)$, $^{58}Ni(n,p)$, $^{27}Al(n,p)$, $^{56}Fe(n,p)$ and $^{27}Al(n,\alpha)$ reaction rate values were used together with spectrometry data to obtain the spectrum. Because of the good agreement of the new measurements with previous ones it has not been thought necessary to revise the NISUS recommended spectrum.

8. CONCLUSIONS

The ratios of measured to calculated cross sections shown in Table 5 confirm and reinforce the trends observed before in NISUS and other reference and standard fields. Particular comment is warranted in the case of the reactions measured in NISUS for the first time:

$^{10}B(n,\alpha)^{7}Li$:- The bias factor of 1.10 is consistent with those found in other fields[17]. This should not be necessarily interpreted as an error in the Boron cross section, because the spectrum of none of the fields in question is reliable in the relevant energy range. Possibly a lack of consistency between $^{10}B(n,\alpha)$ and $^{197}Au(n,\gamma)$ cross sections is implied, since the latter has been used in evaluation of all three spectra.

$^{103}Rh(n,n')^{103m}Rh$:- This reaction is not found in the ENDF/BIV dosimetry file and so the UKNDL file has been used. The result is significant and shows good consistency between this cross section and the Category I cross sections, at least so far as NISUS is concerned. This reaction is potentially very valuable and should perhaps be more widely used than it has been. Its exclusion from the ENDF/B file is regretable.

$^{236}U(n,f)$:- Also not in the ENDF/B file, the excitation function of this reaction is intermediate between $^{237}Np(n,f)$ and $^{238}U(n,f)$. Davey's evaluation has been used here and the result shows fairly good consistency with the Category I reactions.

Apart from the conclusions which may be drawn on the cross sections, the value of NISUS in testing and validation of experimental techniques, and for intercomparison continues to be apparent.

REFERENCES

1. BESANT, C.B., EMMETT, J., CAMPBELL, C.G., KERRIDGE, M., and JONES, T.C., Nucl. Engng. International, 18, 425 May (1973).

2. HANNAN, A.H.M.A., and WILLIAMS, J.G., IAEA-208, Vol. II, 209 (1978).

3. FABRY, A., WILLIAMS, J.G., HANNAN, A.H.M.A., and AZIMI-GARAKANI, D., IAEA-208, Vol. II, 191 (1978).

4. RAHBAR, M., Ph.D. Thesis, University of London (1978).

5. FARRAR IV, H., McELROY, W.N., LIPPINCOTT, E.P., Nucl. Techn. 25, 305 (1975).

6. WILLIAMS, J.G., and HANNAN, A.H.M.A., IAEA-208, Vol. II, 63 (1978).

7. GRUNDL, J.A., GILLIAM, D.M., DUDEY, N.D., POPEK, R.J., Nucl. Techn. 25, 237 (1975).

8. GLOVER, K.M., Conf. on Standardization of Radionuclides, IAEA, Vienna (1967).

9. Vendor Certificate, AERE, Harwell, Didcot, Berks., U.K. (1976).

10. AZIMI-GARAKANI, D., Ph.D. Thesis, University of London (1975).

11. PINTER, M., et al., Proc. Nuclear Cross Sections and Technology Conference, NBS Special Publication 425, Vol. I, 258 (1975).

12. GOLD, R., Proc. of the First ASTM - EURATOM Symposium on Reactor Dosimetry, Petten 1975, EUR 5667e/F Part II, 175 (1977).

13. GILLIAM, D.M., and KNOLL, G.F., Annals of Nucl. Energy, 2, 637 (1975).

14. JAFFEY, A.H., Rev. Sci. Intr., 25, 349 (1954).

15. Summary Report, IAEA-208, Vol. I, Para. IV.B.9, 28 (1978).

16. BENTON, E.V., and NIX, W.D., Nucl. Instr. and Meth., 67, 343 (1969).

17. FABRY, A., et al., IAEA-208, Vol. I, 233 (1978).

18. GRUNDL, J., and EISENHAUER, C., IAEA-208, Vol. I, 53 (1978).

19. DAVEY, W.G., Nucl. Sci. Engng. 32 , 35 (1968).

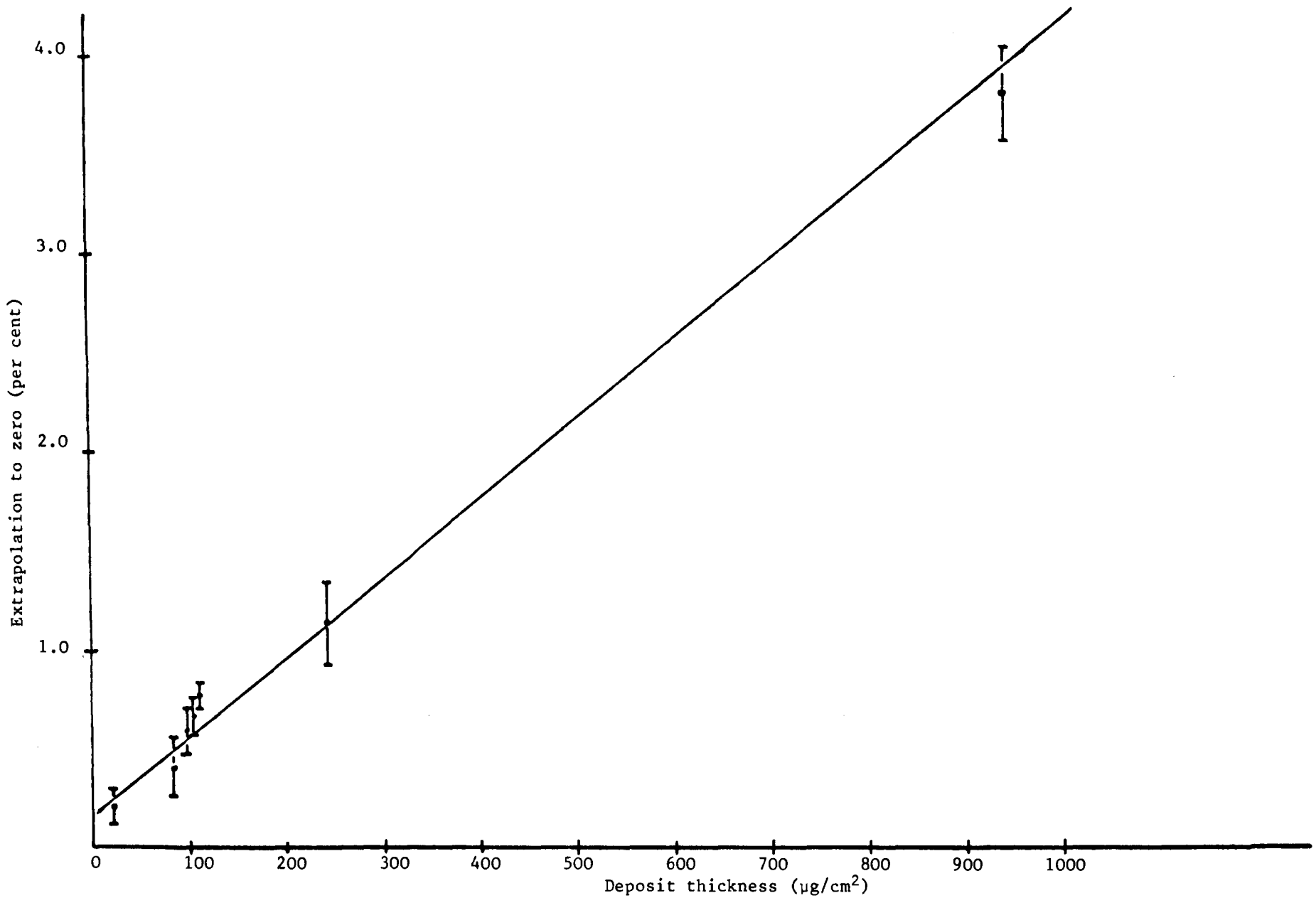

Fig. 1 The extrapolation to zero pulse height distribution in unit of per cent

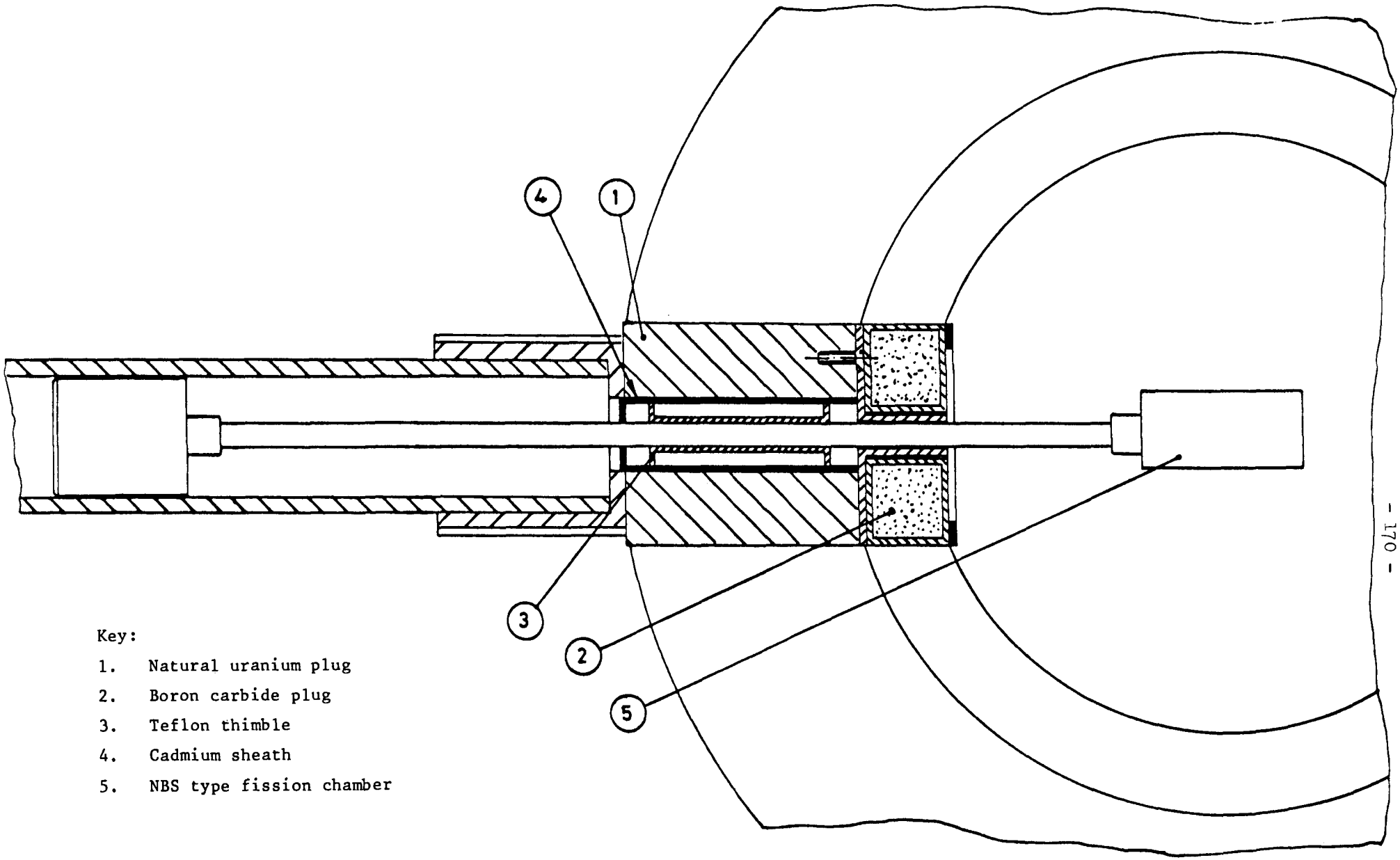

Key:

1. Natural uranium plug
2. Boron carbide plug
3. Teflon thimble
4. Cadmium sheath
5. NBS type fission chamber

Fig. 2 NBS Type double fission chamber at the centre of NISUS

TABLE 1

CHARACTERISTICS OF THE FISSIONABLE DEPOSITS

Principal isotope	Deposit identification	Isotopic concentration (atom per cent)	Mass of principal isotope (μg)	Correction for absorption in deposit (2π geometry)	Impurity fission correction
^{235}U	ULRC-4	^{235}U : 93.0; ^{238}U : 7.0	73.2 ± 1.3%	1.0025 ± .0035	0.9958 ± .0002
^{235}U	ULRC-5	as above	319.4 ± 1.3%	1.0067 ± .0035	as above
^{235}U	ULRC-6	as above	326.3 ± 1.3%	1.0067 ± .0035	as above
^{239}Pu	ULRC-7	^{239}Pu : 100.0	343.8 ± 0.5%	1.0071 ± .0035	1.000
^{237}Np	ULRC-9	^{237}Np : 99.96; ^{239}Pu : 0.04	305.2 ± 0.5%	1.0083 ± .0035	0.9988 ± .0001
^{236}U	ULRC-8	^{236}U : 99.68; ^{235}U : 0.119 ^{238}U : 0.112	257.6 ± 1.0%	1.0053 ± .0035	0.9898 ± .0003
^{238}U	ULRC-3	^{238}U : 99.965; ^{235}U : 0.035	780.6 ± 1.9%	1.0167 ± .0042	0.9938 ± .0002

TABLE 2

FISSION RATES

Isotope	Fissions per nucleus per monitor count x10^{19}	CROSS SECTION RATIO		
		NISUS		Mol-ΣΣ[11]
		present work	Fabry[3]	
^{235}U	0.5309 ± 1.6%	1.000 (ref.)	1.000 (ref.)	1.000 (ref.)
^{239}Pu	0.6244 ± 1.1%	1.176 ±1.8%	1.175 ±2.3%	1.173 ±2.1%
^{237}Np	0.2054 ± 1.0%	0.386 ±1.8%	0.383 ±3.0%	0.381 ±2.8%
^{236}U	0.0640 ± 1.4%	0.1206 ±2.0%	-	-
^{238}U	0.0298 ± 2.1%	0.0561 ±2.6%	0.0568 ±2.7%	0.0564 ±2.5%

TABLE 3

FISSION RATES

Isotope	Fissions per nucleus per monitor count $\times 10^{19}$		
	S S T R	Fission chamber	SSTR / fission chamber
^{235}U	0.5354 ± 2.0%	0.5309 ± 1.6%	1.008 ± .015
^{239}Pu	0.6391 ± 1.3%	0.6244 ± 1.1%	1.024 ± .012
^{237}Np	0.2143 ± 1.6%	0.2054 ± 1.0%	1.043 ± .015
^{236}U	0.0633 ± 1.8%	0.0640 ± 1.4%	0.989 ± .015

TABLE 4

ACTIVATION MEASUREMENTS

Reaction	Reactions per nucleus per monitor count $x10^{22}$		RATIO
	present work	Hannan[2]	present / Hannan
$^{103}Rh(n,n')^{103m}Rh$	106.23 ± 4.0%	-	-
$^{115}In(n,n')^{115m}In$	19.25 ± 2.4%	19.25 ± 2.8%	1.000
$^{58}Ni(n,p)^{58}Co$	8.98 ± 2.5%	9.07 ± 3.0%	0.990
$^{27}Al(n,p)^{27}Mg$	0.332 ± 3.3%	0.327 ± 4.8%	1.015
$^{56}Fe(n,p)^{56}Mn$	0.0880 ± 2.5%	0.0870 ± 3.1%	1.011
$^{27}Al(n,\alpha)^{24}Na$	0.0551 ± 2.6%	0.0537 ± 3.0%	1.026

TABLE 5

INTEGRAL CROSS SECTIONS IN NISUS

Reaction	Measured (mb.)	Calculated [a] (mb.)	Measured/ Calculated
$^{197}Au(n,\gamma)\ ^{198}Au$	391 ± 10	387	1.011
$^{10}B\ (n,\alpha)\ ^{7}Li$	1736 ± 108	1576	1.102
$^{115}In(n,\gamma)^{116m}In$	238 ± 7	-	-
$^{235}U\ (n,f)$	1506 ± 24	1546	0.974
$^{239}Pu(n,f)$	1770 ± 18	1759	1.006
$^{237}Np(n,f)$	580.6 ± 5.9	602	0.964
$^{103}Rh(n,n')^{103m}Rh$	300.8 ± 11.9	293.5 [b]	1.025
$^{236}U\ (n,f)$	181.3 ± 2.5	191.3 [c]	0.948
$^{115}In(n,n')^{115m}In$	54.5 ± 1.1	54.0	1.009
$^{238}U\ (n,f)$	85.0 ± 1.1	85.0	1.000
$^{58}Ni(n,p)\ ^{58}Co$	25.5 ± 0.6	24.6	1.037
$^{64}Zn(n,p)\ ^{64}Cu$	7.76 ± 0.22	-	-
$^{27}Al(n,p)\ ^{27}Mg$	0.935 ± 0.028	0.880	1.063
$^{56}Fe(n,p)\ ^{56}Mn$	0.248 ± 0.006	0.250	0.992
$^{24}Mg(n,p)\ ^{24}Na$	0.345 ± 0.011	-	-
$^{27}Al(n,\alpha)\ ^{24}Na$	0.154 ± 0.004	0.150	1.027

a ENDFB/IV cross sections, except for ^{103}Rh and ^{236}U.

b UKNDL cross sections, DFN 94.

c Cross sections from Davey[19].

Integral cross section measurements in the Cf-252 neutron spectrum

Z.Dezső, J.Csikai[x]

In a Cf-252 benchmark neutron field a number of average cross sections have been measured by the activation method for selected nuclei important in neutron dosimetry. The results obtained in our experiment are in rather good agreement with recently published literature values thus they can provide integral tests for evaluated differential cross section data.

Introduction

Average cross sections obtained in reference neutron fields - especially in the U-235 fission neutron spectrum - are widely used for checking evaluated and measured energy dependent neutron cross section data. In spite of the improvements performed in this field during the past five years there are still inconsistencies between measured and computed average cross sections as it has been outlined in the Summary Report of Reactor Dosimetry Conference held in Vienna, 1976 [1]. Since the Californium-252 fission neutron spectrum is very well established especially in the 0.25-8 MeV energy range [2], integral measurements in this standard neutron field may resolve the discrepancies observed in many cases for threshold reactions. Although the applicability of average cross sections is clearly seen, up to now only

[x]Inst.Exp.Phys. Kossuth Univ. Debrecen, Hungary

very few measurements have been performed in this benchmark. In order to improve the data base, a number of integral cross sections have been measured in the ^{252}Cf-neutron spectrum. The reactions investigated in this work were selected on the basis of the recommendations of ref. [1].

Experimental Procedure

Samples of metallic foils of 10 mm diameter and about 0.8 mm thick were irradiated with neutrons from an 0.4 mg ^{252}Cf source in a scattering free arrangement. The source together with the sample was suspended from the ceiling of a large room for the irradiations with the nearest surface ~3 meters away. The activity of indium foils as a function of distance from 2 cm up to 30 cm has been measured through the ^{115}In/n,n'/ reaction, to determine the average neutron flux close to the surface of the neutron source. In most cases the distance between the samples and the center of the source was about 2 cm. The activity measurements of the samples were performed using a 40 cm^3 volume Ge/Li/ detector connected to a multi-channel analyser.

For the determination of the absolute cross sections the efficiency-curve of the Ge/Li/ detector has been measured with ^{226}Ra standard of the same dimension as the samples. Data for half-life, gamma energy, and intensity were taken from the table given by Erdtmann and Soyka [3], exept for ^{115m}In, where the gamma emission probability published by

Hansen et. al. [4] has been accepted. The decay properties of the reaction products are summarised in Table 1. In the case of $^{238}U/n,f/$ cross section measurement light deposit of 230 times depleted $^{238}UF_4$ on 0.2 mm thick aluminium backing were used. The mass of the target was matched to $\pm$ 3 %. The detection of fission fragments was performed using a light weighted fission chamber made of 0.2 mm thick aluminium box. Fission events counted by the chamber were recorded by a pulse-height analyser. Corrections have been developed for undetected fission fragments : extrapolation of the pulse height distribution to zero energy, and absorption of fission fragments in the deposit.

Results and Discussion

The average cross sections measured in this work together with those taken from the literature [5,6,7,8,9,10] are presented in Table 2. The quoted uncertainties correspond to a confidence level of 68 % and were calculated by quadratic summation of all contributions, namely errors due to source strength and effective distance determination, photopeak effieiencies and counting statistics.

The results given in Table 2, are also compared with computed integral cross sections. For the calculations the evaluated spectral form of Grundl and Eisenhauer [2] has been used for the Cf-252 neutron spectrum, while for

the energy-dependent cross section the ENDF/B-IV [11], the SAND-II [12] files and recently evaluated $\sigma(E)$ data [13] were used respectively.

The renormalised value of our earlier $^{115}In/n,n'/$ cross section measurement [14] is in very good agreement with those obtained by other authors [5,6,7,8]. Since there are five independent $\langle\sigma\rangle$ measurement for this reaction with quoted uncertainties not more than 5 % and the results of individual measurements are consistent within the error limits, the average of the published data should be considered as recommended average cross section for $^{115}In/n,n'/^{115m}In$ reaction. The ratio of this value $/\langle\bar{\sigma}\rangle$ = 196.4 mb/ to the calculated one /using evaluated spectral form of Grundl and ENDF/B-IV cross section file/ is 1.028 which is in very good agreement with the same quantity for ^{235}U fission spectrum [15], namely 1.037. Since the deviation of the two ratios is less then 1 %, it is possible to establish a bias factor of 1.04 for the $^{115}In/n,n'/$ exitation function.

Our results for category I. reactions including $^{56}Fe/n,p/^{56}Mn$; $^{27}Al/n,\alpha/^{24}Na$ and $^{238}U/n,f/$ respectively are in fair agreement with the data obtained by other groups [5,9] especially for $^{56}Fe/n,p/^{56}Mn$ reaction, where an exellent agreement can be found. Although the ENDF/B-IV dosimetry file is recommended by the IAEA Consultants' Meeting /Vienna, 1976/ [1] for spectrum

unfolding procedures without introducing any bias factors for category I. reactions, one should observe that the measured to computed values for $^{56}Fe/n,p/$ reaction in the Cf-252 and U-235 benchmark fields are 0.983 in all the two cases /see ref. [15] for U-235/. This discrepancy between measured and calculated values can be removed accepting the 0.983 value as bias factor for $^{56}Fe/n,p/$ exitation function.

Due to the high threshold energy of $^{63}Cu/n,2n/^{62}Cu$ reaction it can be useful for the determination of the high energy tail of a reactor spectrum, and on the other hand it can play an important role in reactor dosimetry related to CTR program. In spite of this there is no other average cross section measurement in a Californium-252 neutron spectrum exept our data, so it is not possible to compare it with other's results. A comparison of our measured value for the $^{63}Cu/n,2n/^{62}Cu$ reaction with the calculated one using NBS spectral shape for Cf-252 neutron spectrum and SAND-II for $\sigma(E)$ shows that there is a very large discrepancy between measured and computed data. Since the same disagreement can be found between data obtained for U-235 fission spectrum too [15], we can consider the SAND-II data file for this reaction to be incorrect.

Our average cross section value for $^{58}Ni/n,p/^{58}Co$ agrees-within the quoted errors - with that of Alberts et.al. [5] and provide cross section validation for this

reaction. However the inconsistency of integral and differential data for the U-235 fission spectrum still remains, but it can probably be resolved by some new measurements in this benchmark.

The relatively large spread in the measured $^{54}Fe/n,p/^{54}Mn$ cross section values does not make them possible for checking the energy-dependent cross section. Further experiments are needed to establish more accurate integral data in order to test the exitation function.

From a detailed comparison of evaluated spectrum--averaged cross sections with the measured values for titanium /n,p/ reactions, the following conclusions can be drawn. In the case of ^{46}Ti, the experimentally determined integral data [this work and ref.5.] support the recent evaluation of Philis et.al. [13]. The measured to computed ratio - depending on the averaging procedure - is lying in the range of 0.985-0.999, while the same quantity, using ENDF/B-IV data file is 1.04-1.07 respectively.
Although the average cross section values for $^{47}Ti/n,p/$ reaction are not in very good agreement, the data measured by different authors are significantly lower than the calculated ones using ENDF/B-IV or the evaluated cross section of Philis, indicating that further investigations of this reaction is needed to remove the present discrepancy between integral and differential data.

For $^{48}Ti/n,p/$ reaction up to now only two integral measurements are available [this work and ref.5] and they do not agree within the errors given by the authors. From the comparison of measured and calculated values it is clearly seen that the ENDF/B-IV data should be incorrect. Although there is a very large difference /almost 20 %/ between the computed $\langle\sigma\rangle$ using SAND-II or the evaluated data of Philis, the 10 % deviation of the measured average cross sections does not make possible the integral testing of the different representations. Further investigations are also needed for this Ti isotope as it has been recommended for ^{47}Ti.

References

[1] Proc. of a Consultants' Meeting on Integral Cross-Section Measurement, Vienna, 1976, IAEA-208, 1978

[2] I. Grundl and C. Eisenhauer: First ASTM-EURATOM Symposium on Reactor Dosimetry, Petten, 1975

[3] G. Erdtmann and W. Soyka: Die γ-Linien der Radionuklide Jül-1003-AC, 1974

[4] H.H. Hansen et.al.: Z. Physik 269, 155 /1974/

[5] W.G. Alberts and I. Bortfeldt: Proc. of Intern. Symp. on Cf-252 Utilization, Paris, 1976.

[6] G.I. Kirouac, H.M. Eiland and C.I. Slavik: Topical Meeting on Irradiation Experimentation in Fast Reactors, Jackson Lake Lodge /1973/ 412.

[7] H. Pauw and A.H.W. Aten Jr.: J. Nucl. Energy 25 /1971/ 457

[8] W. Mannhart: in ref. 1. Vol.II. p.227

[9] D.M. Gilliam et.al.: Proc. Conf. on Nucl. Cross Sections and Technology, p.270. NBS-425 /1975/

[10] V.M. Adamov et.al.: Preprint RI-52, Leningrad /1976/

[11] B.A. Magurno: BNL-NCS-50446 /1975/

[12] R.L. Simons and W.N. McElroy: BNWL-1312 /1970/

[13] C. Philis, et al.: ANL/NDM-27 /1977/

[14] M. Buczkó, et al.: in ref. 5

[15] A. Fabry, et al.: in ref.1. Vol.I. p.233

Table 1.: Reactions and Decay Properties

Reaction	Sample		Reaction Product	
	Isotopic abundance	Half-Life	Gamma-Ray Detected	Gamma-Emission Probability
$^{46}Ti/n,p/^{46}Sc$	8,0 %	83.9 d	889.3 1120.5	1.0000 1.0000
$^{47}Ti/n,p/^{47}Sc$	7.5 %	3.4 d	159.4	0.7000
$^{48}Ti/n,p/^{48}Sc$	73.7 %	43.68 h	983.3 1037.4 1311.7	1.0000 0.9800 1.0000
$^{54}Fe/n,p/^{54}Mn$	5.8 %	312.5 d	834.81	0.9998
$^{56}Fe/n,p/^{56}Mn$	91.7 %	2.576 h	846.6	0.9900
$^{58}Ni/n,p/^{58}Co$	67.76 %	71.3 d	810.6	0.9944
$^{27}Al/n,\alpha/^{24}Na$	100 %	15.03 h	1368.55	1.0000
$^{115}In/n,n'/^{115m}In$	95.7 %	4.486 h	336.3	0.459
$^{59}Co/n,2n/^{58}Co$	100 %	71.3 d	810.6	0.9944
$^{63}Cu/n,2n/^{62}Cu$	69.1 %	9.73 min	511.0	1.9600

Table 2. Average Cross Sections in the Cf-252 Fission Spectrum

Reaction	Measured <σ> [mb] This work	Others	Calculated <σ> [mb]	χ(E)	σ(E)	Ref.
$^{46}Ti/n,p/^{46}Sc$	13.4±1.1	13.8±0.3				[5]
		12.4±1.2				[6]
			12.87	NBS	ENDF/B-IV	[15]
			13.81	NBS	Philis	[13]
$^{47}Ti/n,p/^{47}Sc$	22.0±0.9	18.9±0.4				[5]
		20.3±1.1				[6]
			23.84	NBS	ENDF/B-IV	[15]
			24.22	NBS	Philis	[13]
			18.58	NBS	SAND-II	[15]
$^{48}Ti/n,p/^{48}Sc$	0.38±0.02	0.42±0.01				[5]
			0.265	NBS	ENDF/B-IV	[15]
			0.383	NBS	SAND-II	[15]
			0.446	NBS	Philis	[13]
$^{54}Fe/n,p/^{54}Mn$	92.5±5.0	84.6±2.0				[5]
		87 ±3				[6]
			89.1	NBS	ENDF/B-IV	[15]
			87.1	NBS	SAND-II	[15]
$^{56}Fe/n,p/^{56}Mn$	1.45±0.06	1.45±0.035				[5]
		1.18±0.08				[6]
			1.475	NBS	ENDF/B-IV	[15]
			1.549	NBS	SAND-II	[15]
$^{58}Ni/n,p/^{58}Co$	113.4±4.8	118 ± 3				[5]
		105 ± 5				[6]
			115	NBS	ENDF/B-IV	[15]
			114.2	NBS	SAND-II	[15]
$^{27}Al/n,\alpha/^{24}Na$	1.08 ±0.05	1.01±0.02				[5]
		0.86±0.5				[6]
			1.059	NBS	ENDF/B-IV	[15]
			1.024	NBS	SAND-II	[15]
$^{238}U/n,f/$	311 ± 14	320 ± 9				[9]
		347 ± 6				[10]
			313	NBS	ENDF/B-IV	[9]

Table 2. cont.

Reaction	Measured <σ> [mb] This work	Others	Calculated <σ> [mb]	χ(E)	σ(E)	Ref.
$^{115}In/n,n'/^{115m}In$	199.2±10.5	198±5				[5]
		202±12				[6]
		188±8				[7]
		195±5				[8]
			191.1	NBS	ENDF/B-IV	[15]
			190.7	NBS	SAND-II	[15]
$^{59}Co/n,2n/^{58}Co$	0.57±0.06		0.57	NBS	ENDF/B-IV	[15]
$^{63}Cu/n,2n/^{63}Cu$	0.30±0.03		0.214	NBS	SAND-II	[15]

ECN-78-163
Restricted distribution

On the consistency between integral and differential cross section data

Willem L. Zijp
Petten, November 1978

Contribution prepared for the IAEA Consultants Meeting on Nuclear Data for Reactor Dosimetry, Vienna, November 13-17, 1978.

SUMMARY

This document is an invited paper for the IAEA Advisory Group Meeting on Nuclear Data for Reactor Dosimetry, held at Vienna, 13-17 November 1978.
It describes the present status of the confrontation of measured cross section values averaged over a benchmark neutron spectrum, with the calculated values, derived from evaluated cross section data and the best available numerical benchmark spectrum data.
Information is collected on three aspects of the comparison:
- the uncertainty in the measured cross section values;
- the accuracy (or bias) of the cross section values;
- the consistency of the observed values.

Available numerical data are presented in a series of tables.
Some concluding remarks are offered for discussion at the Consultants' meeting.

The status of current international efforts to develop standardized sets of evaluated energy dependent neutron cross section data for reactor dosimetry has been discussed in the past few years on several occasions. The following documents give information on the situation and the progress:

1. Status report on neutron cross section data for reactor radiation measurements (Vlasov, 1972, ref. |1|).
2. Proceedings of the IAEA Consultants Meeting on Nuclear Data for Reactor Neutron Dosimetry (Vlasov and Dunford, 1973 |2|).
3. The review papers in the special issue of Nuclear Technology in August 1975. Of special interest is here the report of the U.S. Interlaboratory LMFBR Reaction Rate (ILRR) program by McElroy and Kellog |3|.
4. The review papers at the first ASTM-Euratom Symposium on Reactor Dosimetry, Petten, September 1975 (see Fabry et al., 1977 |4|).
5. Status report on neutron cross section data for reactor dosimetry presented at the Lowell conference, July 1976 (Vlasov et al., 1977 |5|).
6. The review papers at the IAEA Consultants meeting on Integral Cross Section Measurements in Standard Neutron Fields, held in Vienna, November 1976 (see Fabry et al. |6|, Vlasov |7|, and Zijp |8|).
7. Review papers presented at the International Specialists Symposium on Neutron Standards and Applications, at NBS, March 28-31, 1977 (see e.g. Zijp, 1977 |9| and Gilliam, 1977 |10|).
8. The review papers at the second ASTM-Euratom symposium, held at Palo Alto, October 1977 (see e.g. Fabry, 1978 |11|).

The recommendations of the IAEA Consultants Meetings in 1973 |2| and 1976 |12| have resulted in a worldwide availability of the ENDF/B-IV Dosimetry File and its acceptance by the community of reactor neutron metrologists.

The aim of arriving at a generally accepted, internationally consistent and extended dosimetry data file based on the ENDF/B specifications, is the corner stone of all efforts in national and international dosimetry benchmark programs.

Dosimetry benchmark fields and benchmark programs serve to establish reliable and consistent information on three related data sets:

- a few well selected accurate neutron spectra serving as standard spectra;

- evaluated energy dependent cross section data for neutron metrology reactions important for reactor development programs (LWR, FBR, CTR);
- precise and accurate experimental reaction rates for important reactions in these benchmark spectra.

In this respect one has to realize that the three physical quantities: reaction rate, cross section, and flux density, are mutually dependent quantities. This holds not only for the parameter values, but also for the associated errors. In fact, one can define an effective or average cross section as a reaction rate per target atom and per unit flux density. In principle one should take into account the correlations and corresponding covariances of all parameters involved. Up till now one has - for reasons of simplicity - often neglected the influence of covariances in the propagation of errors, since covariance information was hardly available.

The study of the "consistency" of "integral" and "differential" cross section data is based on the comparison of measured and calculated values of spectrum averaged cross sections, where the measured value is obtained by irradiation of an activation (or fission) detector (an "integral" detector) in the spectrum field, and the calculated value is obtained by folding numerical information on the spectrum with energy dependent ("differential") cross section data.

The quality of the comparison can be based on three aspects:
- the *uncertainty* in the measured values;
- the *accuracy* (or bias) of the observed values;
- the *consistency* of the observed values.

As a measure of the uncertainty in the experimental cross section value we take the fractional error (denoted by v) as stated by the experimenter.
As a measure of the accuracy we take the absolute value of the fractional difference (denoted by Δ) between measured value $\langle\sigma_m\rangle$ and the value $\langle\sigma_c\rangle$ calculated from the evaluated cross section file.
Thus

$$\Delta = \left| \frac{\langle\sigma_m\rangle - \langle\sigma_c\rangle}{\langle\sigma_m\rangle} \right| .$$

Instead of looking at the difference Δ one often considers the ratio $\langle\sigma_m\rangle/\langle\sigma_c\rangle$. As a measure of the consistency between measured cross section and calculated cross section one can take the ratio of the frac-

tional difference and its stated fractional error v.

A more general approach to study the consistency is the following. Consider a set of n measured reaction rates per target atom, combined in a vector A^o. Let ϕ denote a set of m group flux densities, combined in a vector Φ, and let σ_{ij}, the cross section of the i-th reaction for the j-th energy group, be an element of matrix S (with n×m elements). In general one has to take into account the covariance matrices for each of the three groups of data involved (activities, group flux densities, and group cross sections).

Let N denote a covariance matrix, and let the transpose of a matrix A be denoted by A^T.

It is assumed that reaction rates, cross sections, and group flux densities are random variables, and that the errors associated to each group are normally distributed.

Perey |13| has shown that there is a unique solution to the unfolding problem. The least squares unfolding approach of Perey implies calculation of the minimum of the following expression

$$\chi^2 = \begin{pmatrix} \Phi - \bar{\Phi} \\ S - \bar{S} \\ A^o - \bar{A} \end{pmatrix}^T \cdot \begin{pmatrix} N_\phi & 0 & 0 \\ 0 & N_S & 0 \\ 0 & 0 & N_A^o \end{pmatrix}^{-1} \cdot \begin{pmatrix} \phi - \bar{\phi} \\ S - \bar{S} \\ A^o - \bar{A} \end{pmatrix} .$$

The values $\bar{\phi}$, $\bar{S}$ and $\bar{A}$ refer to values of the solution, i.e. those values which minimize the χ^2-function.

It can be shown (Perey, |14|) that for unfolding purposes the minimum value of χ^2 can be written as

$$\chi^2_{min} = (A^o - A)^T \cdot (N_A + N_A{}^o)^{-1} \cdot (A^o - A)$$

where the covariance matrix N_A is made up of two contributions, one from N_ϕ and one from N_S. If one writes these as N_A^Φ and N_A^S, one has

$$N_A = N_A^\Phi + N_A^S$$

where

$$N_A^\Phi \equiv \{n_{ij}{}^\Phi\} = \{S^{iT} . N_\phi . S^j\}$$
$$N_A^S \equiv \{n_{ij}{}^S\} = \{\Phi^T . N_S^{ij} . \Phi\}.$$

Such an approach may be used to test the consistency between the input quantities, taking into account their variances and covariances. Since one may expect that each of the n activation rates con-

tributes 1/n-th part to χ^2_{min}, one may test for the presence of one or a few outlying reaction rates. A (too) large contribution to χ^2_{min} from a particular reaction rate should be investigated carefully.
Perey's computer program STAY'SL |15| can provide estimates for the separate χ^2 contributions. Such an approach should be followed in a further consistency study.

MEASUREMENT ERRORS

Many interlaboratory comparisons of reaction rate measurements, and especially in the USA the ILRR program, have contributed to improve the precision and accuracy of measurements of source strengths, activities and fission rates.
From tables 1, 2, 3, 5 and 10, which list the results of some recent measurements, one may observe that the measurement errors reported are smallest for the ^{252}Cf spectrum. For the ^{235}U spectrum, the CFRMF spectrum and the ΣΣ spectrum the measurement errors are frequently larger than 3%.

DISCREPANCIES

Vlasov, Fabry, and McElroy | 5 | have recently mentioned in a status report that for some important reactions large discrepancies were observed between measured cross section values and cross section values derived with aid of the ENDF/B-IV dosimetry file.
The reactions were:
$^{48}Ti(n,p)^{48}Sc$, $Ti(n,x)^{46}Sc$, $^{47}Ti(n,p)Sc$, $^{63}Cu(n,\alpha)^{60}Co$, $^{63}Cu(n,2n)^{62}Cu$, $^{90}Zr(n,2n)^{89}Zr$, and $^{58}Ni(n,2n)^{57}Ni$.
For the first three reactions new data have been reported by the Argonne National Laboratory (Philis et al., 1977 |16|).

$^{48}Ti(n,p)$

The situation is as follows:

	^{235}U spectrum	^{252}Cf spectrum
measured cross section (in mb) |6|	0.300±0.018	0.42±0.01
calculated value, based on ENDF/B-IV file and NBS spectrum form (in mb) |16|	0.193	0.289
based on Argonne data (in mb) |16|	0.303	0.446

$Ti(n,p)^{46}Sc$

For a ^{235}U fission neutron spectrum this reaction is practically equal to the $^{46}Ti(n,p)^{46}Sc$ reaction: the contribution to the total production of ^{46}Sc in natural titanium is about 99% \|5\|.

	^{235}U spectrum	^{252}Cf spectrum
measured cross section (in mb) |6|	11.8±0.75	13.8±0.3
calculated value, based on ENDF/B-IV file and NBS spectrum form (in mb) |16|	10.08	12.87
based on Argonne data (in mb) |16|	10.88	13.81

$^{47}Ti(n,p)^{47}Sc$

The contribution of the $^{48}Ti(n,np)^{47}Sc$ reaction to the production of ^{47}Sc is important above 12 MeV, but is negligible (<0.1%) in the case of a fission spectrum \|5\|.

	^{235}U spectrum	^{252}Cf spectrum
measured cross section (in mb) |6|	19.0±1.4	18.9±0.4
calculated value, based on ENDF/B-IV file and NBS spectrum form (in mb) |16|	21.24	24.00
based on Argonne data (in mb) |16|	21.38	24.22

The reaction $^{63}Cu(n,\alpha)^{60}Co$

No new measurements have been reported. There is not yet a generally accepted explanation for the well known discrepancy between measured and predicted cross section values (subthreshold activation, underestimation of the cobalt impurities in the foil materials and of the

thermal neutron flux density contribution). New measurements, especially near threshold, and in the 90% response energy range, are needed to solve the present discrepancies |5|.

The n,2n reactions

It is worthwhile to repeat two remarks from the status report |5| mentioned above.

In the case of these high threshold reactions the large discrepancies between calculated and measured values depend strongly upon the representations of the fission neutron spectrum used for the calculation. Because of the strong fission spectrum dependence of the calculated integral values for these high threshold reactions it is not expected that the differential integral discrepancies are due to the unsatisfactory knowledge of the excitation functions alone.

Summary list

Table 5, reproduced from ref. | 6 |, largely reflects the state-of-the-art of integral data testing of the ENDF/B-IV dosimetry cross section file in the energy range above 0.1 MeV.

Recent trends

At a meeting of the Task Force on Reactor Dosimetry, held at NBS, 25-28 March 1977, convened by the USA Cross Section Evaluation Working Group (CSEWG) it was communicated that the ENDF/B-V dosimetry file was expected to be released at the end of 1978. Furthermore at that meeting a list was established of reactions for which a need was expressed to include them in a dosimetry file. This list covers the most urgent European needs, as well as those of fusion neutron dosimetry. This list, with the exception of (n,γ) reactions, is given in table 7. It is based on the communications by Vlasov et al. |17|, |18|. The status of the evaluations is also summarized in this table.

A recent evaluation of the $^{58}Ni(n,2n)^{57}Ni$ reaction has been reported by L. Adamski et al. from the Institute of Nuclear Research in Warsaw, Poland |19| .

An evaluation of the cross sections for the reactions $^{24}Mg(n,p)^{24}Na$, $^{64}Zn(n,p)^{64}Cu$, $^{63}Cu(n,2n)^{62}Cu$ and $^{90}Zr(n,2n)^{89}Zr$ is being performed by

H. Vonach at the "Institut für Radiumforschung und Kernphysik" in Vienna |20|.
At BCMN at Geel work is being performed on the determination of the excitation function of $^{103}Rh(n,n')^{103}Rh^{m}$ |21|.
A report on the work at Geel with respect to cross section measurements for the reaction $^{115}In(n,n')^{115}In^{m}$ below 4 MeV is in preparation |22|. These data are essentially in agreement with the data of D.L. Smith at Argonne |23|.

Consistency study

In order to study the consistency between evaluated energy dependent cross section data (e.g. present in the ENDF/B-IV dosimetry file) and the measured spectrum-averaged cross section values obtained in benchmark spectra, use has been made of the value of the chi-square parameter which can be calculated by means of the computer program STAY'SL |15|. In this study the following four benchmark spectra have been considered:
1) the ^{235}U thermal neutron fission spectrum; 2) the ^{252}Cf spontaneous fission neutron spectrum; 3) CFRMF; 4) the ΣΣ facility.
Furthermore we took all reactions for which energy dependent cross section data and experimental spectrum-averaged cross sections as well as the corresponding accuracies are known or can be estimated.
We had to eliminate the inaccuracies in the spectrum information, since no computer program for the necessary data treatment was present.
For the present purpose it was therefore assumed that the benchmark spectra have no inaccuracies.
The cross section data were taken from the dosimetry cross section file DOSCROS77 |24|, which has the 620 group structure as used in the SAND-II program, and is,where possible, based on the well known ENDF/B-IV dosimetry file (except for the three Ti(n,p) and the In(n,n') reactions).
The method implies that also uncertainties in the group cross section data have to be taken into account. Since for all reaction no appropriate covariance matrix for the cross section data was available, we used in our calculation basically the SAND-II evaluated error scheme in 15 groups, as published by McElroy and Kellogg in 1975 |3|. This

scheme presents for 40 activation and fission reactions the percent standard deviation uncertainties (see table 8) for the 15 groups, which are also used in the SAND-II Monte Carlo error analysis. The group structure used is shown in figure 1.

Method

The general chi-square expression as applied in the program STAY'SL contains contributions related to the covariance matrices for reaction rates α_i (i=i ... n), for group flux densities ϕ_j (j=1 ... m) and for reaction group cross sections σ_{ij} (i=1 ... n; j=1 ... m). In the present study it is assumed that the flux density covariance matrix comprises only zero elements.

A large inconsistency, visible from a large value of chi square, can arise from various sources:

- imprecisions (i.e. random errors) in measured reaction rates which have been stated too small;
- imprecisions (i.e. random errors) in group cross section data which have been stated too small;
- inaccuracies (i.e. systematic errors) in the measured reaction rates which have been overlooked or neglected;
- inaccuracies (i.e. systematic errors) in the group cross sections derived from the evaluated cross section file;
- incorrect representation of the actual neutron spectrum;
- the normalization procedure of the spectrum (this aspect is important in case of unfolding applications, and not for the case of calculations of average cross sections).

A list of possible physical causes for the various random and systematic errors mentioned above has been given at the previous meeting [25].

In order to reduce the number and the size of inconsistenties, one should take the following approaches:

- evaluate and reduce the errors in measured reaction rates by means of interlaboratory comparison of counting techniques, and also by exchange of calibrated reference sources;

- use the best evaluated cross section data files;
- apply only well known benchmark spectra;
- look for systematics in observed χ^2-values (e.g. for trends with increasing values of the effective reaction thresholds).

With respect to this last point we remark that in tables 9,10 and 11 the reactions are listed in order of increasing mean response energy for non-threshold reactions, and in order of increasing effective threshold energy for threshold reactions.

The *mean response energy* $\langle E_r \rangle$ is defined by the expression:

$$\langle E_r \rangle = \frac{\int_0^\infty E.\sigma(E).\phi_E(E).dE}{\int_0^\infty \sigma(E).\phi_E(E).dE}$$

where $\phi_E(E) \propto 1/E$.

The *effective threshold energy* E_{eff} is defined by the minimum value of the expression

$$Q(E_{eff}) = \int_0^\infty \chi_E(E).\{\sigma(E)-S(E)\}^2.dE$$

where $\chi_E(E)$ represents the normalization fission neutron spectrum of ^{235}U;

$$S(E) = \begin{cases} 0 & \text{for } E < E_{eff}; \\ \sigma_{eff} & \text{for } E \geq E_{eff}. \end{cases}$$

$$\sigma_{eff} = \int_0^\infty \chi_E(E).\sigma(E).dE \Big/ \int_{E_{eff}}^\infty \chi_E(E).dE.$$

The actual calculations of $\langle E_r \rangle$ and E_{eff} are performed by replacing the spectrum functions and the cross section functions by corresponding histogram representations using a multigroup structure.

Calculations

The ^{235}U thermal neutron fission spectrum is calculated in the 620 groups structure by the SAND-II program package, based on the following spectrum representation [26]:

$$\phi_E(E) = \mu(E).(0.7501).\sqrt{E}.\exp(-1.5/1.97E)$$

where $\mu(E) = 0.847 + 0.8\,E$ for $E < 0.25$ MeV;
$= 1.087 - 0.14E$ for 0.25 MeV $< E < 0.8$ MeV;
$= 0.938 + 0.04E$ for 0.8 MeV $< E < 1.5$ MeV;
$= 9.983 + 0.01E$ for 1.5 MeV $< E < 6.0$ MeV;
$= 1.043.\exp(-0.06/1.043(E-6.0))$ for $E > 6$ MeV.

The ^{252}Cf spontaneous neutron spectrum in 620 groups is derived from the following representation [26]:

$$\mu_E(E) = \mu(E).(0.6672).\sqrt{E}.\exp(-1.5/2.13E)$$

where $\mu(E) = 0.763 + 1.2\,E$ for $E < 0.25$ MeV;
$= 1.098 - 0.14\,E$ for 0.25 MeV $< E < 0.8$ MeV;
$= 0.9668 + 0.024\,E$ for 0.8 MeV $< E < 1.5$ MeV;
$= 1.0037 - 0.006\,E$ for 1.5 MeV $< E < 6.0$ MeV;
$= \exp(-0.03E + 0.18)$ for $E > 6.0$ MeV.

The ΣΣ neutron spectrum is derived from the 136 groups spectrum data given in ref. [27].
The CFRMF spectrum in 620 groups has been calculated on the basis of the data reported by Rogers et al. [28], who give the spectrum data in 71 energy groups with 0.25 lethargy width from 21.17 MeV downwards. This spectrum was obtained using transport, Monte Carlo and resonance theory computerized methods. In preparing the 620 groups representations the SAND-II program package makes, where necessary, an extrapolation at the low energy side with the $\phi_E = k.E$ distribution; if the largest energy value in the input spectrum is smaller than 18 MeV, the SAND-II code gives an extrapolation with a fission neutron distribution.

The four benchmark spectra, now available in the 620 groups structure, were then used as weighting functions in the calculations of the 15 group sections, starting from the DOSCROS77 library [24]. The spectra were also condensed to 15 group flux densities by application of two utility programs.
The experimental spectrum-averaged cross section values and their uncertainties were taken from a recent review by Fabry [6].
The subprogram FCOV of STAY'SL [15] filled the complete input flux density covariance matrix with zero elements. No correlations are as-

sumed to exist between the cross sections of the various reactions, and between the various group cross sections of each reaction.
Using the input data mentioned above, the program STAY'SL calculated the uncertainties in the calculated reaction rates, resulting from the uncertainties in the group cross section data. These values are combined with the uncertainties in the measured reaction rates (or in the average cross sections proportional to these reaction rates).
With all these calculated data a chi-square value for each reaction has been calculated.
The general expression takes in the present simplified and preliminary study the following form:

$$\chi_i^2 = \frac{(\alpha_i^m - \alpha_i^c)^2}{\text{var } \alpha_i^m + \text{var } \alpha_i^c}$$

where α_i^m and α_i^c denote the measured and calculated values for the i-th reaction rate per target atom;

$$\alpha_i^c = \sum_{j=1}^{k} \sigma_{ij}.\phi_j \ ;$$

$$\text{var } \alpha_i^c = \sum_{j=1}^{k} \phi_j^2.\text{var}(\sigma_{ij}).$$

where k is the number of energy groups.

Results

The results for the discrepancies between measured spectrum averaged reaction rates and calculated spectrum averaged reaction rates are presented in table 9.

The results for the consistency investigation by means of the χ^2 values defined above for the separate reaction rates are given in table 10. This table lists also the uncertainties of the calculated reaction rates $s(\alpha_c)$, arising from the uncertainties in the cross section data, next to the uncertainties in the experimental reaction rates, $s(\alpha_m)$. The table shows for each combination of reaction and spectrum a consistency (say if $\chi^2 < 3$), or an inconsistency (say if $\chi^2 > 3$), or just a lack of data.

We have listed the reactions into 3 groups, on the basis of the occurrence of consistencies and inconsistencies.

The χ^2-results of 34 reactions in 4 benchmarks can be summarized as follows:

No indication of inconsistencies

$^{59}Co(n,\gamma)$, $^{55}Mn(n,\gamma)$, $^{6}Li(n,\alpha)$, $^{58}Fe(n,\gamma)$, $^{63}Cu(n,\gamma)$, $^{235}U(n,f)$, $^{239}Pu(n,f)$, $^{237}Np(n,f)$, $^{232}Th(n,f)$, $^{31}P(n,p)$, $^{32}S(n,p)$, $^{58}Ni(n,p)$, $^{54}Fe(n,p)$, $^{46}Ti(n,p)$, $^{24}Mg(n,p)$, $^{48}Ti(n,p)$, $^{59}Co(n,\alpha)$, $^{127}I(n,2n)$.

Consistency together with inconsistency

$^{115}In(n,\gamma)$, $^{197}Au(n,\gamma)$, $^{238}U(n,\gamma)$, $^{115}In(n,n')$, $^{238}U(n,f)$, $^{47}Ti(n,p)$, $^{27}Al(n,p)$, $^{56}Fe(n,p)$, $^{27}Al(n,\alpha)$.

No indication of consistencies

One observation : CFRMF: $^{10}B(n,\alpha)$, $^{45}Sc(n,\gamma)$, $^{64}Zn(n,p)$,
^{235}U: $^{63}Cu(n,\alpha)$, $^{90}Zr(n,2n)$, $^{58}Ni(n,2n)$.
Two observations: $^{63}Cu(n,2n)$.

With respect to the results obtained for the CFRMF, where the number of reactions is quite large, we observe that some inconsistencies occur at the low energy side for the following reactions: $^{10}B(n,\alpha)$, $^{45}Sc(n,\gamma)$, while also an inconsistency occurs at the high energy response: $^{27}Al(n,\alpha)$. It should be noted that in those regions the neutron group flux densities are rather low.
An occurrence of inconsistencies at both ends of the spectrum is also observed for $\Sigma\Sigma$: at the low energy side for the capture reactions $^{115}In(n,\gamma)$, $^{197}Au(n,\gamma)$, and $^{238}U(n,\gamma)$; at the high energy side for the reaction $^{56}Fe(n,p)$. For the ^{235}U spectrum we observe that the (n,2n) reactions for ^{63}Cu, ^{90}Zr and ^{58}Ni, which have very high effective threshold, show strong inconsistencies.
Alone from table 10 one cannot deduce the origin of the inconsistencies observed: e.g. data which are incorrect, or errors which are quoted too small, or insufficient knowledge of the spectrum tails.

Summary table

In table II a summary is presented of the results obtained thus far in the study of uncertainties, discrepancies and consistencies involved in dosimetry reactions.
The following code is used to visualize the present situation.

category	uncertainty	discrepancy	consistency
++	$0\% < v < 2\%$	$0\% < \Delta < 2\%$	$\chi^2 < 1.5$
+	$2\% < v < 4\%$	$2\% < \Delta < 4\%$	$1.5 < \chi^2 < 3$
0	$4\% < v < 6\%$	$4\% < \Delta < 6\%$	$3 < \chi^2 < 4.5$
-	$6\% < v < 8\%$	$6\% < \Delta < 8\%$	$4.5 < \chi^2 < 6$
--	$8\% < v$	$8\% < \Delta$	$6 < \chi^2$

Future work

It is planned to extend the present study in the near future in several ways:

- inclusion of some reactions which have not yet been included, such as $^{103}Rh(n,n')$, $^{55}Mn(n,2n)$, $^{59}Co(n,2n)$ and $^{93}Nb(n,2n)$; these reactions were excluded since no cross section error scheme was readily available. Moreover no evaluated cross section data for $^{93}Nb(n,2n)$ were readily available;
- inclusion of other benchmark spectra, such as INSF, BIG-TEN;
- application of the ENDF/B-V dosimetry file, when this file becomes available;
- inclusion of the covariance matrices, when these become available.

DISCUSSION

The following remarks are offered for discussion at the Consultants Meetings.

1. The present situation for the ^{235}U spectrum is unsatisfactory, since the measurement errors exceed 2.5%.
2. For many reactions good measurements of average cross sections for a fission neutron spectrum are still missing.
3. Attempts should be made to reduce the relatively large uncertainty in the measured average cross sections for the following reactions
   $^{232}Th(n,f)F.P.$ (problem of fission product yield?)
   $^{27}Al(n,p)^{27}Mg$ (problem due to short half-life?)
   $^{63}Cu(n,\alpha)^{60}Co$ (problem of purity of target material?)
   the (n,2n) reactions (problem of very low induced activities).
4. Cross section problems seem to exist for the reactions $^{115}In(n,n')$, $^{47}Ti(n,p)$, $^{31}P(n,p)$, $^{64}Zn(n,p)$ and for the (n,2n) reactions.
5. For the reaction $^{63}Cu(n,\alpha)^{64}Cu$, applied in the ^{235}U fission spectrum, one observes a discrepancy of 18% combined with a consistency of the input data. This is mainly due to a large error in the measured average cross section (15%), which is appreciably larger than the errors in the calculated cross section. In this case there is reason to assume that the cross section error scheme is appropriate, since its influence on the χ^2 value is rather small.
6. For the reaction $^{47}Ti(n,p)$ we observe a discrepancy in cross section values of 24% for the ^{252}Cf spectrum, and of 18% for the CFRMF spectrum. The errors in the calculated cross sections are appreciably larger than the errors in the measured cross sections.
   The cross section error scheme plays an important role in this case. Reduction of cross section errors will immediately raise the level of inconsistency, since the measurement error is less important here.
7. A surprisingly large (13%) discrepancy is observed between the measured and calculated cross section of the reaction $^{59}Co(n,\gamma)^{60}Co$ applied to the CFRMF spectrum. Since the reaction shows no appreciable errors in the nuclear data, and offers no special problems in counting the product activity, the reason for the discrepancy might be related to the large and narrow response peak at the first resonance.
8. The χ^2 value for a reaction should not be considered by itself, but always in connection with the discrepancy between measured and calculated cross sections, and the standard deviations in these cross sections.

REFERENCES

|1| Vlasov, M.F., et al.: "Status of neutron cross section data for reactor radiation measurements"
INDC(NDS)-47/L (IAEA, Vienna, 1972).

|2| Vlasov, M.F., and Dunford, C.: "Proceedings of Consultants Meeting on Nuclear Data for Reactor Neutron Dosimetry"
INDC(NDS)-56/U (IAEA, Vienna, 1973).

|3| McElroy, W.N., and Kellogg, L.S.: "Fuels and Materials Fast Reactor Dosimetry Data Development and Testing"
Nuclear Technology 25 (1975) no. 2, p. 180.

|4| Fabry, A., et al.: "Reactor dosimetry integral reaction rate data in LMFBR benchmark and standard neutron fields: status, accuracy and implications", Proc. first ASTM-Euratom Symposium on Reactor Dosimetry, held at Petten, September 1975,
Report EUR 5667 e/f, supplement, p. 23 (C.E.C., Luxembourg, 1977).

|5| Vlasov, M.F., Fabry, A., and McElroy, W.N.: "Status of neutron cross sections for reactor dosimetry", Contribution to Proceedings of the International Conference on the Interaction of Neutrons with Nuclei, Lowell, U.S.A., July 1976,
CONF-760715, vol. 2, p. 1187.
Also issued as INDC(NDS)-84/L+M (IAEA, Vienna, March 1977).

|6| Fabry, A., et al.: "Review of Microscopic Integral Cross Section Data in Fundamental Reactor Dosimetry Benchmark Neutron Fields", Contribution to "Neutron Cross Sections for Reactor Dosimetry", Technical Report IAEA-208, Vol. I, Review papers, p. 233
(IAEA, Vienna, 1978).

|7| Vlasov, M.F.: "Comments on excitation functions of threshold reactions used in reactor neutron dosimetry", Contribution to "Neutron Cross Sections for Reactor Dosimetry",
Technical Report IAEA-208, Vol. I, Review papers, p. 353
(IAEA, Vienna, 1978).

|8| Zijp, W.L., Nolthenius, H.J., and Baard, J.H.: "Ratios of measured and calculated reaction rates for some known spectra", Contribution to "Neutron Cross Sections for Reactor Dosimetry",
Technical Report IAEA-208, Vol. I, Review papers, p. 265
(IAEA, Vienna, 1978).

|9| Zijp, W.L.: "Reactor Core Dosimetry Standards", Contribution to "Neutron Standards and Applications", Proc. of the International Specialists Symposium, held at NBS, Gaithersburg, M.D., March 28-31, 1977, edited by C.D. Bowman et al., NBS Special Publication 493, p. 128-136 (U.S. Government Printing Office, Washington D.C., October 1977).

|10| Gilliam, D.M.: "Integral Measurement Results in Standard Fields", Proc. of the International Specialists Symposium on Neutron Standards and Applications, held at NBS, Gaithersburg, M.D., March 28-31, 1977, edited by C.D. Bowman et al., NBS Special Publication 493, p. 299-303 (U.S. Government Printing Office, Washington D.C., October 1977).

|11| Fabry, A., et al.: "Status report on dosimetry benchmark field development, characterization and application", Proc. Second ASTM-Euratom Symposium on Reactor Dosimetry, Palo Alto, California, October 3-7, 1977, Report NUREG/CP-0004, Vol. 3, p. 1141 (U.S. Nuclear Regulatory Commission, Washington D.C., 1978).

|12| Vlasov, M.F., editor: "IAEA Consultants Meeting on Integral Cross Section Measurements in Standard Neutron Fields", held at Vienna, November 15-19, 1976, Summary Report, Conclusions and Recommendations INDC(NDS)-81/L+M (IAEA, Vienna, March 1978).

|13| Perey, F.G.: "Uncertainty analysis of dosimetry spectrum unfolding", Contribution to Proc. of the second ASTM-Euratom Symposium on Reactor Dosimetry, held at Palo Alto, Calif., October 3-7, 1977, NUREG/CP-0004, Vol. 3, p. 1449 (U.S. Nuclear Regulatory Commission, Washington D.C., 1978).

|14| Perey, F.G.: "Spectrum unfolding by the least squares method", Paper presented at the IAEA Technical Committee on Current Status of Neutron Spectrum Unfolding, Oak Ridge, Tenn., Oct. 10-12, 1977 (at present unpublished).

|15| Perey, F.G.: "Least squares dosimetry unfolding. The program STAY'SL" ORNL-TM-6062; ENDF-254 (Oak Ridge National Lab., October 1977).

|16| Philis, L., et al.: "Evaluated (n,p) cross sections of ^{46}Ti, ^{47}Ti and ^{48}Ti"
ANL/NDM-27 (Argonne National Laboratory, Argonne, January 1977).

|17| Vlasov, M.F., et al., Review of differential neutron data for important reactions not yet included in ENDF/B-V dosimetry file", Proc. of the 2nd ASTM-Euratom Symposium on Reactor Dosimetry, held at Palo Alto, October 3-7, 1977,
Report NUREG/CP-0004, Vol. II, p. 855 (U.S. Nuclear Regulatory Commission, 1978).

|18| Report of the Nuclear Data Section to the International Nuclear Data Committee (March 1977 to August 1978).
Report INDC(NDS)-97/LNA (IAEA, Vienna, 1978).

|19| Adamski, L., Herman, M., and Marcinkowsk, A.: "Evaluation of the $^{58}Ni(n,2n)^{57}Ni$ reaction cross section"
Report INDC(POL)-8/L; INR 1709 /1/ PL/A (IAEA, Vienna, Nov. 1977).

|20| Tagesen, S., and Vonach, H.: "Evaluation of the cross sections for the reactions $^{24}Mg(n,p)^{24}Na$, $^{64}Zn(n,p)^{64}Cu$, $^{63}Cu(n,2n)^{62}Cu$ and $^{90}Zr(n,2n)^{89}Zr$", Contribution to Int. Conference on Neutron Physics and Nuclear Data for Reactors and Other Applied Purposes, Harwell, 25-29 September 1978.

|21| Paulsen, A., et al.: "Determination of excitation function for the threshold reaction $^{103}Rh(n,n')^{103}Rh$", Contribution to CBNM Nuclear Data Progress Report 1977,
Report NEANDC(E)-192"U" bis, Vol. III, Euratom;
INDC(EUR)-11/G bis, page 5 (IAEA, Vienna, 1977).

|22| Liskien, H., et al.: "Cross sections for the threshold reaction $^{115}In(n,n')^{115}In^{m}$ below 4 MeV neutron energy", Contribution to CBNM Nuclear Data Progress Report 1977,
Report NEANDC(E)-192"U" bis, Vol. III, Euratom;
INDC(EUR)-11/G bis, page 5 (IAEA, Vienna, 1977).

|23| Smith, D.L.: "Evaluation of the $^{115}In(n,n')^{115}In^{m}$ reaction for the ENDF/B-IV dosimetry file",
ANL/NDM-26 and erratum (Argonne National Lab., Argonne, Dec. 1976).

|24| Zijp, W.L., Nolthenius, H.J., and Van der Borg, N.J.C.M.: "Cross section library DOSCROS77 (in the SAND-II format)", Report ECN-25 (Netherlands Energy Research Foundation ECN, Petten, August 1977).

|25| Zijp, W.L.: "General Remarks on the Benchmark Studies", Contribution to "Neutron Cross Sections for Reactor Dosimetry", Technical Report IAEA-208, Vol. II, Contributed papers, p. 189 (IAEA, Vienna, 1978).

|26| Grundl, J., and Eisenhauer, C.: "Fission Rate Measurements for Materials Neutron Dosimetry in Reactor Environment", Proc. of the first ASTM-Euratom Symposium on Reactor Dosimetry, held at Petten, September 22-26, 1975, Report EUR-5667 e/f, Part I, p. 425 (C.E.C., Luxembourg, 1977).

|27| Fabry, A., De Leeuw, G., and De Leeuw, S.: "The Secondary Intermediate Energy Standard Neutron Field at the Mol-ΣΣ Facility", Nuclear Technology 25 (1975), no. 2, p. 349.

|28| Rogers, J.W, Harker, Y.D., and Millsap, D.A.: "The coupled fast reactivity measurements facility (CFRMF)", Contribution to "Neutron Cross Sections for Reactor Dosimetry", Technical Report IAEA-208, Vol. II, Contributed Papers, p. 117 (IAEA, Vienna, 1978).

|29| Fleming, R., and Spiegel, V.: "Measurement of threshold reaction cross section ratios in fission neutron fields", Proc. Second ASTM-Euratom Symposium on Reactor Dosimetry, held at Palo Alto, October 3-7, 1977, Report NUREG/CP-0004, Vol. 2, p. 953 (U.S. Nuclear Regulatory Commission, Washington D.C., 1978).

|30| Mannhart, W.: "Comparison between measured and calculated average cross sections in the ^{252}Cf neutron fission spectrum", Contribution to Progress Report on Nuclear Data Research in the Federal Republic of Germany, Report NEANDC(E)-192"U", Vol. V; INDC(Ger)-20/4+Special (KFA, Jülich, April 1978).

Table 1. Measured and calculated average fission cross sections in a ^{252}Cf neutron field* |10|.

reaction	$\langle\sigma\rangle^f$ in millibarn		$\langle\sigma_m\rangle/\langle\sigma_c\rangle$
	measured	calculated	
$^{235}U(n,f)$	1210 ± 2.0%	1241	0.975
$^{238}U(n,f)$	319 ± 2.5%	315	1.013
$^{239}Pu(n,f)$	1800 ± 2.2%	1789	1.006
$^{237}Np(n,f)$	1332 ± 2.8%	1351	0.986

*Calculated cross sections were derived from ENDF/BIV data, and the neutron energy spectrum given in the NBS evaluation |26|. Measured cross sections are averaged for the ^{252}Cf neutron fields at NBS and the University of Michigan.

Table 2. Fission cross section ratios in benchmark fields. Comparison of measured and calculated values [10].

benchmark field	cross section ratio R	measured value R_m	calculated value R_c	ratio R_m/R_c
^{252}Cf fission spectrum	$\langle\sigma^f(^{235}U)\rangle/\langle\sigma^f(^{239}Pu)\rangle$	0.672±1.6%	0.693	0.970
	$\langle\sigma^f(^{238}U)\rangle/\langle\sigma^f(^{239}Pu)\rangle$	0.177±1.7%	0.176	1.007
	$\langle\sigma^f(^{237}Np)\rangle/\langle\sigma^f(^{239}Pu)\rangle$	0.740±2.2%	0.754	0.981
^{235}U fission spectrum	$\langle\sigma^f(^{235}U)\rangle/\langle\sigma^f(^{239}Pu)\rangle$	0.664±2.2%	0.697	0.953
	$\langle\sigma^f(^{238}U)\rangle/\langle\sigma^f(^{239}Pu)\rangle$	0.169±2.2%	0.166	1.016
	$\langle\sigma^f(^{237}Np)\rangle/\langle\sigma^f(^{239}Pu)\rangle$	0.734±3.0%	0.741	0.991
BIG-TEN	$\langle\sigma^f(^{235}U)\rangle/\langle\sigma^f(^{239}Pu)\rangle$	0.835±1.5%	0.853	0.979
	$\langle\sigma^f(^{238}U)\rangle/\langle\sigma^f(^{239}Pu)\rangle$	0.0311±1.9%	0.0324	0.960
	$\langle\sigma^f(^{237}Np)\rangle/\langle\sigma^f(^{239}Pu)\rangle$	0.265±2.2%	0.285	0.930
CFRMF	$\langle\sigma^f(^{235}U)\rangle/\langle\sigma^f(^{239}Pu)\rangle$	0.873±1.6%	0.893	0.978
	$\langle\sigma^f(^{238}U)\rangle/\langle\sigma^f(^{239}Pu)\rangle$	0.0428±1.9%	0.0431	0.993
	$\langle\sigma^f(^{237}Np)\rangle/\langle\sigma^f(^{239}Pu)\rangle$	0.309±2.3%	0.325	0.951
SIGMA-SIGMA	$\langle\sigma^f(^{235}U)\rangle/\langle\sigma^f(^{239}Pu)\rangle$	0.857±2.1%	0.869	0.986
	$\langle\sigma^f(^{238}U)\rangle/\langle\sigma^f(^{239}Pu)\rangle$	0.0483±2.5%	0.0467	1.034
	$\langle\sigma^f(^{237}Np)\rangle/\langle\sigma^f(^{239}Pu)\rangle$	0.333±2.8%	0.348	0.957
ISNF	$\langle\sigma^f(^{235}U)\rangle/\langle\sigma^f(^{239}Pu)\rangle$	0.866±1.8%	0.898	0.964
	$\langle\sigma^f(^{238}U)\rangle/\langle\sigma^f(^{239}Pu)\rangle$	0.0799±1.8%	0.0757	1.055
	$\langle\sigma^f(^{237}Np)\rangle/\langle\sigma^f(^{239}Pu)\rangle$	-	-	-

Calculated cross section ratios were derived from ENDF/B-IV data, and the neutron energy spectra as tabulated in the compendium by Grundl and Eisenhauer [26].

Table 3. Activation cross section ratio in benchmark fields. Comparison of measured and calculated values, based on preliminary results by Fleming and Spiegel [29].

benchmark field	cross section ratio R	measured value R_m	calculated value R_c	ratio R_m/R_c
^{235}U fission spectrum	$\langle\sigma_i(^{58}Ni)\rangle/\langle\sigma(^{54}Fe)\rangle$	1.346±0.03	1.308	1.029
^{252}Cf fission spectrum	"	1.326±0.03	1.290	1.028

TABLE 4. INTEGRAL TESTING OF DOSIMETRY CROSS SECTION FILES[a] IN THE URANIUM-235 THERMAL FISSION SPECTRUM NEUTRON FIELD, X_{25} |5|

REACTION[b]	EFFECTIVE THRESHOLD (MeV)	BIAS FACTOR[c] FOR $X_{25}(E)$: NBS EVALUATION (E = 1.98 MeV)	BIAS FACTOR[c] FOR $X_{25}(E)$: SAND-II ADJUSTED (E = 2.01 MeV)	RELIABILITY[d]
$^{115}In(n,\gamma)^{116m}In$	-	0.990	0.996	
$^{197}Au(n,\gamma)^{198}Au$	-	0.987	0.972	
$^{63}Cu(n,\gamma)^{64}Cu$	-	0.846	0.834	x
$^{235}U(n,f)$	-	0.969	0.968	?
$\underline{^{239}Pu(n,f)}$	-	1.017	1.017	
$\underline{^{237}Np(n,f)}$	0.6	0.994	1.000	
$^{115}In(n,n')^{115m}In$	1.2	1.037	1.019	
$^{232}Th(n,f)$	1.4	1.174	1.149	x
$\underline{^{238}U(n,f)}$	1.5	1.031	1.010	
$^{47}Ti(n,p)^{47}Sc$	2.2	0.888	0.852	x
$^{31}P(n,p)^{31}Si$	2.4	[1.092]	[1.041]	x
$\underline{^{58}Ni(n,p)^{58}Co}$	2.8	1.068	1.020	
$^{32}S(n,p)^{32}P$	2.9	1.042	0.987	
$^{54}Fe(n,p)^{54}Mn$	3.1	1.026	0.977	
$Ti(n,x)^{46}Sc$	3.9	1.181	1.155	x
$^{27}Al(n,p)^{27}Mg$	4.4	0.937	0.917	x
$\underline{^{56}Fe(n,p)^{56}Mn}$	6.0	0.983	1.004	
$^{59}Co(n,\alpha)^{56}Mn$	6.8	0.966	0.973	
$^{63}Cu(n,\alpha)^{60}Co$	6.8	1.420	1.445	x
$^{24}Mg(n,p)^{24}Na$	6.8	[0.977]	[0.993]	
$\underline{^{27}Al(n,\alpha)^{24}Na}$	7.2	1.017	1.022	
$^{48}Ti(n,p)^{48}Sc$	7.6	1.734	1.714	x
$^{127}I(n,2n)^{126}I$	10.5	0.885	0.778	x
$^{55}Mn(n,2n)^{54}Mn$	11.6	0.996	0.803	x
$\underline{^{63}Cu(n,2n)^{62}Cu}$	12.4	[1.407]	[0.897]	
$^{90}Zr(n,2n)^{89}Zr$	13	[2.951]	[1.715]	x
$\underline{^{58}Ni(n,2n)^{57}Ni}$	13.5	2.050	1.120	

(a) ENDF/B-IV, except for bias factors within brackets where the SAND-II file was used.
(b) Underlined reactions are considered Category I and form the basis for X_{25} spectral shape adjustments.
(c) Measured/computed integral cross sections.
(d) Crosses (x) if $\sigma(E)$ in file is deemed seriously unreliable for the energy response range of the reaction in X_{25}.

Table 5. Measured and calculated average activation cross sections in a ^{252}Cf neutron field [30].

reaction	cross section (in mb) measured* $\langle\sigma_m\rangle$	calculated** $\langle\sigma_c\rangle$	ref.	$\langle\sigma_m\rangle$ $\langle\sigma_c\rangle$ ***
$^{197}Au(n,\gamma)^{198}Au$	76.2 ± 2.4%	76.50	a)	0.996±0.047 (0.069)
$^{115}In(n,\gamma)^{116}In^m$	124.1 ± 2.9%	130.3	b)	0.952±0.043 (0.109)
$^{115}In(n,n')^{115}In^m$	195 ± 2.6%	189.1	c)	1.032±0.033 (0.077)
$^{113}In(n,n')^{113}In^m$	160 ± 2.5%	142.7	c)	1.121±0.033 (0.077)
$^{47}Ti(n,p)^{47}Sc$	18.9 ± 2.1%	24.06	d)	0.786±0.032 (0.077)
$^{58}Ni(n,p)^{58}Co$	118 ± 2.5%	115.0	b)	1.026±0.035 (0.106)
$^{54}Fe(n,p)^{54}Mn$	84.6 ± 2.4%	85.58	e)	0.989±0.033 (0.077)
$^{64}Zn(n,p)^{64}Cu$	39.4 ± 2.5%	37.31	e)	1.056±0.034 (0.078)
$^{46}Ti(n,p)^{46}Sc$	13.8 ± 2.2%	13.46%	d)	1.025±0.040 (0.080)
$^{56}Fe(n,p)^{56}Mn$	1.450± 2.4%	1.476	b)	0.092±0.057 (0.076)
$^{48}Ti(n,p)^{48}Sc$	0.42 ± 2.4%	0.4092	d)	1.026±0.071 (0.099)
$^{27}Al(n,\alpha)^{24}Na$	1.006± 2.2%	1.059	b)	0.950±0.076 (0.091)
$^{197}Au(n,2n)^{198}Au$	5.50 2.5%	5.646	a)	0.974 0.103 (0.144)

* Measurements performed by PTB Braunschweig, and reported by
- Alberts, W.G., Günther, E., Matzko, M., and Rass, G., EUR 5667 e/f, Part II (1977), p.131.
- Mannhart, W., NEANDC(E)-182U, Vol. V (1977), p.84.

** Calculations are based on the NBS spectrum representation [26] using cross section data from the ENDF/B-IV file, from the ENDF/B-V file under preparation, and from recent experiments.
a) Mughabghab, S.F., Private communication to Mannhart (1977).
b) Magurno, B.A., BNL-NCS-50446 (April 1975).
c) Smith, D.L., and Meadows, J.W., ANL/NDM-14 (July 1975).
d) Philis, L., Bersillon, O., Smith, D., and Smith, A., ANL/NDM-27 (January 1977).
e) Smith, D.L., and Meadows, J.W., ANL/NDM-13 (July 1975).

*** The standard deviation comprises uncertainties of $\langle\sigma_m\rangle$ and of the spectrum, the value given in brackets additionally includes the uncertainty of the $\sigma(E)$ data.

TABLE 6. RATIO OF MEASURED[a] TO COMPUTED[b] INTEGRAL CROSS SECTIONS IN DOSIMETRY BENCHMARK NEUTRON FIELDS |6|,|11|.

REACTION	NEUTRON FIELD				
	X_{82}	X_{25}	ΣΣ	CFRMF	BIG-10
$^{59}Co(n,\gamma)^{60}Co$	-	-	-	1.123	1.027
$^{58}Fe(n,\gamma)^{59}Fe$	-	-	-	0.989	1.382
$^{63}Cu(n,\gamma)^{64}Cu$	-	0.846	0.932	0.946	0.924
$^{197}Au(n,\gamma)^{198}Au$	1.000	0.987	1.076	1.014	1.036
$^{238}U(n,\gamma)^{239}U$	-	-	(~0.95[c])	0.946	0.992
$^{10}B(n,\alpha)^{7}Li$	-	-	-	1.068	1.131
$^{45}Sc(n,\gamma)^{46}Sc$	-	-	-	1.175	1.114
$^{115}In(n,\gamma)^{116m}In$	0.962	0.990	0.842	0.932	-
$^{6}Li(n,\alpha)^{3}H$	-	-	-	0.977	1.015
$^{235}U(n,f)$	0.969	0.969	0.991	0.976	0.990
$^{239}Pu(n,f)$	1.008	1.017	1.017	1.001	1.013
$^{237}Np(n,f)$	0.986	0.994	0.966	0.951	0.944
$^{115}In(n,n')^{115m}In$	1.036	1.037	1.014	0.977	0.980
$^{238}U(n,f)$	1.015	1.031	1.044	0.983	0.979
$^{47}Ti(n,p)^{47}Sc$	0.793	0.888	-	0.815	0.858
$^{58}Ni(n,p)^{58}Co$	1.026	1.068	1.139	1.017	1.058
$^{54}Fe(n,p)^{54}Mn$	0.949	1.026	-	0.989	1.028
$Ti(n,x)^{46}Sc$	1.102	1.181	-	1.145	1.207
$^{27}Al(n,p)^{27}Mg$	0.992	0.937	1.131	0.929	-
$^{56}Fe(n,p)^{56}Mn$	0.983	0.983	1.130	-	-
$^{27}Al(n,\alpha)^{24}Na$	0.950	1.017	1.007	0.910	1.089
$^{48}Ti(n,p)^{48}Sc$	1.585	1.734	-	1.578	1.980

(a) Normalized by $^{239}Pu(n,f)$ transfer from californium, text Section 2.1.

(b) $\int_0^\infty \sigma_r^i(E)\,\phi(E)\,dE$; $\sigma_r^i(E)$:ENDF/B-IV file; $\phi(E)$: as recommended, 1975, normalized $\int_0^\infty \phi(E)\,dE = 1$.

(c) Applying the spectral shielding correction computed for CFRMF.

Table 7. List of reactions to be included in the dosimetry file |17|, |18|.

reaction	priority	application	status comments
^{14}N (n,p)^{14}C	L	C	2
^{19}F (n,2n)^{18}F	I	B_1	1
^{23}Na(n,2n)^{22}Na	L	A_3	3
^{24}Mg(n,p)^{24}Na	L	A_1	1
^{31}P (n,p)^{31}Si	L	A_1	1
^{45}Sc(n,2n)$^{44}Sc^{m,g}$	I	B_1	4
^{54}Fe(n,α)^{51}Cr	I	B_1	6
^{59}Co(n,p)^{59}Fe	I	B_1	6
^{63}Cu(n,2n)^{62}Cu	I	A_1, B_2	1
^{64}Zn(n,p)^{64}Cr	L	A_1	1
^{90}Zr(n,2n)^{89}Zr	I	A_1, B_1	1
^{93}Nb(n,n')$^{93}Nb^{m}$	I	A_2, B_3	1
^{93}Nb(n,2n)^{92}Nb	I	A_1, B_1, B_2	5
^{103}Rh(n,n')$^{103}Rh^{m}$	I	A_1, A_2	1
^{197}Au(n,2n)^{196}Au	I	B_1	5
^{197}Au(n,3n)^{195}Au	I	B_1	5
^{197}Au(n,4n)^{194}Au	L	B_1	5
^{199}Hg(n,n')$^{199}Hg^{m}$	L	A_2, A_1	2
^{241}Am(n,f)F.P.	L	A_4	7

For comments see next page.

For notes to the reactions see page 32.

COMMENTS TO TABLE 7

Priorities: I - immediate need.

L - long range need.

Application:

A. Fission Reactor Dosimetry
   - A1 Neutron Spectra Unfolding
   - A2 Neutron Fluence Monitor
   - A3 Activation of Fast Breeder Cooling
   - A4 Burn-up Calculation

B. Fusion Reactor Dosimetry
   - B1 Neutron Spectra Unfolding
   - B2 Neutron Fluence Monitor
   - B3 Structural Material Activation

C. Differential Neutron Spectrometry

Status Comments:

1. Evaluation by Prof. Vonach's group, Vienna, Austria.
2. No sufficient data are available, new measurements required.
3. Evaluation by Marcinkowki's group, Warsaw, Poland.
4. Evaluation by NDS, IAEA, Vienna, Australia.
5. Recently was evaluated by Philis et al., France.
6. Evaluation by Vasiliu's group, Bucharest, Romania.
7. Recently was evaluated by Patrick et al., UK.

Notes to the reactions listed in table 7

^{14}N (n,p) ^{14}C : No data between 5 and 15 MeV.

^{19}F (n,2n) ^{18}F : Discrepancy near threshold.

$^{23}Na(n,2n)^{22}Na$: Strong disagreement between Liskien 69*, Menlove 67* and Picard 65*.

$^{24}Mg(n,p)^{24}Na$: Excitation function reasonably well established. Fluctuation appears in 12 to 14 MeV (Ferguson 67*).

^{31}P (n,p) ^{31}Si : Easier to perform new measurement than to analyse the old results. Measurement required in 10 to 14 MeV.

$^{45}Sc(n,2n)^{44}Sc^{m,g}$: No evaluation available. Urgently required.

$^{54}Fe(n,\alpha)^{51}Cr$: No data available between 6 and 13 MeV.

$^{59}Co(n,p)^{59}Fe$: No data between 10 and 14 MeV. Widely scattered experimental results around 14 MeV.

$^{63}Cu(n,2n)^{62}Cu$: Measured integral cross section is higher than the calculated one. New measurement $\sigma(E)$ near threshold required.

$^{64}Zn(n,p)^{64}Cu$: Integral data support preferably the lower values by Smith 75*.

$^{90}Zr(n,2n)^{89}Zr$: Measurement of $\sigma(E)$ threshold up to 14 MeV would be desirable.

$^{93}Nb(n,n')^{93}Nb^{m}$: No measurements with monoenergetic neutrons. Large uncertainties amoung the measured values of half-life.

$^{93}Nb(n,2n)^{92}Nb$: New evaluation needed urgently due to corrected of Nethaway's* results.

$^{103}Rh(n,n')^{103}Rh^{m}$: Excitation function established by two sets of measurements in Chalk River (Santry and Butler*).

$^{197}Au(n,xn)$: Recent evaluation by Philis et al.* (1976) is available.

$^{199}Hg(n,n')^{199}Hg^{m}$: Practically no information on excitation function commonly used in U.S.S.R.

$^{241}Am(n,f)F.P.$: Measurement required between 4 and 14 MeV.

*For complete reference see |17|.

TABLE 8.

SAND-II-Evaluated Cross-Section Error Assignment

Reaction	Percent Standard Deviation Uncertainty														
$^{6}Li(n, tot. {}^{4}He)$	0.5	1	1	10	10	20	20	20	20	20	20	20	20	20	20
$^{10}B(n, tot. {}^{4}He)$	0.5	1	1	7	10	20	20	20	20	20	20	20	20	20	20
$^{23}Na(n, \gamma)$	1	2	8	8	10	10	10	10	10	10	10	10	10	10	10
$^{24}Mg(n, p)$	0	0	0	0	0	0	0	0	0	50	50	10	10	10	10
$^{27}Al(n, \alpha)$	0	0	0	0	0	0	0	0	0	30	20	6	6	10	10
$^{27}Al(n, p)$	0	0	0	0	0	0	0	30	10	8	8	8	8	20	20
$^{28}Si(n, p)$	0	0	0	0	0	0	0	0	0	50	50	15	15	15	15
$^{31}P(n, p)$	0	0	0	0	0	0	50	6	12	12	12	10	10	10	10
$^{32}S(n, p)$	0	0	0	0	0	0	100	20	8	8	8	8	8	8	8
$^{34}S(n, \alpha)$	0	0	0	0	0	0	0	0	0	50	50	25	15	10	10
$^{35}Cl(n, \alpha)$	0	0	0	0	0	0	0	30	20	20	30	30	30	30	30
$^{45}Sc(n, \gamma)$	2	4	8	10	10	10	15	15	15	15	15	15	15	15	15
$^{46}Ti(n, p)$	0	0	0	0	0	0	50	50	25	20	20	10	10	20	20
$^{47}Ti(n, p)$	0	0	0	0	50	50	50	50	15	15	15	15	15	15	15
$^{48}Ti(n, p)$	0	0	0	0	0	0	0	0	50	50	25	15	15	15	15
$^{54}Fe(n, p)$	0	0	0	0	30	30	30	10	10	8	8	7	7	10	10
$^{55}Mn(n, \gamma)$	0.8	2	8	8	10	10	15	15	15	15	15	15	15	15	15
$^{56}Fe(n, p)$	0	0	0	0	0	0	0	0	8	8	8	6	6	15	15
$^{58}Fe(n, \gamma)$	8	8	28	15	15	15	15	15	15	15	15	15	15	15	15
$^{58}Ni(n, p)$	0	0	0	0	0	20	10	5	5	5	6	6	6	10	10
$^{59}Ni(n, 2n)$	0	0	0	0	0	0	0	0	0	0	0	0	0	30	20
$^{59}Co(n, \alpha)$	0	0	0	0	0	0	0	0	0	30	15	10	10	10	10
$^{59}Co(n, \gamma)$	4	5	10	10	10	10	10	10	10	10	10	10	10	10	10
$^{60}Ni(n, p)$	0	0	0	0	0	0	50	50	50	50	15	10	10	10	10
$^{63}Cu(n, \alpha)$	50	50	50	50	50	50	50	50	50	50	25	10	10	10	10
$^{65}Cu(n, \gamma)$	5	5	10	10	10	10	10	10	10	10	10	10	10	10	10
$^{63}Cu(n, 2n)$	0	0	0	0	0	0	0	0	0	0	0	0	0	8	8
$^{64}Zn(n, p)$	0	0	0	0	50	50	50	50	15	15	15	15	15	15	15
$^{90}Zr(n, 2n)$	0	0	0	0	0	0	0	0	0	0	0	0	0	30	15
$^{115}In(n, n')$	0	0	0	0	30	20	10	10	10	8	8	8	8	10	10
$^{115}In(n, \gamma)$	2.5	5	5	5	5	10	17	17	17	17	17	17	17	17	17
$^{127}I(n, 2n)$	0	0	0	0	0	0	0	0	0	0	0	0	30	30	15
$^{197}Au(n, \gamma)$	0.5	4	5	6	6	7	7	7	7	7	7	7	7	7	7
$^{232}Th(n, \gamma)$	1.4	5	8	8	8	10	10	10	10	10	10	10	10	10	10
$^{232}Th(n, f)$	0	0	0	0	0	30	25	20	10	10	10	10	10	10	10
$^{235}U(n, f)$	0.5	8	8	8	7	6	4	3	3	3	4	6	6	10	10
$^{237}Np(n, f)$	16	10	10	10	20	5	4	3	3	3	4	10	10	10	10
$^{236}U(n, f)$	0	0	0	0	30	30	4	3	3	3	4	6	6	10	10
$^{238}U(n, \gamma)$	1.5	5	8	8	8	8	8	8	8	8	8	8	8	10	10
$^{239}Pu(n, f)$	0.5	8	8	8	7	6	5	5	5	5	6	8	8	10	10
SAND-II[a] Group No.	1-162[a]	162-226	226-361	361-406	406-440	440-455	455-463	463-471	471-481	481-491	491-501	501-521	521-551	551-571	571-621
Energy[b] Bounds (MeV)	1^{-10}-4^{-7}[b]	4^{-7}-1^{-5}	1^{-5}-1^{-2}	1^{-2}-1^{-1}	1^{-1}-6^{-1}	6^{-1}-1.4	1.4-2.2	2.2-3.0	3.0-4.0	4.0-5.0	5.0-6.0	6.0-8.0	8.0-11.0	11.0-13.0	13.0-18.0

[a] SAND-II group numbers.

[b] SAND-II group energy bounds: Note: $1^{-10} = 1 \times 10^{-10}$ MeV, etc.

Table 9. Discrepancies between measured and calculated cross sections, averaged over benchmark spectra. The cross sections are expressed in millibarn. Calculated values refer to the DOSCROS-77 dosimetry cross section file. Measured values are taken from the review by Fabry et al. |6|.

reaction	$\langle E_r \rangle$ or E_L (in MeV)	^{235}U			^{252}Cf			CFRMF			ΣΣ		
		$\langle\sigma_m\rangle$	$\langle\sigma_c\rangle$	$\frac{\langle\sigma_m\rangle}{\langle\sigma_c\rangle}$	$\langle\sigma_m\rangle$	$\langle\sigma_c\rangle$	$\frac{\langle\sigma_m\rangle}{\langle\sigma_c\rangle}$	$\langle\sigma_m\rangle$	$\langle\sigma_c\rangle$	$\frac{\langle\sigma_m\rangle}{\langle\sigma_c\rangle}$	$\langle\sigma_m\rangle$	$\langle\sigma_c\rangle$	$\frac{\langle\sigma_m\rangle}{\langle\sigma_c\rangle}$
$^{115}In(n,\gamma)$	0.08×10^{-3}	134.5	134.4	1.00	125.3	129.1	0.97	281.5	297.1	0.95	240	276.3	0.87
$^{197}Au(n,\gamma)$	0.14×10^{-3}	83.5	82.60	1.01	79.9	78.19	1.02	424	404.3	1.05	402	356.6	1.13
$^{59}Co(n,\gamma)$	0.27×10^{-3}	-	-	-	-	-	-	91.6	81.07	1.13	-	-	-
$^{238}U(n,\gamma)$	0.60×10^{-3}	-	-	-	-	-	-	223	232.9	0.96	174	206.7	0.84
$^{10}B(n,\alpha)$	0.64×10^{-3}	-	-	-	-	-	-	1814	1660	1.09	-	-	-
$^{55}Mn(n,\gamma)$	0.81×10^{-3}	-	-	-	-	-	-	-	-	-	36.0	34.21	1.05
$^{45}Sc(n,\gamma)$	1.48×10^{-3}	-	-	-	-	-	-	23.5	19.52	1.20	-	-	-
$^{6}Li(n,\alpha)$	1.97×10^{-3}	-	-	-	-	-	-	948	943.6	1.00	-	-	-
$^{58}Fe(n,\gamma)$	2.18×10^{-3}	-	-	-	-	-	-	6.12	6.255	0.98	-	-	-
$^{63}Cu(n,\gamma)$	4.89×10^{-3}	9.30	10.74	0.87	-	-	-	45.4	46.52	0.98	36.2	37.25	0.97
$^{235}U(n,f)$	5.25×10^{-3}	1203	1242	0.97	1203	1242	0.97	1557	1582	0.98	1512	1500	1.01
$^{239}Pu(n,f)$	6.08×10^{-3}	1811	1785	1.01	1804	1792	1.01	1783	1779	1.00	1764	1751	1.01
$^{237}Np(n,f)$	0.568	1312	1337	0.98	1332	1365	0.98	551	601.3	0.92	586.5	641.4	0.91
$^{115}In(n,n')$	1.30	189	177.4	1.07	198	185.6	1.07	51.0	52.64	0.97	56.0	56.67	0.99
$^{232}Th(n,f)$	1.4	81	70.81	1.14	-	-	-	-	-	-	-	-	-
$^{238}U(n,f)$	1.5	305	302.0	1.01	320	321.0	1.00	75.6	82.03	0.92	84.8	88.05	0.96
$^{47}Ti(n,p)$	2.3	19.0	21.38	0.89	18.9	23.78	0.79	4.18	5.265	0.79	-	-	-
$^{31}P(n,p)$	2.4	35.5	32.81	1.08	-	-	-	-	-	-	-	-	-
$^{32}S(n,p)$	2.7	66.8	65.42	1.02	-	-	-	-	-	-	-	-	-
$^{58}Ni(n,p)$	2.7	108.5	102.6	1.06	118	115.5	1.02	24.0	24.81	0.97	26.5	24.82	1.07
$^{64}Zn(n,p)$	2.7	29.9	42.81	0.70	-	-	-	-	-	-	-	-	-
$^{54}Fe(n,p)$	3.0	79.7	77.96	1.02	84.6	89.02	0.95	17.5	18.45	0.95	-	-	-
$^{27}Al(n,p)$	4.4	3.86	4.059	0.95	5.1	5.043	1.01	0.874	0.9703	0.90	0.983	0.8995	1.09
*$Ti(n,X)^{46}Sc$	4.4	11.8	10.52	1.12	13.8	13.10	1.05	2.61	2.502	1.04	-	-	-
$^{56}Fe(n,p)$	6.0	1.035	1.019	1.02	1.45	1.422	1.02	-	-	-	0.260	0.2334	1.11
$^{24}Mg(n,p)$	6.6	1.48	1.451	1.02	-	-	-	-	-	-	-	-	-
$^{63}Cu(n,\alpha)$	6.6	0.500	0.3372	1.48	-	-	-	-	-	-	-	-	-
$^{48}Ti(n,p)$	6.8	0.300	0.2573	1.17	0.42	0.3866	1.09	0.0688	0.06993	0.98	-	-	-
$^{59}Co(n,\alpha)$	6.8	0.143	0.1421	1.01	-	-	-	-	-	-	-	-	-
$^{27}Al(n,\alpha)$	7.2	0.705	0.6614	1.07	1.006	1.010	1.00	0.161	0.1827	0.88	0.153	0.1548	0.99
$^{127}I(n,2n)$	10.1	1.05	1.137	0.92	-	-	-	-	-	-	-	-	-
$^{63}Cu(n,2n)$	12.4	0.122	0.08699	1.40	0.30	0.2026	1.48	-	-	-	-	-	-
$^{90}Zr(n,2n)$	12.9	0.247	0.08273	2.99	-	-	-	-	-	-	-	-	-
$^{58}Ni(n,2n)$	13.4	0.00577	0.002621	2.20	-	-	-	-	-	-	-	-	-

*) $\sigma(E)$ of $^{46}Ti(n,\gamma)$ has been used.

Table 10. Uncertainties (in per cent) in measured and calculated cross sections; χ^2 values. Measured uncertainties are taken from the review by Fabry et al. |6|.

reaction	$\langle E_\Gamma \rangle$ or E_L (in MeV)	^{235}U			^{252}Cf			CFRMF			ΣΣ		
		$s(\sigma_m)$	$s(\sigma_c)$	χ^2	$s(\sigma_m)$	$s(\sigma_c)$	χ^2	$s(\sigma_m)$	$s(\sigma_c)$	χ^2	$s(\sigma_m)$	$s(\sigma_c)$	χ^2
$^{115}In(n,\gamma)$	0.08×10^{-3}	4.46	5.53	0.000	3.44	5.61	0.204	3.91	2.77	1.285	3.75	2.81	9.310
$^{197}Au(n,\gamma)$	0.14×10^{-3}	5.99	3.24	0.025	3.63	3.22	0.198	3.30	3.16	1.080	2.49	2.84	10.151
$^{59}Co(n,\gamma)$	0.27×10^{-3}	-	-	-	-	-	-	3.92	8.63	1.794	-	-	-
$^{238}U(n,\gamma)$	0.60×10^{-3}	-	-	-	-	-	-	4.93	4.25	0.443	4.02	3.97	9.195
$^{10}B(n,\alpha)$	0.64×10^{-3}	-	-	-	-	-	-	3.30	3.73	3.181	-	-	-
$^{55}Mn(n,\gamma)$	0.81×10^{-3}	-	-	-	-	-	-	-	-	-	5.56	5.95	0.394
$^{45}Sc(n,\gamma)$	1.48×10^{-3}	-	-	-	-	-	-	3.83	5.08	8.832	-	-	-
$^{6}Li(n,\alpha)$	1.97×10^{-3}	-	-	-	-	-	-	4.11	6.21	0.004	-	-	-
$^{58}Fe(n,\gamma)$	2.18×10^{-3}	-	-	-	-	-	-	3.59	15.35	0.19	-	-	-
$^{63}Cu(n,\gamma)$	4.89×10^{-3}	15.03	4.68	0.945	-	-	-	5.73	5.89	0.089	5.52	5.36	0.137
$^{235}U(n,f)$	5.25×10^{-3}	2.49	2.23	0.929	2.49	2.13	0.968	3.41	3.44	0.108	3.63	3.40	0.026
$^{239}Pu(n,f)$	6.08×10^{-3}	3.32	2.40	0.126	2.49	2.33	0.040	3.36	3.35	0.003	3.69	3.32	0.023
$^{237}Np(n,f)$	0.568	3.81	2.03	0.193	2.78	1.95	0.517	3.81	3.75	2.664	3.41	3.63	3.208
$^{115}In(n,n')$	1.30	4.23	4.74	0.996	2.53	4.59	1.574	5.88	5.69	0.149	2.50	5.82	0.035
$^{232}Th(n,f)$	1.4	6.66	8.80	1.529	-	-	-	-	-	-	-	-	-
$^{238}U(n,f)$	1.5	3.29	2.04	0.065	2.81	1.94	0.008	3.96	2.66	3.014	2.95	2.73	0.877
$^{47}Ti(n,p)$	2.3	7.37	12.33	0.634	2.12	11.52	3.106	4.79	13.07	2.291	-	-	-
$^{31}P(n,p)$	2.4	7.61	5.69	0.669	-	-	-	-	-	-	-	-	-
$^{32}S(n,p)$	2.7	5.54	6.85	0.057	-	-	-	-	-	-	-	-	-
$^{58}Ni(n,p)$	2.7	4.98	2.27	1.019	2.54	2.24	0.405	3.33	2.26	0.685	3.02	2.31	2.911
$^{64}Zn(n,p)$	2.7	5.35	11.18	6.551	-	-	-	-	-	-	-	-	-
$^{54}Fe(n,p)$	3.0	6.15	3.95	0.090	2.30	3.80	1.263	3.44	3.92	1.025	-	-	-
$^{27}Al(n,p)$	4.4	6.48	3.80	0.456	9.80	3.78	0.011	3.78	3.77	3.812	10.15	3.82	0.627
*$Ti(n,X)^{46}Sc$	4.4	6.36	7.98	1.292	2.17	7.55	0.461	3.83	7.66	0.248	-	-	-
$^{56}Fe(n,p)$	6.0	7.25	3.69	0.037	2.41	3.63	0.195	-	-	-	3.08	3.70	4.718
$^{24}Mg(n,p)$	6.6	5.54	6.56	0.054	-	-	-	-	-	-	-	-	-
$^{63}Cu(n,\alpha)$	6.6	11.18	6.42	7.377	-	-	-	-	-	-	-	-	-
$^{48}Ti(n,p)$	6.8	6.00	8.96	2.132	2.38	8.70	0.905	4.36	8.78	0.028	-	-	-
$^{59}Co(n,\alpha)$	6.8	6.99	6.01	0.004	-	-	-	-	-	-	-	-	-
$^{27}Al(n,\alpha)$	7.2	5.67	3.89	0.842	2.19	3.86	0.007	3.10	3.87	6.288	3.27	3.89	0.053
$^{127}I(n,2n)$	10.1	6.19	18.10	0.162	-	-	-	-	-	-	-	-	-
$^{63}Cu(n,2n)$	12.4	10.72	5.91	6.205	10.00	6.05	9.036	-	-	-	-	-	-
$^{90}Zr(n,2n)$	12.9	6.88	13.43	65.397	-	-	-	-	-	-	-	-	-
$^{58}Ni(n,2n)$	13.4	5.38	19.36	28.025	-	-	-	-	-	-	-	-	-

* $\sigma(E)$ of $^{46}Ti(n,\gamma)$ has been used.

Table 11. Scheme of cross section agreement and consistency.

cat-egory *	reaction	$\langle E_r \rangle$ or E_{eff} (in MeV)	precision of α_m				discrepancy $\alpha_m - \alpha_c$				consistency χ^2			
			^{235}U	Cf	CFRMF	ΣΣ	^{235}U	Cf	CFRMF	ΣΣ	^{235}U	Cf	CFRMF	ΣΣ
II	$^{115}In(n,\gamma)$	0.08×10^{-3}	0	+	+	+	++	+	0	--	++	++	++	--
I	$^{197}Au(n,\gamma)$	0.14×10^{-3}	0	+	+	+	++	+	0	--	++	++	++	--
IIa	$^{59}Co(n,\gamma)$	0.27×10^{-3}			+				--				+	
IIa	$^{238}U\ (n,\gamma)$	0.60×10^{-3}			0	0			0	--			++	--
II	$^{10}B\ (n,\alpha)$	0.64×10^{-3}			+				--				0	
II	$^{55}Mn(n,\gamma)$	0.81×10^{-3}				+				0				++
II	$^{45}Sc(n,\gamma)$	1.48×10^{-3}			+				--				--	
II	$^{6}Li(n,\alpha)$	1.97×10^{-3}			0				++				++	
II	$^{58}Fe(n,\gamma)$	2.18×10^{-3}			+				+				++	
II	$^{63}Cu(n,\gamma)$	4.89×10^{-3}	0		0	0	--		+	+	++		++	++
IIa	$^{235}U\ (n,f)$	5.25×10^{-3}	+	+	+	+	+	++	++	++	++	++	++	++
I	$^{239}Pu(n,f)$	6.08×10^{-3}	+	+	+	+	++	++	++	++	++	++	++	++
I	$^{237}Np(n,f)$	0.568	+	+	+	+	++	++	--	--	++	++	++	0
IIa	$^{115}In(n,n')$	1.3	0	+	0	+	-	--	+	++	++	+	++	++
II	$^{232}Th(n,f)$	1.4	-				--				+			
I	$^{238}U\ (n,f)$	1.5	+	+	+	+	++	++	-	+	++	++	0	++
II	$^{47}Ti(n,p)$	2.3	-	+	0		--	--	--		++	0	+	
II	$^{31}P\ (n,p)$	2.4	-				--				++			
IIa	$^{32}S\ (n,p)$	2.7	0				+				++			
IIa	$^{58}Ni(n,p)$	2.7	0	+	+	+	0	+	+	-	++	++	++	+
II	$^{64}Zn(n,p)$	2.7	0				--				--			
IIa	$^{54}Fe(n,p)$	3.0	-	+	+		++	0	+		++	++	++	
II	$^{27}Al(n,p)$	4.4	-	--	+	--	0	++	--	--	++	++	0	++
II	$^{46}Ti(n,p)$	4.4	-	+	+		--	0	0		++	++	++	
I	$^{56}Fe(n,p)$	6.0	-	+		+	++	++		--	++	++		--
II	$^{24}Mg(n,p)$	6.6	0				++				++			
II	$^{63}Cu(n,\alpha)$	6.6	--				--				--			
II	$^{48}Ti(n,p)$	6.8	-	+	0		--	--	++		+	++	++	
IIa	$^{59}Co(n,\alpha)$	6.8	-				++				++			
I	$^{27}Al(n,\alpha)$	7.2	0	+	+	+	0	++	--	++	++	++	--	++
II	$^{127}I\ (n,2n)$	10.1	-				--				++			
I	$^{63}Cu(n,2n)$	12.4	--	--			--	--			--	--		
II	$^{90}Zr(n,2n)$	12.9	-				--				--			
I	$^{58}Ni(n,2n)$	13.4	0				--				--			

*Remark: category IIa denotes a candidate category I reaction.

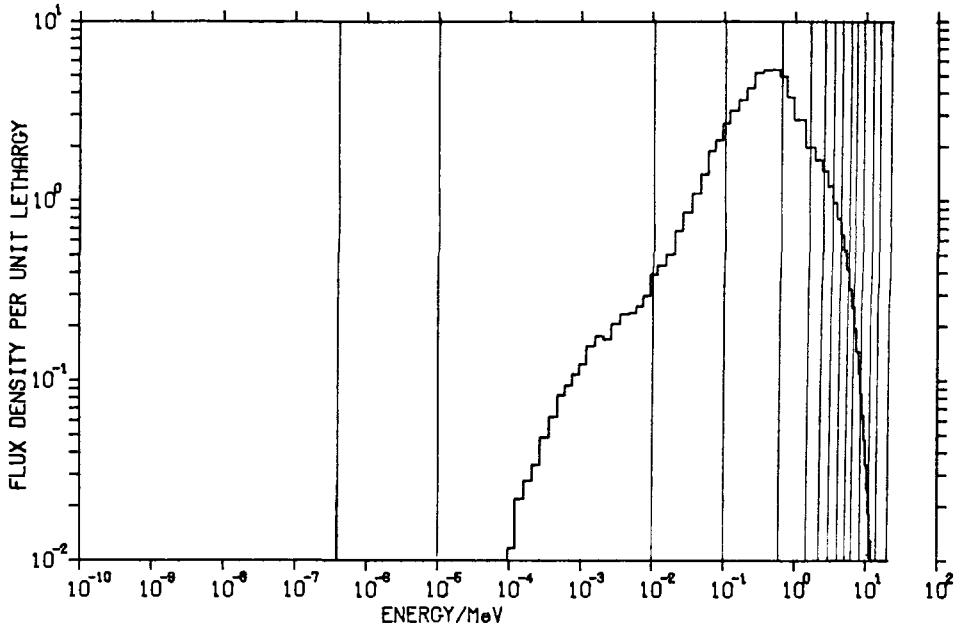

Fig. 1.

CFRMF spectrum and group boundaries of the cross section error library.

group	group boundaries (in MeV)
1	10^{-10} ... 4.10^{-7}
2	4.10^{-7} ... 10^{-5}
3	10^{-5} ... 10^{-2}
4	10^{-2} ... 10^{-1}
5	10^{-1} ... 6.10^{-1}
6	6.10^{-1} ... 1.4
7	1.4 ... 2.2
8	2.2 ... 3.0
9	3.0 ... 4.0
10	4.0 ... 5.0
11	5.0 ... 6.0
12	6.0 ... 8.0
13	8.0 ...11.0
14	11.0 ...13.0
15	13.0 ...18.0

ATTEMPTS AT THE ADJUSTMENT OF DETECTOR CROSS SECTIONS

A.K. McCracken and A. Packwood *

1 Introduction

A previous paper (1) described the simultaneous unfolding with the experimental data processing code RADAK (2) of flux spectra sampled by hydrogen-filled proportional counters and the Rh103 (n,n') Rh103m, S32 (n,p) P32 and In155 (n,n') In 115m threshold reactions. The measurements were made at various depths of penetration in a block of iron and in a simulated fast reactor breeder region in the ASPIS facility on NESTOR. Although the different measurement positions showed spectral differences all the spectra measured were rather soft. In the unfolding process the absolute counting efficiencies of both spectrometers and activation detectors were treated as samples of random variables with estimated standard deviations and were included in the maximum likelihood adjustment process which produced the flux spectra. Rather small adjustments of the threshold detector efficiencies were indicated. This exercise was extended in the case of Rh to include the multigroup reaction cross-sections. Again, consistency between the Rh count rates and cross-sections and those of the other detectors was such that small adjustments of the Rh cross-section were suggested even in the energy region of the threshold. We came to the following conclusions:-

(i) That useful refinement of both detector efficiencies and cross-sections might be achieved by demanding total maximum likelihood consistency with extensive measurements made in the same environment. In our case this was provided by measurements made with five gas filled proportional counters. A standard spectrum, well-validated by measurement and calculation, would have served equally well provided realistic uncertainties could be ascribed to the spectrum.

(ii) The absolute counting efficiencies of S and In we used seemed about right and both the efficiency and the cross-sections (UKNDL - DFN 96) used for Rh seemed very satisfactory.

In the above exploratory exercise adjustments of the Rh cross section were attempted in a one-eighth lethargy group scheme which was arbitrarily chosen and estimates of the uncertainties of the detector cross-sections were subjective. Moreover the two measurement environments which were considered did not include a fairly hard spectrum. These qualifications do not vitiate the conclusions drawn but their removal would greatly increase the usefulness of analysis of the type attempted in the previous paper.

In this paper we extend the scope of the previous work by considering several other activation detectors, by the inclusion of measurements made in a rather hard spectrum and by the use of refined uncertainty estimates for the detector cross-sections together with a resolution of adjustment appropriate to these estimates.

2 Measurements and Reaction-Rate Calculations

The measurements comprise:-

(i) Spectrum A: S32 (n,p) P32, In115 (n,n') In115m, and Rh103 (n,n') Rh103m at a penetration of 50.8 cm in iron from a fission source.

(ii) Spectrum B: The detectors of (i) in simulated fast reactor breeder.

* Radiation Physics & Shielding Group
Reactor Physics Division
Building B21
AEE Winfrith

(iii) Spectrum C: The detectors of (i) and U238 (n,f), Ni58 (n,p) Co58, Ti47 (n,p) Sc47, Fe54 (n,p) Mn54, measured in a lead/steel/water shield in NESTOR Cave B in a spectrum rather similar to that which obtains inside the pressure vessel of a pressurised water reactor.

In each of the above measurement positions extensive measurements were carried out with hydrogen-filled proportional counters and an NE213 organic liquid scintillator cell. The three spectra separately unfolded by RADAK from the spectrometry counts are shown in Figure 1.

The one-eighth lethargy group structure employed in this work is shown in Appendix I together with the detector group cross-sections employed - in each case the last cross-section is that for group 60 of the fine group scheme. Standard deviations assumed for the detector cross-sections are given in Table 1. With minor differences in energy boundaries these values, quoted by Zijp (3), are those used by Simons and McElroy in the SAND-II code. (It will be noted that these are given in a broad group structure which is adopted for the adjustment of detector cross-sections.)

Detector fine-group cross-sections were derived from the following sources:-

(i) S32 (n,p) P32: UK Nuclear Data Library DFN 97 with E^{-1} weighting to 1 MeV and fission spectrum weighting above 1 MeV.

(ii) Rh103 (n,n') Rh103m: UK Nuclear Data Library DFN 94 with E^{-1} weighting.

(iii) All other reactions were taken from the SAND II 640-group library and collapsed to our 60-group structure with E^{-1} weighting.

In seeking a maximum likelihood adjustment of the variables it is necessary to specify any correlations which are thought to exist between the variables. In the case of the detector cross sections we have interpreted McElroy's table to mean that cross-sections are fully correlated within the broad groups and that the broad group cross-sections are independent of each other. This is obviously an over simplification since the table in (3) gives the same broad group uncertainty boundaries for forty detectors.

The calculated reaction-rate of each detector channel i can be written:-

$$C_i = f_i \sum_{j,K} h_{iK} \phi_j \sigma_{ij}$$

where f_i is the absolute counting efficiency of the detector, ϕ_j, σ_{ij} are the fine group fluxes and detector cross-sections,

h_{iK} is the factor by which the cross-sections in broad group K corresponding to fine group i are adjusted.

f_i and h_{iK} are originally set to unity.

Each of the proton-recoil spectrometers has a single f only for every channel, and the h_{iK} are not adjusted - ie it is taken that the response matrix shape, but not its magnitude is well-known. RADAK unfolds the fine group fluxes and the perturbations δf_i, δh_{iK} such that:

$$\sum_i \omega_{Mi}\left[C_i - M_i + C_i\frac{\delta f_i}{f_i} + f_i\sum_{j,K}\delta h_{iK}\,x_{ij}\right]^2 + \sum_i \omega_{fi}(\delta f_i)^2 + \sum_{iK}\omega_{hiK}(\delta h_{iK})^2$$

is a minimum where:-

M_i is the measurement corresponding to C_i ; $\omega_{Mi}, \omega_{fi}, \omega_{hiK}$ are the respective inverse variances of M_i, f_i and h_{iK}

The percentage perturbations in h_{iK} which are greater than 1% and in f_i for the three spectra separately unfolded are shown in Table 2. Separate calculations with all detector calibration uncertainties reduced to 5% are also shown in the table.

3 Discussion

By analogy with sensitivity analysis one can define the group cross-section sensitivity of a reaction as the fractional change in the calculated total reaction-rate per unit fractional change in the group cross-section. Thus if

$C_i = f\sum_j \phi_j x_{ij}$ is the calculated reaction-rate then

$$\frac{\delta C_i}{C_i}\Big/\frac{\delta x_{ij}}{x_{ij}} = \frac{\phi_j x_{ij}}{\sum \phi_j x_{ij}} = U_{xij} \quad \text{say.}$$

Similarly sensitivities to the group fluxes and the absolute efficiencies can be found:-

$$U_{\phi ij} = \frac{\phi_j x_{ij}}{\sum_j \phi_j x_{ij}} \; ; \quad U_{fi} = 1$$

The cross section sensitivity profiles for S and Rh in spectrum A and spectrum C are shown in Figure 2 and Table 3 shows the sensitivities of all detectors in the broad group scheme for all three of the spectra investigated. Typical maximum sensitivities in this coarse grouping over which adjustments were attempted are about 0.3 with the largest of all being 0.53 for Fe in spectrum A. Maximum likelihood data adjustments are an increasing function of $U_{xiK}\,g_{xiK}$ where g_{xiK} is the fractional standard deviation of the broad group cross section σ_{iK}. It is immediately clear then, since $U_{fi} = 1$ that significant refinement of cross sections can only take place if

$$U_{xiK}\,g_{xiK} > g_{fi}$$

Table 4 shows the most significant of the quantities $U_{x\kappa}\ g_{x\kappa}$ for the detectors in the three environments employed. With most of the f_i being about 0.1 it is clear that spectrum C affords little hope of useful adjustment with the exception of sulphur in group 4, Ti in groups 4 and 5 and Rh in group 3. Table 2 shows that small adjustments are made for these cross-sections. The softer spectra A and B afford more scope for adjustment which is statistically significant and again Table 2 shows a close correspondence of the adjustments with the size of the elements in Table 4, Determination of the variance-covariance on the adjustments requires small alterations to the sampling routine in RADAK which have not yet been made. Nevertheless without this precise information we can see that with the cross-section uncertainty information adopted we should need to guarantee absolute calibration factors to within one or two percent before significant cross-section adjustment over a wide energy range could be achieved. The fact that some cross-sections have not been adjusted in Table 2 does not mean that they are right, rather that we do not have the information necessary for this process. The importance of the cross-section uncertainty information is also clear from the above discussion - broadening the range of correlations so that adjustment is made in coarser groups will increase the cross-section sensitivity and enable the cross-sections to be refined at the expense of the absolute efficiencies. The most noticeable adjustments achieved are for the absolute counting efficiencies f_i. Quite large reductions, $\sim$ 10%, are indicated for Fe and Ni. Of Rh, In and S which are common to all three spectra the Rh results are the most consistent - a reduction of some 3% to 4% seems justified, S seems about right and there is a small inconsistency with In.

Where the cross-section adjustments appear to be inconsistent they are not necessarily so; for example group 2 adjustments of In in spectra A and B of respectively -8.4% and -1.4% must be seen in the context of a quoted 30% standard deviation on this group cross-section. Again one is hampered by lack of a full error analysis on the adjustments but in general the larger adjustments (corresponding to the larger experimental sensitivities) are the more reliable; thus a reduction of some 7% in groups 2 and 3 for In is entirely justifiable from the facts presented.

The use of E^{-1} weighted cross-sections is not strictly justified and an obvious refinement would be the use of flux-weighted cross sections. The use of the former is not a serious limitation of this work. Table 5 shows the uncertainties in spectrum A predicted with the numbers of Table 1 together with the ratio of the reaction-rates predicted with E^{-1} and flux-weighted cross-sections. The effect of weighting - at least for our one-eighth lethargy structure - is seen to be relatively unimportant in this case, except for Ni.

TABLE 5

PREDICTED UNCERTAINTIES SPECTRUM A

Reaction	Predicted Uncertainty %	Ratio $\frac{E^{-1} \text{ weight}}{\text{Flux weight}}$
Fe54 (n,p)	13.7	1.02
S32 (n,p)	29.4	1.03
Ni58 (n,p)	6.0	1.06
Ti47 (n,p)	23.7	1.10
U28 (n,f)	12.3	1.04
In115 (n,n')	15.5	1.05
Rh103 (n,n')	22.5	1.02

If serious disquiet is justified over the uncertainties in detector cross-sections the following procedure seems necessary if improvement is to be sought by means of integral experiments.

(i) Make every effort to reduce by conventional means the uncertainties on the absolute counting efficiencies of the detectors.

(ii) Use a standard validated neutron field like spectrum C which shows little structure in the sensitivity profiles to adjust the efficiency factors and, using a full error analysis, determine the reduced standard deviations on the detectors.

(iii) Use the detectors now in different validated fields, for example spectra A and B, where some sensitivity structure is apparent. Determine the adjustments with the reduced fractional standard deviations.

(iv) In all the above use the best possible estimates of the detector cross-section uncertainties bearing in mind that the correlation laws used will influence the answer.

By validated field we mean

(a) Quality measurements made with spectrometers for use with a code like RADAK, or

(b) A standard spectrum determined accurately by both calculation and measurement, in this case a reliable estimate of the variance - covariance relations of the group fluxes is required together with the appropriate unfolding software - (RADAK without modification is not equipped to deal with this problem).

Acknowledgement

We are obliged to Mr M D Carter for the proton-recoil spectrometry measurements.

References

(1) A K McCracken; A Packwood. Some remarks on the choice of detectors, the adjustment of cross sections and the unfolding of flux spectra. Proceedings of Consultants Meeting on Integral Cross-sections Measurements for Reactor Dosimetry. IAEA-208 (1976).

(2) A K McCracken; M J Grimstone. The Experimental Data Processing Program RADAK. Proceedings of the First ASTM - EURATOM Symposium on Reactor Dosimetry. Petten (1975).

(3) W L Zijp. Review of Activation Methods for the Determination of Neutron Flux Density Spectra, Reactor Centrum Nederland, R M G Note 75/19 (1975)

TABLE 1 FRACTIONAL UNCERTAINTIES IN DETECTOR CROSS-SECTIONS

Energy KeV	5.53 98.03	98.03 639.3	639.3 1353	1353 2231	2231 3247	3247 4169	4169 5353	5353 6065	6065 7788	7788 10000	Fractional Uncertainty in f
Fine Group Nos	1 - 23	24 - 38	39 - 44	45 - 48	49 - 51	52 - 53	54 - 56	56	57 - 58	59 - 60	
Broad Group No	1	2	3	4	5	6	7	8	9	10	
Reaction											
$Fe^{54}(n,p)$		.30	.30	.30	.10	.10	.08	.08	.07	.07	.10
$S^{32}(n,p)$				1.00	.20	.08	.08	.08	.08	.08	.15
$Ni^{58}(n,p)$			.20	.10	.05	.05	.05	.06	.06	.06	.10
$Ti^{47}(n,p)$		.50	.50	.50	.50	.15	.15	.15	.15	.15	.10
$U^{238}(n,f)$		.30	.30	.04	.03	.03	.03	.04	.06	.06	.10
$In^{115}(n,\acute{n})$		.30	.20	.10	.10	.10	.08	.08	.08	.08	.05
$Rh^{103}(n,\acute{n})^{+}$	1.00	.30	.20	.10	.10	.10	.08	.08	.08	.08	.10

+ No figures available so these values equated with those of In except for Group 1

TABLE 2 PERCENTAGE PERTURBATIONS IN CROSS-SECTIONS AND CALIBRATION EFFICIENCIES

Reaction and Spectrum	Broad Group Number Cross-Section Changes 1	2	3	4	5	6	7	8	9	10	f Change
Spectrum A $S^{32}(n,p)$				+9.4 (+13.1)							+2.3 (0)
$In^{115}(n,\acute{n})$		-8.4 (-8.4)	-6.1 (-6.2)								-4.3 (-4.3)
$Rh^{103}(n,\acute{n})$											-4.1 (-1.3)
Spectrum B $S^{32}(n,p)$				-1.0 (-2.8)							-0.8 (-0.2)
$In^{115}(n,\acute{n})$		-1.4 (-1.4)	-3.0 (-3.0)	-2.0 (-2.0)	-2.0 (-1.9)						-5.9 (-6.0)
$Rh^{103}(n,\acute{n})$											-2.6 (-1.1)
Spectrum C $Fe^{54}(n,p)$				-1.6 (-2.8)							-10.0 (-4.2)
$S^{32}(n,p)$				-2.8 (-6.2)							-3.0 (-0.6)
$Ni^{58}(n,p)$											-12.0 (-5.2)
$Ti^{47}(n,p)$				-1.2 (-1.5)	-3.8 (-4.7)						-1.4 (0.4)
$U^{238}(n,f)$											-0.5 (-0.2)
$In^{115}(n,\acute{n})$											± 1.2 (± 1.2)
$Rh^{103}(n,\acute{n})$			-1.1 (-1.8)								-4.3 (-1.8)

TABLE 3 REACTION-RATE SENSITIVITIES TO CROSS-SECTIONS IN THREE SPECTRA

Reaction and Spectrum	Sensitivities in Broad Groups									
	1	2	3	4	5	6	7	8	9	10
Spectrum A										
$S^{32}(n,p)$				2.8,-1	4.2,-1	1.7,-1	6.6,-2			
$In^{115}(n,\acute{n})$		3.8,-1	5.3,-1	8.2,-2	1.1,-2					
$Rh^{103}(n,\acute{n})$	2.2,-2	7.3,-1	2.4,-1	1.0,-2						
Spectrum B										
$S^{32}(n,p)$				8.4,-2	3.5,-1	2.3,-1	1.9,-1	5.8,-2		
$In^{115}(n,\acute{n})$		4.7,-2	2.0,-1	3.5,-1	2.5,-1	7.4,-2				
$Rh^{103}(n,\acute{n})$	1.2,-2	3.3,-1	1.8,-1	1.0,-1	3.1,-2					
Spectrum C										
$Fe^{54}(n,p)$			3.9,-3	7.9,-2	1.3,-1	1.4,-1	2.7,-1	1.3,-1		
$S^{32}(n,p)$				7.4,-2	2.5,-1	1.7,-1	2.3,-1	9.6,-2		
$Ni^{58}(n,p)$				1.0,-1	2.1,-1	1.3,-1	2.4,-1	1.2,-1		
$Ti^{47}(n,p)$			7.5,-3	1.4,-1	3.4,-1	1.4,-1	1.7,-1	7.5,-2		
$U^{28}(n,f)$			4.7,-2	4.7,-1	2.3,-1	7.0,-2				
$In^{115}(n,\acute{n})$		2.0,-2	2.0,-1	3.7,-1	2.1,-1	6.6,-2				
$Rh^{103}(n,\acute{n})$	2.0,-3	1.3,-1	3.8,-1	2.5,-1	1.1,-1	3.5,-2				

TABLE 4 THE FACTORS UxG IN THREE SPECTRA

Reaction and Spectrum	Broad Group Number 1	2	3	4	5	6	7	8	9	10
Spectrum A										
$S^{32}(n,p)$				.28	.08	.02				
$In^{115}(n,n)$		.11	.11	.1						
$Rh^{103}(n,n)$	.02	.22	.05							
Spectrum B										
$S^{32}(n,p)$				.08	.07	.02				
$In^{115}(n,n)$		.01	.04	.04	.03					
$Rh^{103}(n,n)$	.01	.09	.07	.02						
Spectrum C										
$Fe^{54}(n,p)$				.024	.013	.014	.02	.01		
$S^{32}(n,p)$				.074	.05	.01	.02	.01		
$Ni^{58}(n,p)$				.01	.01	.01				
$Ti^{47}(n,p)$				.07	.07	.02				
$U^{28}(n,f)$			.01	.02						
$In^{115}(n,n)$			.04	.04	.02					
$Rh^{103}(n,n)$		.04	.08	.025	.01					

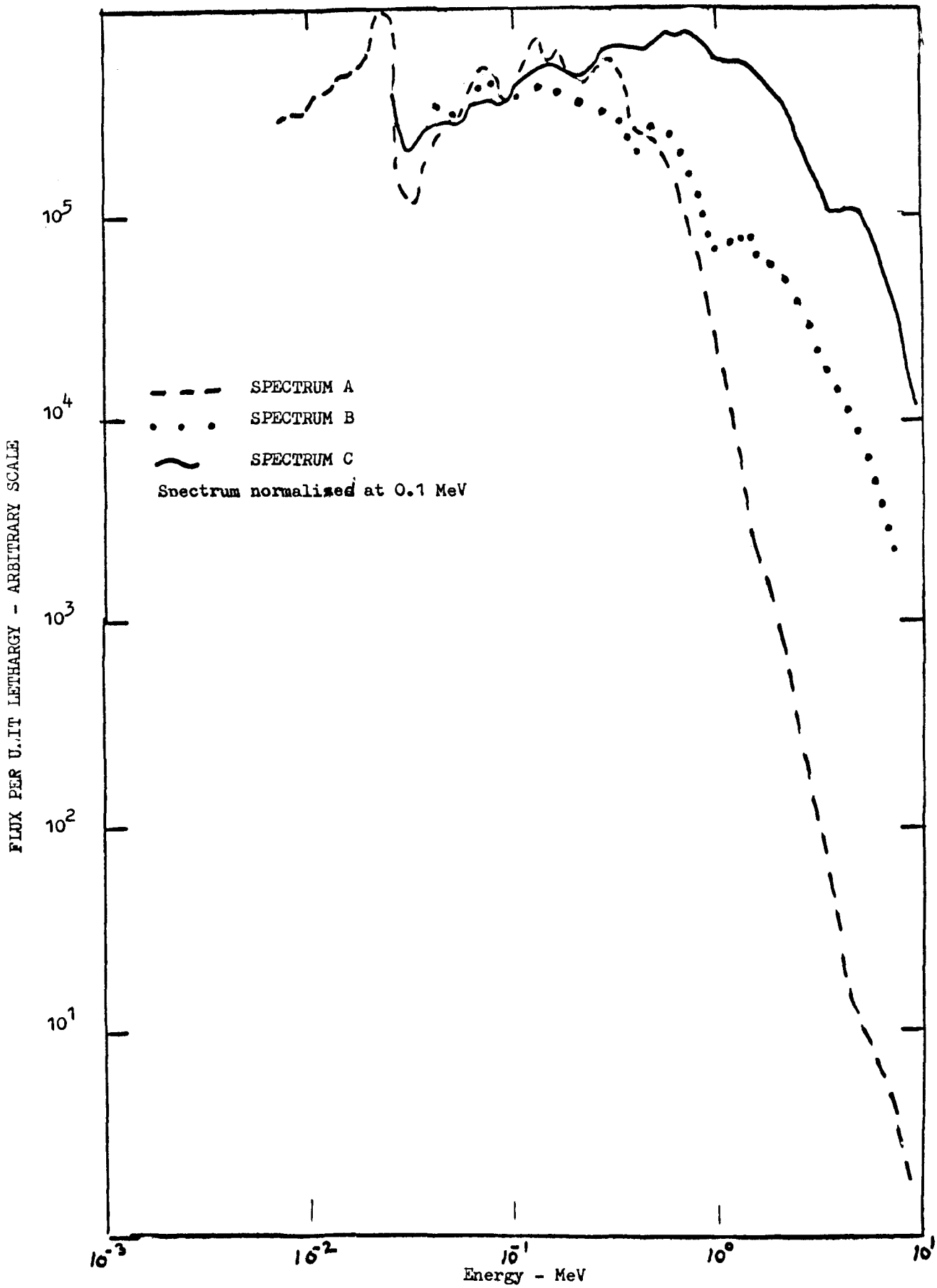

FIG 1. THE IRRADIATION SPECTRA

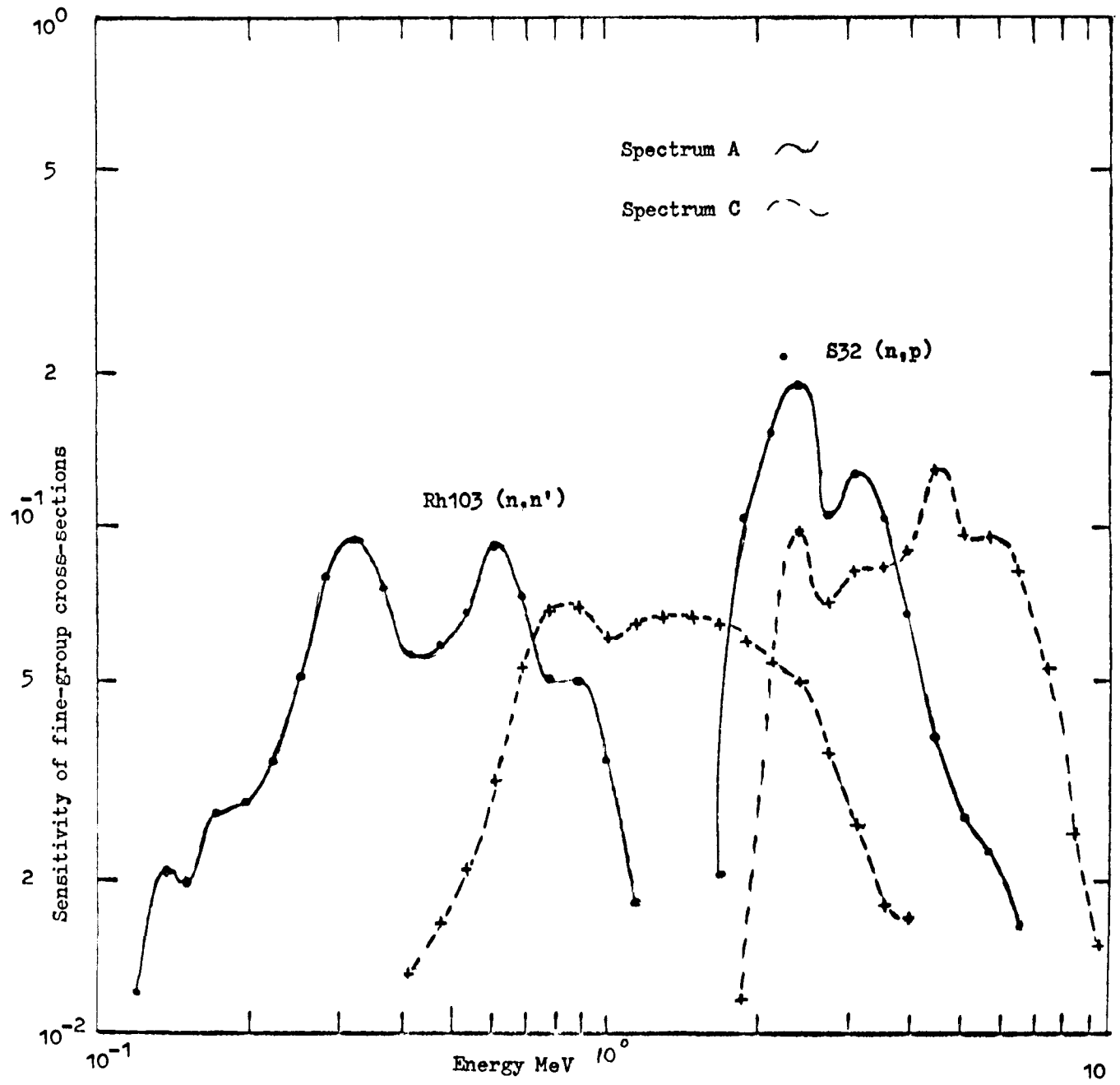

FIGURE 2 Sensitivities of Sulphur and Rhodium Reaction-Rates to Cross-sections

APPENDIX

Fine Group Cross-sections and Energy Boundaries

```
 AL27(NA)NA24  SAND2  1/E WEIGHTING.
53*0.0       8.34955E-07 7.15442E-05
8.37433E-04 6.36696E-03 2.31160E-02 4.60710E-02 7.51178E-02
 MG24(N,P)NA24  SAND2  1/E WEIGHTING.
54*0.0       1.50225E-05
5.95330E-04 2.14392E-02 5.79608E-02 1.19397E-01 1.31309E-01
 FE54(N,P)MN54  SAND2  1/E WEIGHTING.
36*0.0       3.68364E-06 9.73558E-06 1.75676E-05 2.52776E-05
3.47111E-05 6.15481E-05 3.18657E-04 1.59397E-03 5.52566E-03
1.14868E-02 1.67659E-02 2.33813E-02 3.72474E-02 5.89426E-02
9.72502E-02 1.75354E-01 2.76603E-01 3.64514E-01 4.33610E-01
4.89184E-01 5.51711E-01 5.87317E-01 5.94773E-01 5.88755E-01
 S32(NP)P32 UKNDL DFN97 1/E WEIGHTING
45*0.0
0.1146E-2 0.1011E-1 0.3823E-1 0.7951E-1 0.8546E-1 0.1380E 0
0.2083E 0 0.2338E 0 0.3001E 0 0.2478E 0 0.2872E 0 0.3303E 0
0.3367E 0 0.3437E 0 0.3671E 0
 NI58(N,P)CO58  SAND2  1/E WEIGHTING.
41*0.0       8.12145E-05 1.90678E-03 4.64987E-03 7.62676E-03
1.44024E-02 2.73950E-02 5.12851E-02 8.86644E-02 1.32094E-01
2.11592E-01 2.23912E-01 3.34532E-01 4.30895E-01 5.03059E-01
5.61330E-01 5.98847E-01 6.14826E-01 6.14806E-01 6.00611E-01
 TI47(N,P)SC47  SAND2  1/E WEIGHTING.
28*0.0       1.39055E-09 6.86056E-08
1.72417E-07 2.85893E-07 4.14117E-07 5.63047E-07 9.67299E-07
2.71804E-06 7.75027E-06 1.98283E-05 3.15638E-05 4.71626E-05
6.82254E-05 1.10740E-04 1.96775E-04 3.89142E-04 8.46124E-04
2.11362E-03 5.68541E-03 1.64970E-02 2.96163E-02 3.74041E-02
4.22530E-02 4.60424E-02 4.99605E-02 5.34134E-02 5.68630E-02
6.09658E-02 6.44507E-02 6.71797E-02 6.93396E-02 7.06155E-02
 U238(N,F)  SAND2  1/E  WEIGHTING.
34*0.0       1.06815E-05
1.98468E-04 4.42362E-04 1.18413E-03 1.54119E-03 2.96860E-03
9.26261E-03 1.71120E-02 2.97809E-02 5.61214E-02 2.24633E-01
3.91678E-01 4.81147E-01 5.16329E-01 5.11282E-01 5.00440E-01
5.01965E-01 5.18530E-01 5.30052E-01 5.35969E-01 5.40026E-01
5.60990E-01 7.46274E-01 9.43531E-01 9.69548E-01 9.69919E-01
 IN115(N,N)IN115M  SAND2  1/E WEIGHTING.
31*0.0       5.97292E-06 4.29972E-04 1.36790E-03 2.57826E-03
4.11483E-03 7.01538E-03 1.16281E-02 1.73089E-02 2.83428E-02
3.98415E-02 5.93810E-02 7.48733E-02 1.09612E-01 1.52840E-01
2.04098E-01 2.45860E-01 2.92507E-01 3.28414E-01 3.43700E-01
3.48680E-01 3.50687E-01 3.50989E-01 3.49583E-01 3.47678E-01
3.42948E-01 3.31851E-01 3.14582E-01 2.88408E-01 2.50323E-01
 RH103(N,N)RH103M UKNDL DFN 94 1/E WEIGHTING
15*0.0
2.85333E-05 7.51485E-04 2.41833E-03 3.27606E-03 4.12701E-03
5.50200E-03 6.89259E-03 8.25420E-03 1.06903E-02 1.29364E-02
1.58232E-02 1.96289E-02 2.50633E-02 3.25183E-02 4.33458E-02
5.76117E-02 7.56026E-02 9.48941E-02 1.10999E-01 1.24051E-01
1.39274E-01 1.65854E-01 2.25507E-01 3.48544E-01 5.04130E-01
6.03937E-01 6.29727E-01 6.57497E-01 6.91670E-01 7.30286E-01
7.80941E-01 8.42511E-01 8.98603E-01 9.61783E-01 1.00822E+00
1.02404E+00 1.04308E+00 1.07018E+00 1.11780E+00 1.18913E+00
1.29531E+00 1.39622E+00 1.39548E+00 1.36894E+00 1.30658E+00
```

APPENDIX contd.

```
 NP237(N,F)     SAND2  1/E  WEIGHTING.
 1.19568E-02 1.22712E-02 1.26255E-02 1.30460E-02 1.34405E-02
 1.40158E-02 1.43396E-02 1.47308E-02 1.51122E-02 1.56175E-02
 1.61471E-02 1.67518E-02 1.74639E-02 1.82594E-02 1.92074E-02
 2.01178E-02 2.12787E-02 2.25122E-02 2.03375E-02 1.62701E-02
 1.20797E-02 1.22399E-02 1.38418E-02 1.55238E-02 1.72008E-02
 1.90933E-02 2.12354E-02 2.36757E-02 2.64194E-02 2.95260E-02
 3.39144E-02 4.51211E-02 7.01989E-02 1.22097E-01 2.13170E-01
 3.42627E-01 5.08865E-01 7.00387E-01 9.04814E-01 1.07546E+00
 1.25020E+00 1.42439E+00 1.53589E+00 1.57348E+00 1.61324E+00
 1.63387E+00 1.65753E+00 1.65338E+00 1.63215E+00 1.60064E+00
 1.56857E+00 1.54690E+00 1.50272E+00 1.46161E+00 1.43046E+00
 1.46776E+00 1.70287E+00 2.01526E+00 2.13080E+00 2.40317E+00
   NEUTRON GROUP BOUNDARIES KeV
5.530 6.267 7.101 8.047 9.118 10.33 11.70 13.26 15.03 17.036
19.30 21.87 24.78 28.09 31.83 36.06 40.86 46.30 52.47 59.462
67.37 76.35 86.52 98.03 111.0 125.8 142.6 161.6 183.1 207.55
235.1 266.4 301.9 342.1 387.7 439.3 497.8 564.1 639.2 724.40
820.8 930.1 1054. 1194. 1353. 1533. 1737. 1969. 2231. 2528.
2865. 3246. 3678. 4168. 4723. 5352. 6065. 6872. 7788. 8825.0
10000.0
```

REVIEW OF ADVANCED METHODS FOR DATA ADJUSTMENTS

by A. Gandini

1. INTRODUCTION

The methods of nuclear data adjustment to be adopted in order to make them consistent with the integral information available, in recent years have developed to formulations quite similar in various laboratories, thanks to the common fundamentals of statistics theory on which they are based. There remain still unsolved, however, a number of problems which are closely connected to our poor ability of adequately representing the real physical situation (e.g., by inaccurate sensitivities, non linearities, etc.) or to negligence (systematic) errors in the cross-section data files. In the following, methods or procedures proposed for coping with these situations are reviewed.

2. SECOND ORDER ADJUSTMENTS

It is felt that second order adjustments may be of relevance, in particular, when analysing perturbatively, in the nuclide field, the accumulation of isotopes produced in the fuel during the reactor operation and when analyzing, in the neutron field, propagation experiments, i.e. made in material blocks (Fe, Na, etc.) in which neutron spectra originated from given sources are detected, particularly when the optical distances (i.e. given in terms of diffusion lenghts) between these sources and the detector positions are large. Generally, we may say that second order methods may be required either when the original data are rather uncertain so that their possible corrections may result too large for a linear approach, or when the second order sensitivities are comparatively too large. Their derivation is based on an iterative use of first order methods of the type given in Ref. /1/. To show this let us consider a number J of different integral quanties Q_j. If we knew the true values of the group cross-sections σ_i (in number of I) and assuming an exact theoretical model has been chosen (as far as energy group structure, geometry, transport approximations adopted) for representing the neutron diffusion processes, we could express the quantities Q_j as functions of σ_i, i.e.

$$Q_j = Q_j (\sigma_1, \sigma_2, \ldots, \sigma_I). \qquad (j = 1, 2, \ldots, J) \qquad (1)$$

If we assume a given set of values $\sigma_{0,i}$ (*), by hypothesis close enough to the true values σ_i, we may expand Eq. (1) disreguarding third and higher order terms and obtain

$$Q_j = Q_j(\sigma_{0,1}, \cdots, \sigma_{0,I}) + \sum_{i=1}^{I} \frac{\partial Q_j}{\partial \sigma_i} (\sigma_i - \sigma_{0,i}) + \\ + \frac{1}{2!} \sum_{i,k=1}^{I} \frac{\partial^2 Q_j}{\partial \sigma_i \partial \sigma_k} (\sigma_i - \sigma_{0,i})(\sigma_k - \sigma_{0,k}) . \\ (j = 1, \ldots, J) \qquad (2)$$

Considering now the fractional changes y_{Q_j} and y_{σ_i} of the integral and differential parameters, respectively (with respect to initial values), eq. (2) may also be written:

$$y_{Q_j} = \sum_{i=1}^{I} s_{j,i}\, y_{\sigma_i} + \sum_{i,k=1}^{I} s_{j,i,k}\, y_{\sigma_i} y_{\sigma_k} \qquad (j = 1, \ldots, J) \qquad (3)$$

where $s_{j,i}$ and $s_{j,i,k}$ represent first and second order sensitivities, directly related to the first and second order derivatives. In an adjustment scheme these equations represent second order constraints to be satisfied in the fit procedure. Assuming estimates $\tilde{y}_{\sigma_i}^{(m-1)}$ are available, the following recurrent scheme may be considered for linearizing these constraints:

$$y_{Q_j}^{(m)} = \sum_{i=1}^{I} \left(s_{j,i} + \sum_{k=1}^{I} s_{j,i,k}\, \tilde{y}_{\sigma_k}^{(m-1)} \right) y_{\sigma_i}^{(m)} \\ = \sum_{i=1}^{I} s_{j,i}^{(m-1)}\, y_{\sigma_i}^{(m)} . \qquad (j = 1, \ldots, J) \qquad (4)$$

Starting with a linear approach for $\tilde{y}_{\sigma_i}^{(o)}$, and adopting iteratively the same standard linear techniques already available, the value $\tilde{y}_{\sigma_i}^{(m)}$ should converge rapidly to the best estimators $\tilde{y}_{\sigma_i}$.

We shall discuss in the following on the various methods to be adopted for calculating the sensitivities (or derivatives).

(*) Generally different from the experimental set considered later on.

3. SENSITIVITIES

As well known, first order sensitivities, or derivatives, of given integral quantities with respect to system parameters, may be obtained by means of the so called and well established generalized perturbation techniques. An extensive letterature on them may be found in Ref. /2/. For what concerns second order methods, we shall distinguish between those in the nuclide field dealing with burn-up and build-up of isotopes in fuel material and those in the neutron field referring to non-multiplying and multiplying systems.

3.1 Isotopic accumulation

The integral quantities of interests Q_j are represented in this case by the amount of isotopes (as fission products or transuranium elements) produced, or decayed, in fuel material subject to a given power, or flux, history, i.e.

$$Q_j = \int_{Vol} n_j(\underline{r}, t_F)\, d\underline{r} \tag{5}$$

where densities n_j, or, better, their vector representation $\underline{n}$, satisfy the equation

$$\frac{\partial \underline{n}}{\partial t} = \mathcal{A}\,\underline{n} \tag{6}$$

where $\mathcal{A}$ represents the burn-up, build-up and decay matrix operator, generally function of flux, microscopic cross-sections, decay constants, fission yields, etc., which we will represent by parameters p_i. Considering a perturbation $\delta\mathcal{A}$ in the time interval (t_o, t_F), the following second order expression for δQ_j may be derived /3/:

$$\delta Q_j = \sum_i \int_{t_o}^{t_F} dt \left\langle \underline{n}^* \frac{\partial \mathcal{A}}{\partial p_i}\,\underline{n} \right\rangle + \frac{1}{2!} \sum_{i,k} \int_{t_o}^{t_F} dt \left(\left\langle \underline{n}^*_{/k} \frac{\partial \mathcal{A}}{\partial p_i}\,\underline{n} \right\rangle + \right.$$

$$\left. + \left\langle \underline{n}^* \frac{\partial \mathcal{A}}{\partial p_i}\,\underline{n}_{/k} \right\rangle \right) \delta p_i\, \delta p_k \tag{7}$$

with $\underline{n}^*$, $\underline{n}^*_{/k}$, $\underline{n}_{/j}$ satisfying equations [and conditions]:

$$-\frac{\partial \underline{n}^*}{\partial t} = \mathcal{A}^T \underline{n}^* \qquad \left[n_j^*(t_F) = \begin{cases} 1 \text{ for } j=i \\ 0 \text{ for } j \neq i \end{cases} \right] \tag{8}$$

$$-\frac{\partial \underline{n}^*_{/k}}{\partial t} = \mathcal{A}^T \underline{n}^*_{/k} + \frac{\partial \mathcal{A}^T}{\partial r_k} \underline{n}^* \qquad [\underline{n}^*(t_F) = 0] \tag{9}$$

$$\frac{\partial \underline{n}_{/k}}{\partial t} = \mathcal{A} \underline{n}_{/k} + \frac{\partial \mathcal{A}}{\partial r_k} \underline{n} \cdot \qquad [\underline{n}(t_0) = 0] \tag{10}$$

The terms in round parenthesis at the right hand side of Eq. (7) multiplied by 1/2! clearly represent the second order sensitivities to be adopted. A similar formulation, with, in particular, a similar objective, was also proposed recently by Bobkov et al. /4/.

3.2 Non-multiplying systems

In these cases quantities Q_j may represent, typically, flux detections in propagation experiments. In general, we may write:

$$Q_j = \int_{t_1}^{t_F} \langle \underline{h}^+(\underline{r},t)\, \underline{\phi}(\underline{r},t) \rangle \, dt \tag{11}$$

where $\underline{h}^+$ represents a given vector function (e.g. a cross-section multiplied by a decay term), while $\underline{\phi}$ is the flux function satisfying the equation:

$$\mathcal{M} \underline{\phi} + \underline{h} = 0 \tag{12}$$

For these equations, the following second order perturbation expression can be derived /5/, not considering, for semplicity, direct effects /i.e. affecting the detector cross-sections or the sources/:

$$\delta Q_j = \sum_i \langle \underline{\Psi}^* \frac{\partial \mathcal{M}}{\partial \sigma_i} \underline{\phi} \rangle \delta\sigma_i + \frac{1}{2!} \sum_{i,k} \left(\langle \underline{\Psi}^*_{/i} \frac{\partial \mathcal{M}}{\partial r_k} \underline{\phi} \rangle + \right.$$

$$\left. + \langle \underline{\Psi}^* \frac{\partial \mathcal{M}}{\partial r_k} \underline{\phi}_{/i} \rangle \right) \delta\sigma_i \, \delta\sigma_k \tag{13}$$

where $\underline{\Psi}^*$, $\underline{\Psi}^*_{/i}$, $\underline{\phi}_{/i}$ satisfy the following equations:

$$\mathcal{M}^* \underline{\Psi}^* + \underline{\omega}^+ = 0 \qquad \left[\underline{\omega}^+(\underline{r}) = \int_{-\infty}^{t_F} \underline{h}(\underline{r},t)\, dt \right] \tag{14}$$

$$\mathcal{M}^{*}\underline{\Psi}^{*}_{/i} + \frac{\partial \mathcal{M}^{*}}{\partial \sigma_i}\underline{\Psi}^{*} = 0 \qquad (15)$$

$$\mathcal{M}\,\underline{\Phi}_{/i} + \frac{\partial \mathcal{M}}{\partial \sigma_i}\underline{\Phi} = 0 \quad . \qquad (16)$$

Here again the terms in round parenthesis at the right hand side of Eq. (13) multiplied by 1/2! represent the second order sensitivities to be adopted. It may be easily shown how these formulations, since referring to steady conditions, can be easily obtained from those, time-dependent, considered in the previous section replacing the Boltzman operator $\mathcal{M}$ in place of the burn-up and decay matrix $\mathcal{A}$ and integrating over the time variable. A similar formulation has been also proposed by Greenspan et al. /6/.

3.3 Multiplying systems

In these cases generally ratios R of functionals linear with (asymptotic) neutron flux are of interest, i.e. of the type

$$R = \frac{Q_A}{Q_B} = \frac{\langle \underline{h}^{+}_{A}\underline{\Phi}\rangle}{\langle \underline{h}^{+}_{B}\underline{\Phi}\rangle} \quad . \qquad (12)$$

Such quantities may represent reaction rate ratios, reactivity worths, prompt neutron lifetimes, etc. If a second order formulation of δR explicitly dependent on a perturbation $\delta\mathcal{M}$ (not affecting the criticality) of the Boltzmann operator is required, the following second order expression should be considered:

$$\delta R = R\left(\frac{\delta\langle \underline{h}^{+}_{A}\underline{\Phi}\rangle}{\langle \underline{h}^{+}_{A}\underline{\Phi}\rangle} - \frac{\delta\langle \underline{h}^{+}_{B}\underline{\Phi}\rangle}{\langle \underline{h}^{+}_{B}\underline{\Phi}\rangle}\right)\left(1 - \frac{\delta\langle \underline{h}^{+}_{B}\underline{\Phi}\rangle}{\langle \underline{h}^{+}_{B}\underline{\Phi}\rangle}\right), \qquad (13)$$

where the term $\delta\underline{\Phi}$, implied in $\delta\langle \underline{h}\,\underline{\Phi}\rangle$, is given by the perturbation expression /6/:

$$\delta\underline{\Phi} = -\sum_{n=2}^{\infty}\frac{\langle \underline{\Phi}^{*}_{n}\,\delta\mathcal{M}\,\underline{\Phi}\rangle}{\lambda_1-\lambda_n}\underline{\Phi}_n + \sum_{n,j=2}^{\infty}\frac{\langle \underline{\Phi}^{*}_{j}\,\delta\mathcal{M}\,\underline{\Phi}\rangle\langle \underline{\Phi}^{*}_{n}\,\delta\mathcal{M}\,\underline{\Phi}_j\rangle}{(\lambda_1-\lambda_n)(\lambda_1-\lambda_j)}\underline{\Phi}_n \quad , \qquad (14)$$

λ_n representing the n-th eigenvalue and $\underline{\phi}_n$, $\underline{\phi}_n^*$ the n-th real and adjoint eigenfunctions satisfying the equations

$$(A+\lambda_n F)\underline{\phi}_n = 0 \tag{15}$$

$$(A^*+\lambda_n F^*)\underline{\phi}_n^* = 0 \tag{16}$$

and the orthonormal condition

$$\langle \underline{\phi}_n^* F \underline{\phi}_m \rangle = \begin{cases} 1 & \text{for } n=m \\ 0 & \text{for } n\neq m \end{cases} . \tag{17}$$

The calculation of these eigenfunctions follows the method suggested by Saito and Katsuragi /7/ extended in /5/ to whatever order. With this method, a source

$$\underline{S}_n = (A+\lambda_1 F)F^{-1}(A+\lambda_2 F)\dots F^{-1}(A+\lambda_{n-1}F)\underline{\phi}^{guess} \tag{18}$$

is defined where $\underline{\phi}^{guess}$ represents an arbitrary (for instance, flat) function and F the fission source operator. Then an iteration scheme is followed of the type:

$$\begin{cases} A\underline{f}_n^{(1)} = \underline{S}_n \\ A\underline{f}_n^{(2)} = -\bar{\lambda}_n^{(1)} F \underline{f}_n^{(1)} \\ \dots\dots\dots \\ A\underline{f}_n^{(i)} = -\bar{\lambda}_n^{(i-1)} F \underline{f}_n^{(i-1)} \qquad (i=2,3,\dots) \end{cases} \tag{18}$$

where

$$\bar{\lambda}_n^{(i-1)} = \frac{-1}{\langle \underline{u} F \underline{f}_n^{(i-1)} \rangle} , \tag{19}$$

$\underline{u}$ being a unit vector. System (18) is shown to converge to the n-th harmonic. It is interesting to note that this iteration scheme, apart from the renormalization of the fission source by means of coefficient $\bar{\lambda}_n^{(i-1)}$ (which converges for $n\to\infty$ to the n-th eigenvalue λ_n), is identical to that followed when calculating the importance functions for the generalized perturbation techniques and

therefore programs already developed for these can be adopted with minor modifications to this new purpose.

Once a second order expression for $\delta\underline{\phi}$ is available, its insertion in the second order expression (13) allows to determine easily the first and second order sensitivities.

For all the problem so far considered, it should be noted that a number of second order terms may be neglected if specified limits of accuracy are assumed, so that only the most relevant parameters are kept, i.e. those affected by larger inaccuracies and for which larger first order sensitivities are found.

Present work under-way at CNEN on the above methods is aimed at developing on one side codes for the evaluation of the auxiliary functions $\underline{\psi}^*_i$ and $\underline{\phi}'_i$ of Eqs. (15) and (16) and on the other one at calculating the eigenfunctions $\underline{\phi}_n$, $\underline{\phi}^*_n$. The reference code has been ANISN and the results so far obtained are promising.

4. NEGLIGENCE (OR SYSTEMATIC) ERRORS

Quite frequently, when adjusting nuclear data with integral measurements, it occurs that the χ^2 test results higher than the expected value. The reason for this may be attributed to various causes, namely:

1. Inadequacy of the theoretical model assumed.
2. Linearization of the constraints equations used in the adjustment procedure.
3. Negligence errors in the integral data and/or understimation of their variances.
4. Negligence errors in the differented data and/or underestimation of their variances.

For what concerns point 1, it is felt that in the majority of cases we should be able to reduce these inaccuracies below an acceptable level by a proper sophystication of the calculational model. For what concerns point 2, this may be of relevance in certain cases and has been considered in the previous sections. The remaining points will be discussed in some detail in the following.

4.1 Understimation of the variance terms

In case in which the χ^2 test performed after the adjustment maintains values significantly higher than expected, the frequently resorted to procedure has been so far that of increasing the original standard deviations of the group constants (and that of the integral quantities so that the adjusted values do not result changed) by a factor such that the χ^2 test results automatically satisfied. This procedure implies the assumption that such high χ^2 value is due to some underestimation of the standard deviations of some group constants, although in practice all the deviations are indistinctly penalized by a common term.

If this source of error is strongly suspected, a significant improvement could be reached by separating those pieces of information in the B_σ matrix wich are well based and assessed from those more probably affected by larger inaccuraces. Only these latter should then be increased

by a common term so that the expected χ^2 value is obtained.

4.2 Negligence errors in the differential parameters

These systematic errors may be originated in the process of determining the microscopic data, and therefore during the differential measurements, or when adopting a theoretical nuclear model, for instance for interpolating a few experimental points. In these cases, again a separation should be effected of well assessed information on the differential data from that more likely affected by errors of this kind. Then, alternative choices (of models or of numerical values of given parameters) should be done so that a more reliable consistency with integral data can be reached. In certain circumstances, i.e. when the structure of the systematic errors may be explicit represented, this should be accomodated in the likelihood function so that only quantities affected by normal (or, at least, not systematic) errors appear in its exponential term. An interesting example of such methodology is that proposed by Mitani and Kuroi /8/ (commented also in Ref. /9/), who considered a particular structure of systematic error, i.e. inherent with the absolute cross-section measurements (at thermal energies). A similar methodology might be adopted so that other more or less sophysticated structures of systematic errors may be accomodated. Such method uses the same derivations of section 2, with a proper reformulation of the dispersion matrix B_σ, and implies that sistematicities inherent with the integral measurements have been in some way sorted out, for instance by a proper use of the χ^2 test.

In case no structure of systematic errors can be defined, the method recently proposed by Y.A. Chao /10/ could be attempted. With this method the difference g, assumed here for simplicity between two independent experimental determinations of the same quantity, is considered as statistically distributed around a mean value $\bar{g}$ (the negligence error). This mean value is in turn distributed with the Gaussian law

$$P = \lambda^2 \exp\left(-\frac{\lambda}{2}\bar{g}^2\right) , \qquad (20)$$

where λ is a parameter to be determined by maximization of the resulting likelihood function. The maximum probability is then associated to $\bar{g} = o$, i.e. to the case of no negligence error. Once negligence errors are accounted for (gross adjustment) a minor (fine) adjustment is proposed by adopting standard fit procedures within data statistically consistent (i.e. satisfying a χ^2 test). Also with this method there seems to remain the difficulty of deciding weather this negligence error should be associated with the differential data, with the integral ones or with both. If this difficulty remains, a still different approach to cope with negligence errors could be adopted, as proposed recently by Perey /11/, who suggests to resort to decision theory and therefore include some "loss functions" as part of the adjustment procedure. This would, of course, cause

the results of the adjustments to be only valid for some specific decision. So the problem seems shifted to the choice of the loss function most appropriate. If there is not a full agreement on this, for instance when loss functions relevant to economics contrast with those relevant to safety, it seems that we should accept the idea of having more than one "ad hoc" adjusted set. Whereas system designers probably prefer a unique set of data and a reliable error dispersion matrix on which to base, for the most important integral parameters, the evaluation of the confidence intervals required to an adequate built-in flexibility of the system.

REFERENCES

1. A. Gandini, CNEN Report, RT/FI(73)5, 1973
2. A. Gandini, Nucl. Sci. Eng., 57, 248 (1975)
3. A. Gandini, Nucl. Sci. Eng., 67, 91 (1978)
4. Y.G. Bobkov, S.M. Gruzd, A.S. Krivtcov, L.N. Usachev, Preprint FEI-871, Obninsk, 1978
5. A. Gandini, Nucl. Sci. Eng., 67, 347 (1978)
6. E. Greenspan, D. Gilai, E.M. Oblow, Nucl. Sci. Eng., 68, 1 (1978)
7. R. Saito and S. Katsuragi, J. Nucl. Sci. Techn., 6, 303 (1969)
8. M. Mitani, M. Kuroi, J. Of Nucl. Sci. Techn., 9 (7), 383 (1972)
9. A. Gandini, CNEN Report, RT/FI(73) 22
10. Y.A. Chao, Proceed. of the Seminar-Workshop on Theory and Application of Sensitivity and Uncertainty Analysis, Oak Ridge, Aug. 1978
11. F.G. Perey, Private communication (1978)